The development, calibration and application of the DO_3SE-Crop model to assess ozone's effect on grain and protein yield in wheat

Joanne Laura Cook

PhD

University of York

Environment & Geography Department

September 2024

Abstract

Wheat is a global staple crop, providing 40% and 47% of daily calories and protein. However, tropospheric ozone (O_3) threatens wheat yields and quality. While several risk assessments have investigated O_3's impacts on wheat yields at varying geographical scales, the reduction in protein has not been included. The Indo-Gangetic Plains in India, a key wheat-growing region, face high and rising O_3 levels. Given India's existing food and nutrition security challenges, understanding O_3's threat to wheat yields and protein is essential to inform policy, mitigation and adaptation strategies. This thesis develops a framework for estimating O_3 effects on wheat protein yields, concentration and quality, suitable for risk assessments, by developing a nitrogen (N) (and protein) module for the stomatal O_3 deposition crop model, DO_3SE-Crop. In paper 1, the module is developed and identifies the key plant process affecting wheat N under O_3 as early senescence onset (simulated as being ~13 days earlier in the very high vs low O_3 treatment). In paper 2, the module is extended for Indian wheat, and a framework is presented for using the model to calculate protein quality, through amino acids and metrics recommended by the Food and Agricultural Organisation. While the lysine and methionine concentrations were simulated well, the decrease in methionine concentrations under O_3 exposure was underestimated by ~10 percentage points. The underestimation was greater for lysine. In the final paper, different risk assessment methods, input data and cultivar O_3 sensitivity are tested and compared with the newly developed model to understand risk assessment uncertainties. Risk assessment method was the largest source of relative yield (RY) variability ($0<RY<1$), followed by input data ($0<RY<0.8$). Cultivar O_3 sensitivity contributed very little to variations in RY estimates (magnitude of 12 percentage points) but had a greater effect on protein (magnitude of ~40 percentage points).

Contents

List of tables

List of figures

Acknowledgements

I am incredibly thankful for the opportunity to undertake this PhD, and there are so many people whose support I am grateful for, without whom this PhD would not have been possible. Firstly I would like to thank the Adapting to the Challenges of a Changing Environment Doctoral Training Partnership (ACCE DTP) for the funding and training support which made this PhD possible. I am also grateful to the University of York Environment and Geography Department. I have never before worked in such a kind, supportive environment, and I have learnt so much from all students and staff here.

Now moving on to more personal thanks, I am beyond grateful for the support of:

- Lisa Emberson, Felicity Hayes and Samarthia Thankappan who have supervised this PhD and provided a consistent source of support during this time. They have challenged and encouraged me and helped me to build up my confidence as a researcher. I couldn't have asked for a better supervisory team.
- The DO_3SE-Crop team: Pritha Pande, Nathan Booth and Sam Bland who have provided valuable assistance as I developed my understanding of the DO_3SE-Crop model, the calibration and evaluation processes, the plant mechanisms underlying these and the statistical approaches.
- The O_3 early career researchers' group: particularly Clare Brewster, Hattie Roberts, Melissa Chang and Mike Perring who helped me to settle into the PhD and provided support throughout, as well as providing a space to "bounce" ideas and practice presentations before conferences. Clare's help was also essential in providing data and assistance to develop the modelling processes in Paper 1 (Section 2) of this thesis. Without Clare's support it would have not have been possible to develop the model in its current format.
- Durgesh Singh Yadav, who provided data for papers 2 and 3 of this thesis, as well as assisting me with any questions that I had relating to the data. His help was invaluable in allowing me to complete this work.
- UoYork environment and ACCE PhD students, particularly my office and Zoom pals, for providing a safe space to share frustrations, valuable advice and plenty of laughter and joy.
- My wonderful housemates Robyn and Donda, who were always there for me and supported me, and were a great distraction when I was feeling stressed or overwhelmed.
- My friends Ellie, Abigail and Hester who have provided continued support all throughout my academic journey and believed in me when I did not believe in myself.
- My entire family, particularly my parents and sister, Rebecca. I will always be grateful to have such a supportive family who not only encourage me, but also remind me of the importance of taking breaks.
- Finally, I'd like to thank my wonderful partner, Jamie. Between buying a house and moving twice the final months of this PhD have not been easy. I am incredibly lucky to have a partner who took so much of the work with regards to the purchase and move so that I had more time to finish writing. When I first started this PhD, we hadn't even met, now I am finishing this PhD unable to imagine my life without her. I will always be grateful to have such a strong and caring woman by my side.

Declaration

This thesis has not previously been accepted for any degree and is not being concurrently submitted in candidature for any degree other than Doctor of Philosophy of the University of York. This thesis is the result of my own investigations, except where otherwise stated. All other sources are acknowledged by explicit references.

The manuscript in chapter 2 of this thesis has been published as follows: Cook, J., Brewster, C., Hayes, F., Booth, N., Bland, S., Pande, P., Thankappan, S., Pleijel, H. and Emberson, L., 2024. New ozone–nitrogen model shows early senescence onset is the primary cause of ozone-induced reduction in grain quality of wheat. *Biogeosciences*, *21*(21), pp.4809-4835.
I developed, coded, calibrated, applied and evaluated the DO_3SE-CropN model, performed all analyses, produced the figures and wrote the manuscript with comments from all co-authors. Author Clare Brewster provided the experimental data.

The manuscript in chapter 3 of this thesis has been accepted for publication as follows: Cook, J., Yadav, D.S., Hayes, F., Booth, N., Bland, S., Pande, P., Thankappan, S. and Emberson, L., 2024. Modelling the nutritional implications of ozone on wheat protein and amino acids. *EGUsphere*, *2024*, pp.1-33. I further developed, coded, calibrated, applied and evaluated the DO_3SE-CropN model, performed all analyses, produced the figures and wrote the manuscript with comments from all co-authors. Author Durgesh Singh Yadav provided the experimental data.

The manuscript in chapter 4 of this thesis is in preparation for submission as follows: Cook, J., Barman, N., Venkataraman, C., Hayes, F., Booth, N., Bland, S., Pande, P., Thankappan, S., Emberson, L.: Relative yield and protein estimates are more sensitive to ozone risk assessment method than input data and cultivar parameterisation
Authors Neeldip Barman and Chandra Venkataraman provided the simulated WRF-Chem meteorological and ozone data.

Throughout the PhD process, I also contributed to the development of the DO_3SE-Crop model, aiding with model calibration approaches, parameterisation and development of modelling processes (Pande et al., 2024a).

Organisation of thesis

This thesis comprises 5 main chapters, accompanied by a list of abbreviations for reference.

Section 1 introduces the thesis discussing the current state of food and nutrition security, the impacts of ozone (O_3) and climate change, and the significance of wheat as the global staple crop studied here. It outlines O_3 production pathways and their effects on crop yields and quality, both alone and combined with climate variables. Methods for estimating O_3-related yield reductions, focusing on crop models, are reviewed, including the model used in this thesis. Given the focus on India in Sections 3 and 4, the section also examines food security challenges in India, the threats posed by climate change and O_3, and previous methods used to assess O_3 impacts on Indian wheat. The introduction concludes by summarizing the research questions and outputs of the thesis.

Section 2 is the first paper of the thesis and describes the mechanisms by which O_3 affects crop yields and nitrogen (N) content and concentration. A mechanistic understanding of O_3's effects on crop N were used to develop, calibrate and evaluate a N module for the DO_3SE-Crop model to allow simulation of how O_3 affects crop N content (gN m^{-2}) and concentration (gN gDM^{-1}). After evaluation the model was used to calculate the plant process that affects crop N the most under O_3 exposure.

Section 3 is the second paper of the thesis, and extends the model developed in Section 2 for Indian wheat. The chapter presents a framework of how to make crop modelling simulations more relevant to human nutrition by simulating amino acids (AA) affected by O_3 that are essential for nutrition and incorporating the FAO-recommended dietary indispensable AA score (DIAAS) to assess protein quality.

Section 4 is the third and final paper of the present thesis and investigates the sensitivity of relative yield and protein estimates to different risk assessment methods and input data that have been commonly used in the literature to identify the yield loss under current or future O_3.

Section 5 is the synthesis chapter of the present thesis. It brings together the key findings of each paper of the thesis (Sections 2-4) along with common themes identified across the papers, the novelty of the results of the thesis and the associated limitations and implications of the findings.

List of abbreviations

The following acronyms and chemical symbols are used throughout the thesis:

AA	Amino acids
Anet	Net photosynthetic rate
AOT	Ambient over threshold
AWS	Automatic weather station
CH4	Methane
CO	Carbon monoxide
CO2	Carbon dioxide
DIAAS	Dietary indispensable amino acid score
DM	Dry matter
DVI	Development index
FACE	Free air CO2/O3 enrichment
GDP	Gross domestic product
GPP	Gross primary productivity
gsto	Stomatal conductance
H2O	Water
IAM	Integrated assessment modelling
IGP	Indo-Gangetic Plain
IMD	Indian meteorological division
LAI	Leaf area index
N	Nitrogen
NO3-	Nitrate ion
NOx	Nitrogen oxides
NPP	Net primary productivity
O3	Ozone
OTC	Open top chamber
PAR	Photosynthetically active radiation
POD	Phytotoxic O3 dose
PPFD	Photosynthetic photon flux density
PSII	Photosystem 2

RCP	Representative concentration pathway
RH	Relative humidity
RMSE	Root mean square error
ROS	Reactive oxygen species
RP	Relative protein
RPC	Relative protein concentration
RuBP	Ribulose-1,5-bisphosphate
RY	Relative yield
RYL	Relative yield loss
SSP	Shared socioeconomic pathway
TOAR	Tropospheric O3 assessment report
VOC	Volatile organic compounds
VPD	Vapour pressure deficit

1. Introduction

This thesis focusses on the effects of tropospheric ozone (O_3) pollution and climate change on food and nutrition security, with a heavy focus in two papers on India. Wheat is a staple crop globally, providing calories, protein, vitamins, minerals and fibre. These quality factors are all essential for humans to lead a healthy life (Peña-Bautista et al., 2017; Shewry and Hey, 2015). To meet the demands of the increasing global population, wheat production needs to increase (Peña-Bautista et al., 2017). Yet wheat is one of the most vulnerable to O_3 and climate change impacts. Global estimates show that present day wheat yields may be reduced by between 6-12% due to tropospheric O_3 pollution (Van Dingenen et al., 2009; Mills et al., 2018b). Additionally, the impacts of climate change will reduce wheat yields further (Asseng et al., 2015; Liu et al., 2019a). Also, both climate change (via heat and water stress and increased carbon dioxide (CO_2) concentrations) and O_3 have been shown to affect the amount and concentration of protein and minerals in wheat (Broberg et al., 2015; Mariem et al., 2021; Broberg et al., 2023; Broberg, Högy and Pleijel, 2017). While several studies have estimated the extent to which national or global wheat yields are reduced under O_3 pollution, with or without the co-occurrence of climate change (e.g. Nguyen et al., 2024; Tai et al., 2021; Mills et al., 2018b), no study has assessed the same for wheat quality. Arguably, one of the most important determiners of quality is the amount and quality of protein in wheat, as a higher amount and quality of dietary protein can protect against stunting and wasting, and provide defence against disease (Peña-Bautista et al., 2017; Shewry and Hey, 2015). Therefore, this thesis aims to understand the effects of O_3 on wheat quality, through the lens of protein.

O_3's effects on wheat yields have commonly been estimated by using concentration-response relationships. In these relationships a metric describing the concentration of O_3 that the plant was exposed to is linked to a subsequent yield loss under the pollutant (Fischer, 2019; Guarin et al., 2019a). Flux-response methods have also been developed which link the accumulated stomatal O_3 that the plant has taken up to a corresponding yield loss. The stomatal flux is estimated using a multiplicative equation that accounts for the effect of temperature, light and water availability on stomatal conductance (CLRTAP, 2017). Hence this method incorporates environmental effects, but as a statistical relationship, rather than simulating the actual plant processes. Crop models are the final method by which O_3 induced crop yield reductions have been estimated. Crop models use equations to represent the plant's development, photosynthesis, biomass distribution, grain growth, senescence and O_3 impacts on these. They also incorporate the effects of environmental factors such as CO_2, water, temperature, wind speed, radiation and humidity on crop growth in a mechanistic manner (Pande et al., 2024a). As a result, flux-response and crop modelling methods are the only methods of assessing the impacts of O_3 pollution on crop yields that can account for the interacting effects of O_3 pollution and climate change. Few studies have developed methods to assess the effects of O_3 on crop protein, and where they have, these are limited to concentration- and flux-response methods (Grünhage et al., 2012; Broberg et al., 2015). However, only a crop model can estimate the effects of O_3 on wheat protein, and how this can interact with climate effects, in a biologically realistic and mechanistic manner. To develop a method to mechanistically estimate the effects of O_3 pollution and climate change on wheat protein in a biologically realistic way, a module was developed for the existing O_3 deposition crop model, DO_3SE-Crop. This module simulates the N, and hence protein, of the wheat crop, and how it is affected by O_3 pollution, and is described in the 1st paper of this thesis.

Wheat is a key staple food in India. Per capita, the greatest amount of wheat is consumed in the west of India and across the IGP where the majority of wheat is grown (Ministry of Statistics and Programme Information, 2012). However, malnutrition is prevalent in India, with 39% of the population in India unable to afford a nutritionally adequate diet, and 78% of the population unable to afford a healthy diet (FAO et al., 2020; Herforth et al., 2020). As temperatures in India are projected to increase, and climatic conditions are expected to favour O_3 production, the effects of climate change and tropospheric O_3 production are expected to pose a greater threat to wheat yields and quality in India (Naaz et al., 2022; Fowler et al., 2008; Rathore, Gopikrishnan and Kuttippurath, 2023). However, while previous studies have estimated the national reduction to Indian wheat yields cause by O_3 pollution, no study to-date has considered the same for wheat protein, thus neglecting a key aspect of wheat quality important for human nutrition. In the 2nd paper of this thesis the modelling processes developed in paper 1 were extended to make them more relevant for simulating Indian wheat and for including the effects of O_3 on protein quality. Paper 2 hence develops a method by which O_3's impacts on wheat protein and protein quality, in addition to yields, at a national scale in India could be assessed.

The studies that have previously estimated O_3 reductions to Indian wheat yields at a national scale have used different input data to perform their assessments, leading to differences in estimated yield loss (Ghude et al., 2014; Sharma et al., 2019). Additionally, there are large differences in the magnitude of the estimates using concentration-response methods depending on the concentration metric used. Concentration-, flux-response and crop modelling methods do not always agree in their estimates of yield loss either (Mills et al., 2018b; Tai et al., 2021). Before estimating yield loss using a flux-response or crop modelling method, a decision has to be made on how to parameterise the function or model which will subsequently influence any answers (CLRTAP, 2017; Pande et al., 2024a). Therefore, in the 3rd paper of this thesis, concentration-, flux-response and crop modelled estimates of the yield loss of Indian wheat using different input data sources were compared to determine the uncertainty associated with input data choices. The current methods available for estimating protein losses were also compared for different input data to enhance current understanding of methods for assessing O_3 and climate impacts on wheat protein. By parameterising the flux-response and crop modelling methods for an O_3 sensitive and tolerant cultivar, the sensitivity of the different methods to parameterisation, in addition to input data, was determined. Therefore, altogether paper 3 provides an overview of the uncertainty associated with the different methods, data and O_3 sensitivity parameterisation for estimating O_3 and climate impacts on Indian wheat yields.

Overall, this thesis expands on existing crop modelling methods to incorporate O_3's effects on wheat protein and protein quality. This expands the relevance of previous risk assessment methods used to estimate O_3 reductions to yield to consider other aspects of wheat quality relevant for human nutrition. The resulting model has been further developed and tested for Indian wheat, as malnutrition in India is prevalent, and with wheat being a staple crop, and O_3 concentrations projected to increase, it is vital to understand O_3's impacts on wheat availability and the quality of nutrition people will get from it. By quantifying the uncertainty associated with input data, method and parameterisation choices, the final paper of this thesis provides the reader with a thorough overview of the benefits and drawbacks of different methods for assessing O_3's impacts on wheat, essential for allowing researchers to make fully informed decisions before performing their assessments.

The following literature review will provide the context, background knowledge and identification of research gaps for the present thesis, and will begin by introducing the current status of global food security and the threats posed by O_3 and climate change.

1.1 O_3, climate change and food security

This section reviews the current state of food and nutrition security, and how it is impacted by O_3 pollution and climate change. While the present thesis focuses on threats to food security that occur due to reductions in food availability due to abiotic stressors, the threats posed by climate change and O_3 pollution to other facets of food security are introduced to provide the reader with a deeper understanding of the complex threats posed by climate change and O_3 to food security. Additionally, this section will explore the significant role played by wheat in global food security to underscore the importance of focussing on wheat.

1.1.1 O_3 and climate change effects on food security

Food and nutrition security is related to having physical, social and economic access to food which provides the necessary nutrition for a person to lead a healthy and active life (FAO et al., 2023; El Bilali et al., 2019). Ensuring food security is dependent on many factors including the availability and access that people have to the food, whether they can utilise it (from a cooking and metabolic perspective), and the stability of the food system that ensures there are no sudden changes to the prior factors (El Bilali et al., 2019). Climate change and O_3 pollution threaten food and nutrition security as they have the capacity to reduce the yield and quality of crops (Mariem et al., 2021; Broberg et al., 2015; Tai, Martin and Heald, 2014). Both stressors are expected to exacerbate food security, particularly in regions that already experience high levels of food insecurity (Tai, Martin and Heald, 2014; Wheeler and Von Braun, 2013). Therefore, it is important to understand the threats they pose to food security and nutrition.

Globally, approximately 30% of the population was moderately or severely food insecure in 2022, which is an increase of 4% compared to pre-pandemic and pre-Ukraine war estimates (FAO et al., 2020, 2023). The cost of a healthy diet increased by 7% globally between 2019 and 2021, attributable to economic downturns caused by the pandemic (FAO et al., 2023). Levels of wasting and stunting, which occur when individuals do not get enough food, or a high enough quality of food, are also high (FAO et al., 2023; Briend, Khara and Dolan, 2015). Currently, 22% of children under the age of 5 suffer from stunting, which puts them at risk of developing non-communicable diseases later in life, and 7% of children under 5 suffer from wasting, which lowers their immunity (FAO et al., 2023). Both stunting and wasting increase the risk of mortality later in life (Briend, Khara and Dolan, 2015). The risk of food insecurity, stunting and wasting is greater in rural areas compared to urban areas, and greater for women compared to men (FAO et al., 2023). Currently, we are not on track to achieve Sustainable Development Goal 2: 'ensuring access to safe, nutritious and sufficient food for all people all year round' and 'eradicating all forms of malnutrition' by 2030 (FAO et al., 2023).

Abiotic stresses, such as climate change and air pollution, present many threats to the key pillars of food security: availability, access, utilisation and stability (El Bilali et al., 2019; FAO et al., 2023). Availability of food will be impacted by reductions to crop yield caused by increased temperatures and O_3 concentrations, extreme weather events and drought (Asseng et al., 2015; Nguyen et al., 2024; Mills et al., 2018b; Myers et al., 2017). O_3 pollution has been found to exacerbate yield losses under heat and water stress, suggesting interaction of the effects of O_3 with heat and water stress(Broberg et al., 2023; Tao et al., 2017; Nguyen et al., 2024). Yield

reductions from climate variability will be greater in tropical areas as compared to more temperate areas, reducing food availability in those locations (Wheeler and Von Braun, 2013; Porter et al., 2014; Mills et al., 2018b). Reductions to yield caused by an abiotic stress can affect the price of a crop under differing policy scenarios (Pandey et al., 2023). Price spikes and price volatility affect the affordability, and hence an individual's access to food (Myers et al., 2017). Utilization of food is also affected by changes to climate and O_3 pollution. Both climate change and O_3 pollution will affect the quality of crops, and hence affect the nutrition a person will get from their diet (Broberg et al., 2015; Myers et al., 2017; Mariem et al., 2021). Stability refers to the situation in which a person has food available, accessible, and utilisable to them consistently over time (Development Initiatives, 2020a; El Bilali et al., 2019). The threat of climate change and O_3 pollution to yields, price shocks and nutrition are all factors that cause instability and reduce food and nutrition security (Khanna-Chopra, 2012; El Bilali et al., 2019; Development Initiatives, 2020a). Location, age, sex, wealth, education level and conflict are additional factors that all influence the quantity and quality of food a person has access to, and hence contribute to their food and nutrition security (Development Initiatives, 2020). These additional factors will interact with climate change and O_3 effects to affect an individual's food and nutrition security.

1.1.2 The global importance of wheat for food and nutrition security

Wheat is a key staple crop, consumed by people all over the world in the form of breads, biscuits, cakes and noodles (Peña-Bautista et al., 2017). Total wheat consumption is greatest in India and China, which are the dominant wheat producers globally (see Figures 1.1 and 1.2 and US Department of Agriculture (2024)). Per capita, however, wheat consumption is more evenly distributed across the world (Figure 1.3). Developing countries (China, India, Pakistan and Ukraine) account for 38% of global wheat production, with China leading at 17%, and India coming in a close second at 14% (Figure 1.1 and US Department of Agriculture (2024)). The dramatic increase in wheat production in the 1960's, termed the green revolution, substantially reduced food insecurity in several developing regions by increasing food availability and raising incomes (Shiferaw et al., 2013). For small-scale wheat farmers, consistent and sufficient income ensures households have the ability to afford and utilise food, reducing food insecurity (El Bilali et al., 2019; Peña-Bautista et al., 2017). Additionally, the wheat grown by the farmers is an easily available and accessible source of food (Peña-Bautista et al., 2017).

Wheat contributes to approximately 20% of global calories and dietary protein (Shiferaw et al., 2013). It also accounts for 40% of calories from cereal consumption and 50% of cereal-based proteins worldwide (Shiferaw et al., 2013). Starch is the key energy source in wheat and comprises 60-70% of the wheat grain (Broberg et al., 2015). Wheat also provides essential amino acids (AA), which are AA that the body cannot produce by itself (Shewry and Hey, 2015). Children require higher amounts of essential AA in their diet for growth as well as maintenance (Shewry and Hey, 2015). If an individual does not get enough protein, or high enough quality of protein through essential AA, then they are at risk of wasting and loss of muscle function (Medek, Schwartz and Myers, 2017). Additionally, wheat products also contain fibre, minerals, vitamins and antioxidants that are beneficial for health and nutrition (Peña-Bautista et al., 2017; Shewry and Hey, 2015).

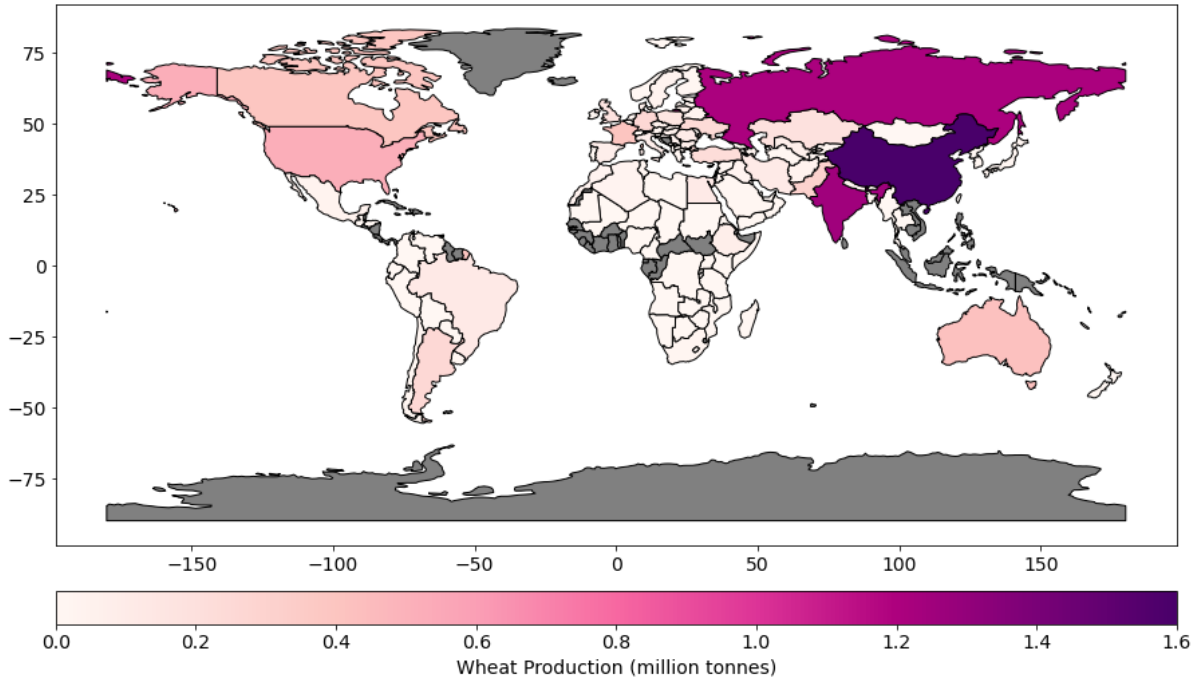

Figure 1.1: Global wheat production in 2022. Plot produced using data compiled by Ritchie, Rosado and Roser (2023) from the Food and Agriculture Organization of the United Nations (2023).

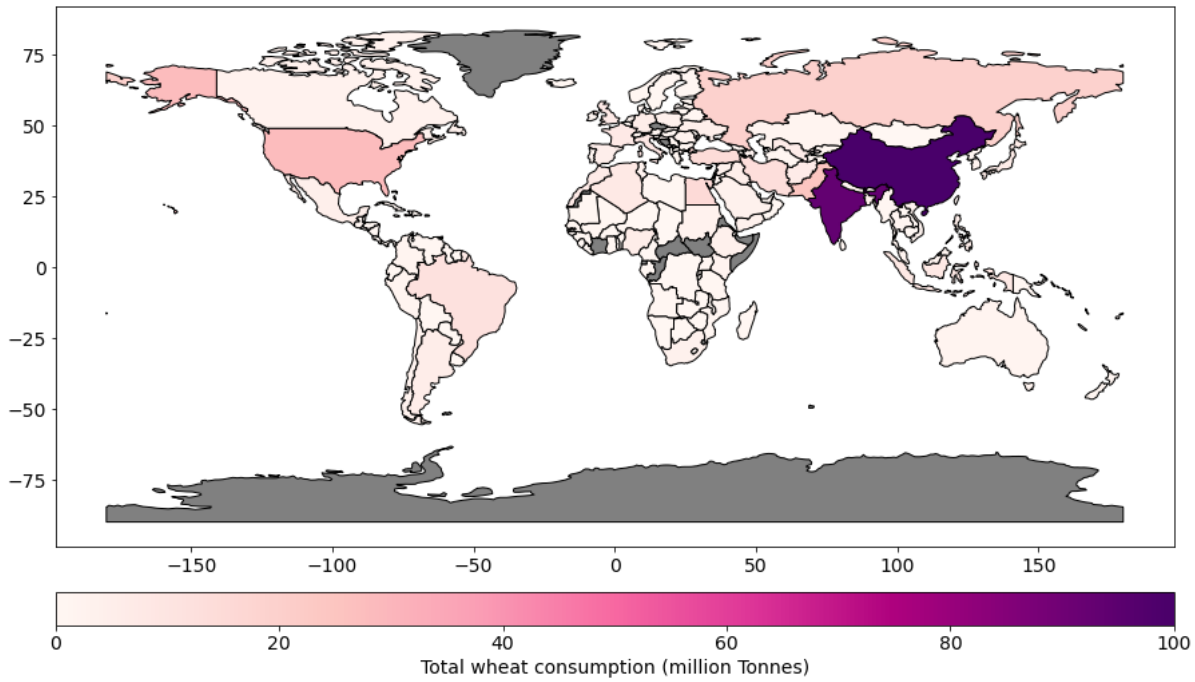

Figure 1.2: Total wheat consumption in 2020 using data compiled by World Population Review (2024) from the food balance sheets of the FAO.

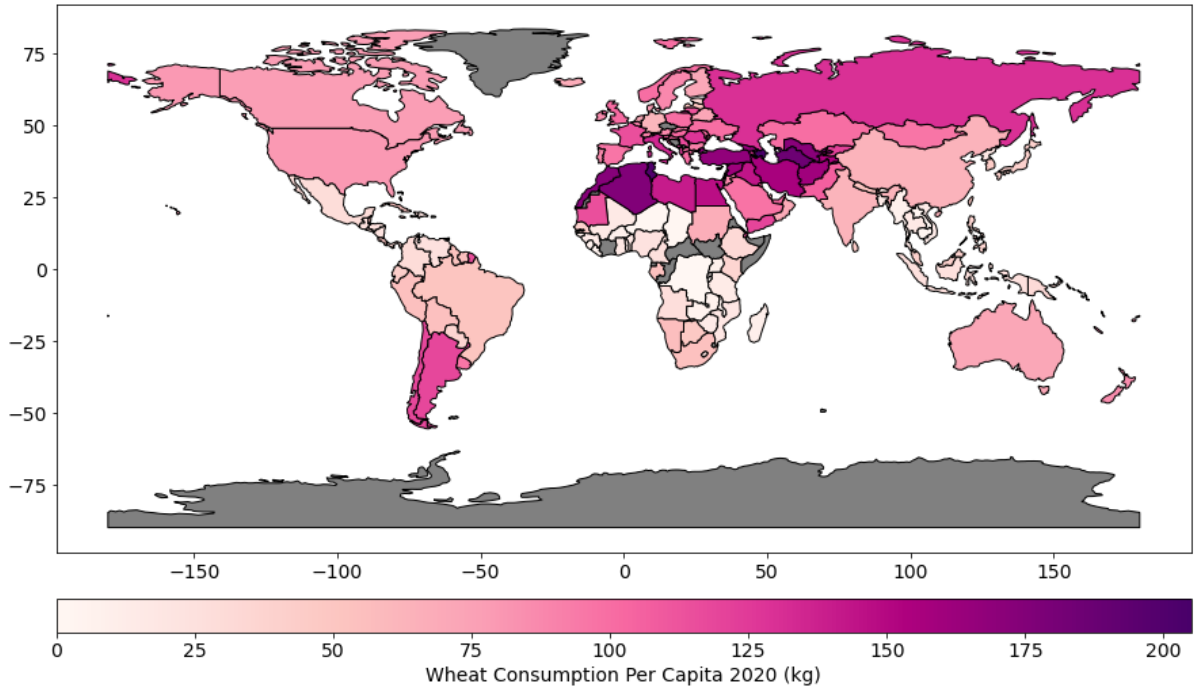

Figure 1.3: Per capita wheat consumption in 2020 using data compiled by World Population Review (2024) from the food balance sheets of the FAO.

1.1.3 Defining wheat quality

In the prior subsections and throughout this thesis wheat quality is often referred to. Wheat quality refers to protein, lipids, carbohydrate, mineral, antioxidant and sensory properties of the wheat (Wang and Frei, 2011). However, in the modelling context of this thesis, quality is simplified to simply mean crop protein, or nitrogen (N) which is a key component of protein and can therefore be used as a proxy for it. In Paper 2 of this thesis, the protein quality (via the AA components that constitute proteins) is also assessed. Protein and AA are important for protecting against wasting and stunting, and for defending against disease. Therefore, they are both vitally important for human nutrition. Understanding the effect of environmental stressors on protein and AA helps understand the effect that these stressors will have on human nutrition.

In summary, this section identified that the key pillars of food and nutrition security are availability, access, utilisation and stability. Each of these pillars will be impacted by climate change and O_3 pollution through reductions to yields, price shocks and reductions in nutritional quality that will impact individual's health and exacerbate malnutrition. Additionally, wheat was identified as a key staple food globally, providing 20% of global calories and dietary protein as well as essential and non-essential AA, minerals, vitamins and antioxidants. The definition of wheat quality as used throughout this thesis was also defined to frame later discussions.

1.2 O_3 production, sources and metrics

Before further exploring the threats posed by O_3 and climate change to wheat, it is crucial to understand how O_3 is formed. This will support the later discussion of current and projected global O_3 concentrations. Additionally, the metrics often used to define O_3 concentrations and assess their damage to crops are described to prepare the reader for future discussions of methods by which yield losses attributable to O_3 are quantified.

1.2.1 O_3 production

In the troposphere, O_3 is formed when precursor gases such as carbon monoxide (CO), methane (CH_4), nitrogen oxides (NO_x) or volatile organic compounds (VOCs) react in the presence of UV radiation. Figure 1.4 shows the process of O_3 formation as well as the sources of O_3 precursors which can be anthropogenic, such as transport and fossil fuel usage, as well as natural, for example wetlands (Fowler et al., 2008).

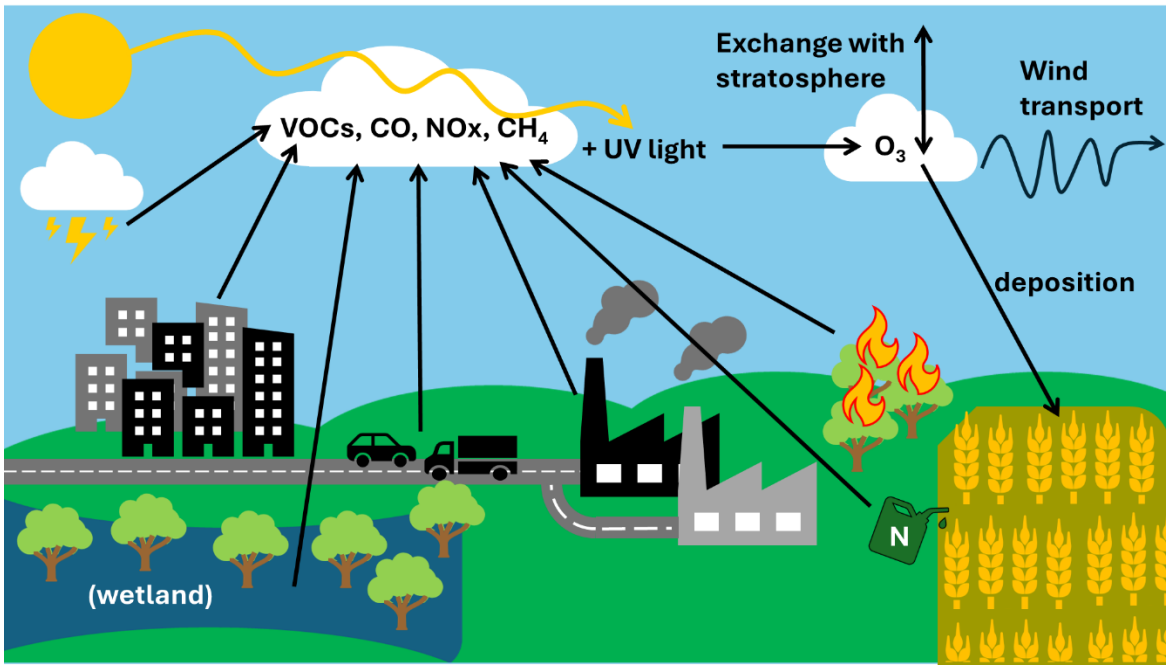

Figure 1.4: Diagrammatic representation of the sources of precursors for O_3 pollution. For detail of the chemical processes involved in O_3 formation please refer to Figure 1.5.

The reactions by which O_3 formation occurs are dependent on precursor concentrations, and therefore regions with different pre-cursor concentrations have different O_3 production pathways (Fowler et al., 2008; Elshorbany et al., 2024). Generally, O_3 formation is NO_x limited, but as NO_x concentrations increase, the limiting factor to O_3 formation becomes VOCs (Fowler et al., 2008). As a result, O_3 formation in rural and agricultural areas tends to be NO_x limited, while in urban areas, which have greater NO_x emissions, O_3 formation tends to be VOC limited (Fowler et al., 2008). O_3 concentrations tend to be greater in rural areas as the NO_x-limited formation pathway means that as NO_x concentrations increase, the rate of O_3 formation increases (Fowler et al., 2008). Elevated O_3 concentrations in rural areas are of particular concern since these are the locations where agriculture predominantly occurs (Fanzo, 2018). Recently, a third regime has been identified in regions with high aerosol concentrations. This aerosol limited regime has been identified as dominating over most of India and China, where the HO_2 radical involved in O_3 formation (see Figure 1.5) adsorbs onto and reacts with the aerosol particles, and is unavailable for further reactions to form O_3 (Archibald et al., 2020a). The cycle of O_3 formation shown in Figure 1.5 is NO_x limited, and as NO_x concentrations increase, so does O_3 formation (Fowler et al., 2008). The concentrations of CH_4, CO and other VOCs have little impact on the rate of O_3 formation in the NO_x limited scenario as there are no side reactions involving the listed gases that could disrupt O_3 generation in the cycle (Fowler et al., 2008).

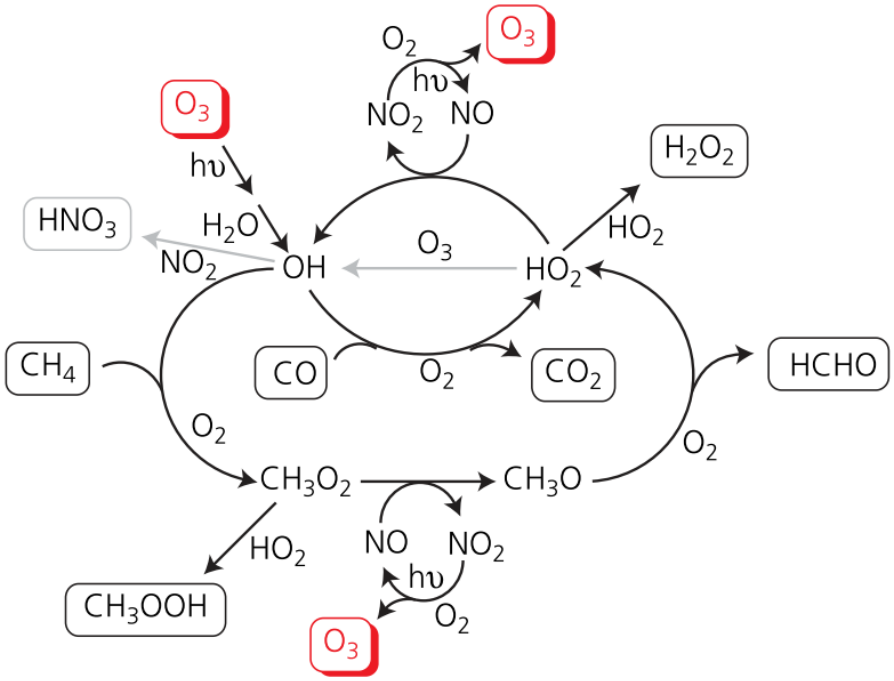

Figure 1.5: Diagrammatic representation of O_3 formation at intermediate NO_x concentrations taken from Fowler et al. (2008)*, where hv represents high frequency light.*

Some of the O_3 found in the troposphere is transported from the stratosphere, where it prevents some of the sun's harmful UV radiation entering the atmosphere (Fowler et al., 2008). Transport of O_3 from the stratosphere to the troposphere is ~ 9 times smaller than the amount of O_3 that is produced from pre-cursor gases in the troposphere (Fowler et al., 2008). In total, around 20% of tropospheric O_3 is deposited to ground surfaces (such as trees or crops), and the remaining 80% undergoes chemical destruction processes in the atmosphere (Fowler et al., 2008). As temperatures increase resulting from climate change, global average O_3 concentrations will also increase if pre-cursor emissions remain the same, as production of the pollutant is favoured by high temperatures and high radiation (Fowler et al., 2008). This means that even if precursor emissions do not change, or reduce by only a small amount, O_3 production could still increase if climatic conditions were favourable (Fowler et al., 2008).

1.2.2 O_3 precursor concentrations

Emissions of O_3 precursors derive from both human activities, such as energy generation, industry, agriculture, transport, biomass burning and deforestation, and natural sources, such as vegetation biogenic emissions, forest fires or lightning (Figure 1.4) (Fowler et al., 2008). Across countries, and over time, precursor concentrations vary due to economic development and emission control measures (Fowler et al., 2008).

(a) *NO_x emissions*

Over the past 50 years, global NO_x concentrations have increased with a peak around 2010 followed by a decline. Globally, the dominant anthropogenic sources of NO_x emissions are energy generation, industry and on-road transportation (McDuffie et al., 2020). NO_x emissions are greatest in China due to the large energy and industrial sector in the country (McDuffie et al., 2020; Duncan et al., 2015). Comparatively, NO_x emissions across Europe, North America and Australasia are $\lesssim$ half of China's NO_x emissions and have decreased over time due to implementation of vehicle and industry

emissions standards (McDuffie et al., 2020; Duncan et al., 2015; Elshorbany et al., 2024). In India, the reliance on solid cooking fuels can also release both VOCs and NO_x gases (Fowler et al., 2008; Chowdhury et al., 2019).

(b) *VOC emissions*
VOC emissions have increased continuously over the past 50 years (McDuffie et al., 2020). The largest anthropogenic source of VOC emissions globally comes from the energy sector, with other sources including on-road transportation, household fuel combustion and solvent usage (McDuffie et al., 2020). Africa and China are the regions with the greatest VOC production globally, which can be attributed to solvent, energy and industry in China, and for Africa is due to residential fuel combustion and the energy sector (McDuffie et al., 2020). In Europe and North America emissions controls for the residential sector and on-road transportation led to comparatively lower VOC emissions (McDuffie et al., 2020).

(c) *CO emissions*
CO emissions peaked around 1990 and then declined. A small increase in CO emissions between 2002-2012 occurred as a result of growth in energy, industry, and residential fuel burning in Asia and Africa (McDuffie et al., 2020). Subsequent declines were associated with emissions control in China and reduced on-road transport emissions for Europe and North America (McDuffie et al., 2020; Elshorbany et al., 2024). CO emissions globally are dominated by on-road transport and residential combustion. China, Africa and other Asian countries (excluding India) have the highest CO emissions. In China, industry and residential combustion are dominant sources, while in other Asian countries residential combustion and on-road emissions are almost equal (McDuffie et al., 2020). For India, CO emissions are mainly from residential fuel combustion due to the reliance on burning solid fuels for cooking and heating (McDuffie et al., 2020; Chowdhury et al., 2019). In Latin America, Africa and Asia, biomass burning is a substantial contributor to NO_x and CO emissions, with the seasonal nature of these activities causing greater emissions during burning periods (Elshorbany et al., 2024; Fowler et al., 2008).

(d) *CH_4 emissions*
Between 2009-2020 global CH_4 emissions have increased, with the waste and agriculture sectors being the dominant contributors to the increase (Janardanan et al., 2024). The countries contributing the most to CH_4 emissions are China, India, North America, Pakistan and Indonesia. The largest anthropogenic contributions to CH_4 emissions in China and Pakistan were waste and gas, in India were agriculture and waste, for North America were oil, gas, coal and agriculture, and for Indonesia were coal (Janardanan et al., 2024). In China, the transition from coal to gas, and increases in the waste sector, will increase CH_4 emissions more over the coming years. Biomass burning is also a contributor to CH_4 emissions in India, Pakistan, South America and parts of West Europe and East Russia, though the contribution is not as large as the previously identified sectors (Janardanan et al., 2024).

1.2.3 O_3 concentrations: Present and future

To effectively assess the impact of tropospheric (ground level) O_3 on crop yields and quality, it is crucial to understand current tropospheric O_3 concentrations. This establishes a baseline with

which to compare projections to identify if future O_3 pollution will have a negative impact on crop yield and quality. Additionally, analysing current tropospheric spatial O_3 concentrations and their projected future trends helps identify regions where crops are likely to experience significant impacts from O_3 pollution. This section begins by providing an overview of current tropospheric global O_3 concentrations, relative to pre-industrial concentrations, and how they vary globally. The section then concludes by considering future tropospheric O_3 projections and identifying regions at risk of adverse O_3 effects on crop and nutrition.

Comparisons of historic tropospheric O_3 records with current measurements are prone to large uncertainties, but it is generally accepted that surface O_3 concentrations have increased by between 30-70% when comparing modern (1990-2014) global tropospheric O_3 concentrations with historic (1896-1975) (Tarasick et al., 2019). The greatest increases in tropospheric O_3 concentrations have been observed in the northern hemisphere, with tropospheric O_3 concentrations between 1950 and 2000 doubling across Europe (Tarasick et al., 2019; Cooper et al., 2014). Globally, tropospheric O_3 concentrations are highest in southern USA, the Mediterranean basin, northern India, parts of China, Republic of Korea, and Japan (Mills et al., 2018c). Tropospheric O_3 concentrations tend to be higher in rural areas than urban, and, seasonally, Europe and North America tend to experience the greatest tropospheric O_3 concentrations in July, while concentrations in East Asia are highest in April and May (Schultz et al., 2017). In Asia, the lowest tropospheric O_3 concentrations coincide with the monsoon period (Schultz et al., 2017; Lu et al., 2018). Between 1980-2010, the greatest increase in tropospheric O_3 concentrations occurred across India (~8 ppb), attributed to increases in anthropogenic activities such as pollution from vehicles and industry, and combustion or burning processes, as well as from some natural sources (Wu et al., 2016).

In the future, O_3 production will vary seasonally according to the key drivers of local O_3 production, which could be changes to precursor emissions and/or changes to local climate and meteorology (Fowler et al., 2008; Fu and Tian, 2019; Meehl et al., 2018). Rising energy and agricultural demands, coupled with increased transportation, will increase precursor emissions, impacting O_3 production (Fowler et al., 2008). Climate change will further influence tropospheric O_3 levels through alterations in precipitation, temperature, humidity, and air movement, with local to regional variations affected by factors like water vapor and pre-cursor concentrations, making future tropospheric O_3 concentration trends uncertain (Fowler et al., 2008; Fu and Tian, 2019).

To perform tropospheric O_3 projections, representative concentration pathways (RCPs) or shared socioeconomic pathways (SSPs) are used. RCPs incorporate a range of greenhouse gas emissions that will result in a target radiative forcing (incoming radiation subtracted by outgoing radiation at the top of the atmosphere) targets (DEFRA et al., 2018). These radiative forcing targets are 2.6, 4.5, 6 and 8.5 Wm^{-2} where RCP 2.6 is a scenario where greenhouse gas emissions are strongly reduced, and RCP 8.5 is a scenario where greenhouse gas emissions grow in an unmitigated manner(DEFRA et al., 2018 and Table 1.1). RCPs 4.5 and 6.0 represent pathways with varying levels of greenhouse gas emissions mitigation (DEFRA et al., 2018).

In contrast with RCPs, SSPs focus on different societal futures and how they may influence emissions. The different societal futures include economic growth, technology and urbanisation (O'Neill et al., 2014). SSPs are often defined in combination with a target RCP and as such provide an indication of the type of societal future that will result in a target radiative forcing. Detailed projections of future O_3 concentrations under differing RCP emission scenarios were performed by Wild et al. (2012), Young et al. (2013), Sicard et al. (2017).

Additionally, Griffiths et al. (2021) projected future O_3 concentrations using SSP370, which has similar radiative forcing to RCP 6.0. For the greatest emissions, scenario, RCP 8.5, Wild et al. (2012), Young et al. (2013b, 2013a), and Sicard et al. (2017) project increases in global tropospheric O_3 concentrations, with vegetation in South America, USA, Asia and Africa in particular threatened by increased O_3 concentrations. Under lower emission scenarios, RCP 2.6 and 4.5, Wild et al. (2012) and Sicard et al. (2017) project a decrease in global tropospheric O_3 concentrations, though some regional variations are observed. The findings of Young et al. (2013b, 2013a) contrast this slightly, as under RCP 4.5 they predict decreases in global tropospheric O_3 concentrations in the northern hemisphere and increases in the southern. Under RCP 6.0 O_3 concentrations were projected to decrease globally (Young et al., 2013b, 2013a). All authors agree that the greatest increases in surface O_3 concentrations will occur across Asia, and in particular South Asia (Wild et al., 2012; Sicard et al., 2017; Young et al., 2013b, 2013a; Griffiths et al., 2021). Figure 1.6 shows a visual representation of future surface O_3 concentrations as projected under various emissions scenarios by 2030 and 2100 from Young et al. (2013b, 2013a).

Table 1.1: Summary of the definitions of the different RCP scenarios (DEFRA et al., 2018; Moss et al., 2010).

RCP	Radiative forcing	Notes
2.6	Radiative forcing stabilised at 2.6 Wm^{-2}	Below the 10th percentile of emissions mitigation scenarios
4.5	Radiative forcing stabilised at 4.5 Wm^{-2}	
6.0	Radiative forcing stabilised at 6.0 Wm^{-2}	
8.5	Radiative forcing stabilised at 8.5 Wm^{-2}	90th percentile of emissions scenarios

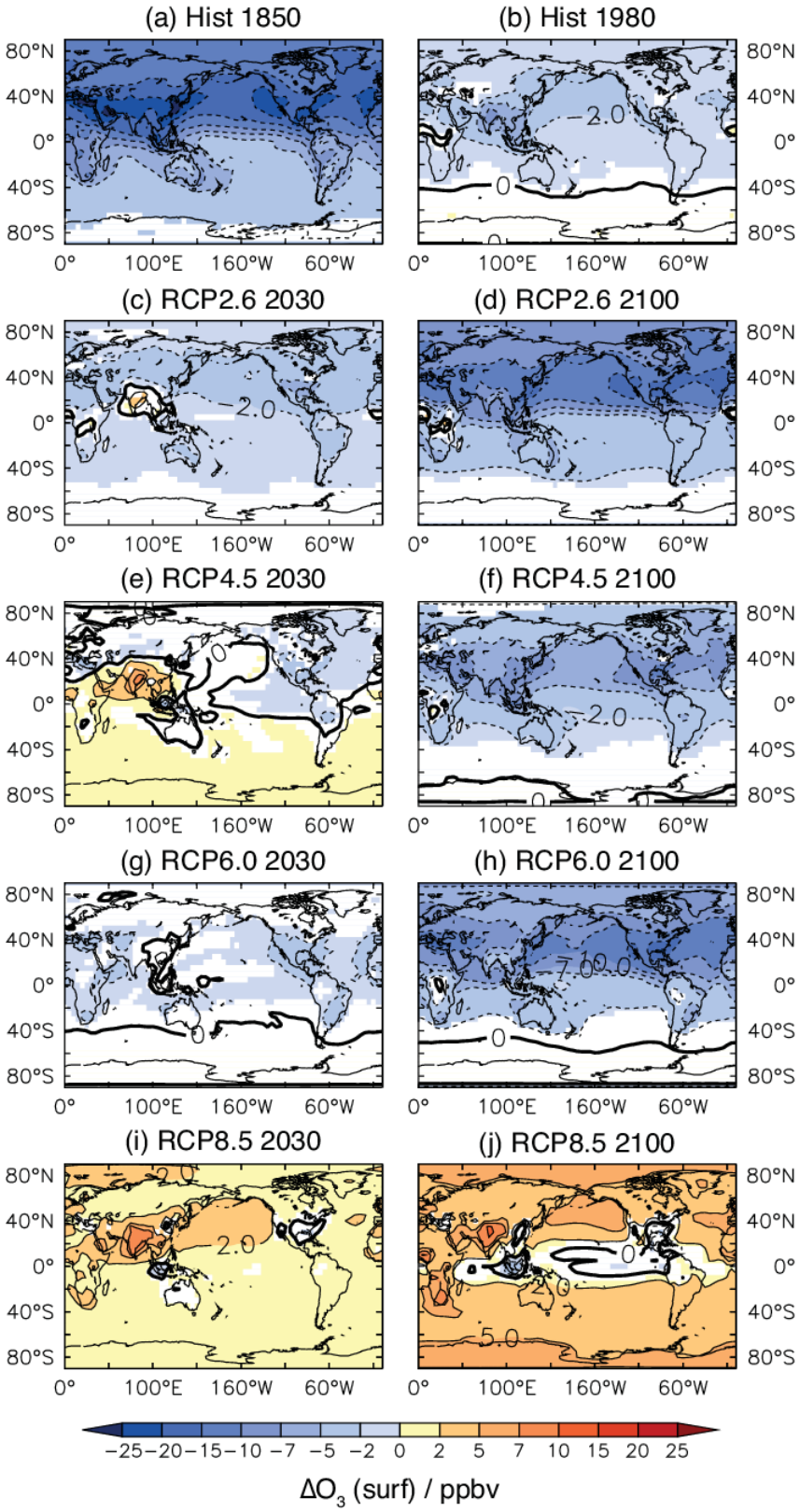

Figure 1.6: Absolute change in surface O_3 (ppbv) for the AC- CMIP ensemble mean compared to the Hist 2000 simulation (ppbv). Top row shows the difference for the Hist 1850 and 1980 time slices. The next four rows show the difference for the 2030 and 2100 time slices of the RCP simulations. Non-white regions indicate where the change is significant at the 5% level, based on the spread of the differences between the models. The red dashed line indicates the position of the annual zonal mean 150 ppbv O_3 contour from the Hist 1850 simulation. This figure and caption was taken from Young et al. (2013b, 2013a)

1.3 Mechanisms by which O_3, climate variables and N influence yields and nutrition

To meet the demands of the increasing global population, wheat production needs to increase (Peña-Bautista et al., 2017). However, wheat is one of the most vulnerable crops to both climate change and O_3 impacts, with both yield and quality threatened (Broberg et al., 2015; Asseng et al., 2019; Tai, Martin and Heald, 2014; Mills et al., 2018b). Increased O_3 concentrations reduce the starch and protein yield (gNutrient m^{-2}) of wheat along with several other nutritionally important minerals (Broberg et al., 2015). While, increased temperatures and water stress will reduce wheat protein content (gProtein m^{-2}) while increasing the concentration of protein (gProtein gDM^{-1}) in the grains (Mariem et al., 2021; Broberg et al., 2023). Although higher carbon dioxide (CO_2) concentrations may mitigate some of the negative yield impacts of O_3 and increased temperatures, they will likely not offset the impact on wheat quality (Broberg et al., 2023). In this section, the impact of O_3 and climate change variables, individually and in combination, on wheat yields and quality are explored, focussing on protein as a measure of wheat quality.

To identify the key mechanisms of damage from O_3 and climate change variables, their effects on the following key plant processes are examined: leaf physiology (stomatal conductance and photosynthesis), antioxidant defence, senescence, biomass, N remobilisation and grain yield & quality. Understanding these processes is crucial for relating the effects of O_3 and climate change to crop growth (biomass and yields) and development (growth stages and senescence). In this section both N and protein are referred to. Since N is a key component of protein, N dynamics are considered as a determinant of final grain protein. The knowledge gained in this section will help identify key processes to include in methods or models for assessing the effects of these stressors on food supply and nutrition.

1.3.1 O_3 mechanisms

Once O_3 diffuses into the plant through the stomata, a series of chemical reactions take place that ultimately end up reducing the rate of photosynthesis and accelerating crop senescence. This leads to a reduction in crop yield and quality (Emberson et al., 2018; Broberg et al., 2015). In this section, the plant processes by which O_3 reduces crop growth, biomass, yield and quality are explained separately.

Stomatal conductance

Stomatal conductance determines how much CO_2 gains entry to the leaf for photosynthesis. As CO_2 diffuses into the leaf, so too will other trace atmospheric gases, including O_3. As such, O_3 diffuses into the leaf via the stomatal pores (Emberson et al., 2018), where the amount of O_3 that enters the leaf depends on the external O_3 concentration and the stomatal conductance of the leaf (Mills et al., 2011). There are also resistances to stomatal O_3 uptake which include aerodynamic resistance and boundary layer resistance (which determine the amount of O_3 transported to the leaf surface and hence available for uptake) and internal resistance from the mesophyll cells, which reduce O_3 uptake by reducing the O_3 concentration gradient between the leaf surface and intercellular spaces inside the leaf (Tiwari and Agrawal, 2018).

Antioxidant defence

Once inside the leaf, O_3 degrades to form reactive oxygen species (ROS) including H_2O_2, O_2^- and OH (Emberson et al., 2018; Tiwari and Agrawal, 2018; Kangasjärvi, Jaspers and Kollist, 2005). Low levels of ROS trigger an acclimation effect, allowing the plant to increase its growth and function as plants naturally contain small amounts of ROS necessary for development (Agathokleous, Kitao and Calabrese, 2019). A small amount of stress, and hence ROS, allows the plant to improve its functioning so that when the plant is exposed to higher amounts of the stress later on it experiences less damage (Reiling and Davison, 1995; Held, Mooney and Gorham, 1991; Mikkelsen and Ro-Poulsen, 1994; Agathokleous, Kitao and Calabrese, 2019; Bellini and De Tullio, 2019). The acclimation effect forms part of the hormesis response in plants, wherein low levels of a stressor produce a positive response for plant growth, whereas higher levels can induce a response detrimental to growth (Bellini and De Tullio, 2019; Agathokleous, Kitao and Calabrese, 2019). If the threshold for ROS to be beneficial has been exceeded, some apoplastic antioxidants (antioxidants located outside of the cell membrane, for example in the cell wall or leaf cuticle) counteract these ROS. The production of such antioxidants increases the demand for carbon (C) which increases the rate of mitochondrial respiration for O_3 detoxification and cell repair (Emberson et al., 2018; Gandin, Dizengremel and Jolivet, 2021). The concentrations of antioxidants in the apoplast of wheat have a diurnal profile induced by the daily variation in O_3 concentrations (Wang et al., 2015). Hence, the time of day of stomatal O_3 uptake will likely affect its ability to be detoxified. If the plant is overwhelmed by the antioxidant demand, then not all ROS are combatted (Emberson et al., 2018). The remaining ROS react with the plasma membrane, creating harmful derivatives with a longer half-life, while antioxidants move from the symplast to the apoplast to help detoxify O_3 at its entry point into the leaf (Tiwari and Agrawal, 2018; Emberson et al., 2018).*Photosynthesis*

Following the attack on the plasma membrane, ROS destroy photosynthetic pigments leading to a reduction in sites available for photosynthetic reactions (Rai and Agrawal, 2012). Further, the ROS cause protein degradation which reduces the amount of Rubisco activase (RA), and subsequently impacts the carboxylation efficiency (rate of fixation of CO_2 during photosynthesis) (Tiwari and Agrawal, 2018; Rai and Agrawal, 2012; Feng et al., 2016; Khanna-Chopra, 2012). A further factor leading to reduced photosynthesis is ROS damages to photosystem II (PSII) where photons are captured. The reduction in photon capture reduces the electron transport rate and the efficiency of photosynthetic reactions (Feng et al., 2011; Tiwari and Agrawal, 2018; Feng et al., 2016). The destruction of photosynthetic pigments also leads to visible damage on the leaf. An example of this is given in Figure 1.7 which shows yellowing on the flag leaf of a wheat plant due to O_3 destruction of photosynthetic pigments.

Figure 1.7: Flag leaf of a wheat plant that has been exposed to high concentrations of O_3. The yellowing shows the effect that O_3 has had on destroying photosynthetic pigments. The effect is called chlorosis. This image is reprinted from ICP Vegetation (2014).

Senescence

During natural senescence, chloroplasts, and Rubisco, are degraded by ROS, to allow for production of proteins for remobilisation to other plant parts, such as the growing wheat grains (Khanna-Chopra, 2012; Feller and Fischer, 1994). During O_3 stress this effect is accelerated as ROS produced as a result of elevated O_3 initiate earlier and faster degradation of chloroplasts and Rubisco, which can lead to early onset and accelerated senescence (Khanna-Chopra, 2012; Feng et al., 2016, 2011; Tiwari and Agrawal, 2018; Rai and Agrawal, 2012). Elevated O_3 may overwhelm the detoxifying antioxidants and ROS will degrade Rubisco and chloroplasts in a greater amount and earlier in the plant's life, again leading to accelerated senescence (Khanna-Chopra, 2012). Both the onset and rate of senescence are accelerated under O_3 exposure. However, the leaf age plays a role in its capacity to defend itself against ROS, with a greater O_3 effect being observed in lower, older leaves compared to the flag leaf (Brewster, Fenner and Hayes, 2024).

Biomass

Subsequently, there is less photosynthate (i.e. assimilated C) available and the plant C allocation processes are modified in order to produce more antioxidants for O_3 defence (Tiwari and Agrawal, 2018; Rai and Agrawal, 2012). Less biomass is directed towards the roots as the plant favours photosynthate partitioning to the shoot to repair O_3 induced damage and continue growth under elevated O_3 (Emberson et al., 2018; Pandey et al., 2018; Broberg et al., 2015). Reduced root biomass means that the uptake of nutrients is less under elevated O_3 (Emberson et al., 2018; Broberg et al., 2015).

Grain DM and starch

O_3 induced accelerated plant senescence results in a shorter period for grain growth and filling (Broberg et al., 2015). Reduced photosynthate production and modified C allocation processes also influence grain biomass accumulation, the size of grains and the number of grains that are filled (Tomer et al., 2015; Broberg et al., 2015). The reduction in biomass partitioning to the grain

under O_3 exposure has also been found to decrease the starch concentration and content of wheat grains (Fuhrer et al., 1990; Broberg et al., 2015; Tomer et al., 2015; Yadav et al., 2019a).

N remobilisation

Pre-anthesis N accumulation in upper plant parts is unaffected by increased O_3 concentrations (Brewster, Fenner and Hayes, 2024). However, after anthesis, due to the acceleration of senescence under O_3 exposure, remobilisation of N from vegetative parts to the grain is reduced (Broberg et al., 2017; Brewster, Fenner and Hayes, 2024; Chang-Espino et al., 2021). It is suggested that there is an additional process that impacts this remobilisation of N, as Brewster, Fenner and Hayes (2024) detected an increase in residual N in the flag leaf, with no change in the timing of senescence. This unknown process could be attributed to antioxidant production for defence against ROS which would reduce the N for remobilisation to the grains (Brewster, Fenner and Hayes, 2024; Sarkar and Agrawal, 2010; Yadav et al., 2019b).

Grain quality

Accelerated senescence activates earlier transfer of protein and micronutrients to the wheat grain (Shewry and Hey, 2015). However, there is a reduction in N remobilisation from the stem and leaves to the grain (Broberg et al., 2017; Brewster, Fenner and Hayes, 2024). Uptake of N from soil is maintained to a larger extent than biomass accumulation under O_3 exposure (Broberg et al., 2015). As a result, the concentration of N (gN gDM^{-1}) in wheat grains generally increases under O_3 exposure while the grain yield (gN m^{-2}) of the mineral decreases as a result of the reduced plant N and reduced N remobilisation to the grain (Broberg et al., 2015, 2020; Feng et al., 2008; Wang et al., 2017). Grain N is a key determiner of grain protein meaning that the concentration of grain protein generally increases under O_3 exposure, while the grain yield of protein decreases (Broberg et al., 2015). The protein quality is also affected under O_3 exposure, with Yadav et al. (2020) finding the concentrations of some AA increased under elevated O_3 while others decreased, which is linked to the plant antioxidant response (Ali et al., 2019).

1.3.2 Climate variables mechanisms

Heat stress, drought stress and increased CO_2 concentrations can impact many of the processes involved in the growth and development of crops. These three climate variables will co-occur under climate change which could offset or exacerbate plant responses. Wheat plants are considered drought stressed at a threshold of 50% relative soil moisture content, below which transpiration and photosynthetic rate and leaf water content rapidly decline (Wang et al., 2023b). Wheat is generally considered to be experiencing heat stress at temperatures > 30°C during the day, and > 20°C during the night, at which point the number of grains declines (Suryavanshi and Buttar, 2016; Stone and Nicolas, 1995; Corbellini et al., 1997; Saini, Sedgley and Aspinall, 1983).

Stomatal conductance

In wheat plants, the stomatal conductance generally decreases with high temperature and drought stress to prevent water loss (Balla et al., 2014, 2019; Shah and Paulsen, 2003). In plants exposed to a combination of heat and drought stress, stomatal conductance decreased to conserve water (Cohen et al., 2021). Increased CO_2 concentrations independently lead to a decreased stomatal conductance (Xu et al., 2016; Ainsworth and Rogers, 2007). When increased CO_2 concentrations co-occur with drought there is a greater decrease in stomatal conductance which leads to greater water conservation (Wall et al., 2006). For wheat grown at elevated CO_2 concentrations, the increase in stomatal conductance over the ~10-35 °C range

was reduced as temperature increased (Bunce, 2000). A summary of the direction of the effects of the climate variables on stomatal conductance as compared to no heat stress, no drought stress and ambient CO_2 is shown in Table 1.2.

Table 1.2: Summary of the combined effects of heat stress, water stress and increased CO_2 concentrations on stomatal conductance. The arrows indicate the direction of the effect.

	Heat stress	Water stress	Increased [CO_2]
Heat stress	↓ (Balla et al., 2014, 2019)	↓ (Cohen et al., 2021)	↓ (Bunce, 2000)
Water stress		↓ (Shah and Paulsen, 2003)	↓ (Wall et al., 2006)
Increased [CO_2]			↓ (Ainsworth and Rogers, 2007)

Photosynthesis

Independently, and in combination, drought and heat stress increase ROS accumulation, which degrades proteins and enzymes, such as Rubisco, located in the chloroplast (Farooq et al., 2011; Lal et al., 2022; Suryavanshi and Buttar, 2016; Rijal et al., 2020; Khanna-Chopra, 2012). Rubisco activase (RA) is the enzyme activating Rubisco, and Rubisco binding protein (RBP) is a protein that ensures Rubisco forms its correct 3D structure from the amino acid chain (Demirevska-Kepova et al., 2005). ROS reduce the activity of RA, leading to lesser Rubisco activity (Lal et al., 2022; Farooq et al., 2011; Demirevska-Kepova et al., 2005; Galmés et al., 2013). Further, the quantity of RBP is also decreased leading to reduced Rubisco activity (Demirevska-Kepova et al., 2005). The destruction of photosynthetic pigments by ROS, reduced electron transport efficiency and reduced Rubisco activity reduces the plant's photosynthetic rate (Rai and Agrawal, 2012; Khanna-Chopra, 2012). Under drought stress, the reduction in stomatal conductance also reduces photosynthetic rate (Bota, Medrano and Flexas, 2004). When drought and heat stress combine, there is a greater reduction to photosynthetic rate than occurs under the individual stressors (Shah and Paulsen, 2003).

Overall, under elevated CO_2, photosynthetic rate increases despite reductions to Rubisco and leaf N content, due to increased C for carboxylation and a reduction in photorespiration (Ainsworth and Rogers, 2007; Kang et al., 2021; Galmés et al., 2013; Tcherkez et al., 2020). Abdelhakim et al. (2021) found that spring wheat cultivars maintained a higher photosynthetic rate under heat stress with elevated CO_2 then they did under the ambient CO_2 treatment. When exposing spring wheat cultivars to an elevated CO_2 treatment and drought stress, the response of photosynthetic rate was mixed (Abdelhakim et al., 2021). A summary of the direction of the effects of the climate variables on photosynthetic rate as compared to no heat stress, no water stress and ambient CO_2 is shown in Table 1.3.

Table 1.3: Summary of the combined effects of heat stress, water stress and increased CO_2 concentrations on the rate of photosynthesis. The arrows indicate the direction of the effect.

	Heat stress	Water stress	Increased [CO_2]
Heat stress	↓ (Farooq et al., 2011)	↓ (Shah and Paulsen, 2003)	↑ (Abdelhakim et al., 2021)

Water stress		↓ (Rijal et al., 2020)	↑↓ (Abdelhakim et al., 2021)
Increased [CO_2]			↑ (Ainsworth and Rogers, 2007)

Plant senescence

Heat stress accelerates senescence onset in plants for several reasons: allocation of plant resources to defence reduces resources available for reproductive development, chlorophyll production is inhibited, and chloroplast components suffer oxidative damage (Farooq et al., 2011; Khanna-Chopra, 2012; Lal et al., 2022). ROS production is also stimulated by drought stress, leading to oxidative damage that accelerates senescence (Khanna-Chopra, 2012; Rijal et al., 2020). Under elevated CO_2, plant development is faster and therefore senescence onset occurs earlier compared to an ambient CO_2 treatment (Wall et al., 2006).

Under drought conditions, senescence onset occurs earlier when plants are also exposed to higher CO_2 concentrations (Wall et al., 2006). Drought stress accelerates the impact of high temperature stress on senescence (Shah and Paulsen, 2003). Although no studies have looked at the interaction of heat stress and increased CO_2 on senescence, based on the literature presented in Table 1.4 it appears most likely that there will be an increase.

Table 1.4: Summary of the combined effects of heat stress, water stress and increased CO_2 concentrations on senescence. The arrows indicate the direction of the effect.

	Heat stress	Water stress	Increased [CO_2]
Heat stress	↑ (Lal et al., 2022)	↑ (Shah and Paulsen, 2003)	↑ (no study to confirm)
Water stress		↑ (Rijal et al., 2020)	↑ (Wall et al., 2006)
Increased [CO_2]			↑ (Wall et al., 2006)

Grain DM (yield) and starch

Wheat yields are increased under elevated CO_2 through an increase in grain number (Piikki et al., 2008). Accelerated senescence under heat and and/or drought stress shortens the period for grain growth leading to reduced grain weight and yield (Lobell, Sibley and Ivan Ortiz-Monasterio, 2012; Broberg et al., 2015; Barutcular et al., 2016). Grain starch concentrations and content (gm^{-2}) were both increased under elevated CO_2 concentrations (Broberg, Högy and Pleijel, 2017). While under heat and/or drought stress, the content and concentration of starch in wheat grains were reduced (Barutcular et al., 2016). Elevated CO_2 concentrations under combined drought and heat stress were found to increase intercellular CO_2 concentrations and improve water-use-efficiency, suggesting a mitigating effect of elevated CO_2 concentrations with the combined stress (Abdelhakim et al., 2021). For a summary of these effects see Tables 1.5 and 1.6.

Grain quality

In their meta-analysis, Broberg, Högy, et al. (2017) found that elevated CO_2 concentrations reduced the grain protein concentration (gProtein gDM^{-1}) but increased the content (gProtein m^{-2}) in wheat. The protein concentration is reduced due to greater accumulation of starch, but also an additional negative impact of CO_2 on nitrate assimilation (Pleijel and Uddling, 2012; Bloom et al., 2010). Barutcular et al. (2016) found that under heat and/or drought stress, grain weight was affected more than protein allocation to the grain, leading to an

increase in grain protein concentration but a decrease in protein yield under the stressors. The combined effect of elevated CO_2 concentrations with heat stress tends to increase grain protein concentration, whereas the combined effect of elevated CO_2 with drought stress decreases both grain protein concentration and content (Zahra et al., 2023). Table 1.6 summarises the effect of environmental variables on wheat quality.

1.3.3 N mechanisms

N is taken up from the soil by wheat mainly in the form of nitrate ions (NO_3^-) (Harper et al., 1987). The NO_3^- ions are transported to the leaf where nitrate reduction reactions take place to form AA; used by the plant for metabolism and growth (Lawlor, 2002). N is stored in the leaves and stem in the form of AA, proteins or nucleic acids (Lawlor, 2002; Feller and Fischer, 1994). The AA stored in the leaves are critical for producing the proteins and enzymes involved in photosynthesis (Lawlor, 2002). If there is a soil N deficiency, then there are less AA in the leaves which impacts chloroplast structure and function and reduces Rubisco concentrations. As a result, photosynthetic rate is reduced (Lawlor, 2002).

After anthesis, the grain is the major sink for N and N remobilisation to the grains starts at senescence (Andersson, 2005; Kong et al., 2016). During leaf senescence, Rubisco and other proteins in the chloroplast are broken down to provide a key source of N for remobilisation to the grains (Feller and Fischer, 1994). Other vegetative plant parts, such as the stem, ear and root also store N which is available for grains, with the stem being a major source of grain N (Kong et al., 2016; Barraclough, Lopez-Bellido and Hawkesford, 2014). Depending on the variety of wheat, remobilisation efficiency of N from the leaves and stem can be up to 85% (Barraclough, Lopez-Bellido and Hawkesford, 2014). Another source of N for developing grains is post-anthesis soil N uptake, which is generally negatively correlated with leaf and stem N remobilisation, implying that for lower remobilisation of N from vegetative parts, more may be taken up from the soil post-anthesis to provide more for the grain (Gaju et al., 2014).

1.3.4 Combined effects of O_3, climate variables and N

The previous sections discussed how increased O_3 concentrations and climate change affect crop yields and quality. In areas where O_3 levels are rising, climate change could further reduce crop yields and quality. To develop a model for assessing these combined effects on crop yields and nutrition, it is essential to understand their combined effects. This section will explore the interactions between O_3, higher temperatures, drought stress, and elevated CO_2 on crop growth and N processes to comprehend their combined effects on crop quality (protein) and yields.

Soil N uptake

Elevated CO_2 and drought reduce plant N uptake from the soil (Broberg, Högy and Pleijel, 2017; Pleijel and Uddling, 2012; Rijal et al., 2020; Faisal et al., 2017). Current literature shows total uptake of N by wheat is unaffected by increased O_3 concentrations (Broberg et al., 2021; Brewster, Fenner and Hayes, 2024). Further, post-anthesis N uptake was not found to be affected by O_3, but plants receiving an extra N application post-anthesis experienced less damage from O_3 demonstrating an ameliorative effect of post-anthesis N application on O_3 damage (Brewster, Fenner and Hayes, 2024).

Stomatal conductance

The reduction in stomatal conductance under heat stress, drought stress, elevated CO_2 concentrations, or any combination of these, would potentially lead to a reduced stomatal

uptake of O_3, leading to a lesser impact of O_3 on yields (Balla et al., 2014; Cohen et al., 2021; Shah and Paulsen, 2003; Bunce, 2000; Wall et al., 2006; Ainsworth and Rogers, 2007; Yadav et al., 2019a). Additionally, soil N stress also decreases stomatal conductance and exacerbates the reduction in stomatal conductance under increased CO_2 concentrations (Li, Kang and Zhang, 2004). Therefore, the changing climate may offer some protective benefits to plants against increased O_3.

Photosynthesis

Yadav et al. (2019) found that under a combined elevated CO_2 and O_3 treatment the photosynthetic rate was similar to the ambient treatment, suggesting a potential offsetting effect of CO_2 on O_3 induced reductions in photosynthetic rate. Broberg et al. (2023) investigated how O_3, drought stress and heat stress interact to affect photosynthetic rate. The authors found that under ambient O_3, photosynthetic rate was higher in the well-watered and ambient treatments, compared to the dry and elevated temperature treatments. However, under elevated O_3 the pattern was reversed, and photosynthetic rates were higher in the dry and elevated temperature treatments (Broberg et al., 2023). Therefore, the negative effect of O_3 on photosynthetic rate is likely to be reduced under increased CO_2, increased temperatures and increased water stress (Broberg et al., 2023; Yadav et al., 2019a).

Plant senescence

Drought, heat stress and increased O_3 concentrations increase ROS accumulation leading to an acceleration of plant senescence (Farooq et al., 2011; Lal et al., 2022; Rijal et al., 2020; Suryavanshi and Buttar, 2016; Emberson et al., 2018; Khanna-Chopra, 2012). The acceleration of senescence under O_3 could be partially offset by increased CO_2 through reduced stomatal conductance (Ewert and Pleijel, 1999). However, some studies have shown an acceleration of flag leaf senescence in wheat under elevated CO_2, due to photosynthetic acclimation to the higher gas concentration (McKee, Bullimore and Long, 1997; Nie et al., 1995; Zhu et al., 2012, 2009). Therefore, the direction of the effect of elevated CO_2 on senescence and whether it will reduce O_3 effects on senescence is unclear.

A higher leaf N can slow down the rate of senescence, and so could potentially reduce O_3 effects on accelerating senescence (Lawlor, 2002). Brewster, Fenner and Hayes (2024) found slight differences in senescence under O_3 exposure for plants that received an extra N treatment at anthesis. The plants that received the extra treatment had slightly delayed senescence in the flag, 2nd and 3rd leaves, suggesting that N application at anthesis can reduce the negative effect of O_3 on plant senescence (Brewster, Fenner and Hayes, 2024).

Grain DM

O_3 reduces wheat yields by reducing 1000 grain weight (Piikki et al., 2008). Whereas elevated CO_2 concentrations increase wheat yields by increasing the number of grains per metre squared of ground (Piikki et al., 2008; Broberg et al., 2019). As a result, increased CO_2 could offset O_3 effects on yield (Yadav et al., 2019a; Piikki et al., 2008). However, increased CO_2 concentrations will likely co-occur with drought and heat stress which both have the potential to decrease yields even further than when considering O_3 stress alone (Nguyen et al., 2024; Tai and Martin, 2017; Xu et al., 2007). In contrast, Broberg et al. (2023) found that drought stress reduces O_3 induced yield losses. Broberg et al.'s (2023) study aimed to mimic conditions where O_3 is elevated for several days before rainfall reduces the pollutant concentration. Therefore, drought stress can offset some O_3 induced reductions in yield if the two stressors co-occur to allow for the reduction in stomatal conductance under drought stress to reduce O_3 uptake (Broberg et al.,

2023). One study assessed the combined effect of elevated CO_2, temperature and O_3 concentrations on wheat yields, finding that yields were significantly reduced in this combined treatment compared to present day conditions (Naaz et al., 2022). Therefore, overall, the interaction between O_3, increased CO_2 concentrations, increased temperatures and drought stress is likely to reduce wheat yields.

Broberg et al. (2017) found that under increased O_3 pollution the grain yield produced for a given quantity of applied N decreases, hence O_3 reduces fertiliser efficiency. The reduction in fertiliser efficiency could be attributed to reduced photosynthesis, reduced grain filling period, lesser plant growth and a smaller root: shoot ratio under O_3 exposure (Broberg et al., 2017). The individual effects of climate variables and O_3 on grain yield parameters are shown in Table 1.5.

Table 1.5: Environmental variables and their influence on wheat yield quantity parameters. The arrow indicates whether there is an increase or decrease in the yield variable under the environmental condition. For the columns where the effect of the environmental condition on the yield parameter was unclear see the text for a discussion of the literature.

	Thousand grain weight		Grain yield (g m^{-2})		Grain size		Grain number	
Heat stress	↓	(Mariem et al., 2021)	↓	(Mariem et al., 2021)	↓	(Farooq et al., 2011)	↓	(Farooq et al., 2011)
Water stress	↓	(Mariem et al., 2021)	↓	(Mariem et al., 2021)	Unclear		↓	(Mariem et al., 2021)
Increased O_3	↓	(Broberg et al., 2015)	↓	(Broberg et al., 2015)	↓	(Piikki et al., 2008)	↓	(Broberg et al., 2015)
Increased CO_2	↑	(Broberg et al., 2019)	↑	(Broberg et al., 2019)	Unclear		↑	(Broberg et al., 2019)

Grain quality

Currently, only one experimental study has looked at the interaction of O_3 with drought and heat stress on wheat grain quality. This study, by Broberg et al. (2023), did not find a significant interaction between O_3 and either drought or heat stress on grain N concentrations (gN gDM^{-1}) or yield (gN m^{-2}). Despite the lack of significant interactions, plants exposed to elevated O_3, increased temperatures and drought stress experienced increased grain N concentration (gN gDM^{-1}) and decreased grain N yield (gN m^{-2}) compared with those in ambient O_3 and temperature, and well-watered treatments (Broberg et al., 2023). The decrease in protein concentration of wheat grains under higher CO_2 cannot be offset by increased O_3 as in addition to the dilution effect, elevated CO_2 impairs nitrate assimilation (Bloom, 2015). Protein and starch concentrations were not significantly different under a combined elevated CO_2 and O_3 as compared to an ambient treatment (Yadav et al., 2019a). Table 1.6 summarises the effects of climate variables and O_3 on wheat quality parameters.

Table 1.6: Environmental variables and their influence on wheat quality parameters. The arrow indicates whether there is an increase or a decrease in the quality variable as a result of the environmental condition.

	Grain starch concentration	Grain protein or N concentration (gProtein gDM^{-1})	Grain protein or N content (gProtein m^{-2})

Heat stress	↓	(Mariem et al., 2021)	↑	(Mariem et al., 2021; Broberg et al., 2023)	↓	(Broberg et al., 2023)
Water stress	↓	(Mariem et al., 2021)	↑	(Mariem et al., 2021; Broberg et al., 2023)	↓	(Broberg et al., 2023)
Increased O_3	↓	(Broberg et al., 2015)	↑	(Broberg et al., 2015, 2023)	↓	(Broberg et al., 2015, 2023)
Increased CO_2	↑	(Mariem et al., 2021)	↓	(Broberg, Högy and Pleijel, 2017)	↑	(Broberg, Högy and Pleijel, 2017)

This section explored the mechanisms by which O_3 and climate change variables interact to affect wheat yields and quality. The key mechanisms affected by O_3 were antioxidant defence, photosynthesis, senescence and N remobilisation, which affect biomass, yields and quality. Additionally, climate variables have the potential to modify O_3 effects on yield and quality through alterations to stomatal conductance, photosynthesis and senescence. For modelling the effects of O_3 and climate change, the inclusion of these processes will provide valuable detail of realistic plant response to stressors. This means the models would be suitable for risk assessment or assessing potential strategies for mitigating yield and nutrition losses. In Section 1.5, the O_3 damage processes included in various crop models will be discussed, while Section 1.6 will explain the specific climate and O_3 mechanisms that are used in the DO_3SE-Crop model, which is the model used throughout this thesis.

1.4 Risk assessment methods

To date, various methods have been used to understand the effects of O_3 on crop yields and protein. To develop a modelling method that can be used to assess O_3 and climate effects on crop yield as well as quality, the merits and limitations of current methods need to be understood. The terms “risk” and “impact” assessment have both been used in the literature to describe the methods by which O_3 and/or climate change effects on crops have been studied (e.g. Emberson (2020), Van Dingenen et al. (2009), Archibald et al. (2020b), Pleijel, Danielsson and Broberg (2022), Nguyen et al. (2024), Tai et al. (2021) and Hoshika et al. (2020)). Usually, risk assessments refer to estimated future environmental impacts of a stressor, while impact assessments refer estimates of current environmental impacts (Challinor et al., 2018; Van Dingenen et al., 2009). The climate change field tends to use impact assessment to describe historic and present day estimated impacts of stressors, while the term risk assessment is used to describe future events which are subject to uncertainty (Challinor et al., 2018). A similar distinction in these terms is not found the O_3 community where risk assessment and impact assessment are used interchangeably. A similar confusion of terms was discussed by Sillmann et al. (2021) in relation to understanding pollution effects on health and agriculture, noting that “risk” assessments should include some aspect of probability or frequency of the impact which is not currently included in what are described as risk assessment studies within the O_3 community. To be consistent with the O_3 community academic literature we use the term risk assessment for any current or future assessment of O_3 effects on crops under for a single situation or scenario. However, it is acknowledged that a true risk assessment should include some aspect probability or uncertainty related to the likely frequency of the occurrence of events that will cause damage. Currently O_3 concentration exposure-response relationships,

flux-based exposure-response relationships and crop models have been used to perform risk assessments of O_3 damage to wheat. Both the exposure-response and flux-based response relationships are informed by experimental data to define their regressions with yield, biomass or visible crop damage under O_3 exposure (Emberson, 2020). Whereas crop models are calibrated based on experimental data before being applied across a country or region of interest (Nguyen et al., 2024; Pande et al., 2024a). This section will discuss concentration and flux-based exposure-response relationships, while crop models will be explored in section 1.5.

Concentration and flux-based exposure-response methods require metrics by which to characterise the O_3 concentrations. The commonly used metrics to assess O_3 damage to crops are M7 (or M12), AOT40 and POD_Y. M7 (or M12) and AOT40 are metrics based on O_3 concentrations. M7 (or M12) is the daily, 7 hour (or 12 hour), mean O_3 concentration during daylight hours and AOT40 is the O_3 accumulated during daylight hours over a threshold concentration of 40 ppb (Fischer, 2019; Guarin et al., 2019a). POD_Y is a flux-based metric; it stands for phytotoxic O_3 dose above a threshold *Y* nmol m^2 PLA s^{-1}. *Y* represents the threshold stomatal flux of O_3, below which the damaging effects of the pollutant are counteracted by antioxidants, and PLA stands for projected leaf area (Mills et al., 2011). POD_Y and AOT40 metrics are often used in combination with a "critical level", where critical level refers to the threshold of the metric above which adverse effects on crops are expected to occur (CLRTAP, 2017).

In the following sections, concentration- and flux-based risk assessment methods are reviewed to support the development of a more robust approach that addresses the limitations of current methods.

1.4.1 Concentration-response

Concentration-response relationships have been derived for crop O_3 risk assessments by regressing O_3 concentration metrics (e.g. M7 or AOT40) with a response metric (such as yield, biomass or visible damage) (Emberson, 2020). A criticism of M7 is that using a mean O_3 concentration averages out peak O_3 events that can overwhelm the plants ability to produce antioxidants and counteract O_3 damage (Emberson et al., 2018; Guarin et al., 2019a). A criticism of the concentration-based M7 and AOT40 approaches is that they fail to account for the mechanistic processes that can support a plants ability to avoid or recover from O_3 damage, or detoxify ROS, and prevent some O_3 damage (Emberson et al., 2018; Tai et al., 2021). Further, the concentration-based approaches do not consider how the impacts of O_3 will interact with environmental factors, such as heat and water availability which could affect stomatal uptake of the pollutant (Tai et al., 2021). In fact, Emberson et al. (2000) found that areas which had the highest AOT40 metric for beech and wheat across Europe, did not always overlap with those which had the greatest O_3 fluxes.

1.4.2 Flux-response

The POD_Y metric accounts for the plants ability to detoxify some O_3 uptake and is calculated using stomatal fluxes which take into consideration vapour pressure deficit, soil water potential, light, and temperature. This means the POD_Y metric incorporates the interaction between O_3 and the environment (Mills et al., 2011). One drawback is that hourly meteorological data are required to calculate the stomatal conductance and hence O_3 uptake (Emberson, 2020). It has been suggested that the POD_Y approach does not give realistic yield loss estimates for wheat in India (Fischer, 2019). Fischer (2019) discusses that the POD_Y method gives lower estimates for O_3 induced yield losses in India than estimates based on AOT40 or M7. Since the POD_Y dose-

response relationships were based on European relationships, Fischer (2019) suggests the discrepancy in yield predictions would imply Indian wheat has a lower stomatal conductance than European wheat - a statement also made in the paper that the data came from (Mills et al., 2018b). However, Fischer (2019) also highlights that experimental data on stomatal conductance of Indian and European wheat does not support this statement. It could be that the environmental conditions Indian wheat is grown in lead it to have a lower stomatal conductance. Nevertheless, even with this discrepancy, flux-based exposure response relationships have been shown to have a stronger statistical relationship with the response metric than concentration-based approaches (Emberson, 2020).

1.5 Usage of crop models for assessing O_3 and climate stress

Crop models can also be used to assess O_3 damage to crops. These models mechanistically simulate crop growth from sowing to harvest by using a series of equations to describe the growth processes occurring inside the plant (Chenu et al., 2017). They offer the flexibility to adjust the underlying code and hence modify the processes simulated. Due to their flexibility, crop models can simulate the effects of multiple stressors simultaneously. In this section, the current modelling methods used to simulate O_3 effects on crops, and the modifying effects of temperature, water and CO_2, are introduced to provide a foundation for the more detailed discussion of the specific model used in the present thesis in section 1.6.

Process-based crop models use meteorological inputs such as temperature, rainfall, soil water, radiation, and CO_2 concentrations to simulate biomass production and crop growth under differing environmental conditions, making them suitable for simulating wheat yields under a changing climate. Some of these models also include algorithms to describe the effects of high temperatures or drought stress, allowing them to account for more extreme events resulting from climate change. Crop models that incorporate O_3 effects are listed in Table 1.7 and their modelling approaches to O_3 and climate, along with their applications are discussed below.

1.5.1 Modelling O_3 effects on yields

Different models consider O_3 effects on yields through various metrics. Most crop models consider O_3 as having a short-term impact reducing photosynthesis and long-term impact accelerating senescence (Table 1.7). For the models that simulate the short- and long-term O_3 effects, several (LINTULCC2, WOFOST, DO_3SE-Crop, MCWLA) base their approach on Ewert and Porter (2000) who use accumulated stomatal O_3 flux as their O_3 measure. LPJml also use the stomatal O_3 flux approach, but they developed their own equations to describe the short- and long-term impacts of O_3. TEMIR, DLEM-Ag, GLAM-ROC and CLM5.0 only consider the short-term impacts of O_3, with CLM5.0 including two O_3 factors to modify stomatal conductance and photosynthetic rate separately while TEMIR and DLEM-Ag just influence photosynthesis. There are some crop models that use concentration-based metrics in their formulations. GLAM-ROC is a transpiration-based crop model and considers the O_3 impact on daily transpiration through the AOT40 metric. Whereas DSSAT's equations use the M7 metric to calculate O_3 effects on photosynthesis and senescence. APSIM takes a different approach to modelling O_3 effects where only the resulting impact on yield is considered using AOT40 as a metric.

It is well understood that O_3 reduces photosynthesis, as well as accelerating senescence in crops (Emberson et al., 2018). Therefore, crop models that incorporate both short- and long-term O_3 effects provide a better representation of plant response to O_3. Additionally, as discussed in section 1.4, M7 and AOT40 approaches are limited as they are calculated from

external O_3 concentrations and are not directly related to the plant's physiology. The stomatal flux-based approach, which considers environmental factors impacting the plant's growth, provides a more representative view of how the plant takes up and interacts with O_3, but is unable to directly relate these mechanisms to variations in plant growth that are ultimately determined by C assimilation.

1.5.2 Modelling the interaction of O_3 and climate effects

Most models consider crop development to occur as an accumulation of thermal time. This means that the effect of increasing temperatures is accounted for through accelerated development as the crop proceeds towards its optimum temperature, and reduced development when temperatures approach, or exceed, the maximum or minimum for growth. Additionally, crop models require radiation inputs to provide an estimate of photosynthate or biomass production which could affect O_3 impacted photosynthetic rates or biomass production in the modelling process.

For the crop models that consider the flux-based approach to simulating the effects of O_3, calculation of stomatal conductance is key. As discussed in Section 1.3, stomatal conductance is affected by environmental conditions such as temperature, CO_2 concentrations and drought (Balla et al., 2014, 2019; Shah and Paulsen, 2003; Ainsworth and Rogers, 2007). DO_3SE-Crop, LINTULCC2, WOFOST, LPJml, TEMIR and MCWLA all include processes to reduce the stomatal conductance under increased CO_2 concentrations and soil water stress which subsequently limits O_3 uptake. A reduction in stomatal conductance then reduces photosynthesis due to the reduced CO_2 uptake. Photosynthesis can also be modified directly to include environmental effects, with MCWLA including a factor accounting for the reduction of photosynthesis under elevated temperatures. DSSAT also includes a high temperatures stress factor, though it is used to accelerate senescence. Similarly, GLAM-ROC accelerates senescence under drought stress. However, at present models do not include the effect of heat stress, water stress and increased CO_2 concentrations in combination on both stomatal conductance and photosynthesis.

Incorporating the effects of CO_2, water stress and increased temperatures in O_3 simulations is key as there are interaction effects that can reduce or exacerbate O_3 damages. The most important effect to consider, as shown by the inclusion in most models, is the impact of the environmental variables on stomatal conductance, which affects the amount of O_3 that is taken up and can go on to cause damage. Changes in stomatal conductance also impact photosynthesis through alterations to CO_2 uptake. The effect of temperature is generally incorporated into models through accumulated thermal time which influences crop development, though some models do incorporate high temperature stress factors to incorporate additional crop damage due to heat shock. The effect of heat stress, water stress and elevated CO_2 concentrations on senescence is not generally incorporated. For models that consider O_3 damage, they only model the effect of O_3 on the rate of senescence, though water, heat stress and elevated CO_2 concentrations all accelerate senescence (Section 1.3, Lal et al., 2022; Shah and Paulsen, 2003; Rijal et al., 2020; Wall et al., 2006). The effects of water, heat and O_3 stress, and increased CO_2 concentrations on grain DM are incorporated implicitly in some models via the effects of these stressors on stomatal conductance and photosynthetic rate which subsequently effects total assimilation. Since some models do not incorporate all of these stressors, or incorporate a selection (Table 1.7), whether the grain DM is affected depends on which stressors were included in the model.

It is not as common to model both crop yield, and grain quality. Commonly N is considered a measure of grain quality in crop modelling as it is the main determiner of protein. Of the models listed in Table 1.7, only DSSAT-NWheat and APSIM model plant N. However, they do not incorporate the effect that O_3 has on plant N remobilisation. Any effects of O_3 or climate variables on grain N would occur implicitly through the effects on biomass and hence nutrient accumulation. Few crop models consider grain quality through a different lens than that of grain N. Liu et al. (2019) modified the CERES-Wheat model to simulate wheat AA concentrations by creating regressions between grain protein and grain AA concentrations. Their model considers the effects of water stress on grain quality as well as photosynthesis, hence biomass accumulation is also affected by the stressor (Liu et al., 2019b). Additionally, SiriusQuality considers the fraction of N that is split between the different proteins in wheat relevant for bread production, considering the effects of water and heat stress on biomass accumulation only (Martre et al., 2006). However, neither model considers the effect of O_3 on grain quality. O_3 and its interaction with heat and water stress, and elevated CO_2 concentrations has been neglected in crop modelling to-date, but as shown in Section 1.3, these interactions will affect grain yield and quality and hence are important considerations for modellers.

Table 1.7: Summary of models that have been, or are currently, in use for simulating O_3 effects on wheat, along with the locations they have been applied. Models indicated with an asterisk (*) are involved in the AgMIP- O_3 project, and will be used for simulating O_3 effects on wheat yields for China, India, Sweden and Wales (Emberson et al., in prep.). *Unfortunately for MATCRO detailed model information is currently unavailable.*

Model Name	Simulates O_3 effects by using…	O_3 impact		Locations applied	Other effects considered	Citations
		Short-term	Long-term			
DO_3SE-Crop*	Stomatal flux	Y	Y	Europe China	Drought -	(Nguyen et al., 2024) (Pande et al., 2024a)
DSSAT-NWheat*	Concentration	Y	Y	Mexico Globally	Temperature, rainfall, CO_2 -	(Guarin et al., 2019a) (Guarin et al., 2024)
WOFOST-O3*	Stomatal flux	Y	Y	Europe	Drought	(Nguyen et al., 2024)
LINTULCC2*	Stomatal flux	Y	Y	Europe	Drought	(Nguyen et al., 2024)
LPJml	Stomatal flux	Y	Y	Globally	Temperature, water	(Schauberger et al., 2019)
MCWLA*	Stomatal flux	Y	Y	China	Temperature, rainfall, CO_2, radiation	(Tao et al., 2017)
TEMIR*	Stomatal flux	Y	N	Globally	CO_2	(Tai et al., 2021)
DLEM-Ag*	Concentration	Y	N	China	Drought	(Tian et al., 2015; Ren et al., 2007)
CLM5.0*	Stomatal flux	Y	N	-	-	(Zhou et al., 2018)
GLAM-ROC	Concentration	Y	N	India	-	(Droutsas, 2020)

APSIM*	Concentration	N	N	China	Temperature, rainfall, CO_2, radiation	(Xu et al., 2023)
MATCRO*	-	-	-	-	-	-

1.5.3 Applications

Several of the listed models have been used to simulate the effects of O_3, in combination with other abiotic stressors, on wheat in locations around the world (Table 1.7), which helps to understand the magnitude of yield losses and vulnerability of different regions to O_3 pollution and climate change. Crop models can also be used to test different management strategies such as irrigation and fertilisation regimes, sowing of different cultivars, altered sowing dates and planting density (Soltani and Hoogenboom, 2007; Cavero et al., 1998; Pathak et al., 2003). As such, the models listed in Table 1.7 have the capacity to investigate management options, that could also consider strategies for improving crop tolerance to O_3. Further, in the past crop models have been integrated with economic models to calculate the financial losses due to crop reduction under climate change (e.g. Rosenzweig et al. (2018)). Given the models in Table 1.7 can simulate yield reductions under O_3 and climate change, they could also be combined with economic models to understand the financial effects of O_3 pollution.

1.6 The DO_3SE-Crop model

In the following section, the DO_3SE-Crop model, used throughout this thesis, is introduced. The first section will introduce the reader to the model by giving a general overview, before going into the detail of phenology, photosynthesis and stomatal conductance, O_3 flux and damage, and biomass partitioning.

1.6.1 Model overview

The DO_3SE-Crop model is an integrated photosynthetic-stomatal conductance crop model calculating the effect of O_3 deposition on photosynthesis, stomatal conductance, senescence and crop yield. An overview of DO_3SE-Crop is given in Figure 1.8 and will be described in the subsequent text. At a minimum, the model takes hourly inputs of radiation, O_3 concentrations, temperature, wind speed, relative humidity, air pressure, precipitation, and soil water. CO_2 concentrations can be specified as an input parameter or as a constant in the model configuration file. To run the DO_3SE-Crop model, the hourly meteorological data specified above are required, along with a configuration file specifying the crop-specific and site parameters for the crop type/cultivar being simulated. Generally, the parameters for the configuration file come from the model calibration. For further details of processes and equations involved in the simulations, please refer to Pande et al. (2024a).

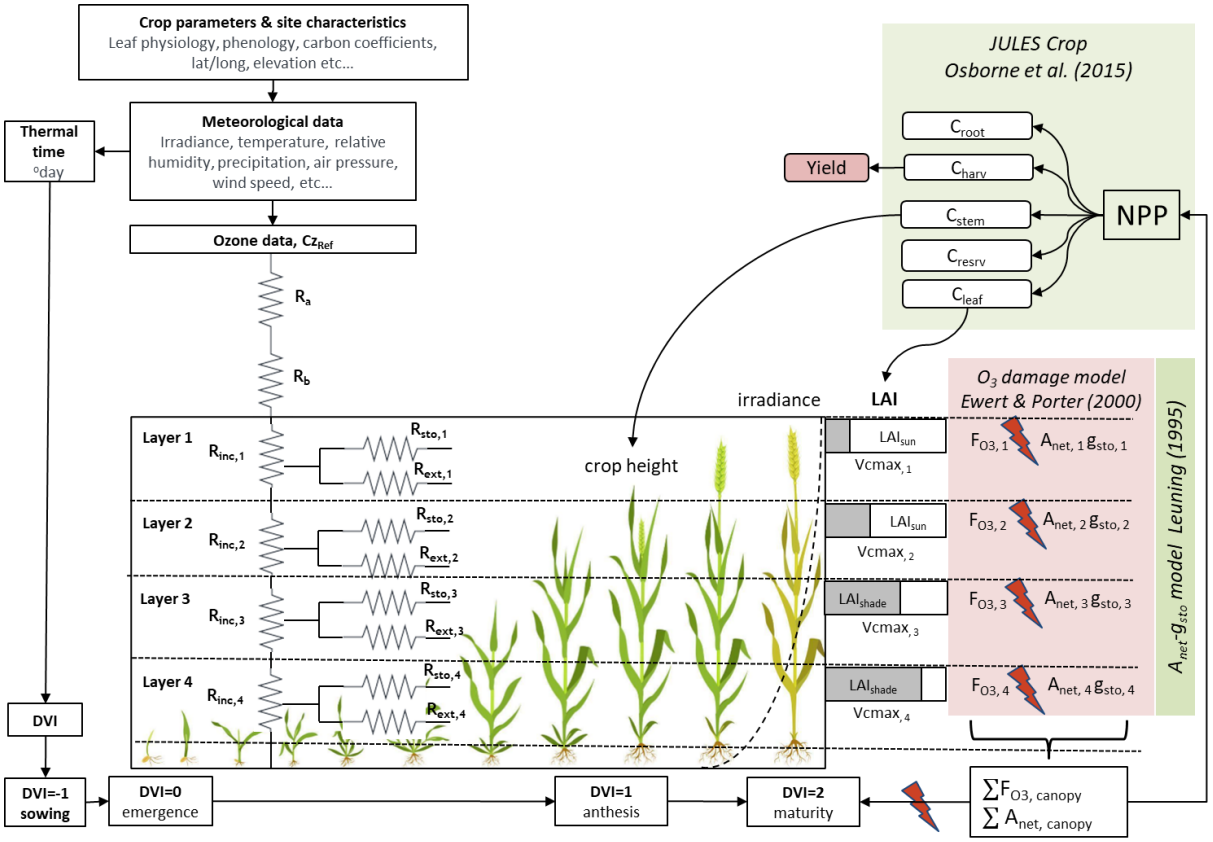

Figure 1.8: The DO₃SE-Crop model as illustrated by Pande et al. (2024a).

1.6.2 Phenology

Phenology in DO$_3$SE-Crop is calculated through an accumulation of effective thermal time T_{eff}, controlled by 3 parameters. T_b is the base temperature for crop growth below which growth does not occur, T_o is the optimum temperature for crop growth at which point growth is a maximum, and T_m is the maximum temperature above which crop growth does not occur. Below T_b, and above T_m, the accumulation of T_{eff} is 0. At temperatures between T_b, and T_m, accumulation of T_{eff} occurs and is a maximum at T_o (Pande et al., 2024a).

The accumulation of effective temperature is used to determine when the key developmental stages occur. The 3 key stages in DO$_3$SE-Crop are: sowing to emergence (-1 < DVI < 0 in Figure 1.8), emergence to start of grain filling (0 < DVI < 1 in Figure 1.8), and the start of grain filling to maturity (1 < DVI < 2 in Figure 1.8), where DVI represents the development index of the crop (Pande et al., 2024a; Osborne et al., 2015).

1.6.3 Coupled photosynthetic-stomatal conductance framework

In DO$_3$SE-Crop there are 3 limiting factors to the rate of photosynthesis based on the work of Sharkey et al. (2007), Farquhar, Caemmerer and Berry (1980) and Medlyn et al. (2002). The limiting factors are: Rubisco activity, ribulose-1,5-bisphosphate (RuBP) regeneration constrained by the speed of electron transport, and the rate of transfer of photosynthetic products (Pande et al., 2024a). The rate of photosynthesis is calculated according to each of the limiting factors, and the lowest rate of photosynthesis is used (Pande et al., 2024a). To calculate the net rate of photosynthesis, the dark respiration is subtracted from the most limiting photosynthetic rate (Pande et al., 2024a). The net rate of photosynthesis is then used in the coupled photosynthetic stomatal conductance framework based on work by Leuning (1995) to

calculate the stomatal conductance to CO_2, from which the stomatal conductance to O_3 can be determined (Pande et al., 2024a).

1.6.4 O_3 flux estimates using multi-layer resistance scheme

Once the stomatal conductance to O_3 has been calculated, it is possible to calculate the flux of O_3 taken up by a leaf per canopy layer (Pande et al., 2024a). To do this, the O_3 concentration for each layer is calculated using the resistance scheme illustrated in Figure 1.8. The resistances to O_3 uptake include: stomatal resistance, leaf boundary layer resistance, and non-stomatal leaf surface resistance. From these resistances, and a defined uniform O_3 concentration at the top and bottom of the canopy, a matrix of equations can be formed to solve for the concentration of O_3 per layer (Waggoner, 1971; Pande et al., 2024a). Once the concentration of O_3 per layer has been calculated, the O_3 flux per layer is obtained through combining the concentration, conductance to O_3 and O_3 resistances. O_3 flux is greater for leaves at the top of the canopy. The top leaves receive the most photosynthetically active radiation due to having the greatest LAI in the sun, and therefore have the highest stomatal conductance to O_3 (see Figure 1.8 and Pande et al. (2024)).

1.6.5 O_3 damage module

The O_3 damage module is based on the work of Ewert and Porter (2000), and modified by Pande et al. (2024). There are short-term and long-term components to O_3 damage that are included in the module.

The short-term damage component considers the instantaneous effect that O_3 has on reducing the Rubisco limited rate of photosynthesis. The reduction in the Rubisco limited rate of photosynthesis occurs when the O_3 flux exceeds the capacity at which the plant can detoxify damaging O_3 species. In DO_3SE-Crop, the leaves recover from O_3 damage overnight. However, as the leaf ages, its capacity to recover from O_3 damage decreases. Therefore, the reduction in the Rubisco limited rate of photosynthesis is greater as the leaf ages (Pande et al., 2024a).

The long-term damage component considers the effect that O_3 has on degrading Rubisco, and hence accelerating the onset and rate of senescence (Gelang et al., 2000; Osborne et al., 2019). Senescence begins to occur once a defined critical O_3 flux is exceeded. Coefficients describing the sensitivity of the cultivar to this threshold, and specifying the onset and end of senescence are also defined (Pande et al., 2024a).

1.6.6 Scaling up: biomass partitioning at the crop level

The O_3 fluxes and their effects on stomatal conductance, photosynthesis and senescence are simulated at the leaf level. To scale things up to the crop level the net rate of photosynthesis per layer is summed, taking into consideration the different rates of photosynthesis for sunlit and shaded leaves, to achieve the net canopy photosynthesis. Once dark, maintenance and growth respiration have been subtracted from the net photosynthesis, the net primary productivity (NPP) is obtained (Pande et al., 2024a). The NPP is partitioned between the roots, leaves, stems and grain depending on the partition coefficients defined by Osborne et al. (2015). The partition coefficients for the root are greatest at the beginning of the growing season, whereas the coefficients for the grain is greatest after anthesis, reflecting the needs of the plant at the time (Osborne et al., 2015).

Equations relating leaf and stem C to LAI and stem height respectively are included in the model (Pande et al., 2024a; Osborne et al., 2015). Once the fraction of dry weight that is C, and grain

moisture content have been taken into consideration, the crop yield is calculated from the grain C (Osborne et al., 2015).

1.6.7 Linking back to O_3 and climate variables mechanisms of damage

In Section 1.3 the mechanisms by which heat, water and O_3 stress and increased CO2 concentrations affect stomatal conductance, photosynthesis, senescence, biomass accumulation, grain DM and quality were discussed. Here we link these mechanisms to how temperature, water availability, O_3 and CO_2 influence simulations in DO_3SE-Crop to identify areas which are not covered.

Stomatal conductance is a function of vapour pressure deficit (VPD) which incorporates the effects of temperature and humidity into the conductance equation. It is also a function of the surface CO_2 concentration which incorporates the effect of increased CO_2 concentrations in a changing climate into stomatal conductance calculations. While the effect of O_3 on stomatal conductance is not modelled explicitly, the coupled nature of the stomatal-conductance-photosynthesis framework in DO_3SE-Crop means that the instantaneous effect of O_3 on reducing photosynthesis does feedback into the calculation of stomatal conductance. Additionally, plant available water is incorporated into the calculation of photosynthetic rate, allowing the effect of water stress on photosynthesis to be integrated. This means that temperature, water and O_3 stress and elevated CO_2 effects are incorporated into the photosynthesis calculations (Pande et al., 2024a).

When it comes to senescence, higher temperatures accelerate the rate of crop development (provided the temperature is below the maximum) which means that senescence onset can be reached earlier in the crop development. However, there is no explicit effect of high temperature stress on accelerating senescence. Similarly, there is no mechanism currently for the effect of water stress or increased CO_2 concentrations on senescence onset or rate. The only stressor explicitly modelled to affect senescence is O_3 (Pande et al., 2024a).

Grain DM is affected by any stressors that affect photosynthesis, as photosynthesis determines biomass accumulation in DO_3SE-Crop. Additionally, if senescence is accelerated then there is less time for remobilisation of DM from the leaf and stem to the grains. This means that in DO_3SE-Crop grain DM is affected by higher temperatures, CO_2 concentrations, water and O_3 stress.

Currently, DO_3SE-Crop does not simulate any metric of grain quality. In the present thesis, the DO_3SE-Crop model will be extended to incorporate the effect of O_3 on leaf and stem N, and hence grain N. Since N is the main component of protein, which is very important nutritionally, the effect of O_3 on the nutritional quality of what can be understood.

In summary, the DO_3SE-Crop model is an integrated photosynthetic-stomatal conductance crop model designed to calculate the effects of O_3 deposition on photosynthesis, stomatal conductance, senescence, and crop yields. Climate effects are included through via the inputs, such as radiation, which affects photosynthesis, temperature effects on phenology, and wind speed and humidity effects on stomatal conductance which influence O_3 uptake.

1.7 Vulnerability of India

In this thesis, two papers focus on India due to its vulnerability to O_3 pollution and climate change which will exacerbate existing malnutrition in the country. The following section provides an overview of these challenges to food security.

1.7.1 Food and nutrition security

Wheat is a staple food source in India, and wheat production is a key contributor to gross domestic product (GDP) and the country's exports (Khatkar, Chaudhary and Dangi, 2015; Tripathi and Mishra, 2017). Production and yield of wheat in India has increased dramatically since 1950 with northern states dominant in producing the cereal (Figure 1.9 and Ministry of Agriculture & Farmers Welfare (2023)). However, as a result of increased production, there are concerns about soil productivity and water resources, pollution and loss of crop diversity, which increases the vulnerability of agriculture to abiotic stresses (Somvanshi, Pandiaraj and Singh, 2020; Chhetri and Chaudhary, 2011). Further, the diversity of wheat varieties has also decreased which will have negative consequences on the adaptation ability of agriculture (Somvanshi, Pandiaraj and Singh, 2020; Chhetri and Chaudhary, 2011). During the green revolution, the production of wheat increased by 97% from 1969 to 1989, which reduced hunger from a caloric perspective (Somvanshi, Pandiaraj and Singh, 2020). However, the production of micronutrient-dense pulses and coarse cereals decreased (Somvanshi, Pandiaraj and Singh, 2020; Pandiyan, Barbhai and Medithi, 2019). The policies that aimed to increase production of cereals to improve hunger, caused a trade-off with dietary diversity (Pandiyan, Barbhai and Medithi, 2019; Pingali, Mittra and Rahman, 2017).

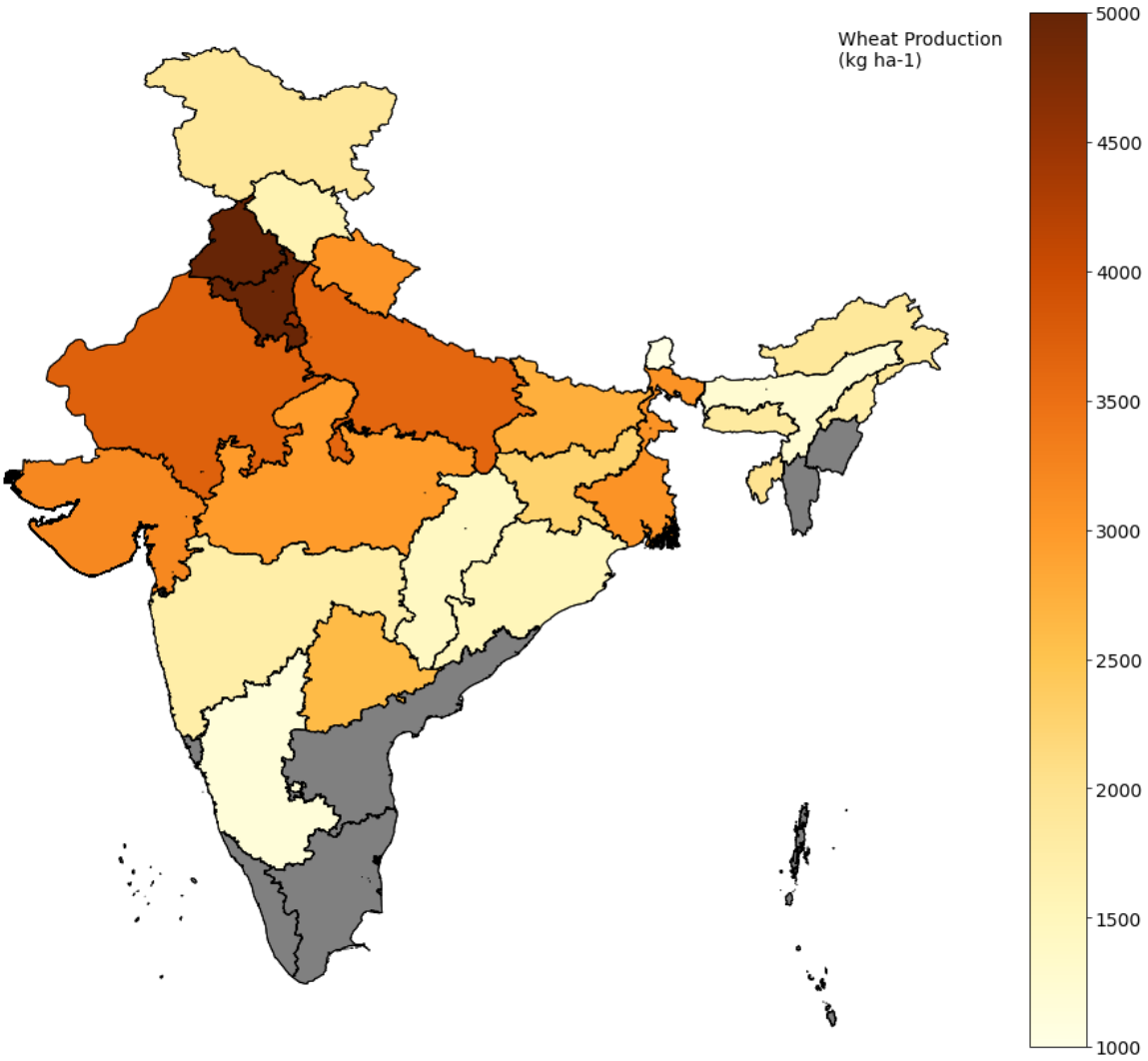

Figure 1.9: Map of India wheat production in kilograms per hectare, compiled using data from Ministry of Agriculture & Farmers Welfare (2023). States in grey indicate locations for which data were missing.

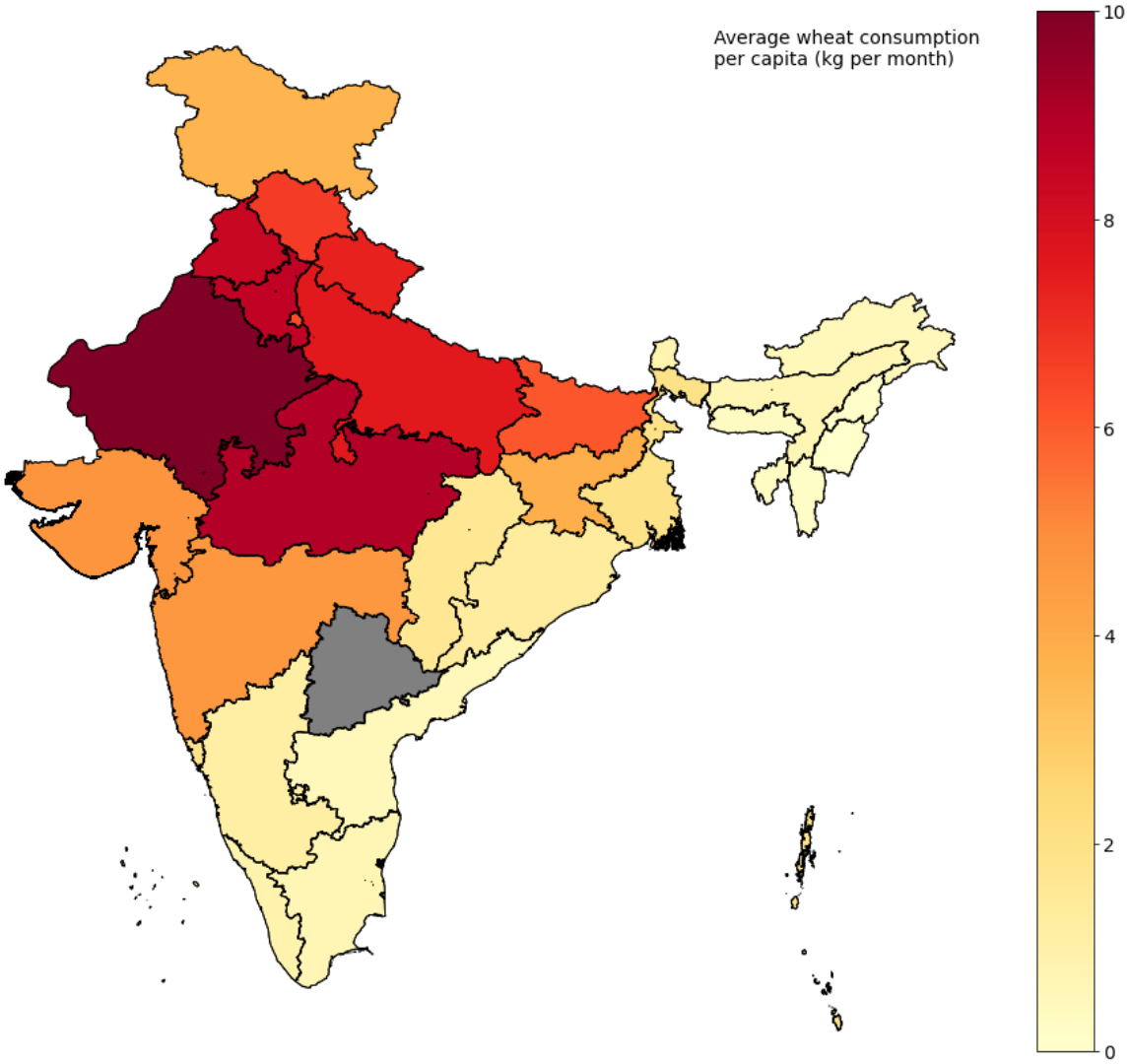

Figure 1.10: Map of per capita monthly wheat consumption in India in kilograms, compiled using data from the Ministry of Statistics and Programme Information (2012). *States in grey indicate locations for which data were missing. The last round of the National Sample Survey was 2011-2012 hence the absolute per capita consumption should be interpreted with caution. Though the distribution is expected to be similar due to the greatest wheat producing states overlapping with the states with the greatest per capita consumption (Figures 1.9 and 1.10).*

Per capita, the greatest amount of wheat is consumed in the west of India and across the IGP where the majority of wheat is grown. Currently, 39% of the population in India cannot afford a nutritionally adequate diet, and 78% of the population cannot afford a healthy diet (FAO et al., 2020; Herforth et al., 2020). Further, 35% of children under 5 suffer from stunting and 17% from wasting due to insufficient or poor-quality food, lacking the necessary micronutrients and calories for growth (Shukla, Tiwari and Prakash, 2014; Gonmei and Toteja, 2018). This causes problems with cognition, stunted growth, osteoporosis and muscular dystrophy (Shukla, Tiwari and Prakash, 2014; Gonmei and Toteja, 2018). Research by Raghunathan et al. (2020) found that individuals living in poverty in India cannot afford a diet that satisfies basic nutritional requirements.

In India, cereals provide around 60% of dietary protein as higher quality protein sources, such as meat, dairy, fish and eggs, are more expensive (Swaminathan, Vaz and Kurpad, 2012; Jain et al., 2023; Raghunathan and Chandrasekaran, 2020; Minocha, Thomas and Kurpad, 2017a). The

quality of protein in cereals is lower than that in pulses and milk for example, which are the next most accessible protein sources (Minocha, Thomas and Kurpad, 2017a). Minocha et al. (2017) found that for most states, at least 30% of people are at risk of not getting a high quality of protein across India. Additionally, Swaminathan et al. (2012) found that a diet containing cereals as its most prominent protein source would likely not fulfil dietary AA requirements. Protein deficiencies are of particular concern for pregnant people, who have additional protein requirements (Swaminathan, Vaz and Kurpad, 2012). Additionally, individuals in poorer socioeconomic circumstances, who may be more likely to experience disease, require a higher quality of protein to fight off infections (Minocha, Thomas and Kurpad, 2017a).

1.7.2 Threats of climate change and O_3 pollution

It is widely recognised that current pollution control measures in India are not sufficient for improving air quality (Singh, Dey and Knibbs, 2023; Wang et al., 2023a). Fossil fuel consumption and emissions of air pollutants in India are projected to increase leading to greater warming and greater O_3 concentrations in the country (Fowler et al., 2008; Rathore, Gopikrishnan and Kuttippurath, 2023). Rathore, Gopikrishnan and Kuttippurath (2023) comment that generally increasing temperature with decreasing precipitation favours O_3 production due to low humidity, whereas increased precipitation and decreased temperatures will reduce the rate of O_3 formation. India is projected to experience a country-wide increase in temperatures, with the greatest increases occurring at the higher latitudes and in the west of the country, which is where most of the wheat is grown (Salunke et al., 2023; Ministry of Agriculture & Farmers Welfare, 2022; Rupa Kumar et al., 2006; Bal et al., 2016). Future projections of precipitation also show an increase (Salunke et al., 2023). Hence, generally it is expected that India's future climate will favour O_3 production and further exacerbate O_3 pollution in the country. Whether an individual state in India experiences an increase or decrease will depend on the regional meteorology and emissions of pre-cursor gases (Jacob and Winner, 2009; Fu and Tian, 2019).

Naaz et al. (2022) found several Indian wheat cultivars experienced significant yield losses under combinations of increased temperature, O_3 and CO_2 concentrations representing climate change scenarios in the country for 2050. Additionally, their modelling study predicted a significant decline in areas climatically suitable for wheat growth by 2050 under RCP 8.5 which is of significant concern giving the increasing nutritional demands of the population (Naaz et al., 2022). Several O_3 risk assessments have quantified current yield loss due to O_3 in the country (see section 1.7.3), which will increase with increasing O_3 concentrations, and the additional stressors of climate change.

1.7.3 Results of O_3 risk assessments for India

Several methods have been employed to estimate yield loss at scale across India, and for different regions of the country (see Table 1.8), including concentration-response methods (Avnery et al., 2011; Van Dingenen et al., 2009; Lal et al., 2017; Ghude et al., 2014; Sinha et al., 2015; Sharma et al., 2019; Tang et al., 2013), flux-based methods (Mills et al., 2018b; Tang et al., 2013; Tai et al., 2021), and crop models incorporating O_3 damage methods (Droutsas, 2020; Tai et al., 2021). The following section will discuss the range in relative yield loss (RYL) predicted using the different methods, the spatial differences in RYL estimates and the requirements of each risk assessment method with their uncertainty. This overview will identify the limitations of current O_3 risk assessments in India to be addressed later in this thesis.

(a) *Range of RYL estimates for India*

Figure 1.11 summarises the RYL estimates for India using various metrics (detailed in Table 1.8), and Figure 1.12 shows the pairwise comparison of M7/M12 and AOT40 when using the same driving data. In both figures it can be seen that the AOT40 metric shows substantially higher and more variable estimates compared to the M7 metric. The boxplot for AOT40 is wider than the M7, indicating greater variability in RYL estimates. The AOT40 metric also shows a skewed distribution (substantially greater median than mean) indicating the presence of lower outlier values. The M7 metric has a more symmetric distribution and narrower range, indicating more consistent yield loss estimates and fewer extreme values. Using a flux-response relationship, Mills et al., (2018a) achieved a RYL consistent with the mean estimates of yield loss when using the M7 metric, while Tang et al.'s (2013) estimate was consistent with the mean RYL when using the AOT40 metric. The estimates by Droutsas (2020), who used an AOT40 based transpiration crop model, were approximately midway between the estimates of Mills et al. (2018a) and Tang et al. (2013). Droutsas' (2020) estimates were also between the estimates using the M7 and AOT40 metrics, but were on the lower end of the AOT40 estimates. These differences underscore the importance of metric choice when performing O_3 risk assessments.

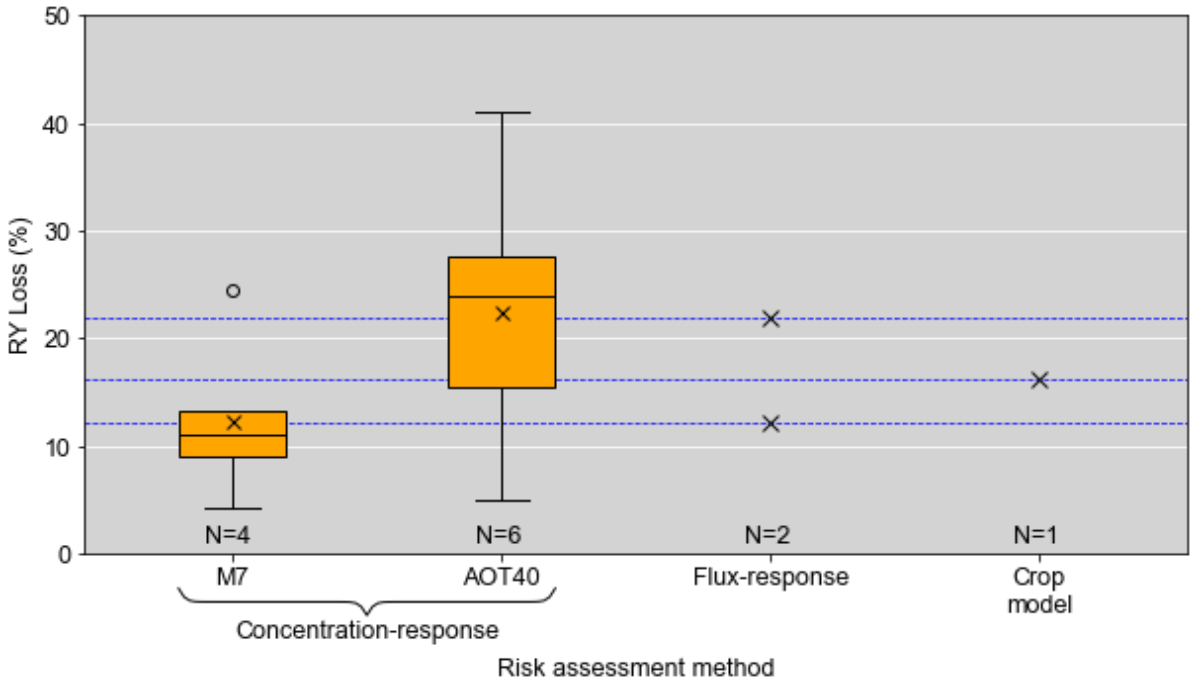

Figure 1.11: Boxplot showing the range of estimates of RYL (%) for all of India using the different risk assessment metrics using data from Table 1.8.

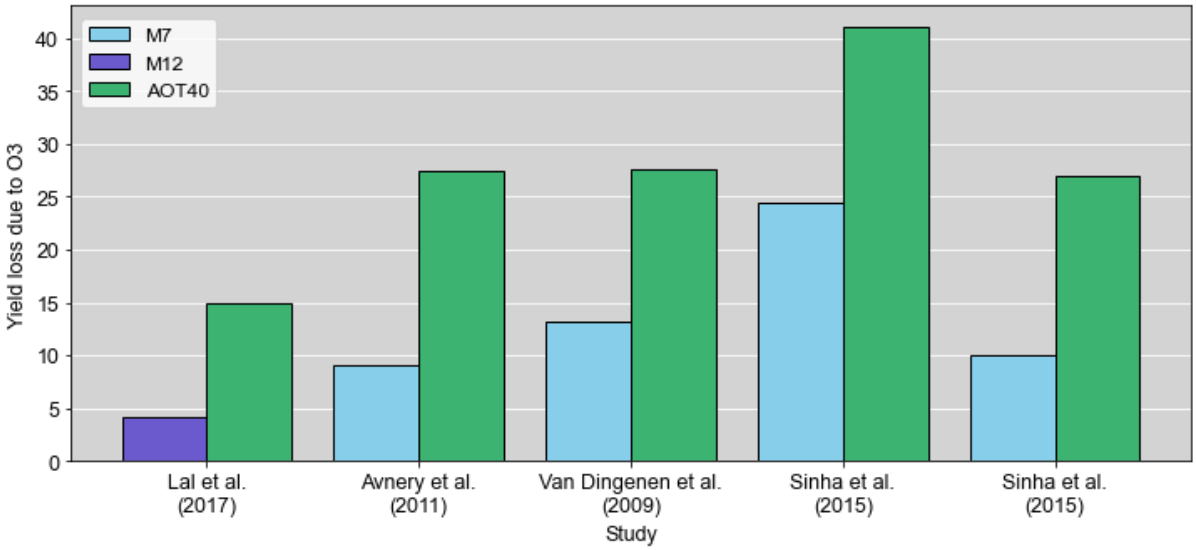

Figure 1.12: Pairwise comparison of M7 or M12 and AOT40 for the listed concentration-response studies in Table 1.8 that calculated both AOT40 and either M7 or M12.

(b) *Spatial pattern of RYL estimates in India*

The Indo-Gangetic Plain (IGP) is the region where most of the wheat in India is grown. It includes Punjab, Haryana, Uttar Pradesh and Bihar (Ministry of Agriculture & Farmers Welfare, 2023). To understand the spatial patterns, the lowest-highest RYL for each author are considered. Similarities in magnitudes of RYL estimates are ignored for now.

Lal et al. (2017) considered the RYL of wheat across the northern IGP, East India (West Bengal, Odisha and Assam), and West India (Gujarat, Rajasthan and Maharashtra), finding the lowest yield losses in the east, followed by the IGP, and the west experienced the greatest. Mills et al. (2018a) mostly agree with Lal et al. (2017), finding the greatest RYL the east, followed by the IGP, and the lowest across the west and central states (Rajasthan, Gujarat, Maharashtra and Madhya Pradesh). Tang et al. (2013) mostly agree with Mills et al. (2018a), finding the greatest yield losses across the northern IGP, and lowest in the west and central states. While Tai et al. (2021) do not report magnitudes of RYL and so their results cannot be incorporated into Table 1.8, their results generally show the greatest RYL across the northern IGP, followed by the east. In contrast, Ghude et al. (2014) find the greatest yield losses in Maharashtra (southwest), followed by Madhya Pradesh (central) and the other western states, with the lowest losses across the IGP. Droutsas (2020) agrees with aspects of Mills et al. (2018a) and Lal et al. (2017), finding the greatest yield loss in Bihar (eastern IGP). However, Droutsas (2020) finds the next greatest yield loss is predicted to be Madhya Pradesh, not the northern IGP, agreeing with Ghude et al. (2014). Droutsas' (2020) estimates of RYL across the northern parts of the IGP are generally lower than yield loss estimates for the other states.

The estimates of RYL by Sharma et al. (2019) are less varied than from the other authors. They find the greatest RYL in Madhya Pradesh, partially agreeing with Droutsas (2020) and Ghude et al. (2014) who predict larger losses in this state (Sharma et al., 2019). Of the most northern IGP states (Uttar Pradesh, Punjab and Haryana), with the exception of Tang et al. (2013), all authors who estimated RYL at these locations found Uttar Pradesh experienced a greater RYL than the other two states (Ghude et al., 2014; Sharma et al., 2019; Mills et al., 2018b; Droutsas, 2020).

(c) *Uncertainties of the different risk assessment methods for estimating RYL in India*

Given the majority of risk assessments have been performed using concentration-based

metrics, there is a lack of understanding of how climate and cultivar choice impact on yield loss estimates. Additionally, most concentration-response methods, with the exception of Sinha et al. (2015), did not use relationships developed using Indian wheat, though it has been shown to be more sensitive to O_3 (Emberson et al., 2009). Instead, concentration-response functions were used for European and North American wheat (Ghude et al., 2014; Avnery et al., 2011; Van Dingenen et al., 2009; Fischer, 2019; Sharma et al., 2019), and Chinese wheat (Tang et al., 2013). For all concentration-based RYL estimates, AOT40 always gave a greater RYL than M7 (Table 1.8, and Figure 1.11 and 1.12). Given that the AOT40 metric has been shown to give greater yield losses, it could be considered a drawback of Droutsas' (2020) model to integrate AOT40 into the crop model, as this could bias it towards greater RYL estimates. However, as Droutsas (2020) calibrated a yield parameter in their model before application, it is likely that biasing issues were corrected for.

For all RYL estimates, a large uncertainty is introduced through the choice of O_3 (and in some cases meteorological) data that is used to obtain the concentrations, flux, or input to the model. Table 1.9 summarises the different driving data used for the studies summarised in Table 1.8. Sharma et al. (2019) and Ghude et al. (2014) both use the WRF-Chem model to simulate the O_3 concentrations across the country. Yet simulated O_3 is sensitive to the choice of emission inventory and chemical mechanisms used when running WRF-Chem (Sharma et al., 2017). Sharma et al. (2019) used different emissions inventories and chemical mechanisms than Ghude et al. (2014) which were shown to better reproduce O_3 concentrations in India (Sharma et al., 2017), and achieved a large difference in RYL estimates as a result.

Table 1.8: Summary of the different approaches that have been used to estimate the RYL of wheat due to O_3 exposure across India. Where ranges were reported these are given, otherwise just the average is given. The average of studied locations is given in the final row of the table. For some studies this represents the entirety of India.

Location	% Wheat prod. 2021	Study	Method	Year	RYL
Uttar Pradesh	31.40%	Mills et al. (2018)	Flux-response	2010-2012**	15-20%
		Droutsas (2020)	AOT40 Transp Model*	1980-2009***	15.5%
		Ghude et al. (2014)	Concentration-response	2005	2.70% (AOT40)
		Sharma et al. (2019)	Concentration-response	2014-2015	21% (AOT40)
		Tang et al. (2013)	Concentration-response	2020	13.2% (AOT40)****
		Tang et al. (2013)	Flux-response	2020	19.9%****
Punjab	16.30%	Mills et al. (2018)	Flux-response	2010-2012**	10-20%
		Droutsas (2020)	AOT40 Transp Model*	1980-2009***	9.8%
		Ghude et al. (2014)	Concentration-response	2005	1% (AOT40)
		Sharma et al. (2019)	Concentration-response	2014-2015	16% (AOT40)
		Tang et al. (2013)	Concentration-response	2020	29.3% (AOT40) ****
		Tang et al. (2013)	Flux-response	2020	31.2%****
Haryana	11.10%	Mills et al. (2018)	Flux-response	2010-2012**	10-20%
		Droutsas (2020)	AOT40 Transp Model*	1980-2009***	10.5%
		Ghude et al. (2014)	Concentration-response	2005	1% (AOT40)
		Sharma et al. (2019)	Concentration-response	2014-2015	16% (AOT40)

		Tang et al. (2013)	Concentration-response	2020	19.1% (AOT40)****
		Tang et al. (2013)	Flux-response	2020	27%****
Northern IGP		Lal et al. (2017)	Concentration-response	2012-2013	4% (M7), 13% (AOT40)
Rajasthan	10.10%	Mills et al. (2018)	Flux-response	2010-2012**	5-15%
		Droutsas (2020)	AOT40 Transp Model*	1980-2009***	15.3%
		Ghude et al. (2014)	Concentration-response	2005	4% (AOT40)
		Sharma et al. (2019)	Concentration-response	2014-2015	19% (AOT40)
		Tang et al. (2013)	Concentration-response	2020	3% (AOT40)****
		Tang et al. (2013)	Flux-response	2020	9.1%****
Gujarat	3.10%	Mills et al. (2018)	Flux-response	2010-2012**	5-10%
		Ghude et al. (2014)	Concentration-response	2005	8% (AOT40)
		Tang et al. (2013)	Concentration-response	2020	13.1% (AOT40)****
		Tang et al. (2013)	Flux-response	2020	21.6%****
Maharashtra	1.70%	Mills et al. (2018)	Flux-response	2010-2012**	5-10%
		Ghude et al. (2014)	Concentration-response	2005	17% (AOT40)
		Tang et al. (2013)	Concentration-response	2020	8.9% (AOT40)****
		Tang et al. (2013)	Flux-response	2020	19.3%****
West		Lal et al. (2017)	Concentration-response	2012-2013	6% (M7), 27% (AOT40)
Bihar (Lower IGP)	5.20%	Mills et al. (2018)	Flux-response	2010-2012**	15-28%
		Droutsas (2020)	AOT40 Transp Model*	1980-2009***	18.9%
		Ghude et al. (2014)	Concentration-response	2005	3.60% (AOT40)
		Tang et al. (2013)	Concentration-response	2020	15.2% (AOT40)****
		Tang et al. (2013)	Flux-response	2020	22%****
East		Lal et al. (2017)	Concentration-response	2012-2013	3% (M7), 7% (AOT40)
Madhya Pradesh	18.20%	Mills et al. (2018)	Flux-response	2010-2012**	5-15%
		Droutsas (2020)	AOT40 Transp Model*	1980-2009***	18.5%
		Ghude et al. (2014)	Concentration-response	2005	8% (AOT40)
		Sharma et al. (2019)	Concentration-response	2014-2015	23% (AOT40)
		Tang et al. (2013)	Concentration-response	2020	5.8% (AOT40)****
		Tang et al. (2013)	Flux-response	2020	13.6%****
Average of studied locations		Mills et al. (2018)	Flux-response	2010-2012**	12.20%
		Droutsas (2020)	AOT40 Transp Model*	1980-2009***	16.20%
		Ghude et al. (2014)	Concentration-response	2005	3.8-6.2% (AOT40)
		Lal et al. (2017)	Concentration-response	2012-2013	4.2% (M7), 15% (AOT40)
		Avnery et al. (2011)	Concentration-response	2000	8-10% (M12), 25-30% (AOT40)
		Van Dingenen et al. (2009)	Concentration-response	2000	13.2% (M7), 27.6% (AOT40)

	Sinha et al. (2015)	Concentration-response	2011-2012	24.5% (M7), 41% (AOT40)
	Sinha et al. (2015)	Concentration-response	2012-2013	11% (M7), 27% (AOT40)
	Sharma et al. (2019)	Concentration-response	2014-2015	21% (AOT40)
	Tang et al. (2013)	Concentration-response	2020	15.7% (AOT40)****
	Tang et al. (2013)	Flux-response	2020	21.9%****

[*] Droutsas (2020) modified the GLAM-Parti model to include O_3 effects on transpiration using AOT40 and included a plant adjustment to O_3 stress

[**] estimated yield loss relative to preindustrial O_3

[***] To estimate yield loss they ran the model with, and without the O_3 functions turned on

[****] Tang et al. (2013) report two estimates using 90 and 75 days AOT40 for their concentration response relationship, and for the flux-response they use POD_6 and POD_{12}. Here the average of the concentration-response and flux-response RYL is reported

Table 1.9: Table stating the data that were used to drive the analyses in each study from Table 1.8

Driving data		**Study**
O_3	**Meteorology**	
EMEP MSC-W chemical transport model	ECMWF-IFS model	Mills et al. (2018)
UKESM1 model	AgMerra climate series	Droutsas (2020)
WRF-Chem regional chemistry transport model	N/A	Ghude et al. (2014)
Ground-level monitoring	N/A	Lal et al. (2017)
MOZART-2 global chemical transport model	N/A	Avnery et al. (2011)
TM5 global chemical transport model	N/A	Van Dingenen et al. (2009)
Ground-level monitoring	N/A	Sinha et al. (2015)
WRF-Chem regional chemistry transport model	N/A	Sharma et al. (2019)
WRF/Chem-CHASER global/regional chemical transport model	NCEP re-analysis dataset	Tang et al. (2013)

In summary, most risk assessments have been performed using concentration-based metrics which do not consider environmental interactions or differences in response between cultivars. Estimates of RYL varied spatially between the different metrics, hence the overall pattern of RYL due to O_3 across India is unclear. To date, no risk assessment method has been applied across India to identify the effect of O_3 on crop nutrition. Given the existing state of malnutrition in the country, this is of critical importance to understand the effects on food security going forward.

1.8 Research questions

It is essential to understand how production of wheat and wheat quality is affected by both O_3 and climate change to further understand these stressors effects on food and nutrition security. O_3 and climate induced reductions in starch and protein are of particular concern since the

crop is responsible for providing 20% of calories and protein globally, and 50% of dietary calories and 60% of dietary protein in India (Tripathi and Mishra, 2017; Swaminathan, Vaz and Kurpad, 2012; Shiferaw et al., 2013). Given that wheat demand will increase as populations increase, reductions to wheat production as a result of O_3 pollution and climate change will cause price increases for consumers (Peña-Bautista et al., 2017; Ruane and Rosenzweig, 2019; Pandey et al., 2023). As the price of the food varies it is likely that some individuals' will no longer be able to afford the food. This puts individuals at risk of food insecurity due not having sufficient food. Additionally, climate impacts on agriculture in India have been predicted to place more people in poverty with the proportion of people in middle-upper income groups decreasing for both rural and urban populations (Kumar and Parikh, 2001). Given that most of India's population cannot afford a healthy diet and a large percentage cannot afford a nutritionally adequate diet (FAO et al., 2020), an increase in poverty and alterations to crop quality raises further issues for individuals' food security in the country.

1.8.1 Paper 1

The first paper of this thesis will identify the processes by which O_3 influences crop yields and quality, and map these in combination with the processes currently included DO_3SE-Crop, to identify areas where the model can be extended to include O_3 effects on nutrition. A module will be developed for DO_3SE-Crop to simulate the effects of O_3 on wheat N, and hence protein. The model will be used to identify the key plant process affecting crop quality under O_3 exposure. This will make the modified DO_3SE-Crop model the first crop model to consider the effect of O_3 on the nutritional quality of the crop (considered through the perspective of N, a key component of protein), and will identify the key plant processes affecting crop quality under O_3 exposure. The following questions will be addressed:

1) How does O_3 exposure affect crop quality (N)?
2) How can N processes be incorporated into an O_3 deposition crop model to simulate how grain protein is affected by O_3 exposure?
3) What are the key plant processes affecting wheat quality (N) under O_3 exposure?

1.8.2 Paper 2

The second paper describes the modification of the DO_3SE-CropN model developed in Paper 1 (Section 2 of this thesis) to ensure its suitability for simulating wheat protein for different environmental conditions. Considering the high ambient O_3 concentrations in countries such as India, antioxidant processes will be incorporated into the model to more realistically represent plant response to O_3. To ensure nutritional relevance of the model, the key AAs for nutrition will be identified and incorporated into simulations. The model will then be tested using data for an O_3 tolerant and O_3 sensitive wheat cultivar.

1) How does O_3 exposure affect crop quality in India?
2) What are the most limiting AAs in wheat that are important for nutrition?
3) How can a model be developed to capture the effect of O_3 on Indian wheat, and protein quality?

1.8.3 Paper 3

The final paper investigates the current risk assessment choices for assessing O_3 effects on crop yields and quality in India by applying a range of risk assessment methods with varying O_3 and meteorological data. The differences between yield and protein loss estimates using

differing input data and risk assessment methods will be investigated to make recommendations of the most suitable choice of method for determining yield and protein losses of Indian wheat under O_3 exposure.

1) How does the choice of input data affect estimates of yield and protein loss under O_3 exposure in India?
2) How does the choice of risk assessment method affect estimates of yield and protein loss under O_3 exposure in India?
3) How can input data for risk assessments be improved for India?

1.9 Research outputs

The output of this PhD will be a N module for the existing DO_3SE-Crop model that can simulate the effect of O_3 on plant N, including the O_3 inhibition of remobilisation from shoots to the grain, and the antioxidant response of the plant. The model will be calibrated and evaluated for European and Indian wheat.

The outputs will also include 3 papers, titled:

1) New ozone-nitrogen model shows early senescence onset is the primary cause of ozone-induced reduction in grain quality of wheat (Pre-print available and article accepted for publication (Cook et al., 2024))
2) Modelling the nutritional implications of ozone on wheat protein and amino acids (submitted for publication)
3) Relative yield and protein estimates are more sensitive to ozone risk assessment method than input data and cultivar parameterisation (in preparation for journal submission)

I also contributed to the DO_3SE-Crop model development throughout my thesis, aiding with calibration approaches, parameterisation of dry matter partitioning, respiration and brown LAI equations, and performing sensitivity analyses to identify the most important parameters for model calibration (see Pande et al., 2024)

2. Paper 1: New ozone-nitrogen model shows early senescence onset is the primary cause of ozone-induced reduction in grain quality of wheat

2.1 Abstract

Ozone (O_3) air pollution is well known to adversely affect both the grain and protein yield of wheat, an important staple crop. This study aims to identify and model the key plant processes influencing the effect of O_3 on wheat protein. We modified the DO_3SE-Crop model to incorporate nitrogen (N) processes, and parameterised the O_3 effect on stem, leaf and grain N using O_3 fumigation datasets spanning 3 years and 4 O_3 treatments. The modifications make the newly developed DO_3SE-CropN model the first crop model to include O_3 effects on N processes, making it a valuable tool for understanding O_3 effects on wheat quality. Our results show the new model captures the O_3 effect on grain N concentrations, and anthesis leaf and stem concentration well, with an R^2 of 0.6 for the increase in grain N concentration and an R^2 of 0.3 for the decrease in grain N content under O_3 exposure. However, the O_3 effect on harvest leaf

and stem N is exaggerated. Overestimations of harvest leaf N range from ~20-120%, while overestimations of harvest stem N range from ~40-120%. Further, a sensitivity analysis revealed that, irrespective of O_3 treatment, early senescence onset (simulated as being ~13 days earlier in the very high vs low O_3 treatment) was the primary plant process affecting grain N. This finding has implications for the breeding of stay-green cultivars for maintaining yield, as well as quality, under O_3 exposure. This modelling study therefore demonstrates the capability of the DO_3SE-CropN model to simulate processes by which O_3 affects N content, and thereby determines that senescence onset is the main driver of O_3 reductions in grain protein yield. The implication of the sensitivity analysis is that breeders should focus their efforts on stay-green cultivars that do not experience a protein penalty when developing O_3 tolerant lines, to maintain both wheat yield and nutritional quality under O_3 exposure. This work supports the second phase of the tropospheric O_3 assessment report (TOAR) by investigating the impacts of tropospheric O_3 on wheat, with a focus on wheat quality impacts that will subsequently affect human nutrition.

2.2 Introduction

The first phase of the tropospheric ozone (O_3) assessment report (TOAR) (https://igacproject.org/activities/TOAR/TOAR-I) built the world's largest database of surface O_3 metrics to identify global distribution of the pollutant and trends in O_3 concentrations over time. The second phase of TOAR (https://igacproject.org/activities/TOAR/TOAR-II), to which this paper contributes, has a broader scope, with one of the additional aims being to investigate the impact of tropospheric O_3 on human health and vegetation. The present work will address these goals by developing riskassessment methods that consider the interaction between O_3 and nitrogen (N) in crops. As N is a key component of protein, effects of O_3 on N have the potential to impact crop quality, and, as a result, human nutrition. Areas for further investigation to provide deeper understanding of O_3-N interactions are identified, and recommendations for future work to mitigate the negative effects of O_3 on both crop yield and protein are discussed.

2.2.1 The importance of wheat for nutrition and the threat of O_3

The Food and Agricultural Organisation of the United Nations (FAO) projects that staple cereals will play a critical role in ensuring food security; particularly in Central and West Asia, and North Africa where wheat provides at least 40% and 47% of dietary calories and protein respectively, compared to ~20% of dietary calories and protein globally (FAO, 2017). There is a large body of evidence, including work from the first phase of TOAR, suggesting that current ambient ozone (O_3) concentrations in key wheat growing locations are causing substantial productivity losses of equal importance to other, more well known, biotic and abiotic stresses (Mills et al., 2018a; Emberson et al., 2009; Mills et al., 2018c). Globally, wheat production is reduced by ~7%, though in some regions with high ambient O_3 concentrations, such as Northern India, the yield loss is much greater (> 15%) (Mills et al., 2018a). There is also a growing body of literature showing that O_3 affects the nutritional quality of the wheat grain and reduces the protein yield (Broberg et al., 2015; Piikki et al., 2008; Yadav et al., 2020, 2019a). Over the next century, increases to global population and economic growth, and changes to climate and land use, will increase emissions of O_3 precursors (NO_x and VOCs) (Fowler et al., 2008). For shared socio-economic pathway (SSP) 3-70 (often termed the "business-as-usual" scenario), projections show that O_3 concentrations will increase in most locations globally, particularly South and East Asia, South America, Africa and the middle East (Szopa et al., 2021). Alterations to local meteorology and carbon dioxide (CO_2) concentrations under climate change will also influence O_3 production (Fu and Tian, 2019), with Zanis et al. (2022) finding that for regions close to emissions sources climatic conditions will likely increase O_3 production. Understanding O_3

impact on the supply and nutritional quality of wheat grown in regions where O_3 concentrations are high/ predicted to increase is crucial (FAO et al., 2020). This will help us understand and address the threats posed by O_3 pollution on the ability of future wheat production to meet increasing demand and nutrient requirements (Shiferaw et al., 2013; Mills et al., 2018b).

2.2.2 The impact of O_3 on wheat quality and the mechanisms by which damage occurs

Reactive oxygen species (ROS), formed from O_3 entering the leaves through the stomata, trigger a series of reactions that reduce grain yield and quality (Emberson et al., 2018; Broberg et al., 2015). The uptake and remobilisation of nutrients under O_3 exposure is affected less severely by O_3 than the O_3-induced reduction in dry matter (DM). This results in a decrease in the nutrient yield of the grains (gNutrient m^{-2}) but an increase in the nutrient concentration (gNutrient gDM^{-1}) (Wang and Frei, 2011; Broberg et al., 2015). Broberg et al. (2015) further found that an increased grain protein concentration caused the baking properties, quantified by the Zeleny value, Hagberg falling number and dry and wet gluten content, to be positively affected by O_3. In some wheat studies, where O_3 concentrations are very high, grain protein concentration is decreased, potentially as a result of N being used for antioxidant production and defence against O_3 (Baqasi et al., 2018; Yadav et al., 2020, 2019b; Mishra, Rai and Agrawal, 2013; Fatima et al., 2018).

The main mechanism by which O_3 reduces wheat yields and impacts on quality is through accelerated senescence (Emberson et al., 2018). Wheat cultivars with delayed senescence, stay-green cultivars, have previously been trialled for their potential to offset yield reductions under stressors such as heat and drought stress (Kamal et al., 2019). However, accelerated senescence typically reduces protein remobilisation and reduces wheat quality (Havé et al., 2017; Sultana et al., 2021). Understanding the mechanisms by which O_3 damages crop yield and influences crop quality is crucial for breeding of O_3 tolerant cultivars. Section 2.3.2.1 provides more detail and a mechanistic description of how wheat yields, and protein, are affected by O_3.

2.2.3 The current status of crop modelling with regards to N and O_3

Current understanding of the effect of O_3 pollution on wheat nutritional quality has been inferred from experimental studies (Mills et al., 2011; Feng, Kobayashi and Ainsworth, 2008; Broberg et al., 2015, 2021). However, experimental work is time consuming and costly, and it can be difficult to control all variables involved. Crop models use environmental inputs to simulate crop growth, for a range of conditions and stressors, in far less time, using fewer resources than required for experimental investigation (Chenu et al., 2017). Developing crop models with experimental data, which provides insights into plant growth processes, allows investigation of realistic plant responses to individual and multiple stressors.

It is possible to simulate the O_3 effect on grain protein through incorporating N processes into an existing crop model considering O_3 damage, and using a simple conversion factor (e.g. Mariotti, Tomé and Mirand (2008)) to convert N to protein. Many models consider N dynamics in wheat (e.g. APSIM-NWheat and CERES-Wheat) (see supplementary Table S1), and others have incorporated O_3 damage (e.g. LINTULLC2, WOFOST, APSIM and DO_3SE-Crop) (Nguyen et al., 2024; Xu et al., 2023). Some models, such as APSIM, can simulate both O_3 effects on yield and grain N, which could be used to calculate grain protein and hence provide a measure of grain quality variation under O_3 exposure. However, to our knowledge, no simulations have yet been performed on the O_3 effect on grain N. Further, these models do not yet include the

mechanisms that relate O_3 with grain N. Currently, no model simulates the reduced remobilisation of N under O_3 exposure from the stem and leaf to the grain, an important determiner of wheat protein under O_3 exposure (Broberg et al., 2021, 2017; Brewster, Fenner and Hayes, 2024; Brewster, 2023; Chang-Espino et al., 2021).

2.2.4 Objectives

This study aims to develop and use the DO_3SE-Crop model to investigate the impact of O_3 on wheat grain N content through the following objectives:

1) Identifying the key mechanisms necessary to model N in crops and the influence of O_3 on these mechanisms.
2) Developing a N module that can be incorporated into the existing O_3 deposition and crop growth model, DO_3SE-Crop, to simulate how grain N (and hence protein), is affected by O_3 exposure (DO_3SE-CropN).

3) Using the developed DO_3SE-CropN model to perform a sensitivity analysis to determine which of the O_3 damage mechanisms (senescence onset, senescence rate/end, and remobilisation of N) affects grain quality the most.

2.3 Model development

2.3.1 Overview of the DO_3SE-Crop model

The DO_3SE-Crop model is used to estimate O_3 deposition to a plant canopy and the impacts (biomass and yield loss) caused by stomatal O_3 uptake (Emberson et al., 2018). The crop phenology is estimated based on thermal time sums. Photosynthesis is simulated at the leaf level, based on a modified version of the biochemical Farquhar model (Farquhar, Caemmerer and Berry, 1980), and scaled to the canopy level by splitting the canopy into equally sized layers of cumulative leaf area index (LAI). The photosynthetic products from each layer are summed to give the net primary productivity (NPP). The NPP is allocated to the root, stem, leaf or grain based on the plant's developmental stage using the approach of Osborne et al. (2015). O_3 transfer from the atmosphere to the leaf is estimated by a resistance scheme incorporating aerodynamic, boundary layer and surface resistances above and within the canopy (Pande et al., 2024a). The instantaneous impact of stomatal O_3 flux on photosynthesis and the impacts of accumulated O_3 flux on senescence, once the cumulative flux exceeds a cultivar specific threshold, are estimated based on the approach of Ewert and Porter (2000) and modified by Pande et al. (2024a). Further details of the DO_3SE-Crop model along with a mathematical description can be found in Pande et al. (2024a). In this study version 4.39.11 of the DO_3SE-Crop model was used (Bland, 2024a).

2.3.2 Development of the N module

2.3.2.1 Identification of which N processes to model

The key plant processes influenced by N and O_3 were identified to guide decisions on which processes to include in the N module for DO_3SE-Crop (Figure 2.1). Figure 2.1 provides an overview of processes already included in DO_3SE-Crop, those to be added in the new N module, and those which are excluded. In brief, DO_3SE-Crop includes an instantaneous short-term effect of O_3 on carboxylation efficiency which subsequently affects photosynthesis. The leaf has the capacity to recover from this O_3 damage overnight, though recovery ability decreases with age. Additionally, we simulate a long-term effect of O_3 on accelerating senescence. Detail of the

DO_3SE-Crop model and associated O_3 damage processes are given by Pande et al. (2024a). Figure 2.1 is separated into numbered sections which are explained in the subsequent text:

#1
Reactive oxygen species (ROS), that are formed when O_3 diffuses through leaf stomata, trigger a series of physiological and stress responses in the plant that lead to accelerated senescence and a reduced photosynthetic rate (Emberson et al., 2018). ROS delay stomatal response to external stimuli, reducing stomatal conductance (Dai et al., 2019; Paoletti and Grulke, 2010). ROS are detoxified by apoplastic anti-oxidants, but an excess of ROS may overwhelm the anti-oxidant response, damaging cell plasma membrane (Emberson et al., 2018; Fatima et al., 2019).

#2
ROS destroy photosynthetic pigments (Emberson et al., 2018). ROS degradation of photosynthetic pigments accelerates crop senescence, during which Rubisco, comprising 50% of soluble leaf protein, is broken down to release N for remobilization to other parts of the plant (Feller and Fischer, 1994; Emberson et al., 2018).

#3
ROS degradation of Rubisco leads to reduced carboxylation efficiency (Emberson et al., 2018). Together with a reduced electron transport efficiency, photosynthetic rate is reduced (Emberson et al., 2018; Rai and Agrawal, 2012). There is an increase in antioxidant and defence proteins triggered by elevated O_3 (Sarkar et al., 2010; Cho et al., 2011; Fatima et al., 2018).

#4
O_3 induced accelerated senescence reduces the green leaf area for photosynthesis, further decreasing carbon assimilation (Emberson et al., 2018). Diminished photosynthesis leads to lesser photosynthate production (Emberson et al., 2018). More photosynthate is used in respiration and for anti-oxidant production to target ROS (Emberson et al., 2018; Khanna-Chopra, 2012). Under O_3 stress, annual crops, such as wheat, prioritise allocation of assimilates to flowers and seeds, reducing the availability for leaves, stems and roots (Emberson et al., 2018).

#5
N taken up by the plant is used to produce all proteins (Lawlor, 2002). Root biomass, and subsequently nutrient uptake, is reduced under stress conditions as assimilate allocation to repair aboveground O_3 damage is prioritised over export to the roots (Emberson et al., 2018; Pandey et al., 2018). While O_3 can induce senescence and reduce photosynthesis, a higher leaf N can delay the onset of senescence and increase the photosynthetic rate (Pilbeam, 2010; Nehe et al., 2020; Martre et al., 2006; Brewster, Fenner and Hayes, 2024). On the other hand, N deficiency can damage the structure and function of the chloroplasts which could exacerbate O_3 impacts on senescence and photosynthetic rate (Kang et al., 2023). Brewster, Fenner and Hayes (2024) found an increase in residual leaf and stem N occurs, potentially as a result of O_3 toxicity.

#6
Wheat yields are decreased due to reduced photosynthesis and grain filling duration (Emberson et al., 2018; Broberg et al., 2015). Wheat grain N comprises N taken up post-anthesis, and N remobilised from the leaves and stem when senescence begins (Havé et al., 2017; Gaju et al., 2014; Nehe et al., 2020; Barraclough, Lopez-Bellido and Hawkesford, 2014). Hence, any

damage mechanism which affects grain filling duration, influences the final N content of the wheat grains. Additionally, as Rubisco is a key source of N for grains, once senescence begins, reductions to Rubisco will impact the amount of N that is available to grains (Feller and Fischer, 1994). Brewster, Fenner and Hayes (2024) and Chang-Espino et al. (2021) find evidence of an additional, unknown process, separate to accelerated senescence, that reduces the remobilisation of N under O_3 exposure.

Generally, grain protein concentrations increase under elevated O_3, due to a smaller decrease in N uptake and re-translocation relative to the O_3-induced decrease in grain DM (Wang and Frei, 2011; Broberg et al., 2015, 2019; Triboi and Triboi-Blondel, 2002; Piikki et al., 2008). However, per metre square of crop the starch and grain protein yield is reduced (Broberg et al., 2015; Feng, Kobayashi and Ainsworth, 2008; Gelang et al., 2000). Some wheat cultivars have shown a decrease in grain protein concentration under O_3 exposure (Yadav et al., 2019a; Baqasi et al., 2018; Mishra, Rai and Agrawal, 2013). This could be because leaf proteins are converted to enzymatic antioxidants to defend against O_3 induced damages, resulting in less proteins available for translocation to the grains (Yadav et al., 2019b; Sarkar et al., 2010; Fatima et al., 2018).

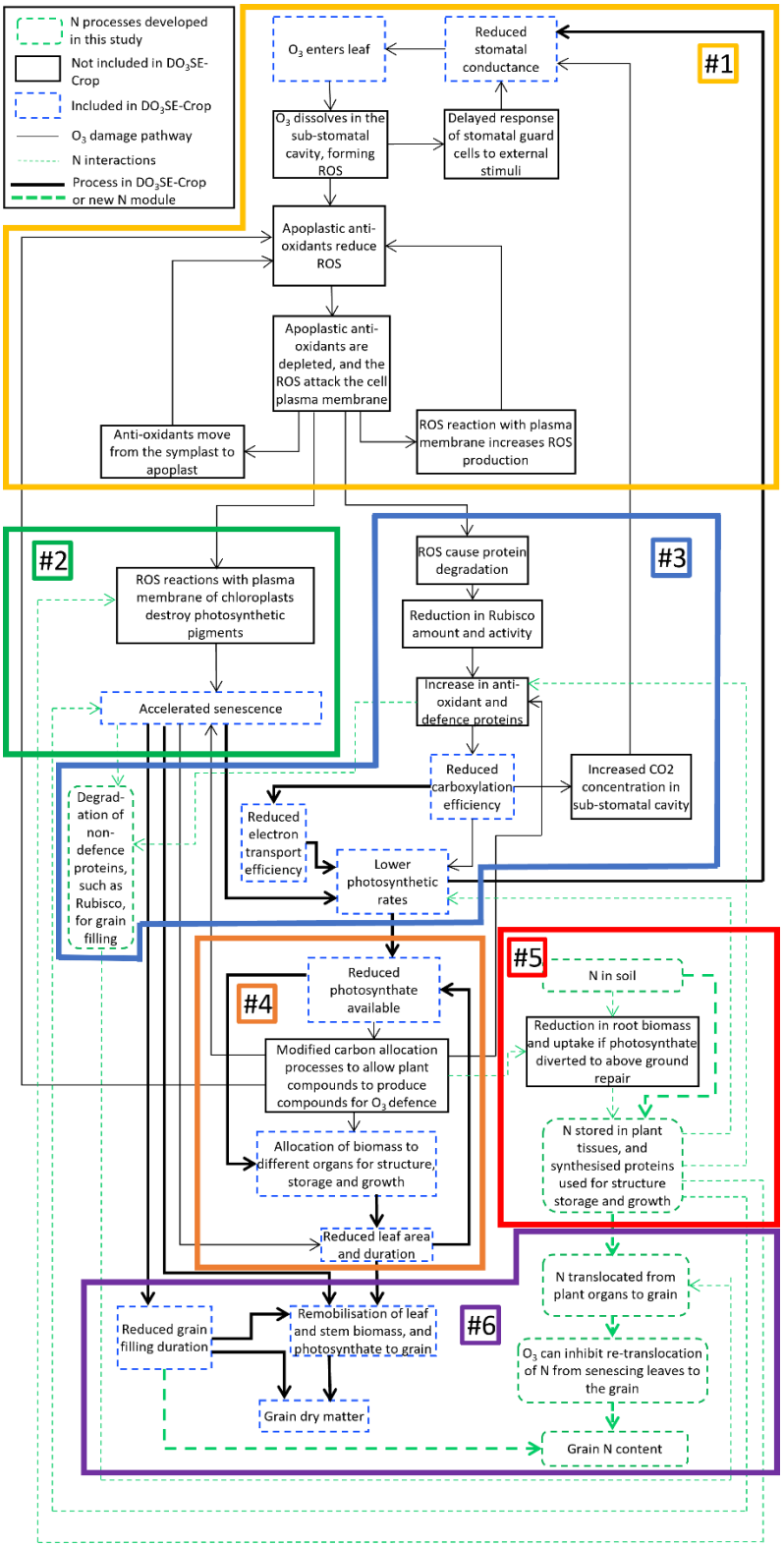

Figure 2.1: A flow chart of the mechanisms by which O_3 causes damage to both grain yields and grain N (or protein) in wheat. The different colours and line styles outlining the individual boxes represent whether the process is included in the DO$_3$SE-Crop model already (blue, dashed outline), not included in the DO$_3$SE-Crop model (black, solid outline), or included in the N module developed for DO$_3$SE-Crop in this study (green dashed outline, rounded edge boxes). The black connector lines represent interactions between the O_3 damage processes and the green dashed connector lines represent where N processes interact with these. The thinner lines represent interactions that are not included in the DO$_3$SE-Crop model or the new N module, whereas thicker lines represent the interactions that are included. The figure has been divided into 6 numbered sections for which the mechanisms are described individually in section 2.3.2.1.

2.3.2.2 Assessment of existing crop models that include N

Supplementary Table S2.1 summarises and discusses the similarities between models that simulate plant N dynamics. Most models simulated leaf and stem N by fulfilling the required N demanded by the respective parts from the N uptake pool, with N demand based on a defined minimum and maximum for that organ. The maximum and minimum N concentrations can be set as constants or defined using the phenological stage of the plant, which in turn is based on the accumulation of thermal time or a temperature sum based on a scheme by van Keulen and Seligman (1987). Most crop models define a labile pool of N available to be translocated to the grain and consisting of N available from post-anthesis uptake, non-structural stem N, and N released from leaf senescence. The N released from leaf senescence is calculated in proportion to the decrease in carbon of green leaf area, as N remobilisation is proportional to carbon remobilisation (Havé et al., 2017). Most of the crop models simulated grain N by calculating and fulfilling a N demand, or simulating a rate at which the grains fill with N.

2.3.2.3 Modifications to the existing DO_3SE-Crop Model for this study

Prior applications of the DO_3SE-Crop model have assumed that the last 33% of the mature leaf lifespan is when leaf senescence occurs (e.g. Pande et al. (2024a)) . In some applications, multiple leaf populations were considered. Given the limitations of available data in parameterising the model for multiple leaf populations, only one leaf population is considered in the present study. As a result, the fraction of mature leaf lifespan that is senescence needed to be modified to instead simulate the fraction of canopy mature leaf lifespan that is senescence. Recent work by Brewster et al. (2024) has shown that the 4^{th} leaves can begin to senesce even before anthesis. Given the importance of senescence in determining N remobilisation (Nehe et al., 2020; Gaju et al., 2014), work by Brewster et al. (2024) was used to re-parameterise the onset of rapid phase senescence as the last 75% of the canopy level mature leaf lifespan for the Skyfall cultivar in DO_3SE-Crop.

2.3.2.4 The DO_3SE-Crop N module for wheat

Based on sections 2.3.2.1 and 2.3.2.2, we identified key processes for inclusion in the N module as: soil N uptake, partitioning of N uptake between leaf and stem, remobilisation of N in leaf and stem to the grains, grain filling with N, and O_3 effects on grain N. At the present stage of the modelling, we do not include any processes relating to usage of N for antioxidant production or utilisation of photosynthate for above ground repair due to lack of data for parameterisation. Full details of equations, sources of equations and model parameterisations are available in Appendix A. Briefly:

(a) Soil N uptake

Pre-anthesis, daily N uptake from the soil is proportional to the increase in LAI and stem mass that day, along with any N deficit that has accumulated over the plant's life, following the work of Soltani and Sinclair (2012). Post-anthesis, we use the formulation from SiriusQuality (Martre et al., 2006) which links post-anthesis N uptake with the capacity of the stem to store N. Pre- and post-anthesis we define a maximum N uptake which cannot be exceeded. Since we did not have data to calibrate for the effects of N stress, the present model assumes optimal soil N availability.

(b) N partitioning

Pre-anthesis, N uptake is allocated to the leaf and stem in accordance with the increase in LAI or stem mass that day, as commonly used by other crop modellers (section 2.3.2.2). The specific equations used closely follow those of Soltani and Sinclair (2012).

(c) N remobilisation

After anthesis, N remobilisation from the stem to the grains begins. N is released from senescing leaves in accordance with the decrease in LAI that day. Released N is stored in the stem where it is available to the grain. The combination of N released from leaf senescence and non-structural stem N creates the labile pool of N for grain filling.

(d) Grain N

The N in the labile pool can be transferred to the grain, or it can remain as part of the stem. In contrast to other crop models, the proportion of labile N transferred to the grain each day follows a sigmoid function. The sigmoid was chosen as it uses only two extra parameters (α_N and β_N) which allows the start and rate of grain fill with N to be customised without the addition of much complexity. The fraction leaving the labile pool increases as the plant develops.

$$N_{to\_grain} = N_{labile} \times \frac{1}{1 + exp(-\alpha_N(DVI - \beta_N))} \quad (2.1)$$

where N_{to_grain} represents the amount of N leaving the labile pool (N_{labile}) to the grains, DVI represents the development index of the plant in DO_3SE-Crop (Pande et al., 2024a). The N_{to_grain} profile for different parameterisations of α_N and β_N is shown in Appendix A, Figure A2.3.

(e) Direct effect of O_3 on grain N

The fraction of N remaining in the leaf and straw increases with O_3 exposure (Broberg et al., 2017, 2021). Additionally, in the work of Brewster et al. (2024) the same effect is observed, where a lower proportion of N stored in these parts at anthesis is moved to the grains. Little data is available on this effect, so we used all available existing data from Broberg et al. (2017) and Brewster et al. (2024) to produce a linear regression of the % of N remaining in the leaf and stem at harvest as a function of M12 (the common metric for the two studies defined as the 12 hour mean O_3 concentration during daylight hours (Guarin et al., 2019b)). The results of this can be seen in Figure 2.2.

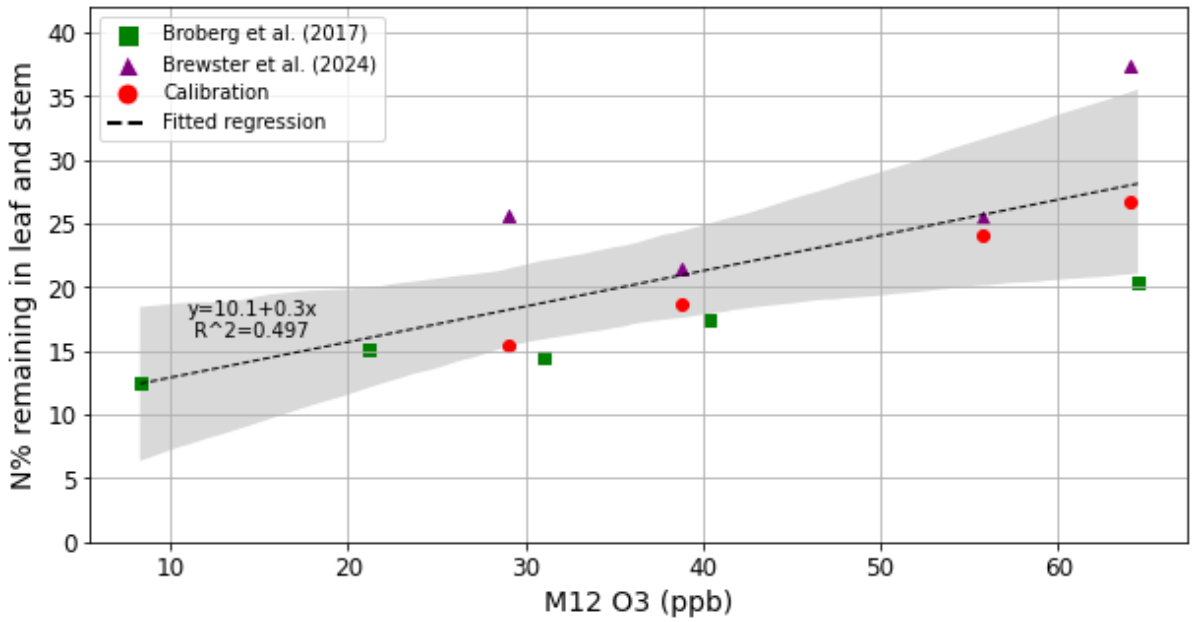

Figure 2.2: The % of N remaining in the leaf and stem as a function of M12 for studies by Broberg et al. (2017) (green square markers) and supplementary data obtained from Brewster, Fenner and Hayes (2024) (purple triangular markers). The grey area represents the 95% confidence interval of the fitted regression (dashed linear line) and the R^2 of the regression is given on the figure. Overlaid are red, circular markers showing the effect of the calibrated $m_{leaf}, c_{leaf}, m_{stem}$ and c_{stem} on overall remobilisation.

The minimum allowed leaf and stem N concentrations were varied to optimise the grain N% and harvest leaf and stem N% simulations, whilst making sure the % of N remaining in the leaf and stem was within the 95% CI of the remobilisation regression. The form of the regressions representing the minimum leaf and stem N concentrations under O_3 exposure are given in Equations (2.2) and (2.3) respectively.

$$\frac{[N_{leaf,min}]}{1\ gN\ LAI^{-1}} * 100 = m_{leaf} \times \frac{[O_{3,M12}]}{1\ ppb} + c_{leaf} \quad (2.2)$$

$$\frac{[N_{stem,min}]}{1\ gN\ DM^{-1}} * 100 = m_{stem} \times \frac{[O_{3,M12}]}{1\ ppb} + c_{stem} \quad (2.3)$$

where $[N_{leaf,min}]$ is the minimum leaf N concentration in gN per unit of LAI, $[N_{stem,min}]$ is the minimum stem N concentration in gN per g of stem DM, and $[O_{3,M12}]$ is the concentration of O_3 using the M12 metric in ppb. The parameterisation for Equations 2.2 and 2.3 is given in Table 2.1 Further details of the process by which the best parameters were obtained is given in Appendix A, section 2.8.4.

Table 2.1: The calibrated values for the newly developed regressions describing how the minimum leaf and stem N concentrations vary under differing O_3 concentrations. All parameters are unitless.

Parameter	Description	Value
	Gradient of Equation (2.2)	
m_{leaf}		0.8

c_{leaf}	Intercept of Equation (2.2)	10.9
m_{stem}	Gradient of Equation (2.3)	0.014
c_{stem}	Intercept of Equation (2.3)	0.23

(f) Indirect effect of O_3 on grain N

In the DO_3SE-Crop model, O_3 accelerates the onset and rate of senescence (Pande et al., 2024a). In this N module, remobilisation of N from senescing leaves occurs once senescence begins. Further, no N is remobilised from the leaves once senescence is complete. DO_3SE-Crop also simulates the impact of O_3 on the rate of photosynthesis and, consequently, biomass production and leaf area expansion (Pande et al., 2024a). In this N module, leaf area determines accumulation of leaf N and stem biomass determines accumulation of stem N, providing an indirect link between O_3 damage in the DO_3SE-Crop model and the newly developed N module.

In combination, the N and DO_3SE-Crop processes are integrated to form the DO_3SE-CropN model as shown in Figure 2.3. Simply, N uptake is partitioned in accordance with demand from the leaf and stem. The N available to the grain comes from senesced leaf area, post anthesis N uptake and non-structural stem N. The amount of N that is transferred to the grain from this available pool is calculated using a sigmoid function. The fraction of N that is available to the grain from the leaf and stem is modified in accordance with daily O_3 concentrations. Further details of the equations used, and processes involved are given in Appendix A. In this study version 1.0 of the N module was used, and the corresponding code can be found at Cook (2024).

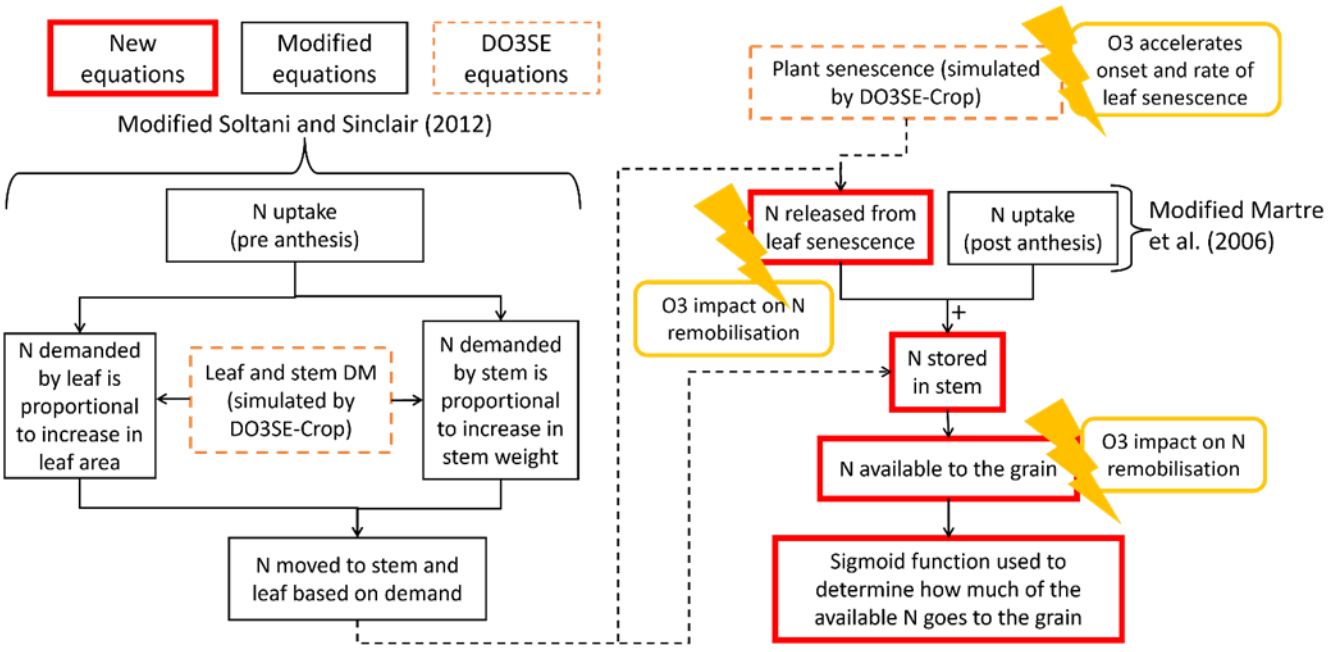

Figure 2.3: Simplified overview of the DO_3SE-Crop N module. Red outlined boxes show the processes developed in this study. Orange outlined boxes are indicating where the N module takes outputs from the DO_3SE-Crop model. Black outlined boxes indicate where equations were taken from the existing literature and modified for the current study. The lightning bolts represent the locations where O_3 impacts on plant N processes in the newly developed DO_3SE-CropN model.

2.4 Parameterisation and calibration of DO_3SE-Crop and new N module

Experimental data have been collated and gap filled (using the AgMIP-Ozone gap-filling methodology (Emberson et al., 2021)) to calibrate and evaluate the DO_3SE-Crop model and newly developed N module. Further details of the gap filling methods can be found in the Supplementary materials.

2.4.1 Experimental datasets

Data from the Centre for Ecology and Hydrology, Bangor, from the years 2015, 2016 and 2021 were used to calibrate the N module for DO_3SE-Crop. For each year, the Skyfall wheat cultivar was grown in solar domes under 4 O_3 treatments, with median O_3 concentrations ranging from 29 – 61.1 ppb. Across the 3 years, the wheat was planted between February 23rd and April 15th and harvested between August 11th – August 17th. O_3 fumigation occurred between stem-elongation (GS30) and harvest (mid-August) (Brewster, Fenner and Hayes, 2024; Broberg et al., 2023; Osborne et al., 2019 with supplementary information from the authors). In this study, only treatments where the plants were well watered and experienced no N or temperature stress were used. No grain data was used for the year 2021 as the plants did not put on any grain (see Brewster, Fenner and Hayes (2024) for further detail). A tabulation of data available from each year can be found in supplementary Table S2.2. Further details of the experimental set up for all years can be found in Brewster et al. (2024), Broberg et al. (2023) and Osborne et al. (2019) and supplementary data obtained from the authors was used for model development.

2.4.2 Model calibration and evaluation

Model calibration was performed in stages, with the calibrated parameters indicated in brackets. Definitions of DO_3SE-Crop parameters, along with the value they were calibrated to and the units are given in supplementary Table S2.3.

1) Phenology ($T_b, T_o, T_m, TT_{emr}, TT_{flag,emr}, TT_{astart}, TT_{amid}, TT_{harv}$)

2) Photosynthesis and respiration ($V_{cmax,25}, kN,\ J_{max,25,}, m, R_{dcoeff}, R_g$)

3) DM allocation and yield, and O_3 effect on yield and senescence (α_{root}, β_{root}, α_{leaf}, β_{leaf}, α_{stem}, β_{stem}, Ω, τ, $E_g, \gamma 3, \gamma 4, \gamma 5$, CLsO3)

4) N allocation and O_3 effect on N remobilisation ($m_{leaf}, c_{leaf}, m_{stem}, c_{stem}$ (section. 2.3.2.4, Table 2.1))

This sequential calibration prevents later adjustments caused by the interdependencies between parameters at different calibration stages. It was necessary to calibrate O_3 effects on yield at the same time as the DM allocation and yield parameters, as O_3 still influences yield, even in the low O_3 treatments. $V_{cmax,25}$ and $J_{max,25,}$ had been measured and so were fixed to their experimentally measured values to limit the numbers of parameters to calibrate. Further, data on photosynthesis at different light concentrations allowed the determination of the rate of dark respiration, and hence we fixed the parameter controlling dark respiration in DO_3SE-Crop. A combination of genetic algorithm and manual calibration was then used to calibrate chosen parameters to achieve the desired output variable. The genetic algorithm is not always the most suitable for model calibration, as it can give parameterisations that maximise the R^2, but don't make sense physiologically. In cases where unrealistic parameterisations were given, a manual

"by-eye" calibration process was also used. By varying one parameter at a time to understand it's effect on a desired output, realistic parameterisations were chosen. For all calibrations the R^2 and RMSE were used to assess the fit between observed data and simulations. Generally, 50% of the combined data for all years, for the low and very high O_3 treatments were used in the calibration, with the remaining data used in the evaluation along with 100% of the medium and high O_3 treatment data for all years. A tabulation of the parameters calibrated for, and the values they were calibrated to, are given in supplementary Table S2.3 along with further details of the calibration process in Section 2.9.4. Parameterisations relating to the newly developed N module are discussed and presented along with their equations in Appendix A.

The model was evaluated by calculating the RMSE and R^2 of the linear regression between observed and simulated values of phenology dates, grain DM, stem and leaf N and grain N%. More emphasis is placed on the relative O_3 impact on yield and quality than simulations of absolute values, as the aim of the study was to develop a model that can capture relative O_3 impacts on crop quality.

2.4.3 Sensitivity Analysis

Sensitivity analyses are used to determine the proportion of variance in a desired model output attributed to a variation in the model input (Saltelli et al., 2008). In this study, we use a sensitivity analysis to identify and rank the sensitivity of grain N to different plant processes simulated by DO_3SE-Crop and the new N module. We identified 3 key mechanisms that can influence grain quality in the crop model: senescence onset, the end/ duration of senescence and the O_3 interruption of N remobilisation of the leaf and stem. A preliminary sensitivity analysis was conducted to identify the key parameters in DO_3SE-Crop influencing these processes. After reduction, 4 parameters which contribute the greatest to the variance of output variables representing these processes were identified for the sensitivity analysis (see Table 2.2). We use an extended Fourier amplitude sensitivity analysis (eFAST) to explain the variation in a chosen output variable attributed to varying selected input variables over a given range (Saltelli et al., 2008). The eFAST method is a commonly used method for sensitivity analyses and has previously been used by crop modellers to improve calibration (Silvestro et al., 2017; Vazquez-Cruz et al., 2014). The benefit of eFAST over other forms of sensitivity analysis is that it allows the interactions between model parameters to be quantified, it can sample the entire parameter space, and it is robust for non-linear relationships (Saltelli et al., 2008; Cariboni et al., 2007). These benefits make it a useful tool for complex systems such as crop models, where interacting, non-linear processes are common (Saltelli et al., 2008; Cariboni et al., 2007). The Python library SaLIB was used for all sensitivity analyses (Herman and Usher, 2019). The first sensitivity index, S1, quantifies the uncertainty in the output variable that is attributed to varying only that parameter. The total sensitivity index, ST, quantifies the uncertainty in the output variable that is attributed to varying a chosen parameter in combination with the other selected parameters (Saltelli et al., 2008). The range of values for the sensitivity analysis were taken from the theoretical maximum and minimum in the DO_3SE-Crop model for those mathematical equations. The ranges for $\gamma 4$ and $\gamma 5$ were determined using the breakpoint method, as described by Pande et al. (2024b). For the leaf and stem remobilisation equations, the minimum gradient is 0 as this assumes no O_3 effect on remobilisation for that plant part, and the maximum gradient was calculated by assuming that the other plant part has had as close to zero O_3 impact on remobilisation as is mathematically possible in the equation formulation. To ensure that the parameters remained within the 95% confidence interval of the experimental data on remobilisation, Figure 2.2 was plotted in Desmos, and the values of

m_{leaf} and m_{stem} were varied. For each case, when one parameter was set to zero, the other was adjusted to ensure that the remobilisation values fell within the specified confidence interval. If no value for m_{leaf} or m_{stem} satisfied this condition, the other parameter was incrementally increased from zero so that it had minimal impact on remobilisation while maintaining consistency with the 95% confidence interval. This approach allowed remobilisation to be reasonably approximated within the bounds of the experimental data.

Table 2.2: The parameters included in the sensitivity analysis along with a specification of the values for the ranges between which they were varied in during the analysis.

Parameter	Unit	Explanation	Minimum	Maximum
$\gamma 4$	-	O_3 long-term damage co-efficient determining onset of senescence	0.1	10
$\gamma 5$	-	O_3 long-term damage co-efficient determining maturity	0.1	1.5
m_{leaf}	-	Gradient of regression determining minimum leaf N concentration under O_3 exposure (influences how much leaf N is available for remobilisation)	0	3.024
m_{stem}	-	Gradient of regression determining minimum stem N concentration under O_3 exposure (influences how much stem N is available for remobilisation)	0	0.0312

2.5 Results

2.5.1 End of season grain DM and N% in grain, leaf and stem

Figure 2.4 shows the evaluation of the grain DM, and grain, leaf and stem N% simulations. Leaf and stem N data were only available in 2021, hence the leaf and stem plots only use data from 2021. Additionally, for 2021, the plant did not put on any grain (the reason for which is unknown (Brewster, Fenner and Hayes, 2024)) which meant it was not possible to use the grain DM or grain N data for that year. However, since this was the only year of data for which stem and leaf N% measurements were available and the plants developed and flowered normally, the decision was made to proceed with these data for stem and leaf parameterisation. For 2016, the model captured the grain DM and the grain N% more precisely than for the year 2015. In 2015, the under-estimate of grain DM resulted in an overestimation of grain N%. The stem and leaf N% at anthesis is better simulated than at harvest. Harvest leaf N is overestimated by between 20-120%, while harvest stem N overestimations range from ~40-120%. However, in both the stem and the leaf, N concentrations are over-estimated at both anthesis and harvest, despite the calibration showing the remobilisation of N from the leaf and stem under the

differing O_3 concentrations was well captured (see Figure 2.2). The R^2 values (calculated using scikit Learn, developed by Pedregosa et al. (2011)) for grain DM and grain N% are negative, implying that the model simulations are worse than using the mean of the observed data (scikit-learn developers, 2023).

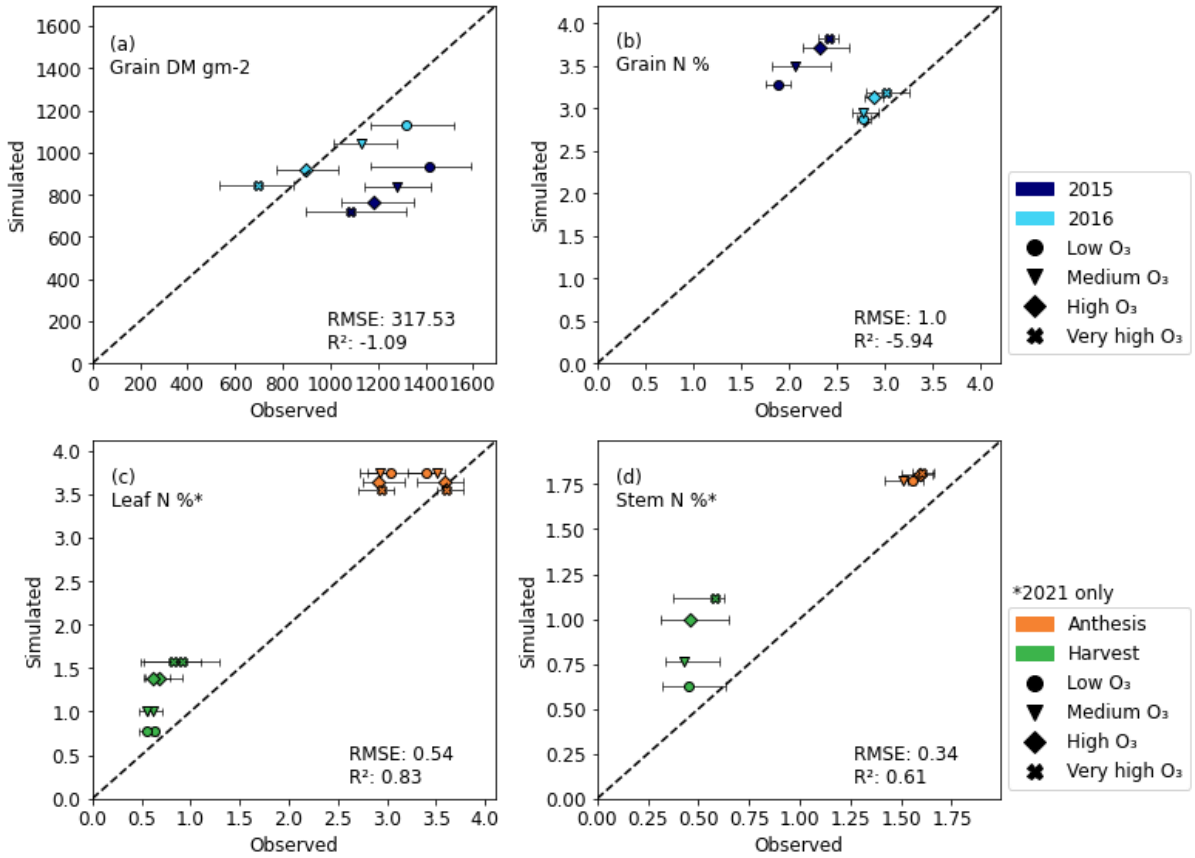

Figure 2.4: Output of the DO_3SE-Crop grain dry matter simulations at harvest (a), and the newly developed N module simulations of grain N% at harvest (b), leaf N% at anthesis and harvest (c), and stem N% at anthesis and harvest (d). The simulations shown are for the evaluation datasets only. The evaluation data available contained grain dry matter and N% for 2015 and 2016, whereas for 2021 the plant did not put on any grain, so this data was not used for evaluation. Leaf and stem N% data was only available for 2021. The RMSE and R^2 of the observed versus simulated data (not including error bars) are shown on the plots. The error bars represent the maximum and minimum of the experimental data, excluding outliers, for comparison with simulations. The leaf N% figure contains data for both the flag and 2nd leaf. DO_3SE-Crop and the new N module do not discriminate between these so simulations of leaf N% for flag and 2nd leaf are the same

The relative yield (RY) loss of the 2015 simulations is much better simulated than the 2016 simulations (Figure 2.5). However, the R^2 is 0, meaning that the simulations work equally well as when using the mean of the observed data (scikit-learn developers, 2023). When considering grain quality, the increase in grain N% that occurs as O_3 concentrations increase, is simulated very effectively with an R^2 of 0.6 and a RMSE of 4.9%. The % decrease in grain N content (grain N content measured in grams of N per m^2 of crop) is not simulated as well as the change in grain N concentration, as is seen from the lower R^2 (0.3) and greater RMSE (14.4). Further, Figure 2.5c shows that the model had trouble capturing the large differences in grain N content that occurred in 2016, compared to the much smaller differences in 2015.

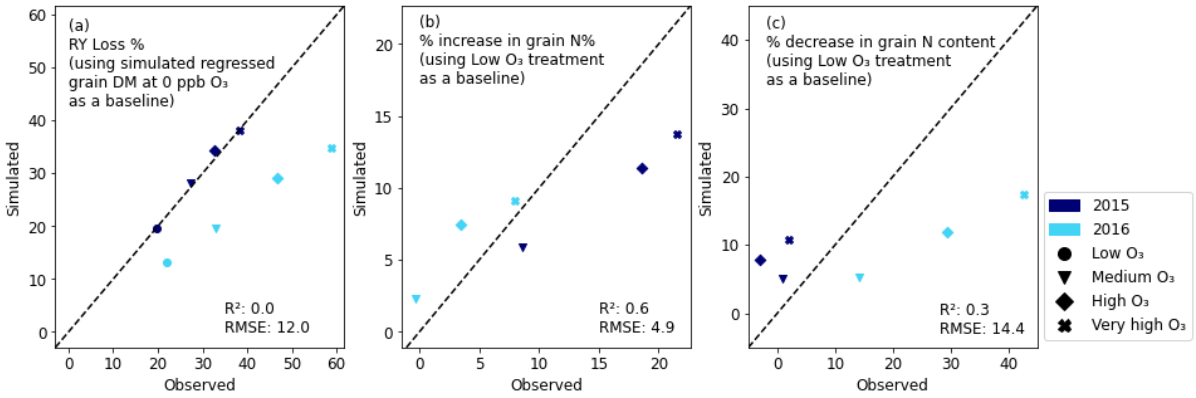

Figure 2.5: Relative plots of the evaluation data. (a) the relative yield (RY) loss of the grain DM when using the grain DM at 0 ppb (obtained by regressing the simulated and observed yields) as a baseline. (b) the % increase in grain N% and (c) the % decrease in grain N content (gm^{-2}) when using the low O_3 treatment as a baseline. The RMSE and R^2 of the observed versus simulated data (not including error bars) are shown on the plots.

2.5.2 Seasonal profiles of grain DM, grain N content, and N% in the grain, leaf and stem

The profile of grain DM accumulation over time for all treatments is shown in Figure 2.6 for 2015 and 2016, and for all years in supplementary Figure S2.5. From the profiles we see that initially accumulation of grain DM is slow, then at days 200 and 192 for 2015 and 2016 respectively, there is a rapid increase. From the plots we can see the O_3 effect on grain DM accumulation begins around 5-10 days post-anthesis.

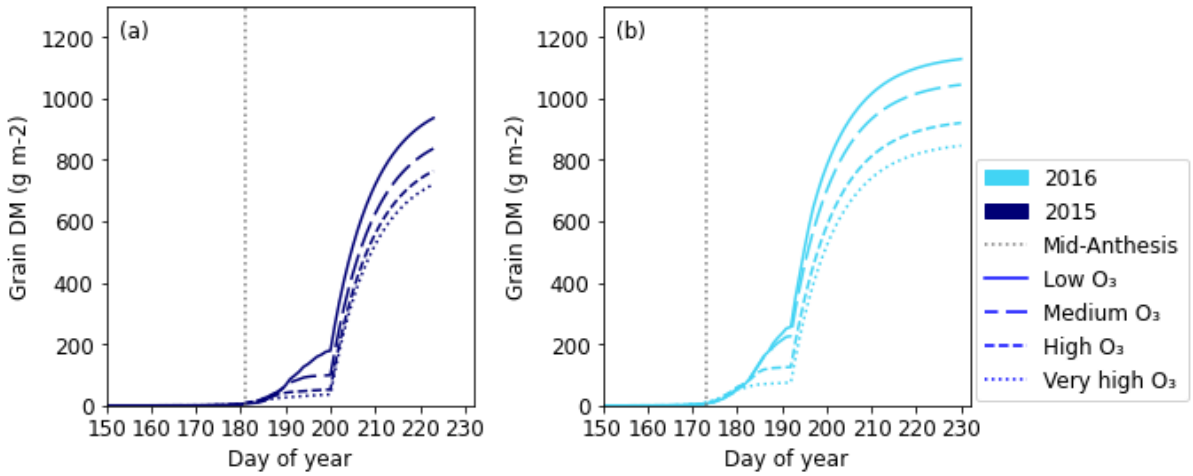

Figure 2.6: The profile of simulated grain DM for 2015 (a) and 2016 (b). Mid-anthesis is indicated on the graph as a vertical dotted line and the different line styles on the plot represent the simulations for the different O_3 concentrations.

Figure 2.7 shows the change in simulated grain N% and grain N content as a function of time under the different O_3 concentrations. As O_3 concentrations increase, the absolute grain N content in gm^{-2} (Figure's 2.7c and 2.7d) decreases for both years. Figures 2.7a and 2.7b appear to show a very sharp increase in grain N% as the grain starts filling with N after anthesis, and then after approximatley 20 days N concentration starts to decrease. This rapid increase is due to a difference in the accumulation rates of grain DM and N in the model, and is not representative of a plant process (see supplementary Figure S2.1). Due to the large spike in initial N concentrations, it is difficult to see the effect of O_3 on the end N concentrations.

Therefore, the end profiles of the grain N concentrations were enlarged in Figure's 2.7a* and 2.7b*. Once magnified, it is possible to see the increase in grain N% with increasing O_3 concentrations.

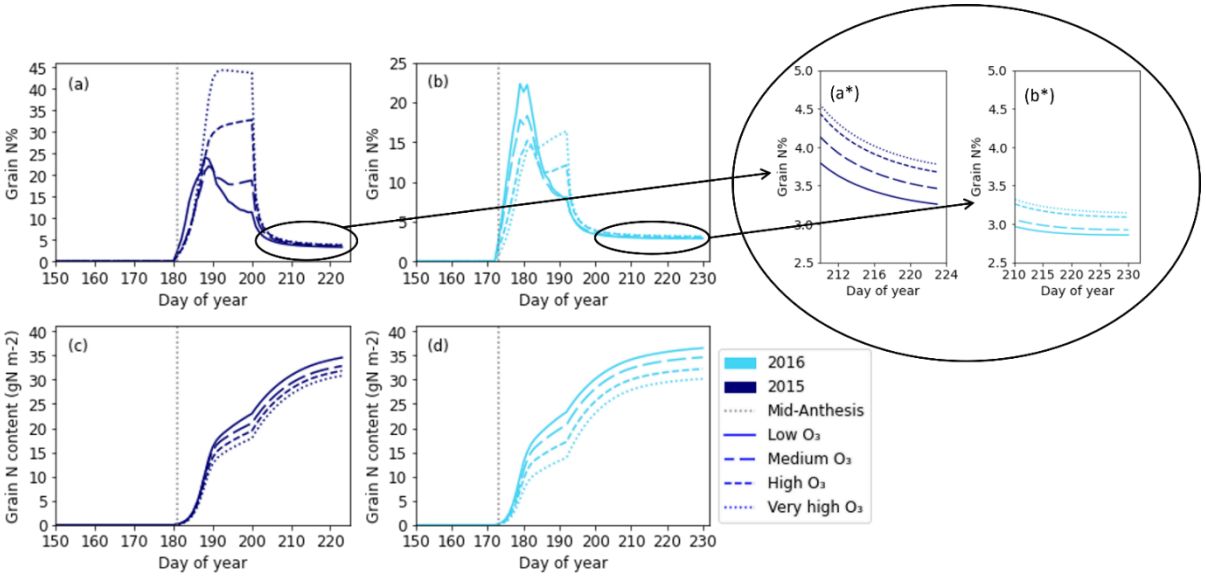

Figure 2.7: The simulated grain N% for 2015 (a), and 2016 (b), and the simulated grain N content in grams per metre squared for 2015 (c) and 2016 (d). The different line styles represent the different O_3 concentrations. Mid anthesis is indicated on the graph as a dashed vertical line for each year. The end points of figures (a) and (b) have been enlarged and are represented as figures (a) and (b*) respectively so that differences at the end points can be distinguished.*

Figure 2.8 shows the seasonal profile of leaf and stem N content and % under differing O_3 concentrations. Simulations of leaf and stem N% (Figures 2.8a and 2.8b) are relatively constant at their target N concentration (see Appendix A for target N explanation), until anthesis, since the model assumes no limitations to soil N uptake. The leaf and stem N content increase in line with increasing biomass. Post-anthesis, the stem begins to transfer N to the grain, and so the N concentration and content in the stem decreases (Figures 2.8b and 2.8d). The remobilisation of N from the stem to the grain continues provided the stem N concentration does not decrease below the minimum (Figures 2.8b and 2.8d). The levelling off of the stem N% in Figure 2.8b shows the minimum stem N concentration for that O_3 treatment has been reached. At higher O_3 concentrations the stem remobilises less N to the grains and the final concentration of N in the stem is greater (Figures 2.8b and 2.8d). Initially leaf N% and content decreases faster in the simulated wheat plants experiencing greater O_3 concentrations, as senescence begins earlier in these treatments (Figures 2.8a and 2.8c). Then, at around 20 days after mid-anthesis the O_3 effect on remobilisation takes over, and the leaf N% and content are greater under increased O_3 concentrations, due to the O_3 inhibition of N remobilisation.

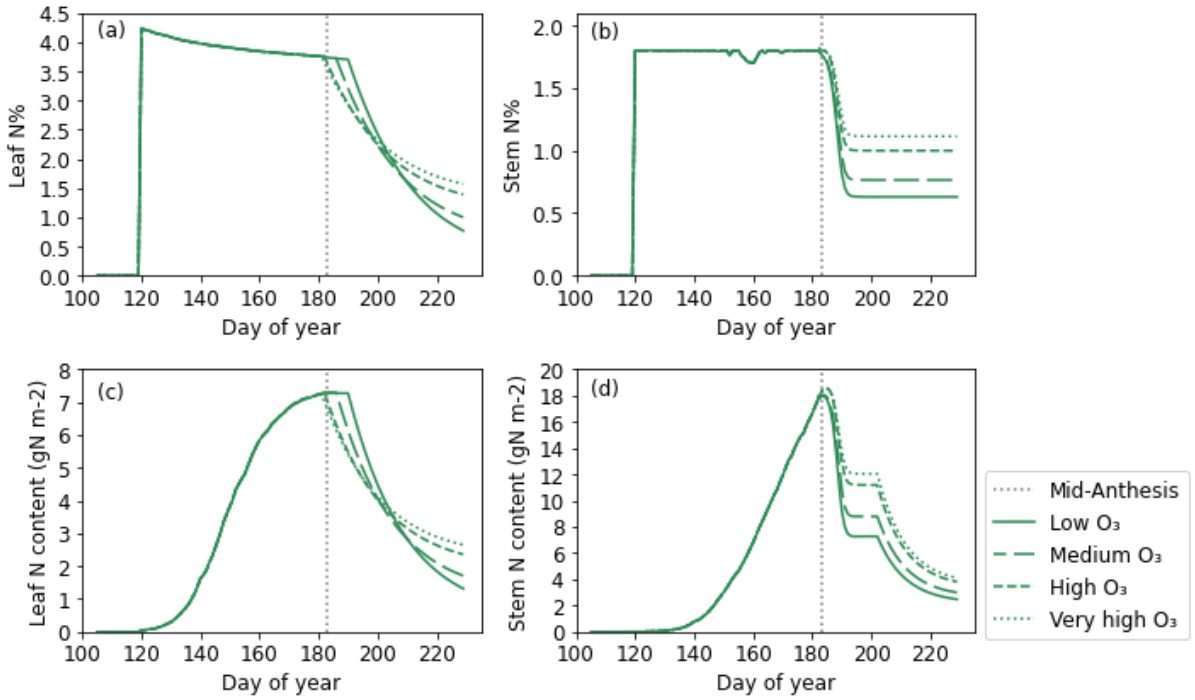

Figure 2.8: The simulated leaf (a) and stem (b) N%'s along with the simulated absolute N content in grams per metre squared for the leaf (c) and stem (d). Mid-anthesis is indicated on the graph as a vertical dotted line and the different line styles on the plot represent the simulations for the different O_3 concentrations. These plots are for the 2021 simulations only.

2.5.3 Sensitivity analysis results

Figures 2.9a and 2.9b illustrate the results of the sensitivity analysis study, and show that greater than 60% of the variance in both grain N content and grain N% in simulations of all O_3 treatments is explained by varying the parameter controlling the onset of leaf senescence. Absolute grain N content (gm^{-2}) is more sensitive to variations in senescence onset than grain N%, and grain N% is more sensitive to variations in senescence-end than grain N content. A threshold of ST > 0.1 was used by Silvestro et al. (2017) to identify influential parameters in their sensitivity analysis. In this study, senescence onset and senescence end were found to be the only influential parameters on grain N content and grain N%. The effect of varying the leaf and stem remobilisation accounts for less than 2% of the variance in both grain N% and grain N content for all O_3 simulations and can be considered non-influential. The interactions between the parameters were close to zero for the grain N%, as shown by a small difference between S1 and ST. Whereas a stronger interaction was seen when considering absolute grain N as the output. The negligible ST terms for leaf and stem remobilisation imply that the larger ST observed for senescence onset in Figure 2.9a must be due to the interaction between senescence onset and end. Onset of leaf senescence was simulated as occurring 15, 11 and 12 days earlier in the very high versus low treatments for 2015, 2016 and 2021 respectively.

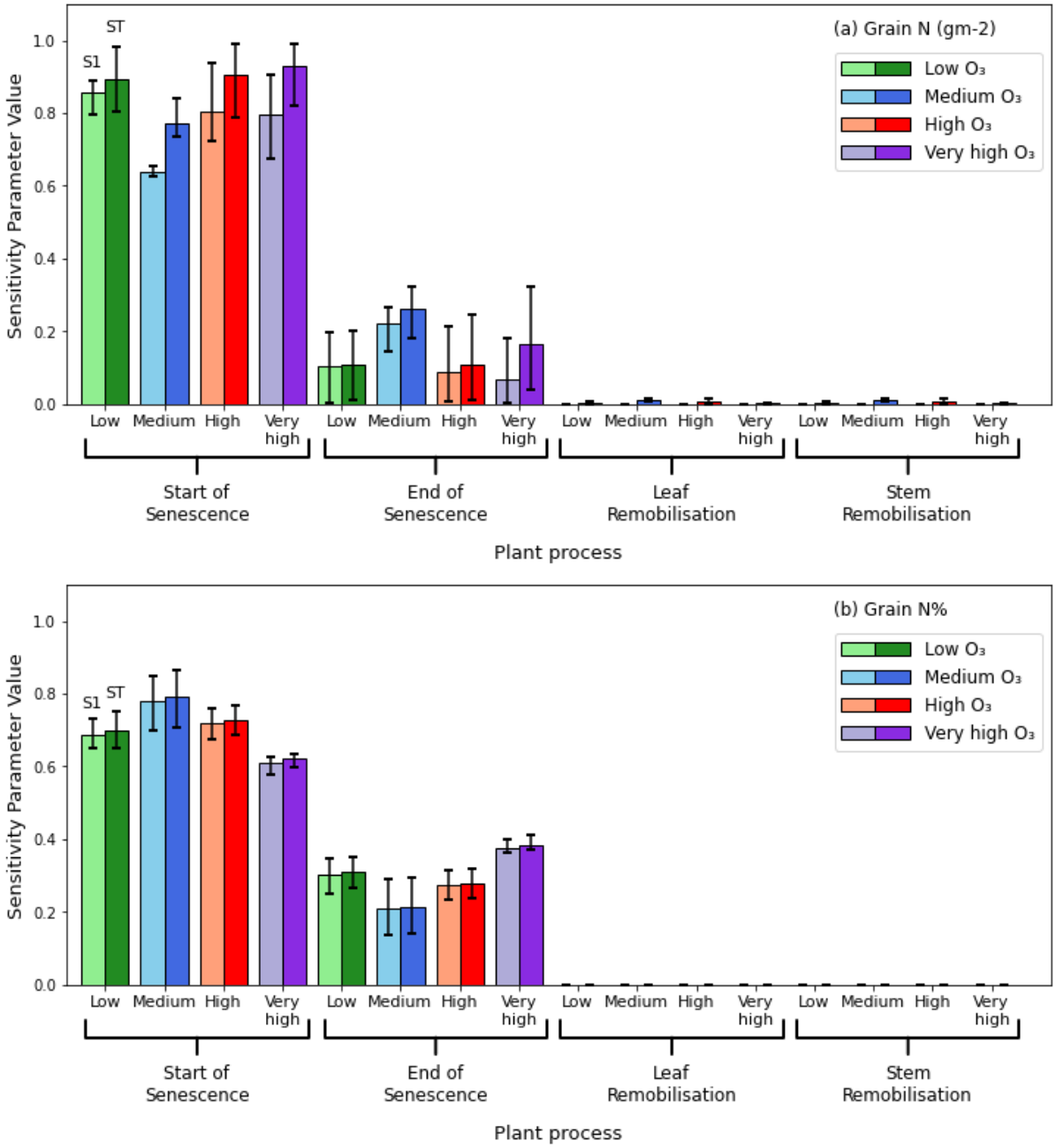

*Figure 2.9: Results of the sensitivity analysis. Lighter bars represent the first sensitivity index, S1, and the darker bars represent the total sensitivity index, ST. The different colours represent the different O_3 treatments and for clarity are also indicated on the x ticks. Braces group together the results of the sensitivity analysis for a particular plant process. The single model parameter chosen to represent each plant process in this analysis is described in section 2.4.3. This graph shows the averaged results for the 3 different years. The coloured bars represent the mean value of the sensitivity index for all 3 years, while the error bars represent the maximum and minimum values for that sensitivity index achieved in the runs for the 3 years. Figure (a) shows the results of the sensitivity analysis when considering the absolute grain N content in gN m^{-2} as the output parameter. Figure (b) shows the results of the sensitivity analysis when considering the percentage of N in the grain as the output parameter (100*gN gDM^{-1})*

2.6 Discussion

2.6.1 Evaluation of grain DM simulations

2.6.1.1 Grain DM simulations at harvest

The relative yield (RY) loss of the wheat in 2015 was more accurately simulated than in 2016, despite the grain DM being better simulated in 2016 than 2015 (Figures 2.4a and 2.5a). The variability of whether grain DM or RY loss is better simulated occurs because it is not possible to calibrate grain DM independently of the O_3 effect on yield loss, due to overnight O_3 concentrations of >20 ppb in the solar domes, which give a pollutant effect on yield even in the lowest O_3 treatment. Subsequently, there is a trade-off between achieving a greater accuracy in either grain DM or RY loss simulations as the current model construct was not able to capture both at the same time. In this study, the decision was made to give priority to greater accuracy on the relative O_3 effect on yield, so that we could better test our simulations of the relative effect of O_3 on grain quality. Further, the splitting of data for calibration and evaluation was randomised. The randomisation resulted in the calibration simulations for 2015 having a slightly lower grain DM, and hence the grain DM for 2015 in the evaluation simulations was underestimated.

2.6.1.2 Seasonal profiles of grain DM accumulation

Grain DM accumulation profiles follow an approximate sigmoid shape, with a "bump" in the grain DM profile occurring when the stem begins to allocate DM to the grain (Figures 2.6a, 2.6b and S2.5). Under higher O_3 concentrations, grain DM is reduced ~5-10 days after mid-anthesis. While profiles of grain DM accumulation have not yet been studied for O_3, they have been studied for other stressors such as drought. Given that both drought stress and O_3 damage are ROS mediated we can expect their effects on the seasonal profiles of DM and N to be similar, where the stresses occur continuously throughout the growing season (Khanna-Chopra, 2012; Emberson et al., 2018). Liu et al. (2020) found that drought-stressed wheat initially had a higher grain weight than well-watered wheat 7 days after anthesis, but by 28 days the well-watered wheat had surpassed the drought stressed wheat in weight. Similarly, Zhang et al. (2015) found the grain weight of drought-stressed wheat was higher 12-20 days after anthesis, but by 36 days had been surpassed by the well-watered wheat. In maize, Guo et al. (2021) found a decrease in kernel fresh weight under drought stress 10 days after anthesis, with the effect consistent to the end of the study, as in the present grain DM profiles for wheat. However, Liu et al. (2020) and Zhang et al. (2015) who did study wheat, did not observe a consistently lower grain DM for the drought-stressed wheat as observed in this study (Figure 2.6). However, their profiles were based on individual grains (Liu et al., 2020) and the thousand grain weight of the 4 main spikes (Zhang et al., 2015). Neither of those values take into consideration the reduced number of grains per plant that occurs under drought stress (Mariem et al., 2021). Reduced grain numbers are also observed under O_3 stress (Broberg et al., 2015). Therefore, a consistently lower grain DM profile when presented as a grain DM per metre squared (as in this study) may be expected for increasing levels of stress. Together, these data suggest that differences in grain DM accumulation under drought stress are evident as early as 7-10 days post-anthesis. Therefore, it is not unreasonable that our simulations to show a decrease in grain DM accumulation in O_3 exposed wheat 5-10 days after mid-anthesis. Further, considering the grain DM per metre squared, we may expect to see a consistently lower grain DM for plants experiencing greater O_3 stress.

2.6.2 Evaluation of grain N simulations

2.6.2.1 Grain N simulations at harvest

Harvest grain N% is simulated well for 2016, when the grain DM is more closely captured (Figure's 2.4a and 2.4b). However, in 2015, when the grain DM is under-estimated, the grain N% is over-estimated. The over-estimation of grain N% is reduced when the observed, rather than simulated, grain DM values are used to calculate grain N% (data not shown). This suggests that the newly developed N module can simulate the absolute grain N% under differing O_3 treatments accurately, provided grain DM is simulated well.

The model captured the increase in grain N% (100*gN gDM^{-1}) under elevated O_3 much better than the decrease in grain N content (gN m-2) (Figure's 2.5b and 2.5c). The model was calibrated to grain N% as the response of grain N% to O_3 was more consistent between years than grain N content. Between the two years of data there were large differences in the grain N content of the wheat at harvest, the reason for which is unclear, though it could partially be due to the differences in grain DM between the two years. Since the grain N content was so different between the 2015 and 2016 datasets for all treatments, the model struggled to match both years when simulating the decrease in grain N content. Additionally, the interdependence between grain DM and N meant that in the calibration, changing one of them subsequently changes grain N%, making the calibration process more difficult (see supplementary Figure S2.1). If the wheat in 2021 had put on grain, the grain N measurements would have been invaluable in determining which of 2015 and 2016 had the more common response of grain N to O_3 for the Skyfall cultivar. Having at least 3 datasets for model calibration allows outliers to be more easily identified, and more physiologically representative data selected for calibration.

2.6.2.2 Seasonal profile of grain N accumulation

The seasonal grain N content profiles (Figures 2.7c and 2.7d) match well with profiles seen in experimental work (Nagarajan et al., 1999; Bertheloot et al., 2008) and that can be constructed from available wheat N data (see supplementary Figure S2.2). There is a "bump" in our simulated grain N content (Figures 2.7c and 2.7d) which matches that of our simulated grain DM profile (Figure's 2.6a and 2.6b). The "bump" occurs because as stem DM decreases (due to remobilisation), it increases the available N for the grain. It is not thought that this "bump" represents the actual rate by which the grain fills with N, but instead occurs due to the complex interconnections between leaf senescence, leaf N remobilisation, stem N remobilisation and required N for the grains in the model.

The seasonal profiles of grain N content (Figures 2.7c and 2.7d) show that O_3 effects are distinguishable ~10 days after mid-anthesis, with the model simulating lower rates of accumulation of grain N content when wheat is exposed to higher concentrations of O_3. To our knowledge, no studies describe how the seasonal profile of grain N content accumulation varies under differing O_3 concentrations. However, again using that both O_3 and water stress are ROS mediated (Khanna-Chopra, 2012; Emberson et al., 2018), the response of grain N accumulation under water stress, compared to a well-watered treatment, could be comparable to grain N accumulation under different O_3 concentrations. Nagarajan et al. (1999) found varying responses in grain N accumulation between cultivars for water-stressed wheat, with some showing similar profiles to the control treatment and others experiencing a negative impact on both total N and rate of accumulation compared to the control.

In a study measuring N accumulation with and without irrigation, Panozzo and Eagles (1999) found that the irrigated wheat accumulated N more slowly per grain, but continued

accumulating for longer and ultimately had a higher N content per grain. In the current study, our simulations show that the grains accumulated less N content under O_3, which occurs due to the explicit modelling of a reduced remobilisation rate under higher O_3 concentrations (Figures 2.7c and 2.7d and Equations (2.2) and (2.3)).

Seasonal profiles of grain N% (Figures 2.7a and 2.7b) under different O_3 treatments are less consistent than the grain N content profiles. Initially, grain N% increases rapidly, then levels-off and decreases. Using data from Nagarajan et al. (1999) who measured grain N and carbon (C) of wheat cultivars at 3 time points post-anthesis under water stress and control conditions, we constructed time profiles of grain N% (see supplementary materials and Figure S2.4). The constructed profiles generally show an initial increase in grain N% which tends to decrease or level-off, as in the present study. Panozzo and Eagles (1999) measured grain weight and N for 7 time points post-anthesis, again allowing a profile of grain N% under dry and irrigated treatments to be constructed. The profiles show that the wheat grain N% decreases from 2.5% and levels off to 2% approximately 21 days after anthesis, matching the shape of our grain N% profile, though our peak grain N% is far too large at 15-45% (Panozzo and Eagles, 1999). In our study, the reason for the large peak in grain N% is that N accumulation occurs more rapidly after anthesis than grain DM, leading to a greater concentration of grain N (see supplementary Figure S2.1). If the initial rate of grain fill with N was slower, or grain DM accumulation was faster, our grain N% profiles would likely match the shape and magnitude of those constructed from Panozzo and Eagles (1999) or Nagarajan et al. (1999). It would be helpful to have measurements of grain N content and DM for multiple time points after anthesis under varying O_3 treatments, to develop a temporal understanding of grain N% response to O_3 for model parameterisation.

In 2015, grain N% is already higher in the elevated O_3 treatments around 10 days after anthesis, whereas in 2016 grain N% is initially higher in the lower O_3 treatments and then around 20 days after mid-anthesis, the elevated O_3 show a higher grain N% (Figures 2.7a and 2.7b). The difference in response of grain N% is due to the differences in the simulated rates of grain N and grain DM accumulation between the years. In the grain N% profiles constructed from Panozzo and Eagles (1999) (see supplementary Figure S2.3), the irrigated (non-stressed) wheat had a lower final grain N% than the dry (stressed) treatment and the difference was clear to see from > 10 days post-anthesis. Toward harvest, the effect of increased O_3 concentrations on increasing the grain N% is seen approximately 20 days after anthesis, when the initial sharp increase levels off and the concentrations reach more reasonable values.

2.6.3 Evaluation of stem and leaf N simulations

2.6.3.1 Stem and leaf N simulations at anthesis and harvest

The anthesis leaf and stem N% are captured well by the model but the effect of O_3 on harvest leaf and stem N% is exaggerated Figures 2.4c and 2.4d). Although the differences between harvest leaf and stem N% were non-significant (Brewster, Fenner and Hayes, 2024), there appears to be a slight decrease in final leaf and stem N% under the medium O_3 treatment and a subsequent increase for the high and very high O_3 concentrations. A potential reason for the decrease under medium O_3 concentrations could be an effect called hormesis, where a stressor initially induces a greater productivity in the plant and then, past a given threshold, has a negative effect (Agathokleous, Kitao and Calabrese, 2019). While it could be argued that hormesis is present for the data of Brewster, Fenner and Hayes (2024) in Figure 2.2 of this study, there are only 4 O_3 treatments which means it is not possible to parameterise the minimum point of the hormetic response. Whereas Broberg et al. (2017) had 5 O_3 treatments, yet did not

observe a hormetic response, and instead found it linear. If future experimental work looks at the O_3 impact on N remobilisation from the leaf and stem to the grain, it would be helpful to place a greater emphasis on O_3 treatments between 30-60 ppb to determine a potential turning point at which higher O_3 concentrations start to limit N remobilisation. This would enable parameterisation of a non-linear hormetic response for N remobilisation in wheat under O_3 exposure.

2.6.3.2 Seasonal profiles of leaf and stem N accumulation

Our simulations of leaf and stem N content and N% over time (Figure 2.8) show that they reach a peak before anthesis and decrease after anthesis, which is also shown by the stem and leaf N profiles constructed from available experimental data (see supplementary Figure S2.2). The levelling-off of the stem N content (Figure 2.8d) profile at approximately 190 days is a result of the model construct in that no N was required for the grains from the stem at that point.

Currently, there are no data in the literature describing the effect of O_3 on leaf or stem N status in crop plants over the course of the growing season to compare with the present study (Figure 2.8). However, one study by Bielenberg, Lynch and Pell (2002) did measure the variation in stem and leaf N content, over time, in hybrid poplar exposed to elevated O_3. In plants receiving the same N treatment, increased O_3 generally reduced the N content of the leaves and stem at each measurement point. Generally, the temporal profiles of N content had the same shape regardless of O_3 treatment (Bielenberg, Lynch and Pell, 2002). In our study, the stem N content was greater at every stage post-anthesis for greater O_3 concentrations due to the reduced remobilisation of nutrients under O_3 exposure (Brewster, Fenner and Hayes, 2024). By contrast, the leaf N content was initially reduced in wheat experiencing greater O_3 concentrations due to accelerated senescence, but the effect of the reduced remobilisation eventually outweighed the senescence effect, leading to greater N content in O_3 stressed wheat at harvest

2.6.4 Suggestions for improving the representation of plant growth in DO_3SE-CropN

It has been suggested that the reduced remobilisation of leaf and stem N under O_3 exposure occurs as a result of reduced N use efficiency, as O_3 accelerated senescence shortens the grain filling period (Broberg et al., 2021, 2017). However, Brewster et al. (2024) found an increase in residual flag leaf N concentration under O_3 exposure, despite not finding a difference in senescence onset, suggesting that the accelerated senescence and subsequent reduced N remobilisation efficiency is not the only factor increasing the residual N concentration in plant parts. Some researchers have suggested the increase occurs as defence proteins accumulate (Brewster, Fenner and Hayes, 2024; Sarkar et al., 2010). In the present study, we simulate the accelerated senescence that occurs under O_3 exposure, and we model the reduced remobilisation using simple linear equations (Equations (2.2) and (2.3)). Future work to understand the mechanism for the increase in residual N in the stem and leaf would help refine the model to more accurately plant processes.

Brewster, Fenner and Hayes (2024) found that N fertilisation reduced the N left in the leaf and stem at harvest under O_3 exposure, delaying senescence and protecting chlorophyll against O_3 damage. The current model construct does not simulate this effect and assumes the plant receives optimum N. No N stress or extra fertilisation was considered. Future iterations of this model incorporating soil N processes could use the work of Brewster, Fenner and Hayes (2024) to include N fertilisation and model the ameliorative effect of variable N fertilisation on O_3

damage. Additionally, this first iteration of the model does not include any feedback of plant N status on photosynthetic or growth processes. Future research may want to consider the feedbacks between leaf N levels and photosynthetic rate, with higher leaf N increasing photosynthetic rate, which could offset O_3 induced reductions (Pilbeam, 2010). Researchers may also want to consider the influence of a higher leaf N in potentially delaying O_3 induced early senescence onset (Nehe et al., 2020; Martre et al., 2006).

2.6.5 Sensitivity analysis results

The sensitivity analysis (Figures 2.9a and 2.9b) showed that the effect of varying leaf and stem remobilisation contributed little, if at all, to variations in grain N content or grain N% under the differing O_3 treatments. Further, the most influential parameter on grain N content and grain N%, was senescence onset; this does not change regardless of the O_3 treatment simulated. These results align with existing literature, which show that a shorter duration for grain fill leads to less time for nutrient remobilisation, subsequently impacting grain quality (Havé et al., 2017). Therefore, it is expected that the senescence parameters would have a large influence on grain N. Further, since the onset of leaf senescence is the beginning of leaf N remobilisation to the grain, it has a larger influence on grain N content and concentration than the end of leaf senescence (Havé et al., 2017). We also observed that the next most influential parameter on grain quality was associated with the end of senescence. It is unsurprising that senescence end also has influences on grain quality, as a later ending for senescence leads to more time for remobilisation. The limited influence of O_3 interruptions to leaf and stem remobilisation on grain quality relative to senescence parameters occurs as a result of the critical role of senescence in determining the start and end of nutrient remobilisation. Therefore, minor changes to remobilisation due to O_3 are constrained by senescence timing which is the ultimate determiner of the amount of N available for grain filling.

In our sensitivity analysis we observed a difference in the magnitude of S1 (the uncertainty in the output variable that is attributed to varying only that parameter) and ST (the uncertainty in the output variable that is attributed to varying a chosen parameter in combination with the other selected parameters) (Saltelli et al., 2008) between the different O_3 treatments. The non-linear response is unsurprising given the complex and interconnected nature of crop modelling. However, it isn't possible to determine whether this response is typical for wheat, since the present study considers data for only one cultivar and one location. If future work investigates multiple growing locations and wheat varieties and uncovers a similar response of the sensitivity indices for the differing O_3 concentrations, then the underlying crop modelling processes could be investigated to determine the reason for this effect.

2.6.6 Implications of sensitivity analysis results for growers

The sensitivity analysis results pose interesting questions around the importance of cultivars having an earlier or delayed senescence for maximising grain protein under O_3 exposure. Generally, a delayed onset of leaf senescence decreases grain protein content as there is a delay to the start of N remobilisation from the leaves to the grain (Havé et al., 2017; Sultana et al., 2021). A delayed senescence also decreases grain protein%, due to the reduction in grain N content and an increased length of photosynthetic activity that increases grain yield (Sultana et al., 2021; Nehe et al., 2020; Bogard et al., 2011). However, this is not always the case as there are several interacting effects from the environment (e.g. temperature, drought, O_3 or pathogens), N application and gene expression (Zhao et al., 2015; Nehe et al., 2020; Bogard et al., 2011; Gaju et al., 2014; Sultana et al., 2021). Stay-green cultivars have previously been

identified as allowing plants to maintain their photosynthetic capacity under heat and drought stress conditions (Kamal et al., 2019). Since O_3 damage is ROS mediated, similar to the damage from heat and drought stress (Khanna-Chopra, 2012), it is expected that stay-green cultivars will provide a similar increased yield for O_3 exposed wheat by delaying the stress induced early senescence onset. The impact of using stay-green cultivars on wheat grain protein under O_3 stress conditions is yet to be investigated. However, a decrease in grain protein content under O_3 exposure may be due to the delayed onset of remobilisation (Havé et al., 2017; Sultana et al., 2021). Zhao et al. (2015) genetically modified wheat plants to investigate the response of senescence, grain yield and grain N% when a senescence delaying gene was over-expressed. In the genetically modified wheat, the grain yields were similar to the control, but grain N% was increased (Zhao et al., 2015). Therefore, stay green wheat cultivars that do not experience a grain protein penalty should be considered by breeders and investigated for their suitability under differing O_3 concentrations.

2.6.7 Potential model applications

Simulations of crop N content can be easily converted into protein through the use of a simple conversion factor, or linear regressions if N or water stress conditions are present that have not been accounted for previously in the simulation (Mariotti, Tomé and Mirand, 2008; Liu et al., 2018; Tkachuk, 1969). Therefore, grain protein% can easily be obtained from grain N%. Further, by using protein%, amino acid concentrations can be simulated using regressions developed by Liu et al. (2019), allowing the model to be extended to simulate protein quality. In addition, by building on the work of Broberg et al. (2015) it would also be possible to link changes in N content under O_3 exposure, to changes in other grain mineral contents, such as zinc, magnesium and starch. Such relations would be simple to integrate given the model already simulates O_3 effects on N, and there seem to be similarities between the effect of O_3 on N and the effect of O_3 on other minerals (Broberg et al., 2015). These improvements would increase the nutritional relevance of the model.

The DO_3SE-Crop model takes inputs of temperature, PPFD, CO_2 concentrations and precipitation. There is also a built in soil moisture module which can simulate the effect of water stress on stomatal O_3 flux (Büker et al., 2012). Because of these features, the DO_3SE model is an ideal candidate for simulating the combined effects of O_3 pollution and climate change on crop yields. With the newly developed N module, this would allow the user to determine how O_3 pollution and climate change effects may interact to affect crop yield, quantity and quality, and hence dietary nutrition.

2.7 Conclusions

In summary, this study identified the key mechanisms for modelling N in wheat as soil N uptake, partitioning of N taken up from the soil between the leaf and stem, remobilisation of N from the leaves and stem to the grain, and the impact of O_3 on N remobilisation. Using these key processes, a new model was developed that can be used in combination with the existing O_3 deposition crop model, DO_3SE-Crop, to simulate the O_3 impact on wheat N. The newly developed model is the first to simulate the effect of O_3 on N in any plant species. After evaluation, a sensitivity analysis was applied to the model to identify the key plant process that affects grain quality under O_3 exposure. It was found that O_3 induced early senescence onset was the key plant processes affecting grain quality under O_3 exposure, regardless of O_3 treatment. We recommend that breeders focussing on stay-green cultivars aim to develop cultivars that do not suffer a protein penalty. If such cultivars can maintain their yield and

quality under abiotic stresses, they may also be tolerant to O_3 in terms of both yield and crop quality; testing this would be beneficial to further understand the implications of O_3 on global food and nutritional security.

2.8 Appendix A

Detailed below are the equations and references for the N module of the DO_3SE-Crop N module. We found Wang & Engel's (2002) approach to writing up their crop model to be very effective so we take inspiration from their approach and present a description of the processes and references in the text, and tabulate the specific equations, with their corresponding references in each section. The values of parameters used in the module and their corresponding sources are tabulated also. For a full mathematical description of the phenology, photosynthesis, carbon allocation and ozone damage processes of DO_3SE-Crop, please refer to Pande et al. (2024).

At the current stage of development, the N module is not integrated within DO_3SE-Crop. It requires the output file from a DO_3SE-Crop run in order to perform the N simulations.

2.8.1 Soil N Uptake

Pre-anthesis a maximum N uptake ($NUP_{pre,max}, in\ gN\ m^{-2}\ day^{-1}$) is defined (Soltani and Sinclair, 2012). The actual N uptake by the crop pre-anthesis ($NUP_{pre}, gN\ m^{-2}\ day^{-1}$) is calculated using the work of Soltani and Sinclair (2012). Daily N uptake is the sum of the N associated with the increase in LAI that day ($LAI_{growth}, m^2\ day^{-1}$), the increase in dry matter of the stem that day ($DW_{stem\_grth}, g\ DW\ m^{-2}\ day^{-1}$) and the N deficit that day ($N_{stem,deficit}, g\ N\ m^{-2}\ day^{-1}$), that has been accumulated over the plant's life:

$$NUP_{pre} = DW_{stem\_grth} \times \left[N_{stem,target}\right] + LAI_{growth} \times [N_{leaf,target}] + N_{stem,deficit}\,. \quad \text{(A2.1)}$$

$\left[N_{stem,target}\right]$ is the target N concentration of the stem and $[N_{leaf,target}]$ is the target N concentration of the leaf (Soltani and Sinclair, 2012). The $N_{stem,deficit}$ is defined as the difference between the target stem N for its mass, and its current N content (N_{stem}):

$$N_{stem,deficit} = DW_{stem} \times \left[N_{stem,target}\right] - N_{stem}. \quad \text{(A2.2)}$$

where DW_{stem} is the dry weight of the stem in $g\ m^{-2}$. If $NUP_{pre} > NUP_{pre,max}$ we set $NUP_{pre} = NUP_{pre,max}$, otherwise, the crop takes up N equal to NUP_{pre}.

Post-anthesis, N uptake is a function associated with the capacity of the stem to hold nitrogen. The basis for this equation is taken from SiriusQuality (Martre et al., 2006). The potential N uptake post anthesis ($NUP_{post,pot}\ gN\ m^{-2}\ day^{-1}$), is calculated as follows:

$$NUP_{post,pot} = NUP_{post,max} \times \frac{T_{grainfill} - T}{T_{grainfill}} \quad \text{(A2.3)}$$

where $NUP_{post,max}$ is the maximum N uptake post-anthesis, $T_{grainfill}$ is the thermal time (in °C days) between the end of grain filling (i.e. harvest in the present model) and the start of anthesis, and T is the current thermal time (in °C days) since anthesis. Subsequently, the stems target capacity to hold N is calculated and compared to the current amount of N stored in the stem. If the current stem N, N_{stem} in $g\ N\ m^{-2}$, exceeds the target capacity, no N is taken up that day (Equation (A4)).

$$NUP_{post} = 0 \;\; if \;\; N_{stem} \geq DW_{stem} \times \left[N_{stem,target}\right] \quad \text{(A2.4)}$$

If the current stem N is less than the target capacity, the N taken up is equal to the minimum of the stem's current capacity and the potential uptake.

$$NUP_{post} = min\left(NUP_{post,pot}, DW_{stem} \times \left[N_{stem,target}\right] - N_{stem}\right) \quad \text{(A2.5)}$$

Table A2.1: Citations and names for equations describing soil N uptake

Equation number	Equation name	Developed according to…
(A2.1)	Actual plant N uptake pre-anthesis	(Soltani & Sinclair, 2012)
(A2.2)	N stem deficit	(Soltani & Sinclair, 2012)
(A2.3)	Potential daily N uptake post-anthesis	(Martre et al., 2006)
(A2.4)	Post-anthesis N uptake if current stem N is greater than target	developed in this study to ensure stem does not get an unlimited supply of N
(A2.5)	Post-anthesis N uptake if current stem N is less than target	(Martre et al., 2006) and adapted in this study to account for current stem N

Table A2.2: Default and present parameterisations for the N module along with citations as to where the original default value was obtained

Parameter	Original Value	Value used in this study	Source for original value
$NUP_{post,max}$	0.4 $g\ N\ m^{-2}\ day^{-1}$	0.4 $g\ N\ m^{-2}\ day^{-1}$	(Martre et al., 2006)
$NUP_{pre,max}$	0.25 $g\ N\ m^{-2}\ day^{-1}$	0.65 $g\ N\ m^{-2}\ day^{-1}$	(Soltani and Sinclair, 2012)
$\left[N_{stem,target}\right]$	0.015 $g\ N\ g^{-1}\ DW$	0.018 $g\ N\ g^{-1}\ DW$	(Soltani and Sinclair, 2012)
$[N_{leaf,target}]$	1.5 $g\ N\ m^{-2}$	1.65 $g\ N\ m^{-2}$	(Soltani and Sinclair, 2012)

2.8.2 N partitioning to the stem and leaf

Pre-anthesis, the equations describing how the uptake of N is split between the leaf and stem are based on the work of Soltani and Sinclair (2012), and no N is allocated to the grains at this time. The stem and leaf have a defined target and minimum N concentration which can be calibrated for different wheat cultivars. In Soltani and Sinclair (2012) both the target and minimum stem and leaf N concentrations are constants. In this study, the minimum N concentrations of the leaf and stem are variable based on the ozone concentrations. This allows a reduction in remobilisation of N from the leaf and stem to the grain, as found by Brewster et al. (2024), under higher ozone concentrations. It is easiest to see the structure of the N partitioning code in Figure A2.1. The write up of pre-anthesis N partitioning to the leaves and stem is split

into 2 sections based on whether the stem is experiencing a N deficit (i.e. stem N is less than its minimum).

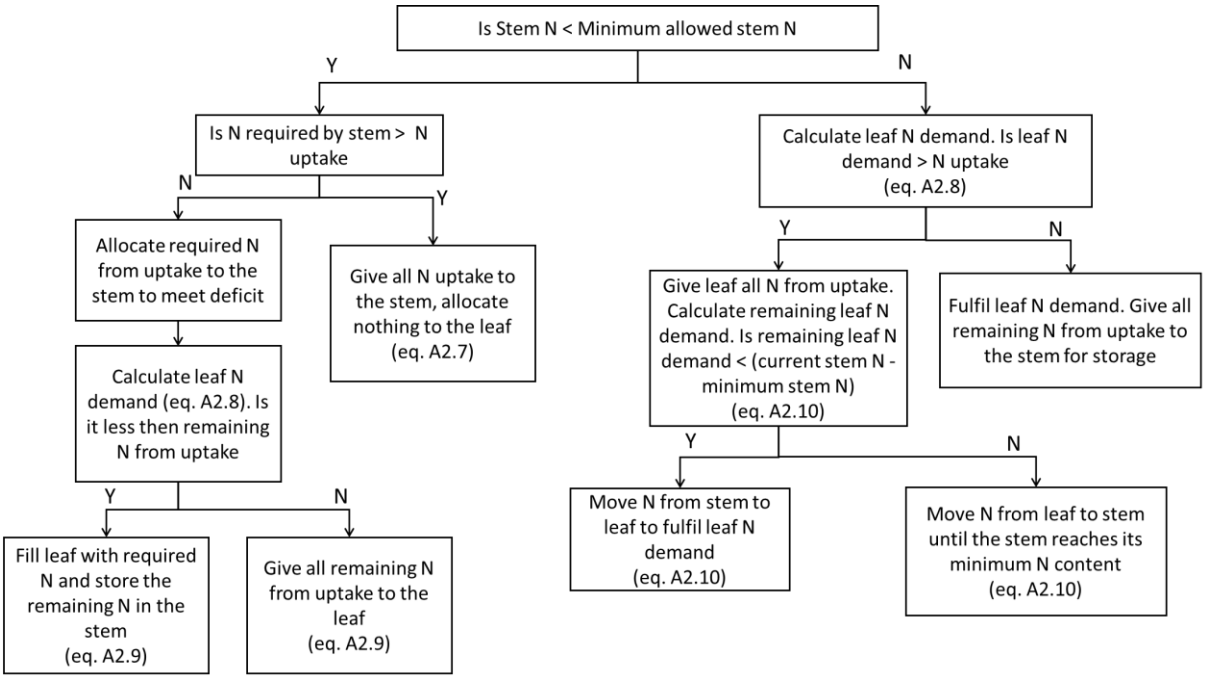

Figure A2.1: Figure showing the allocation of N to the stem and leaf before anthesis. Y and N represent "yes" and "no" respectively. Equation definitions are referenced appropriately. Where equation numbers are not indicated additional information can be found in the text. Equations and model structure for N allocation are based on those of Soltani & Sinclair (2012) and modified for the purposes of this study.

Firstly, the current stem N concentration is compared to the minimum allowed stem N concentration, $\left[N_{stem,min}\right]$.

2.8.2.1 If Current stem N concentration is less than the minimum stem N concentration (N deficit)

If the current stem N concentration is less than the minimum concentration, then allocation of N to the stem is prioritised.

$$N_{req,stem} = DW_{stem} \times \left[N_{stem,min}\right] - N_{stem} \quad \text{(A2.6)}$$

where $N_{req,stem}$ is the N required by the stem to meet its deficit in $g\ N\ m^{-2}$. If $N_{req,stem}$ is greater than the amount of N taken up that day ($NUP, g\ N\ m^{-2}$), the N entering the stem pool ($N_{into,stem}, g\ N\ m^{-2}$) is capped at the amount of N taken up.

$$if\ N_{req,stem} > NUP_{pre} \quad \begin{cases} N_{into,stem} = NUP \\ N_{leaving,leaf} = 0 \\ N_{leaving,stem} = 0 \\ N_{into,leaf} = 0 \end{cases} \quad \text{(A2.7)}$$

Equation (A2.7) has been modified from Soltani and Sinclair (2012) who allow leaf area to senesce and provide the stem with N if there is not enough to meet the stem's N demand. The senescing of leaf area to provide N was removed in the current iteration of DO_3SE-CropN. Currently, there is no interdependencies between the N module and DO_3SE-Crop. The DO_3SE-Crop model runs and then the N module is applied to the output of DO_3SE-Crop to calculate crop N. It is therefore not possible to senesce leaf area to provide N in the current version of the N module as the leaf area was already determined in DO_3SE-Crop.

If there was enough N to meet the deficit of the stem, then $N_{into,stem} = N_{req,stem}$ and $N_{leaving,stem} = 0$. Then, the N required for maintaining leaf area growth at its target N concentration ($N_{req,leaf}, g\ N\ m^{-2}$) is calculated using equation (A2.8).

$$N_{req,leaf} = LAI_{growth} \times [N_{leaf,target}] \quad \text{(A2.8)}$$

If $N_{req,leaf}$ can be fulfilled by the N left over after maintaining the stem growth at minimum N concentration, then N is partitioned to the leaves and any leftover N is partitioned to the stem for storage. If the leftover N cannot fulfil the demand of the leaf, then the remaining N from uptake is partitioned to the leaves (Soltani and Sinclair, 2012).

$$N_{into,leaf} = \begin{cases} N_{req,leaf} & if\ N_{req,leaf} \leq NUP - N_{into,stem} \\ NUP - N_{into,stem} & if\ N_{req,leaf} > NUP - N_{into,stem} \end{cases} \quad \text{(A2.9)}$$

2.8.2.2 If Current stem N concentration is not less than the minimum stem N concentration (no N deficit)

If the stem N is not below its minimum, then N is first allocated to the leaves. The N required by the leaves is calculated in accordance with equation (A8). If the N required by the leaves is less than the N uptake that day, the N required by the leaves is transferred to them: $N_{into,leaf} = N_{req,leaf}$ and $N_{leaving,leaf} = 0$. Subsequently, the remaining N from uptake is transferred to the stem, $N_{into,stem} = NUP - N_{into,leaf}$ and $N_{leaving,stem} = 0$

If the leaves required more N than was taken up by the crop, the extra demand is fulfilled by using some of the stem N. The N from the stem is removed only until the stem reaches its minimum concentration.

$$N_{leaving,stem} = \begin{cases} 0 & if\ N_{req,leaf} \leq NUP \\ \min\left(N_{req,leaf} - NUP,\ N_{stem} - (DW_{stem} \times [N_{stem,min}]\right) & if\ N_{req,leaf} > NUP \end{cases} \quad \text{(A2.10)}$$

In equation (A10), the minimum function ensures that the stem N does not fall below its minimum. In the scenario that the leaves required more N than taken up by the crop, $N_{leaving,leaf} = 0$ and $N_{into,stem} = 0$.

Table A2.3: Citations and names for equations describing N partitioning to the stem and leaf

Equation number	Equation name	Developed according to...
(A2.6)	The N required by the stem for growth	(Soltani and Sinclair, 2012)
(A2.7)	The N partitioned to the leaf and stem if the stem has a N deficiency and N uptake is not great enough to meet it	Soltani and Sinclair (2012) and adapted to remove leaf senescence releasing N in this study
(A2.8)	The N required for leaf area expansion	(Soltani and Sinclair, 2012)

(A2.9)	The N going into the leaf pool if N uptake met the stem N deficit	(Soltani and Sinclair, 2012)
(A2.10)	The N leaving the stem to maintain leaf area expansion under no stem N deficit	Soltani and Sinclair (2012) and adapted in this study to ensure stem N does not go below its minimum

2.8.3 N partitioning to the grain

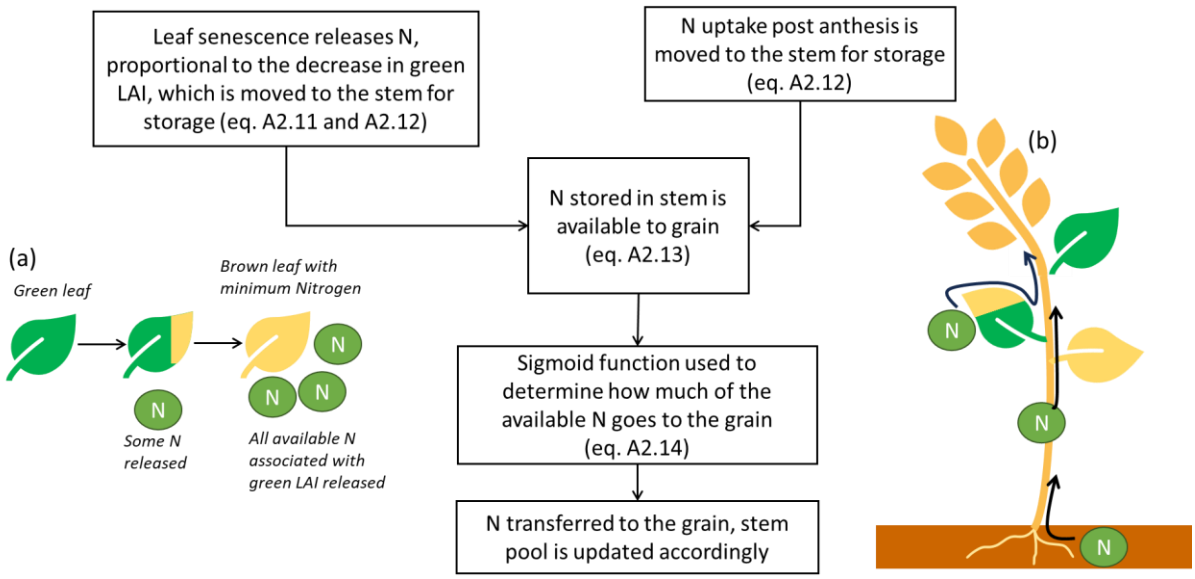

Figure A2.2: Figure showing the allocation of N to the wheat grains post-anthesis with equations indicated appropriately. Sub-image (a) is a visual representation of a leaf releasing N as the leaf area senesces. Sub-image (b) shows the 3 locations where N is transferred to the grain from: post anthesis N uptake, N stored in the stem, senescing leaf area.

After anthesis, the grain begins to fill with N and the model equations change to reflect that the priority is grain fill, not leaf area expansion or growth. After anthesis $N_{into,leaf} = 0$ always. As leaf area senesces, N is released:

$$N_{leaving,leaf} = \left(LAI_{yesterday} - LAI_{today}\right) \times \left(\frac{N_{leaf}}{LAI_{yesterday}} - \left[N_{leaf,min}\right]\right) \quad \text{(A2.11)}$$

where $LAI_{yesterday}$ and LAI_{today} represent the values of the leaf area index yesterday and today as calculated in DO_3SE-Crop. N released from the leaf, and N taken up by the plant post-anthesis are added to the stem N pool for storage, as they would have to travel through the stem to reach the grains (Sanchez-Bragado, Serret and Araus, 2017). The stem Nitrogen is then updated accordingly:

$$N_{into,stem} = N_{leaving,leaf} + NUP_{post} \quad \text{(A2.12)}$$

Not all of the N in the stem is available to be transferred to the grain as the stem has a minimum N concentration. Therefore, the available stem N (often referred to as the labile pool in other crop models) is calculated as:

$$N_{available} = N_{stem} - \left(DW_{stem} \times \left[N_{stem,min}\right]\right) \quad \text{(A2.13)}$$

The fraction of $N_{available}$ that is transferred to the grain each day is determined through a sigmoid function. The sigmoid was chosen as it uses only two extra parameters which allows the start and rate of grain fill with N to be customised without the addition of much complexity. The N in the $N_{available}$ pool can be transferred to the grain, or it can remain as part of the stem. The sigmoid determines the fraction of N going to the grain from $N_{available}$. The fraction increases as the plant develops. Multiplying $N_{available}$ by the sigmoid function gives the amount of N transferred to the grain that day. α_N and β_N are the coefficients that customise the onset and rate of grain fill. They can be calibrated to customise grain fill.

$$N_{to\_grain} = N_{available} \times \frac{1}{1 + exp(-\alpha_N(dvi - \beta_N))} \quad \text{(A2.14)}$$

Once N has been transferred to the grain, the leaf and stem N pools are decreased according to their N availability to account for this transfer. Figure A2.2 diagrammatically represents the grain filling process and Figure A2.3 shows an illustration of the sigmoid function with varying parameterisations to control grain fill.

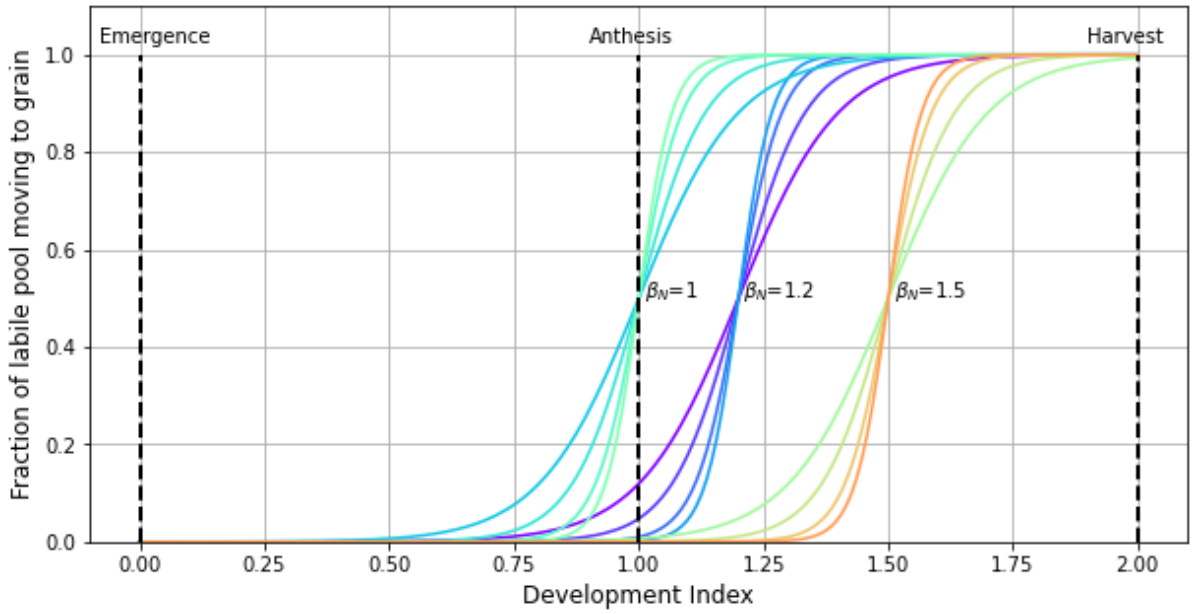

Figure A2.3: Plot showing example parameterisations of α_N and β_N for customising the sigmoid function describing the fraction of labile N moving to the grain. For each value of β_N, values of α_N of 10, 15, 23 and 30 are plotted to show how the rate, start and end of grain fill can be customised. Though $\beta_N = 1$ has been plotted to illustrate how the shape of the function can be customised, care should be taken if using this value, as for lower values of α_N it can imply grain filling with N begins midway between emergence and anthesis. Sensible parameterisations should be chosen.

Table A2.4: Citations and names for equations describing grain filling with N

Equation number	Equation name	Developed according to...

(A2.11)	N released from senescing leaves	Based on the equations in Soltani & Sinclair (2012) describing release of N from the leaves, but adapted for this study to match desired variables
(A2.12)	Update stem N pools	(this study)
(A2.13)	Calculate available N in stem	Based on the equations in Soltani & Sinclair (2012) describing release of N from the stem, but adapted for this study to match desired variables and incorporate post anthesis N uptake
(A2.14)	Grain N sigmoid function	(this study)

Table A2.5: Parameterisation of α and β parameters for grain filling

Parameter	Value used in this study	Source
α_N	23	(this study)
β_N	1.2	(this study)

2.8.4 O_3 impact on N remobilisation

The effect of ozone on grain N has been described in the main body of this study but will be discussed with relation to the equations and how they link with the previously described model structure here. Broberg et al. (2017) and Brewster et al. (2024) found that as ozone concentrations increased, the fraction of N in the leaf and stem at harvest, that was present at anthesis, increased. In essence, the remobilisation of N from the leaves and stem to the grains decreased. A regression of the combined data from Broberg et al. (2017) and Brewster et al. (2024) representing the remobilisation is shown in Figure 2.2 of the main body of the study.

To represent the reduced remobilisation under increased ozone exposure, the remobilisation regression was used to calculate new values of $[N_{stem,min}]$ and $[N_{leaf,min}]$ under ozone exposure. The fraction of N remaining in the leaf and stem at harvest that was there at anthesis (fN_{remob}) is approximated by:

$$fN_{remob} = \frac{DM_{leaf,harv} \times [N_{leaf,min}] + DM_{stem,harv} \times [N_{stem,min}]}{DM_{leaf,anth} \times [N_{leaf,targ}] + DM_{stem,anth} \times [N_{stem,targ}]} \quad \text{(A2.15)}$$

Equation (A15) assumes the anthesis leaf and stem N concentration is the same as the target N concentration, as the first iteration of the model assumes no N limitation. Additionally, for calibration purposes, the "harvest" N concentration was assumed to be the same as the minimum N concentration. In the model itself this would not occur as not all available N will be remobilised due to ozone effects on senescence. However, for calibration purposes equation (A15) is a good approximation. Using equation (A2.15), minimum values of leaf and stem N for the differing ozone treatments were manually altered for each ozone concentration, to estimate values for the N remobilisation (red points on Figure 2.2) that form a linear regression fitting inside the 95% CI. The leaf and stem minimum N concentrations of each red point were extracted. The minimum leaf N concentration, and minimum stem N concentration, were regressed separately with M12 to give regressions describing how the minimum N concentration in the plant part varies with ozone concentration:

$$\frac{[N_{leaf,min}]}{1\ gN\ LAI^{-1}} \times 100 = m_{leaf} \times \frac{[O_{3,M12}]}{1\ ppb} + c_{leaf} \quad \text{(A2.16)}$$

$$\frac{[N_{stem,min}]}{1\ gN\ DM^{-1}} \times 100 = m_{leaf} \times \frac{[O_{3,M12}]}{1\ ppb} + c_{stem} \quad \text{(A2.17)}$$

Table A2.6: Citations and names for equations describing the O_3 effect on N remobilisation

Equation number	Equation name	Developed according to...
(A2.15)	The fraction of N remaining in the leaf and stem at harvest that was there at anthesis	(this study)
(A2.16)	Ozone effect on minimum leaf N concentration	(this study)
(A2.17)	Ozone effect on minimum stem N concentration	(this study)

Table A2.7: Parameterisation of parameters associated with the ozone effect on N grain filling as used in the DO$_3$SE-CropN model

Parameter	Value	Source
m_{leaf}	0.798	(this study)
m_{stem}	0.0138	(this study)
c_{leaf}	10.89	(this study)
c_{stem}	0.2293	(this study)

2.8.5 Calculating leaf N concentration

In the DO$_3$SE-Crop model, green leaves are photosynthesising leaves, and brown leaves are senesced leaves. In the N module, the N associated with the senesced LAI is released (as described in section 2.8.3). Leaf area which has senesced will have the minimum leaf N concentration. Green leaf area which has not senesced will have a higher N concentration. An average leaf N concentration can be calculated by taking the absolute N in both green and brown leaves and dividing it by the total (green + brown) leaf DM.

2.9 Supplementary information

2.9.1 Comparison of crop models that simulate N processes

Table S2.1: Summary of the processes employed by each crop model to simulate N. ' Indirect Env. Impacts' indicates whether water (W), CO2, or heat/ temperature are used at any stage in the model and could indirectly influence grain N through their impacts on biomass, uptake or photosynthesis, for example. ' Direct Env. Impacts' indicates which environmental variables (heat or water stress (WS) or O_3) are included as a direct influence on the grain N. The key is as follows: N demand of plant part is determined by a minimum and maximum, and/or critical N concentration = N_Dem_Part, N demand at crop/plant level is determined by a minimum and maximum, and/or critical N concentration = N_Dem_Crop, Define a N pool available to grain and set a daily rate of transfer from pool to grain = N_Grn_Rate, Define a N pool available to grain and fulfill a daily grain N demand from pool = N_Grn_Dem, N is defined on a shoot/crop basis so grain/harvest N is not distinguishable = N_Shoot, Relative C:N ratios between different plant parts = C_N. Phenology modified by N stress speeding up aging = Phen, Senescence accelerated by N stress = Sen, Biomass accumulation modified by N availability = Bio, Photosynthesis modified by N availability = Photo, Leaf area modified by N availability = L_A, O = Other, / = not simulated

Model	N partitioning	Grain/ harvest/ storage organ N	Plant processes	Indirect env. Impacts	Direct env. Impacts	Source
AFRCWheat2	N_Dem_Part	N_Grn_Dem	Phen, Sen, Bio, L_A	W, CO_2, Heat	/	(Porter, 1993)
APSIM-NWheat	N_Dem_Part	N_Grn_Dem	Phen, Sen, Bio	W, CO_2, Heat	Heat	(Zheng et al., 2015)
CERES-Wheat	N_Dem_Part	N_Grn_Rate	Sen, Photo, L_A	W, CO_2, Heat	Heat	(Godwin and Allan Jones, 1991)
CN-Wheat	O*	O*	Photo	W, CO_2, Heat	/	(Barillot, Chambon and Andrieu, 2016b)
CropSIM-Wheat	N_Dem_Part	N_Grn_Dem	Bio, L_A	W, CO_2, Heat	Heat	(Hunt and Pararaiasingham, 1995)
CropSyst	N_Dem_Crop	N_Shoot	Bio	W, CO_2, Heat	WS	(Stöckle, Donatelli and Nelson, 2003)
Daisy	N_Dem_Part	N_Shoot	Photo	W, CO_2, Heat	/	(Hansen et al., 1991)
DO_3SE-CropN	N_Dem_Part	O (this study)	/	W, CO_2, Heat	O_3	This study
EcoSys	N_conc_grad	N_Shoot	/	W, CO_2, Heat	/	(Grant, 1998)
EPICWheat	N_Dem_Crop	/	Bio	W, Heat	/	(Williams et al., 1989)

Table S2.1 (continued)

Model	N partitioning	Grain/ harvest/ storage organ N	Plant processes	Indirect env. Impacts	Direct env. Impacts	Source
Expert-N-Sucros	N_Dem_Part	Unclear	Unclear	W, CO_2, Heat	Unclear	(Kropff and Laar, 1993; Priesack, Gayler and Hartmann, 2006)
FASSET	N_Dem_Part	N_Dem_Part	Bio, Photo, L_A	W, CO_2, Heat	/	(Lægdsmand, 2011)
InfoCrop	N_Dem_Part	N_Grn_Dem	Phen, Bio, (Photo?), Sen	W, CO_2, Heat	Heat	(Aggarwal et al., 2006)
Jules	C_N	/	Photo	W, CO_2, Heat	/	(Best et al., 2011; Clark et al., 2011)
LPJml	C_N	C_N	Photo, Bio	W, CO_2, Heat	/	(Sitch et al., 2003; Von Bloh et al., 2018)
Pan et al. (2006)	O**	N_Grn_Rate	Sen	W, Heat	Heat, WS	(Pan et al., 2006)
SiriusQuality2	N_Dem_Part	N_Grn_Rate, C_N	Sen, L_A	W, CO_2, Heat	/	(Martre, 2014; Martre et al., 2006)
Soltani and Sinclair (2012)	N_Dem_Part	N_Grn_Dem	Sen, L_A	W, CO_2, Heat	/	(Soltani and Sinclair, 2012)
SPASS	N_Dem_Part	N_Grn_Dem	Sen, Photo, L_A	W, CO_2, Heat	Heat	(Wang, 1997)
STICS	N_Dem_Part	O***	Sen. Photo, L_A	W, CO_2, Heat	/	(Brisson et al., 1998, 2003)

** CN-Wheat calculates rate of growth, death and synthesis of proteins including protein synthesis in photosynthetic organs and the grain*
*** Leaf N is as a function of LAI and stem N is a function of degree days from sowing. Relations have been empirically determined.*
**** Grain N is calculated using a N harvest index*

2.9.2 Summary of experimental data

Table S2.2: Summary of the data measured in each experiment on the Skyfall cultivar under varying levels of ozone exposure at Bangor CEH. Y=Yes data was available for this item, N=No data was not available for this item. For 2021 grain DM and grain N data was collected. However the plants did not put on any grain (Brewster, 2023) *and so the grain data for this experiment was not used*

Year	Phenology	Photosynthetic	Respiration	Straw DM	Stem & Leaf DM	Grain DM	Stem & Leaf N	Grain N
2015	Y	Y	N	Y	N	Y	N	Y
2016	Y	Y	Y	Y	N	Y	N	Y
2021	Y	N	N	Y	Y	/	Y	/

2.9.3 Gap filling protocol

PPFD data were obtained from NASA Power and converted to hourly PAR (NASA, 2023). All other input variables were extracted from observed meteorological data. The AgMIP Ozone gap filling protocol was followed where possible on missing experimental meteorological data (Emberson et al., 2021). Briefly, the AgMIP ozone protocol states that single hours of missing data should be filled by taking the average of neighbouring values, and several consecutive missing values should be filled by taking the average of the day before and day after. In some cases, there was not enough data available to follow the protocol. For large periods of missing temperature data, regressions from previous years between external and internal solar dome temperatures were constructed, and used to calculate internal dome temperatures. Similarly, regressions between the relative humidity (RH) of heated and ambient domes in previous years were used along with the RH of heated domes for the year of study to calculate the RH of the ambient temperature domes. All the temperature, ozone, RH and PPFD data were averaged to hourly values. Additional inputs required by DO_3SE-Crop are air pressure, precipitation and wind speed which were assumed to be constant inside the solar domes and had values of 101.1818 kPa, 5 mm per hour, and 0.9 ms^{-1} respectively to account for watering and the fans inside the solar dome.

2.9.4 Further details of model calibration

For the purposes of this study, the focus was the calibration and evaluation of grain quality parameters and the testing of the new nitrogen module. Therefore, 100% of the available data for phenology, photosynthesis and respiration was used for calibration as these will be key determiners of the dry matter and nitrogen accumulation. For all datasets the base temperature was set as 0°C, commonly used when multiple base temperatures are not considered (Savin and Slafer, 1991). The optimum temperature was set as 21°C, which is within the range of the average optimum growth temperature over the entire growing season (Porter and Gawith, 1999; Khan et al., 2021). The maximum temperature was set as 40°C as above this temperature irreversible damage to photosynthetic organs and processes occurs (Khan et al., 2021). Following the setting of the temperature parameters, the thermal time intervals of key growth dates were calibrated using the genetic algorithm so that one set of parameters was obtained for all 3 datasets. The genetic algorithm requires specification of a starting point for the parameter, as well as a range in which to vary it. The simulated value of the growth stage (or other modelling parameters for the later calibration stages) is then compared to the observed

value and the parameters are varied within the range to reduce the RMSE and achieve the maximum R^2. The starting parameters for the algorithmic model calibration came from a default parameterisation used in prior DO_3SE-Crop runs that can be obtained from example config files in the DO_3SE-Crop repository (Bland, 2024a). The range of parameters used to refine the model parameters comes from looking at previous model parameterisations and observing the range in parameter values for different geographical locations. Additionally, it can be observed from the output of the calibration whether the optimisation algorithm is setting a parameter to its minimum or maximum value in the defined range, which suggests the range needs altering.

$V_{cmax,25}$ and $J_{max,25}$ were fixed at their 90th percentile values, as determined from the experimental data, to exclude outliers (148 μmol m^{-2} s^{-1} and 215 μmol m^{-2} s^{-1} respectively) for Skyfall. The dark respiration coefficient was fixed at 0.0115 by averaging the experimentally measured photosynthetic rate at 0 PAR for the ambient and elevated O_3 treatments for Skyfall. $D0$ was fixed at 2.2. The m value was calibrated to a value of 5.641 algorithmically by maximising the R^2 between the simulated and average experimental values of stomatal conductance (535 μmol O_3 m^{-2} s^{-1}) and net photosynthetic rate (28 μmol CO_2 m^{-2} s^{-1}).

There was a problem with the 2021 dataset in that the plants did not grow any grain (see Brewster, (2023)). Therefore, the 2021 dataset was not used to calibrate or evaluate any grain or dry matter parameters. The ratio of stem to leaf dry matter in the 2021 dataset was used to calculate a stem and leaf dry matter for the 2015 and 2016 experiments from the straw DM. These parameters ensured the splitting of straw biomass between the leaf and stem pools in the model made physiological sense. For calibration of the grain and straw (leaf + stem) dry matter the low ozone treatments from 2015 and 2016 were used. The datasets were split in half so that half of the data would be used for calibration and half for evaluation. The rationale for using a 50:50 ratio was that the Bangor 2015 dataset only had 4 recordings of dry matter; splitting any differently than 50:50 would result in only 1 data point from the 2015 experiment in either the calibration or evaluation set. The DM parameters were calibrated using the genetic algorithm by maximising the R^2 between the grain yield, the estimated leaf and stem DM and LAI by assuming a peak LAI of 5 (obtained via communication with the experimentalists).

To calibrate the effect of O_3 damage on grain DM, 50% of the low and very high O_3 treatments from 2016 were used. The 2015 experiment was not used to calibrate O_3 damage as the grain DM difference between the low and very high treatments was lower than expected for this cultivar and would result in an underestimated ozone effect on yield. The O_3 damage parameters were then calibrated using the genetic algorithm by maximising the R^2 between the simulated and observed RY loss.

To calibrate the stem and leaf N, 50% of the low ozone treatment data from both anthesis and harvest in the 2021 dataset was used. Additionally, we used only the percentage of N in these plant parts, as the model would likely not achieve the exact correct stem and leaf DM so the absolute grams of N would likely not match the experimental data. For the leaves, the % of N was measured for flag and 2nd leaf. However, we simulate the leaf canopy as a whole. Using Barraclough et al. (2014) we understand that the flag and 2nd leaves contain more N than 3rd and 4th leaves and we expect the observations of N% in the flag and 2nd leaf to be an upper end estimate when modelling.

To calibrate grain N, 50% of the low ozone treatment data from 2016 was used. To calibrate the impact of ozone on the re-mobilisation of leaf N to the grain, 50% of the low and very high grain N % data was used from 2016. The N parameters were then calibrated using the genetic algorithm by maximising the R^2 between the simulated and observed leaf and stem N at anthesis and harvest, and the grain N at harvest. As the N module is new, the starting parameters could not come from the default DO₃SE-Crop config. Instead, the initial parameters used came from the locations where the equations were extracted from where possible (see Section 2.8). For the algorithmic calibration, ranges for all parameters and the starting values for any parameters that were new were estimated by manually trialling different combinations of values in tools such as Desmos (Desmos, 2023).Table S2.3: The parameters that were calibrated for (changed from the default parameterisation) in DO₃SE-Crop Model

Process	Parameter description	Parameter	Calibrated Value	Unit
Phenology	Base temperature	T_b	0	°C
	Optimum temperature	T_o	21	°C
	Maximum temperature	T_m	40	°C
	Plant emergence	TT_{emr}	194.7	°C days
	Flag emergence	$TT_{flag,emr}$	763.2	°C days
	Start anthesis	TT_{astart}	1271.3	°C days
	Mid-anthesis	TT_{amid}	1290.6	°C days
	Harvest	TT_{harv}	2017	°C days
Photosynthesis	Maximum carboxylation capacity at 25 °C	$V_{cmax,25}$	148	$\mu mol\ CO_2\ m^{-2}s^{-1}$
	Leaf vertical N co-efficient	kN	0	-
	Maximum rate of electron transport at 25 °C	$J_{max,25}$	215	$\mu mol\ CO_2\ m^{-2}s^{-1}$
	m	m	5.49	-
Respiration	dark respiration	R_{dcoeff}	0.0115	-
	growth respiration	R_g	0.125	-
DM parameters	Coefficient for determining DM partitioning	α_{root}	16.5	-
	Coefficient for determining DM partitioning	β_{root}	-18.61	-
	Coefficient for determining DM partitioning	α_{leaf}	18.054	-
	Coefficient for determining DM partitioning	β_{leaf}	-18.876	-
	Coefficient for determining DM partitioning	α_{stem}	17.18	-
	Coefficient for determining DM partitioning	β_{stem}	-14.384	-
	Coefficient determining specific leaf area	Ω	22.8	$m^2\ kg^{-1}$

	Fraction of stem carbon in the reserve pool	τ	0.7	-
	Fraction of DM in the harvest pool that goes to the grains (rest goes to the ear)	E_g	0.75	-
Ozone damage	O_3 long term damage coefficient	$\gamma 3$	$9x10^{-5}$	$(\mu mol\ O_3\ m^{-2})^{-1}$
	O_3 long term damage coefficient determining senescence onset	$\gamma 4$	4.5	-
	O_3 long term damage coefficient determining maturity	$\gamma 5$	1.2	-
	Critical accumulated stomatal O_3 flux that determines the onset of leaf senescence	$CLsO_3$	13000	$\mu mol\ O_3\ m^{-2}$

2.9.5 Relationship between grain DM, grain N (gm^{-2}) and grain N%

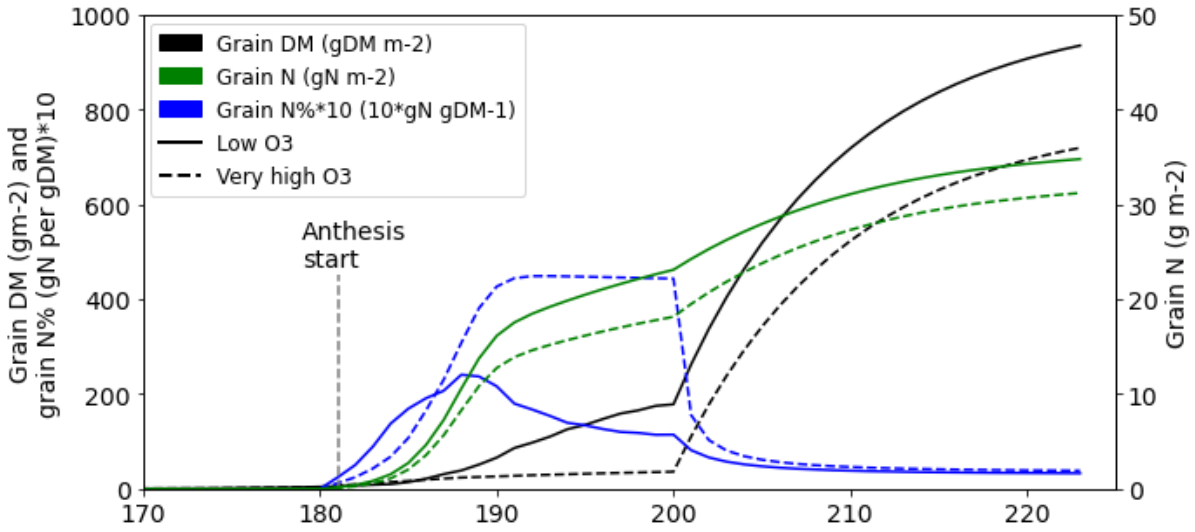

Figure S2.1: A conceptual figure illustrating the interdependencies between grain DM, grain N content and concentration in the newly developed DO_3SE-CropN model. This figure was generated using the low and very high ozone treatment data from Bangor 2015, though all years had very similar patterns. All grain N% data has been multiplied by 10 to make the figure easier to read.

2.9.6 Constructing N profiles from existing literature

Data was taken from all 6 field experiments of Groot (1987). For each experiment the date, Zadoks value, green leaf and dead leaf nitrogen, stem nitrogen and grain nitrogen were extracted. The nitrogen treatments were ignored at this stage. The green and dead leaf nitrogen were summed to give a total leaf nitrogen. Data were extracted for measurements in g kg^{-1} and

kg ha^{-1} separately as these were measured using different methods (Groot, 1987). Additional data was extracted on leaf, stem and grain nitrogen using WebPlotDigitizer (https://automeris.io/WebPlotDigitizer/) , from Bertheloot et al. (2008) and Nagarajan et al. (1999). Bertheloot et al. (2008) and Nagarajan et al. (1999) recorded the time points of their measurements in degree days after anthesis and days after anthesis respectively. For all 3 sources, the stem, leaf and grain nitrogen measurements cover a range of soil types, cultivars, countries, nitrogen treatments and water stress; though these conditions were not taken into consideration and the data has been grouped together.

Each of the datasets had recorded the time using different metrics. Therefore, the first stage of analysis was to convert them all to the same units. Using the Groot (1987) data, a regression was fit between the number of days after sowing, and the Zadoks value for each nitrogen treatment of each experiment. Assuming a Zadoks value of 61 corresponds to anthesis, the regression was solved to calculate the number of days after sowing that anthesis occurred. Although the relation between days after sowing and the Zadoks scale is not linear, some treatments and experiments only had 2 data points so it was not possible to account for greater complexity in the relationship. Using the date of anthesis for each treatment and experiment, the number of days after anthesis was calculated for each measurement in the Groot (1987), making it the same scale as the Nagarajan et al. (1999) data. The Bertheloot et al. (2008) was measured in degree days after anthesis not days after anthesis. To calculate the time measurement in days after anthesis, the anthesis dates and final measurement dates (assumed to be harvest) were matched to calculate a conversion factor between the two.

For the leaf, stem and grain, the total nitrogen of these plant parts was summed for every time point of each treatment and experiment, and the fractional leaf, stem and grain nitrogen calculated by dividing the component nitrogen by the total. The 95% confidence intervals were calculated and smoothed using Loess smoothing in Python. The resulting plot is shown in Figure S2.2 and can be used to describe how the N content in the stem, leaves, and grains changes over time respective to each other.

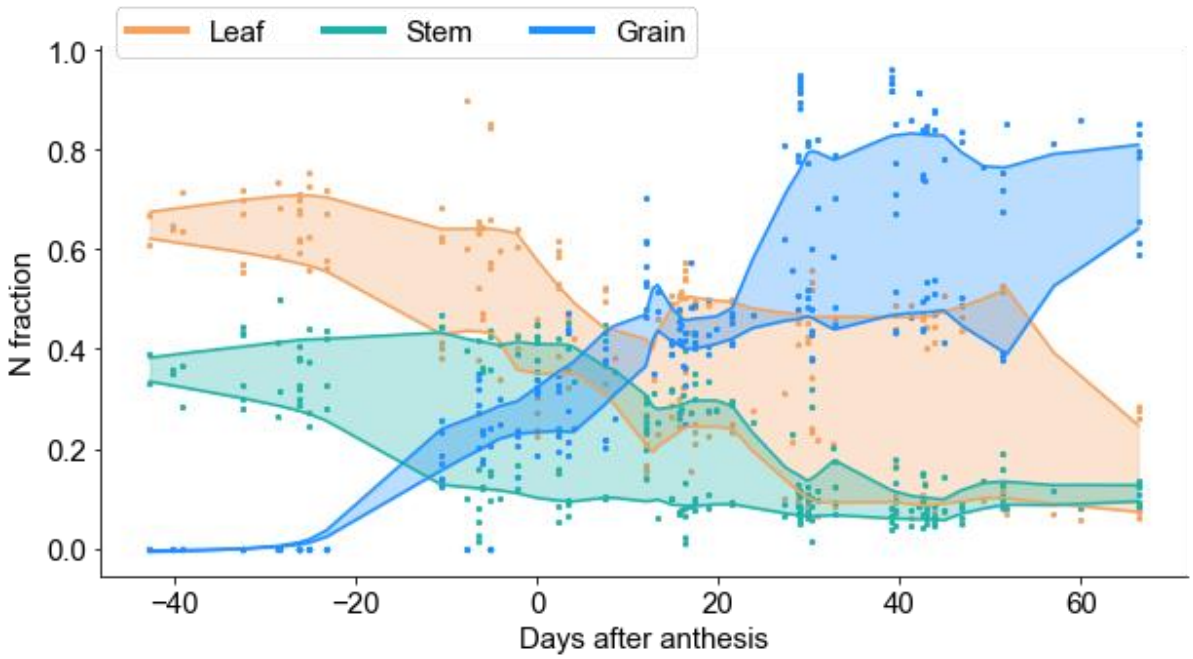

Figure S2.2: The proportion of total plant N stored in the leaf, stem and grain of the wheat plant using experimental data from Bertheloot et al. (2008), Groot (1987), and Nagarajan et al. (1999). The points represent the experimental

data, and the solid lines indicate the upper and lower bounds of the 95% confidence interval applied using a LOESS smoothing factor of 0.2.

The grain weight (mg), and the grain N (mg per grain) were extracted from Figures 1 and 2 of Panozzo and Eagles (1999) using WebPlotDigitizer (https://automeris.io/WebPlotDigitizer/). From this the grain N% could be calculated for each treatment and timepoint. The mean of the irrigated and dry treatment data for each timepoint was calculated and the resulting profile of grain N% over time is given in Figure S2.3.

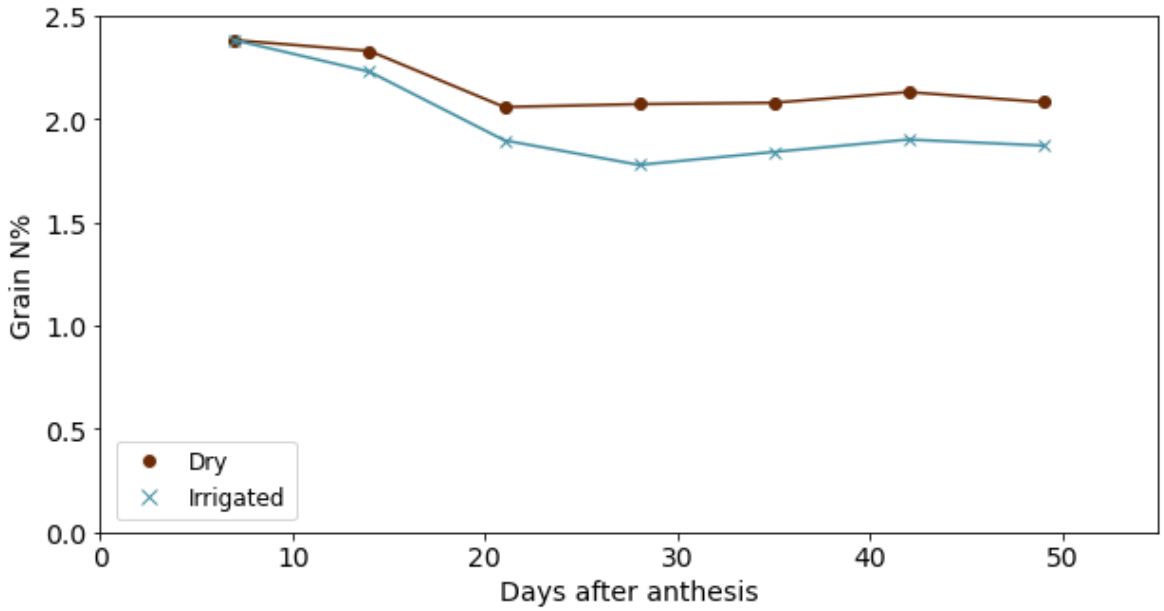

Figure S2.3: The dynamic profile of grain N% as calculated from available data in Panozzo and Eagles (1999) for wheat kept under dry and irrigated conditions. Figures 1 and 2 from which this data was extracted used averaged data from 4 wheat cultivars: Rosella, Hartog, Halberd and Eradu.

Profiles of grain N% were also constructed from data available in Nagarajan et al. (1999). The carbon and nitrogen content were extracted from Figures 4 and 5 in Nagarajan et al. (1999) using WebPlotDigitizer (https://automeris.io/WebPlotDigitizer/). By assuming the fraction of C in DM is 50% (Osborne et al., 2015), the existing data was used to construct the profile in Figure S2.4.

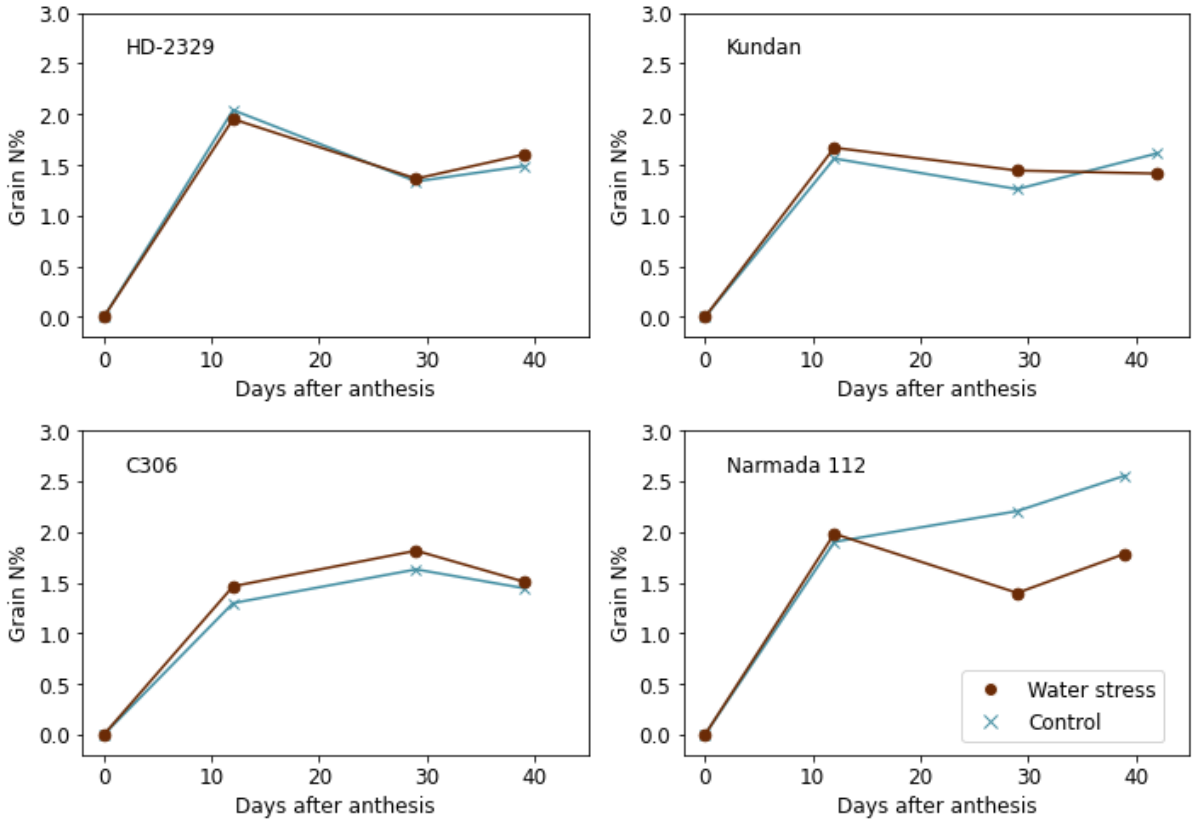

Figure S2.4: The temporal profile of grain N% for the 4 wheat cultivars measured by Nagarajan et al. (1999) for water stress and a control treatment.

2.9.7 Temporal profile of simulated grain DM

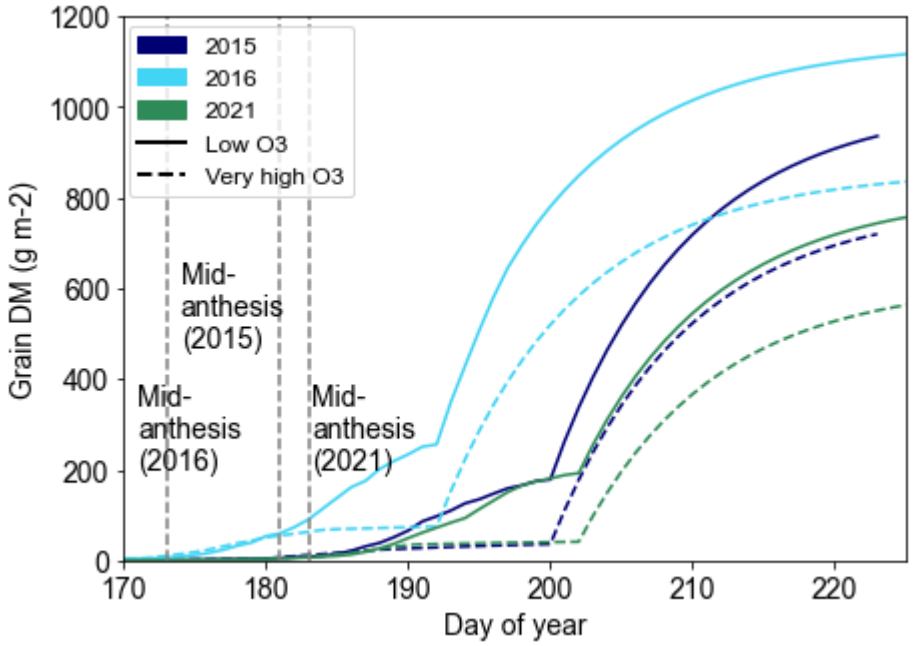

Figure S2.5: Profile of grain DM from just before anthesis to harvest for all years of the present study. The low and very high O_3 treatments are indicated for comparison of grain DM accumulation between years and treatments.

3. Paper 2: Modelling ozone-induced changes in wheat amino acids and protein quality using a process-based crop model

3.1 Abstract

Ozone (O_3) pollution reduces wheat yields as well as the protein and micronutrient yield of the crop. O_3 concentrations are particularly high in India, and are set to increase, threatening wheat yields and quality in a country already facing challenges to food security. This study aims to improve the existing DO_3SE-CropN model to simulate the effects of O_3 on Indian wheat quality by incorporating antioxidant processes to simulate protein, and the concentrations of nutritionally relevant amino acids. As a result, the improved model can now capture the decrease in protein concentration that occurs in Indian wheat exposed to elevated O_3. The structure of the modelling framework is transferrable to other abiotic stressors and easily integrable into other crop models, provided they simulate leaf and stem N, demonstrating the flexibility and usefulness of the framework developed in this study. Further, the modelling results can be used to simulate the FAO recommended metric for measuring protein quality, the DIAAS, setting up a foundation for nutrition-based risk assessments of O_3 effects on crops. The resulting model was able to capture grain protein, lysine and methionine concentrations reasonably well. As a proportion of dry matter, the simulated percentages ranged from 0.26% to 0.38% for lysine, and from 0.13% to 0.22% for methionine, while the observed values were 0.16% to 0.38% and 0.14% to 0.22%, respectively. For grain and leaf protein simulations, the interdependence between parameters reduced the accuracy of their respective relative protein loss under O_3 exposure. Additionally, the decrease in lysine and methionine concentrations under O_3 exposure was underestimated by ~10 percentage points for methionine for both cultivars, and by 37 and 19 percentage points for lysine for HUW234 and HD3118 respectively. This underestimation occurs despite simulations of relative yield loss being fairly accurate (average deviation of 2.5 percentage points excluding outliers). To provide further mechanistic understanding of O_3 effects on wheat grain quality, future experiments should measure nitrogen (N) and protein concentrations in leaves and stems, along with the proportion of N associated with antioxidants, which will aid in informing future model development. Additionally, exploring how grain protein relates to amino acid concentrations under O_3 will enhance the model's accuracy in predicting protein quality and provide more reliable estimates of the influence of O_3 on wheat quality. This study builds on the work of Section 2 of the present thesis, and supports the second phase of the tropospheric O_3 assessment report (TOAR) by investigating the impacts of tropospheric O_3 on Indian wheat and the potential of this to exacerbate existing malnutrition in India.

3.2 Introduction

A growing body of literature from Europe, China and India has shown that exposure to O_3 reduces wheat protein and micronutrient yields (Broberg et al., 2015; Yadav et al., 2020; Mishra, Rai and Agrawal, 2013; Feng, Kobayashi and Ainsworth, 2008). This is important as cereals often make up the most available protein source per capita and wheat is the dominant dietary cereal globally (Shiferaw et al., 2013). Therefore, any reduction in yield, protein and micronutrient contents caused by O_3 could threaten both food and nutrition security, especially in countries such as India where O_3 concentrations are high and food security is low (FAO et al., 2020;

Herforth et al., 2020; Mills et al., 2018c). The first phase of the tropospheric ozone (O_3) assessment report (TOAR) (https://igacproject.org/activities/TOAR/TOAR-I) compiled information on surface O_3 metrics to produce the world's largest database for identification of global distribution and trends of O_3. The second phase of TOAR (https://igacproject.org/activities/TOAR/TOAR-II), for which this paper is a part, expands on the goals of the first phase, to investigate O_3 impacts on human health and vegetation. This study contributes to the second phase of TOAR by examining the impacts of tropospheric O_3 on wheat yield and quality in India, enhancing our understanding of the broader implications for food and nutrition security. Understanding the interplay of different factors affecting O_3 induced reductions in wheat yield and quality will be important for current, and future, food and nutritional security risk assessments.

3.2.1 Malnutrition and the importance of wheat in India

Malnutrition is prevalent in India with ~40% of the population unable to afford a nutritionally adequate diet, and ~80% unable to afford a healthy diet (FAO et al., 2023). In India, ~35% of children under the age of 5 are affected by stunting and ~20% affected by wasting, with the prevalence of wasting in India being one of the highest in the world (Development Initiatives, 2020b). Stunting and wasting occur when an individual does not have sufficient calories or micronutrients in their diet to grow and develop (Gonmei and Toteja, 2018). Wasting and muscle function loss can result from a poor quantity, or quality, of dietary protein (Medek, Schwartz and Myers, 2017). For most Indian states, at least 30% of the population are at risk of protein deficiency, which is of concern for people who are pregnant or in poorer socioeconomic circumstances, who require higher qualities of protein for growth or fighting infections (Swaminathan, Vaz and Kurpad, 2012; Minocha, Thomas and Kurpad, 2017b).

In India, cereals are the most available protein source per capita, and are a key dietary protein source (Minocha, Thomas and Kurpad, 2017b). Wheat makes up the dominant dietary cereal in the north of India where the majority of the crop is grown (Khatkar, Chaudhary and Dangi, 2015). Globally, India has the greatest area under wheat cultivation, 31.6 million hectares, and produced 109.5 million tonnes of wheat in 2021, second only to the amount of wheat produced by China (Ministry of Agriculture & Farmers Welfare, 2022). As a result, the country is self-sufficient/reliant when it comes to wheat (Tripathi and Mishra, 2017). Consumption of wheat varies by state with the dominant wheat producing states (Punjab, Rajasthan, Haryana and Madhya Pradesh) consuming the most. Resulting from population growth and increases to income, the total demand for wheat is increasing (Tripathi and Mishra, 2017). However, numerous experimental and modelling studies have shown that O_3 is substantially reducing wheat yields across India (Sharma et al., 2019; Sinha et al., 2015; Mills et al., 2018b; Yadav, Agrawal and Agrawal, 2021; Mishra, Rai and Agrawal, 2013).

3.2.2 O_3 pollution in India

Ground level O_3 is a secondary pollutant, formed when precursor gases (predominantly volatile organic compounds and nitrogen oxides) react in the presence of ultraviolet light (Fowler et al., 2008). Current literature, and the first phase of TOAR, identified that South Asia, and in particular India, experience some of the highest O_3 burdens of any region or country worldwide (Mills et al., 2018c; Emberson, 2020). Geographically, the highest O_3 concentrations in India occur in the northern part of the country and the Indo-Gangetic planes (IGP), where the majority of wheat is grown (Rathore, Gopikrishnan and Kuttippurath, 2023; Lu et al., 2018; Ministry of Agriculture & Farmers Welfare, 2022). In the future, the changing climate will affect O_3

concentrations, with climatic conditions across the north of India favouring greater O_3 production (Stevenson et al., 2013; Li et al., 2022a). Comparative to present day, Kumar et al. (2018) showed the greatest increase in O_3 concentrations across India would be during the dry (wheat growing) season across the IGP. This is a critical finding given the majority of wheat is grown in the north of India, across the IGP (Ministry of Agriculture & Farmers Welfare, 2022).

3.2.3 Effects of O_3 pollution on wheat yields

O_3 diffuses into wheat leaves via the stomates and impacts photosynthesis and senescence when antioxidant defences are compromised (Emberson et al., 2018; Tiwari and Agrawal, 2018; Rai and Agrawal, 2012). Accelerated senescence shortens the grain filling period, and the decline in photosynthesis decreases biomass production, ultimately leading to lower crop yields (Tiwari and Agrawal, 2018; Emberson et al., 2018).

Several experimental studies using wheat cultivars commonly grown in India have shown decreases in yield due to elevated O_3 exposure (Yadav, Agrawal and Agrawal, 2021; Pandey et al., 2018; Tomer et al., 2015; Naaz et al., 2022). National estimates of relative yield (RY) loss due to O_3 across India vary between 3.8-41% between studies (Ghude et al., 2014; Lal et al., 2017; Avnery et al., 2011; Van Dingenen et al., 2009; Sinha et al., 2015; Sharma et al., 2019; Droutsas, 2020). The effects of O_3 on wheat yield also vary spatially (Mills et al., 2018b; Droutsas, 2020; Ghude et al., 2014; Lal et al., 2017; Sharma et al., 2019). Mills et al. (2018) found the greatest yield losses across the north of the country as the meteorological conditions are more favourable to O_3 uptake. Lal et al. (2017) also found the greatest wheat yield losses due to O_3 in the north and west of India, where the majority of wheat is grown. Further, Naaz et al. (2022) exposed Indian wheat cultivars to different conditions representing future O_3 and climate scenarios, finding that areas suitable for wheat cultivation will be reduced in the future.

3.2.4 Effects of O_3 pollution on wheat quality

Studies have shown that the starch, protein and micronutrient yield of wheat decreases under elevated O_3 exposure (Broberg et al., 2015; Tomer et al., 2015; Piikki et al., 2008). Pre-anthesis, the accumulation of nitrogen (N) in upper plant parts is unaffected by elevated O_3 concentrations (Brewster, Fenner and Hayes, 2024). However, after anthesis, the O_3 induced acceleration of plant senescence limits the remobilisation of N from the leaves and stem to the grain (Broberg et al., 2017; Brewster, Fenner and Hayes, 2024; Chang-Espino et al., 2021). Brewster, Fenner and Hayes (2024) also suggest that an additional process affects N remobilisation to the grain, as they found an increase in residual N in the flag leaf, despite not detecting a difference in senescence onset. It is possible that the residual N is in the form of antioxidants (for example glutathione) which the plant creates for defence against O_3 induced reactive oxygen species (ROS) (Brewster, Fenner and Hayes, 2024; Sarkar and Agrawal, 2010; Yadav et al., 2019b). Overall, the reduction in N remobilisation, leads to reduced N deposition to the grain and a reduced grain N, and protein, yield (Broberg et al., 2015; Yadav et al., 2020; Section 2 of this thesis). In wheat, since the grain yield is decreased to a greater extent than proteins and micronutrients under increased O_3, the concentration of protein and micronutrients in the grains generally increases (Feng and Kobayashi, 2009; Piikki et al., 2008). However, some wheat varieties, particularly Indian wheat, have shown a different pattern, where the protein yield and concentration of the grains decreases under O_3 exposure (Baqasi et al., 2018; Yadav et al., 2020; Mishra, Rai and Agrawal, 2013).

Indispensable amino acids (AA's) are most important for nutrition as they cannot be synthesised by the body and must be obtained through diet (Brestenský et al., 2019). Additionally, the quantity of N containing compounds consumed is important for synthesis of dispensable AA (Brestenský et al., 2019). Nevertheless, while dispensable AA can be produced by the body, their consumption is still important for supporting metabolic functions (Brestenský et al., 2019). The production of different proteins in the body requires AA in differing proportions (Shewry and Hey, 2015). The AA that is available in the lowest proportion, the most limiting AA, determines protein production (Elango, Ball and Pencharz, 2008; Shewry and Hey, 2015). Un-utilised AA cannot be stored so if they are not used for protein production they are oxidised (Elango, Ball and Pencharz, 2008; Brestenský et al., 2019). Yadav et al. (2020) looked at the AA profiles of a modern (HD3118), and old (HUW234), wheat cultivar exposed to O_3, finding indispensable and dispensable AA decreased under O_3 exposure. The effect of O_3 on protein quality of wheat is of particular concern given the existing state of malnutrition in India.

3.2.5 Crop modelling for O_3 and nutrition

Several crop models have been used to investigate the impacts of O_3 pollution on crop yields in a wide range of countries and globally (Nguyen et al., 2024; Guarin et al., 2019a, 2024; Schauberger et al., 2019; Tao et al., 2017; Tai et al., 2021; Tian et al., 2015; Zhou et al., 2018; Droutsas, 2020; Xu et al., 2023). Ebi et al. (2021) highlight the usefulness of models for such risk assessments, while stressing that most do not consider aspects relevant for human nutrition in their simulations. Currently, only one model has been developed which captures the effect of O_3 on crop nutrition: DO_3SE-CropN (Section 2 of this thesis). DO_3SE-CropN is built on the existing DO_3SE-Crop model and simulates explicitly the effect of O_3 on reducing the amount of N from the leaves and stems that is available for the grain. From the grain N content (gN m^{-2}), grain protein content (gProtein m^{-2}) is easily obtained using conversion factors (Mariotti, Tomé and Mirand, 2008).

The DO_3SE-CropN model was originally developed to capture the increase in N concentration (100gN gDM^{-1}) and decrease in N yield (gN m^{-2}) that occurs under O_3 exposure in European wheat (Section 2 of this thesis). However, Indian wheat experiences a decrease in grain protein concentration as well as a decrease in grain protein yield under elevated O_3 concentrations (Mishra, Rai and Agrawal, 2013; Yadav et al., 2020). In India, the ambient O_3 concentrations are high, leading to ROS production and subsequent yield losses (Tiwari and Agrawal, 2018; Sinha et al., 2015; Sharma et al., 2019). The production of antioxidants by the plant to defend against ROS reduces the proportion of proteins that would otherwise be remobilised to the grain, reducing grain protein (Yadav et al., 2019b, 2020). Therefore, to capture the decrease in the protein concentration of Indian wheat under O_3 exposure, the inclusion of antioxidant processes is essential. Further, the inclusion of such processes will improve the wider applicability of the model for simulating O_3 effects on wheat quality for regions with high O_3 concentrations.

To expand the nutritional relevance of the model, it would be useful to simulate the effect of O_3 on protein quality. This can be done through simulating AA concentrations, which can subsequently be used to calculate the recommended metric for measuring protein quality by the FAO: the dietary indispensable AA score (DIAAS). The inclusion of protein quality would allow for risk assessments of O_3 effects on wheat nutrition in addition to yield.

3.2.6 Aims

In the present study, the DO_3SE-CropN model was further developed and applied with two years of meteorological data. The model was calibrated using phenology, photosynthesis and yield data collected for two cultivars (HUW234 and HD3118) grown under both ambient and elevated O_3 treatments. All data were available from Yadav, Agrawal and Agrawal (2021). Grain quality data were obtained from an experiment on the same cultivars a year prior, however hourly meteorological and O_3 data were not available for this year (Yadav et al., 2020). In the absence of further data, this study assumes that the grain protein concentration and grain protein quality will respond similarly to O_3 between years. The aims of the present study were to use the available data for the following:

1) Develop a framework to simulate the antioxidant response of wheat under O_3 exposure for incorporation into the existing DO_3SE-CropN model.
2) Develop a method for simulating the impact of O_3 exposure on the protein quality of wheat, focussing on AA essential for human nutrition, for incorporation into the existing DO_3SE-CropN model.

3.3 Methods

3.3.1 Integrating antioxidant processes into DO_3SE-CropN

The DO_3SE-Crop model is a coupled stomatal conductance-photosynthesis model, which simulates stomatal O_3 uptake and its impact on photosynthesis, recovery from O_3 damage overnight, as well as O_3 induced accelerated crop senescence (Pande et al., 2024a). Daily photosynthate is partitioned between the leaves, stem, roots and grains according to the plant's growth stage (Pande et al., 2024a; Osborne et al., 2015). Development of DO_3SE-Crop has allowed the O_3 impact on wheat production in China and Europe to be estimated (Pande et al., 2024a; Nguyen et al., 2024). The N module for DO_3SE-Crop, developed in Section 2 of this thesis, takes inputs of daily stem and leaf dry matter (DM), as well as the onset of crop senescence, to simulate the N accumulated by the leaf and stem. The remobilisation of N from the leaf and stem to the grain after anthesis is simulated using a sigmoid function. To account for the reduction in N remobilisation under O_3 exposure, a relationship linking accumulated O_3 flux to the minimum N levels in the leaf and stem is incorporated (Section 2 of this thesis; Brewster, Fenner and Hayes, 2024). The model allowed the decrease in grain N yield ($gN\ m^{-2}$) and increase in grain N concentration ($100gN\ gDM^{-1}$) of European wheat under O_3 exposure to be simulated (Section 2 of this thesis). A full write up of the equations and processes of the DO_3SE-Crop model is given in Pande et al. (2024). Additionally, a full description of the equations and processes of version 1.0 of the N module developed for DO_3SE-Crop is given in Section 2 of this thesis. In this study version 4.39.16 of the DO_3SE-Crop model was used, along with version 2.0 of the N module (Cook, 2024; Bland, 2024b).

The first iteration of the N module for DO_3SE-Crop (Section 2 of this thesis), did not consider the utilisation of leaf/stem N in creating defence proteins, yet for Indian wheat this may be an important process to explain the decrease in grain protein concentration as well as yield (Yadav et al., 2019b, 2020). Here we propose a method by which the leaf and stem N involved in antioxidant production may be quantified (Figure 3.1).

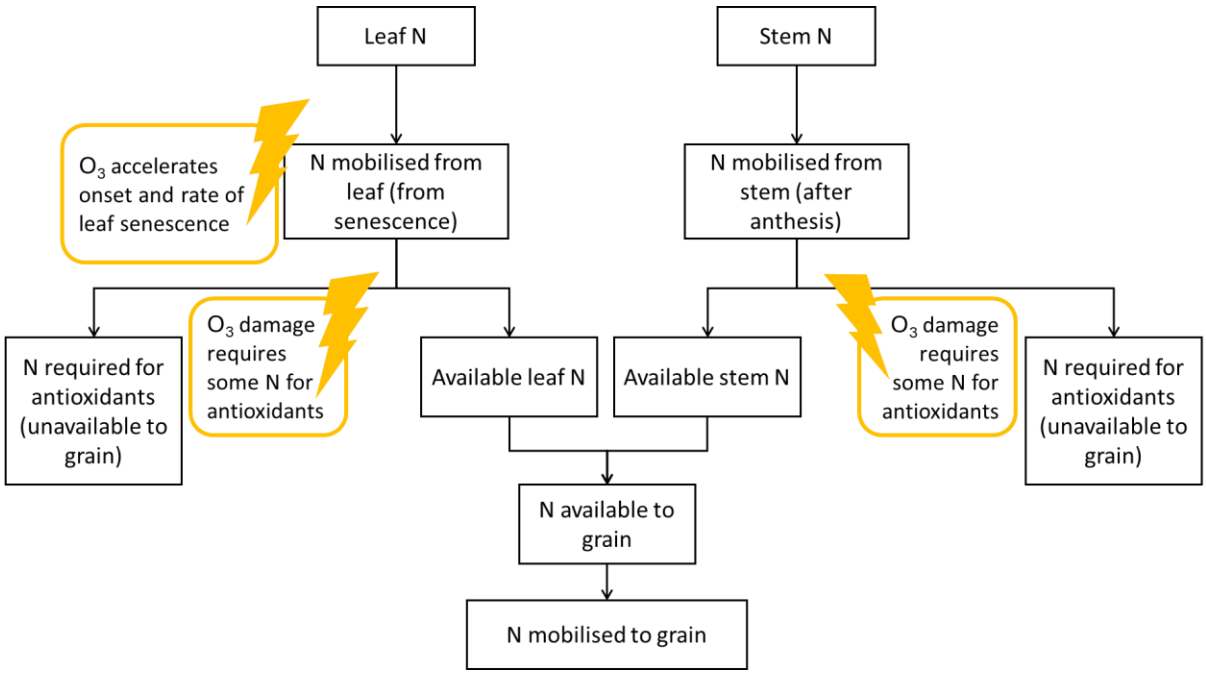

Figure 3.1: Diagram of the proposed method for integrating antioxidant response under O_3 exposure into the existing N module for DO_3SE-Crop. The lightning strikes represent where O_3 can interrupt plant N processes.

Figure 3.1 shows how antioxidant processes can be integrated within the existing DO_3SE-CropN framework. When the leaf senesces, N is released from the leaf. The N module is linked to the existing DO_3SE-Crop model so that increasing stomatal O_3 flux accelerates senescence, which accelerates N release from the leaf. N is released until the minimum leaf N concentration is reached. Previously, the minimum leaf N concentration increased with O_3 concentration to represent the increase in residual N (Section 2 of this thesis). Now it is hypothesised that this increase in residual N is due to the leaf and stem using N for antioxidants which remain in the leaf. After a threshold of accumulated O_3 flux has been exceeded, we allocate a proportion of the released N to an antioxidant pool, which means it is unavailable to the grain. Since the stem is also involved in antioxidant response and defence against ROS (Bazargani et al., 2011; Gao et al., 2018; Li et al., 2022b), the same mechanism is used for the stem. We determine the proportion of N that will be allocated to the antioxidant pool using an equation that follows a similar structure as the drought stress factor of Liu et al. (2018), as both O_3 and drought stress are ROS mediated (Khanna-Chopra, 2012). Liu et al. (2018) use their drought stress factor to empirically modify the N:protein conversion factor under drought stress. Here, we introduce this method to the DO_3SE-CropN model via Equation (3.1) as a more mechanistic approach. Instead of modifying the N:protein conversion factor under an abiotic stress, we use the structure of Liu et al.'s (2018) equation to determine N allocation to the antioxidant pool, thereby reducing the N available to the grain, and subsequently affecting grain protein.

The proportion of N allocated to the antioxidant pool, $f_{O_3,Antioxidants}$, takes the following form:

$$f_{O_3,Antioxidants} = \begin{cases} 0, & fst_{acc} < cL_{O_3} \\ \dfrac{fst_{acc} - cL_{O_3}}{a_{part} \times fst_{end} - cL_{O_3}}, & fst_{acc} \geq cL_{O_3} \end{cases} \quad (3.1)$$

where fst_{acc} is the current stomatal accumulation of O_3 flux in the DO_3SE model, fst_{end} is the stomatal accumulation of O_3 flux when N is only allocated to antioxidant pool and is not available to the grain, cL_{O_3} is the critical level above which O_3 flux starts affecting the onset of

senescence in the DO$_3$SE-Crop model, and a_{part} is a constant modifier that can be calibrated to customise the O_3 effect on antioxidants for each plant part (leaf and stem). a_{part} must be equal to or greater than $\frac{cL_{O_3}}{fst_{end}}$ for the antioxidant factor equation to show a decrease in released N with accumulated O_3 flux. Further, fst_{end} must be greater than cL_{O_3}. Of the N released that day, the proportion available to the grain is $1 - f_{O_3,Antioxidants}$. The cL_{O_3} term was chosen as the O_3 stress factor as if O_3 has exceeded a critical threshold and is affecting senescence onset, we can hypothesise that the allocation of N to antioxidants to protect against O_3 stress will be increased. fst_{end} was incorporated into the equation to allow the end point of the slope to be customised. For varying values of a_{part}, the O_3 stress factor is used to calculate the proportion of N available to the grain as a function of accumulated stomatal O_3 flux according to Figure 3.2.

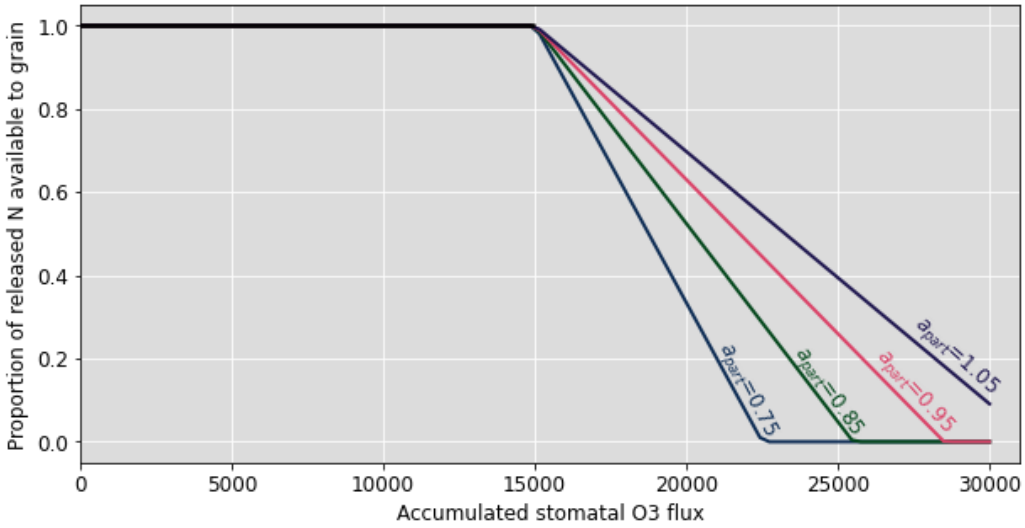

Figure 3.2: Proportion of N released from stem or leaf senescence that is available to the grain for varying values of a_{part}. The plot uses fst_{end} = 30000, and cL_{O_3} = 15000.

3.3.2 Identification of nutritionally relevant AA for O_3 exposed wheat

The quality of a protein depends on the proportions of indispensable and dispensable AA's in the food. While Yadav et al. (2020) found that dispensable AA's were reduced to a greater extent than indispensable AA's under O_3 exposure, the most limiting for protein production were the indispensable AA's lysine and methionine. Additionally, the concentrations of lysine and methionine were reduced under O_3 exposure for both the HD3118 and HUW234 cultivars (Yadav et al., 2020). Therefore, to simulate the protein quality under O_3 exposure, lysine and methionine were focussed on.

3.3.3 Protein and AA calculations

The DO$_3$SE-CropN model outputs a grain N yield (gN m^{-2}) and concentration (100gN gDM^{-1}). From the grain N content, the protein content can be calculated by considering a standard N:protein conversion factor. The Jones' factors are commonly used to convert from N to protein, however, these factors vary between foods and within the same food group (Jones, 1941; Mariotti, Tomé and Mirand, 2008). On average for whole wheat, the conversion factor is 5.49, which is used in this study to convert grain N to protein (Mariotti, Tomé and Mirand, 2008). The regressions used to calculate lysine and methionine concentrations of the wheat grain from grain protein percentage are taken from Table 5 of Liu et al. (2019).

3.3.4 The DIAAS score

The metric recommended by the FAO for evaluating food protein quality is the dietary indispensable AA score (DIAAS), which corrects for the AA digestibility at the end of the small intestine (FAO, 2013). It therefore reflects the fact that the nutritional quality of protein should account for the AA required for metabolism (FAO, 2013). The metric also varies for different age groups which have different protein quality requirements (FAO, 2013). Currently, no crop model has incorporated a nutrition measure such as the DIAAS into their models. Additionally, no model has considered the impact of O_3 pollution on protein quality which is critical for risk assessments of O_3 stress on food and nutrition security.

There are two steps in calculating the DIAAS score. First, the DIAAS reference ratio is calculated for each AA as follows:

$$\underset{reference\ ratio}{DIAAS} = \frac{True\ ileal\ IAA\ Digestibility \times mg\ of\ AA\ in\ 1g\ of\ the\ dietary\ protein}{mg\ of\ digestible\ indispensible\ AA\ in\ 1g\ of\ the\ dietary\ protein} \quad (3.2)$$

where IAA stands for indispensable AA.

Once the AA concentrations have been obtained from grain protein simulations, as detailed in Section 3.3.3, then Equation 3.2 is re-written using the parameters used in the crop modelling as:

$$\underset{reference\ ratio}{DIAAS} = \frac{True\ ileal\ IAA\ Digestibility \times \frac{1000 \times Grain\ AA\ (\%\ in\ DM)}{Grain\ protein\ (\%\ in\ DM)}}{mg\ of\ digestible\ indispensible\ AA\ in\ 1g\ of\ the\ dietary\ protein} \quad (3.3)$$

In the second step, the lowest DIAAS reference ratio is selected and used to calculate the DIAAS score as in Equation 3.4. The lowest reference ratio is selected as this corresponds to the AA which is most limiting in the food, and is available in the smallest proportion relative to a person's requirements (Elango, Ball and Pencharz, 2008). The AA with the lowest availability determines protein production, and quality, and the other AA which are in excess of the most limiting one will be oxidised (Elango, Ball and Pencharz, 2008).

$$\underset{score}{DIAAS} = 100 \times lowest(reference\ ratio) \quad (3.4)$$

The true ileal IAA digestibility coefficients for wheat flour required for Equation 3.3 can be obtained from Shaheen et al. (2016) for the different AA. Additionally, the mg of digestible indispensable AA in 1g of the dietary protein are tabulated for the different AA and age groups in FAO (2013). There are different requirements for different age groups as adults only require AA for maintenance, whereas children require them for growth and maintenance (Shewry and Hey, 2015).

3.4 Parameterisation and calibration of the DO_3SE-CropN model

3.4.1 Experimental datasets

Datasets for training and evaluation of the DO_3SE-CropN model were taken from three years of field experiments for wheat harvested between March 2016-2018 at the Botanical Garden, Banaras Hindu University, Varanasi, India using the HUW234 and HD3118 cultivars. The cultivars are both late sown and heat tolerant wheat varieties. For all years, O_3 fumigation began 3 days after seed germination, the 13th, 14th and 15th of December respectively for the 2015,

2016 and 2017 sowing on the 14th of December. The wheat was exposed to ambient O_3 concentrations and an elevated O_3 treatment (ambient + 20 ppb), with the seasonal maximum O_3 concentrations ranging from 80-100 ppb, and an average ambient M7 of 48 ppb across 2017 and 2018. Across all experiments the wheat was sown on the 5th of December and harvested on the 30th of March. The wheat was grown in non-filtered open top chambers across all three years. The wheat did not experience any soil water or N stress. For greater detail of the experimental set up and measurements taken, the reader is referred to Yadav et al. (2020) and Yadav et al. (2021). A scaling factor was applied to each AA concentration in Yadav et al. (2020) based on the mean concentration of AA in Siddiqi et al. (2020) to ensure values were consistent with the wider literature on AA concentrations for Indian wheat.

The meteorological data for the model input was taken from an onsite weather and O_3 monitoring system. The input temperature data were corrected for the heating effect of the open top chambers, with the chambers found to be approximately 2°C warmer than the ambient air (see supplementary information). Due to gaps in the hourly meteorological data, gap filling was performed according to Emberson et al. (2021).

3.4.2 Model calibration and evaluation

3.4.2.1 Model calibration

The calibration for DO_3SE-CropN is performed sequentially to allow the interactions between parameters at each stage to be limited (Section 2 of this thesis). The key parameters calibrated in the DO_3SE-CropN model are given in Section 2 of this thesis, and the same method of calibration is used in this study. In the present study, there are 3 additional parameters to calibrate based on the newly introduced antioxidant module: fst_{end}, a_{leaf} and, a_{stem}.

The maximum catalytic rate at 25°C ($V_{cmax,25}$) and the maximum rate of electron transport at 25°C ($J_{max,25}$) were fixed at the values provided by Yadav et al. (2020) in their supplementary data. The author's supplementary data on maximum photosynthetic rate were combined with data provided by the authors on maximum stomatal conductance to vary the species-specific sensitivity of stomatal conductance to assimilation rate (m), and the parameter describing variation in stomatal conductance in response to VPD (VPD_0), until a close match between photosynthetic rate and stomatal conductance was achieved (Yadav et al., 2020). Additional data provided by the authors of Yadav et al. (2020) were utilised to calculate the dark respiration rate; allowing calibration of the dark respiration coefficient for all simulations. Subsequently, the parameters controlling biomass accumulation and O_3 damage were calibrated using biomass data provided and assuming a seasonal maximum LAI of 5. The O_3 damage parameters were incorporated at this stage due to high ambient O_3 concentrations which caused an O_3 induced reduction in yield even under the ambient treatment. The parameters controlling leaf and stem N were varied to achieve a close match for the leaf and grain protein simulations, as no stem N data was available for calibration. During this stage of the calibration, the gradient of the equations describing the effect of O_3 on N remobilisation of the leaf and stem were set to 0 to allow the newly developed antioxidant processes to be tested, as it was hypothesised in Section 2 of this thesis that the O_3 impact on N remobilisation occurs due to antioxidant processes. However, as the calibration was performed, the best results were achieved when the new antioxidant processes were used in combination with the previously developed O_3 effect on remobilisation. Therefore, the parameters controlling N remobilisation from the leaf and stem (calibrated in Section 2 of this thesis) were varied as little as possible from their defaults to allow the newly developed antioxidant processes to be parameterised. For a tabulation of

parameters calibrated for, and the values they were calibrated to, please refer to the supplementary data.

Model parameters were calibrated using a combination of genetic algorithm and a trial-and-error approach, to minimise the difference between simulated and observed values while also retaining parameterisations that are physiologically realistic for the plant. For further details of the calibration method see Section 2 of this thesis.

3.4.2.2 Model evaluation

The input data available for the present study were limited. Initially, the data were split in half with the 2017 data used for model calibration and the 2018 data used for the model evaluation. However, when looking at the results of the evaluation it was clear that the limited input data led to overfitting of the 2017 dataset (see supplementary Fig.'s S8 and S9). Therefore, to focus on the development of the modelling framework, all available data were used for model calibration. The root mean square error (RMSE) and R^2 were used to evaluate the model's suitability at simulating the yields and protein contents of the two cultivars using Scikit-Learn (Pedregosa et al., 2011). Using the R^2 calculation from Pedregosa et al. (2011) can give negative R^2 values, where a negative value means that using the mean of the observed values is a better fit to the data than using the model. In this paper the units of the RMSE are the same as the units of the model variable, e.g. for yield RMSE is reported in in g m^{-2} and for protein percentage (% or 100gProtein/gDM^{-1}) RMSE is reported as percentage points.

3.5 Results

3.5.1 Biomass and protein simulations

Overall, the calibrations for grain yield, and leaf and grain protein, were reasonable for both cultivars. The grain yield and RY loss simulations performed better for 2018 than 2017. However, there was little difference in the model's capacity to capture the leaf and grain protein concentrations, and the relative loss in these, under O_3 exposure between the years. From Figure 3.3a, the grain yield calibration was satisfactory with a RMSE of 141 gm^{-2}, however it is clear that the calibration was able to simulate the grain DM better for 2018 than 2017. The underestimation of the grain DM in the 2017 dataset ranged between 35-46%. Further, the negative R^2 implies that using the mean of the observed data would be a better estimate of grain DM than the model (Pedregosa et al., 2011). The RY loss was captured much better than the grain DM. In Fig. 3b, the model captures the RY loss of cultivar HD3118 well. However, cultivar HUW234 has a large difference in RY loss between the two years which the model was unable to capture. The average deviation of RY loss from the observed value is 2.5 percentage points excluding the HUW234 cultivar for 2018. When this cultivar is included, the deviation increases to 7 percentage points.

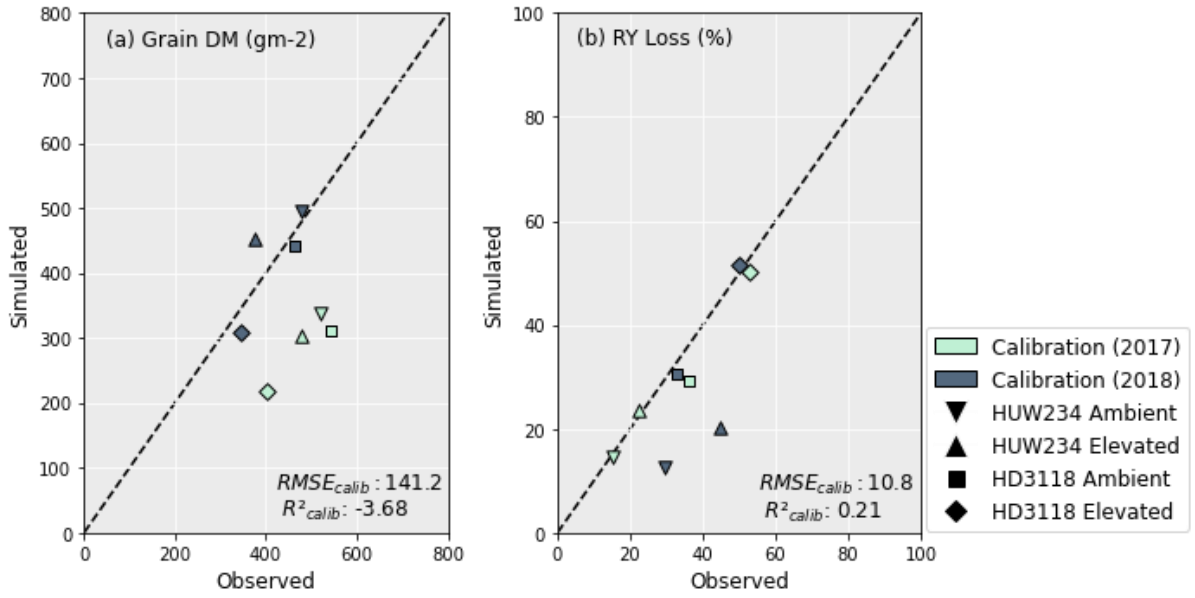

Figure 3.3: Calibration of grain DM (a) and RY loss (b) using the DO_3SE-Crop model for the Varanasi dataset. RY loss was calculated comparative to preindustrial O_3 concentrations (CLRTAP, 2017).

Figure 3.4 shows the grain and leaf protein simulations, and the relative protein (RP) loss between the ambient and elevated treatments. The grain protein (Fig. 4a) is captured better for 2017 than 2018, but overall, the results are good, with an R^2 of 0.5 and a RMSE of only 1.3%. The grain RP loss between the ambient and elevated O_3 treatment is slightly overestimated for the HUW234 cultivar, and for the HD3118 cultivar in 2017 it is slightly underestimated, all by ~2.5 percentage points. However, in 2018 the grain RP loss of the HD3118 cultivar was heavily overestimated by ~6.5 percentage points.

The simulations of leaf protein (Figure 3.4c) showed a good fit to the experimental data and were closer to the observed values than grain protein simulations, with an R^2 of 0.6 and a RMSE of 0.8%. Nevertheless, the model captured the pattern of the grain protein concentrations under ambient and elevated O_3 concentrations better than the pattern of the leaf protein concentrations (Figures 3.4a and 3.4c). The leaf RP loss (Figure 3.4d) was not well captured. For the HD3118 cultivar, the leaf RP loss was underestimated, and for the HUW234 cultivar it was overestimated. For the HUW234 cultivar leaf RP loss was overestimated by ~42 percentage points and for the HD3118 cultivar, the RP losses were more variable, with the leaf RP loss underestimated by ~13.5 and ~25 percentage points for 2017 and 2018 respectively.

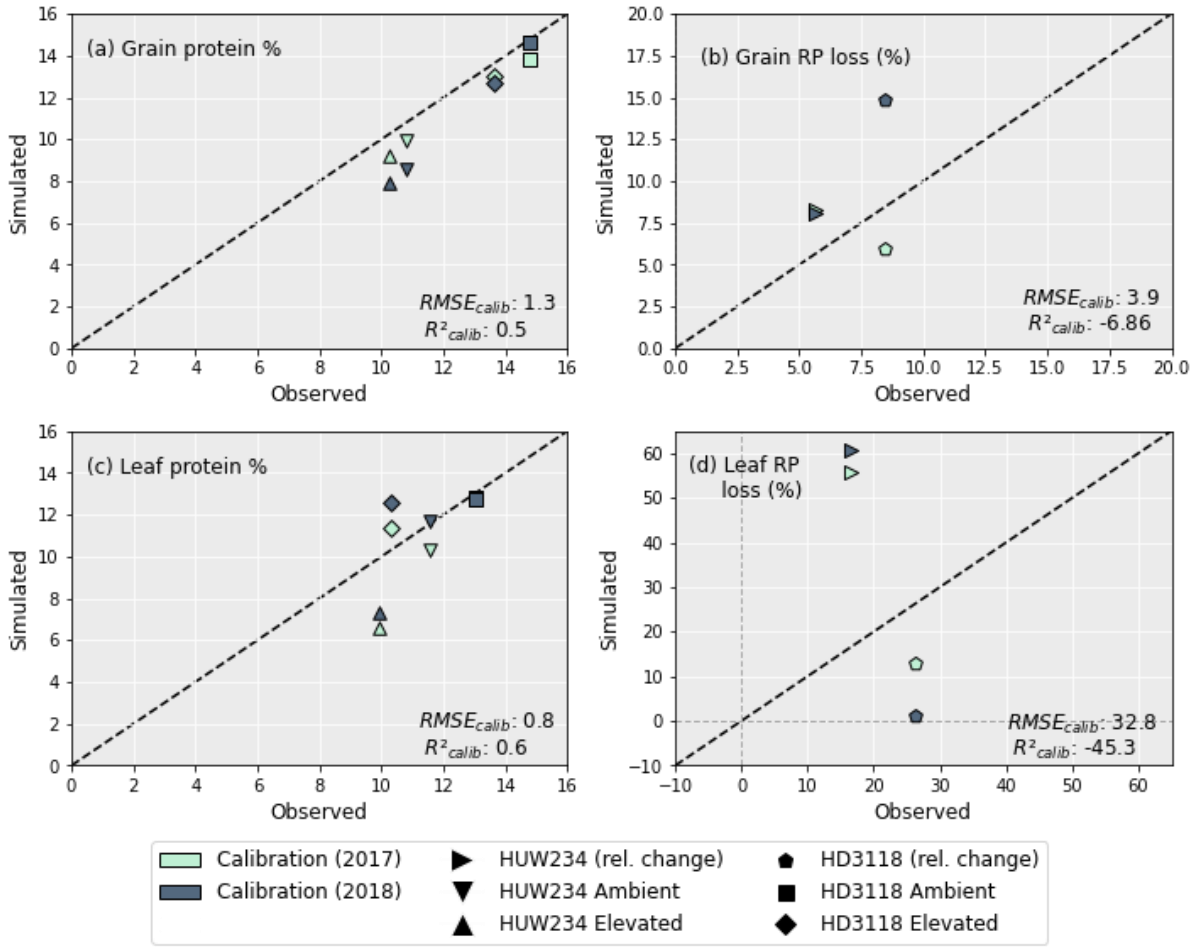

Figure 3.4: The concentration of grain (a) and leaf (c) protein of HUW234 and HD3118 cultivars under ambient and elevated O_3. Calibration of the RP loss in grain (b) and leaf (d). In figure (b) the relative change in grain protein for the HUW234 cultivar for the years 2017 and 2018 was almost identical, hence the overlaid points. In figure (c) the leaf protein concentration for HD3118 cultivar in the ambient treatment was almost identical for 2017 and 2018, giving the overlaid points. The RMSE and R^2 of the calibration are indicated on the plot.

3.5.2 AA simulations

Lysine and methionine were the key AAs focussed on as they were found to be the most limiting to protein production under O_3 exposure (Yadav et al., 2020). To calculate their concentrations the grain protein concentrations (Figure 3.4) were used along with the regressions from Liu et al. (2019). Figures 3.5a and 3.5c show the concentration of methionine in the wheat grains is predicted better than the lysine concentrations, with a higher R^2 of 0.73 (compared with 0.31) and a lower RMSE (0.02 compared with 0.06). However, the decrease in both AA concentrations under O_3 exposure was not captured as well (Figures 3.5b and 3.5d). For both lysine and methionine, the decrease in AA under O_3 exposure was heavily underestimated. The decrease in methionine for HUW234 and HD3118 was underestimated by 9 and 10.5 percentage points respectively. The decrease in lysine concentrations were underestimated by 37 and 19 percentage points for HUW234 and HD3118 respectively. The decrease in AA concentration for HUW234 was similar between years for both methionine and lysine, whereas for the HD3118 cultivar, the simulations showed a drastically different decrease in AA concentration between years.

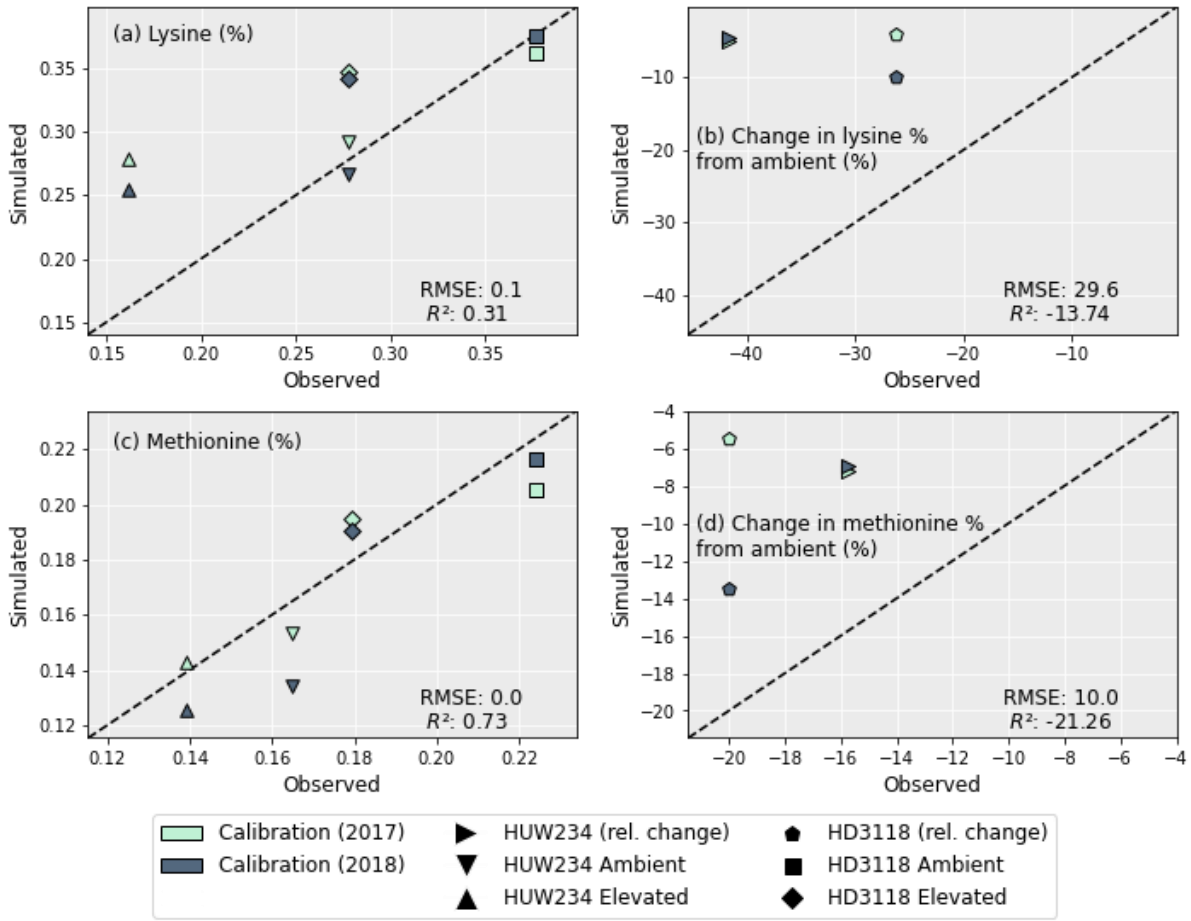

Figure 3.5: A comparison of the simulated concentrations of lysine (a) and methionine (c) for the different cultivars and years of treatment. The change in AA from ambient for lysine (b) and methionine (d) is also shown for both cultivars.

3.5.3 DIAAS of the nutritionally relevant AA

Methionine and lysine are the most limiting AA for protein production for the HUW234 and HD3118 cultivars, and experience a decrease in concentration under O_3 exposure (Yadav et al., 2020). Since the relative impact of O_3 on the AA concentrations was not captured well, the observed concentrations of the AA were used to calculate the DIAAS score, with the value that would be obtained if using the simulated outputs in brackets. After calculating the reference ratios for lysine and methionine using Equation (3.3), lysine was found to give the lowest reference ratio for all O_3 treatments and cultivars, and was used to calculate the DIAAS using Equation (3.4). Table 3.1 shows the results of the DIAAS calculation. Using the observed data, both cultivars experience a decrease in protein quality under elevated O_3 with the HUW234 cultivar experiencing a greater reduction than the HD3118 cultivar. Overall, the quality of wheat protein was lower for children aged between 6 months – 3 years than for older children and adults (>3 years). When using the simulated outputs to calculate the DIAAS, there is an increase in protein quality under O_3 exposure. This discrepancy occurs due to the construct of the DIAAS equation. As the decrease in AA concentrations under O_3 were underestimated by DO_3SE-CropN in comparison to the grain protein (see Figures 3.4 and 3.5), it led to a greater ratio of grain AA to grain protein (Equation (3.3)). The greater ratio under elevated O_3 then led to a higher value DIAAS under the treatment compared to the ambient, though this would not be the case in reality.

Table 3.1: The DIAAS for the HUW234, and HD3118 cultivars under the two O_3 treatments and for the age categories 6 months – 3 years, and for older children and adults (>3 years). The reduction in DIAAS under O_3 for the HUW234 and HD3118 cultivars was also calculated. The numbers in brackets represent the DIAAS score calculated using model outputs, the average AA and protein concentrations across the 2017 and 2018 simulations were used in the calculation.

	DIAAS					
Age category	HUW234 Ambient	HUW234 Elevated	HUW234 rel. change	HD3118 Ambient	HD3118 Elevated	HD3118 rel. change
DIAAS Score (> 3 years)	49.9 (59.1)	31.0 (61.1)	- 37.9% (+3.3%)	49.9 (50.8)	39.9 (52.4)	- 20.1% (+3.2%)
DIAAS Score (6 months - 3 years)	42.0 (49.80)	26.1 (51.5)	- 37.9% (+3.3%)	42.0 (42.8)	33.6 (44.1)	- 20.1% (+3.2%)

3.5.4 Difference between 2017 and 2018 simulations

After performing the simulations for 2017 and 2018 in section 3.5.1, it was clear there was a large difference in grain DM for the two years. The reasons for this discrepancy are important to understand since uncertainties on grain DM simulation will compound errors in protein concentration and yield (Section 2 of this thesis). To investigate the grain DM discrepancy further, the meteorological variables, stomatal conductance and photosynthetic rate were plotted for both years. The accumulation of biomass each day and the LAI were overlaid to see if there were any differences that could explain the large difference in biomass. The temperature in 2018 was greater at the beginning and end of the growing season compared to 2017 (Figure 3.6). The reverse was true for relative humidity (Figure S3.2). With relation to the other inputs, air pressure, precipitation and wind speed had negligible differences between the years (Figures S3.1, S3.3 and S3.4). O_3 concentrations were generally greater in 2017 than 2018 (Figure 3.7), and photosynthetic photon flux density (PPFD) was greater at the start of the growing season in 2018 (Figure 3.8). Daily photosynthetic rate was mostly greater in 2018 than 2017 and showed the same pattern for both cultivars (Figures 3.9 and S3.5). The difference in stomatal conductance between the years for both cultivars mimicked the shape of the photosynthetic rate plots (Figures S3.6 and S3.7). Given that the O_3 effect is more strongly determined by senescence than the instantaneous impact on photosynthesis (Pande et al., 2024b), and senescence onset did not differ strongly between years (Figure S3.11), it is unlikely that the differences in yield were caused by O_3 effects. Instead, it is likely that 2018's higher early-season PPFD and temperatures, along with lower RH, promoted earlier LAI development and increased biomass production in simulations.

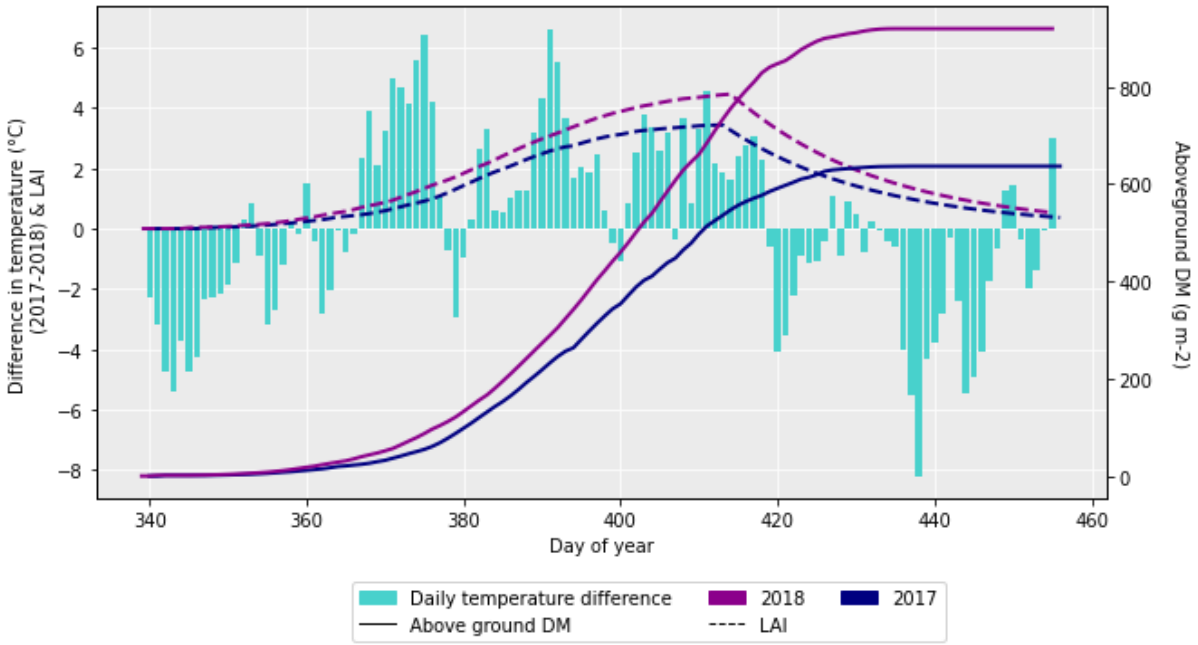

Figure 3.6: Plot of the difference in daily temperature between 2017 and 2018, along with the difference in aboveground DM accumulation for the ambient treatment for both years and the LAI profiles. The LAI and aboveground DM profiles are for the HUW234 cultivar.

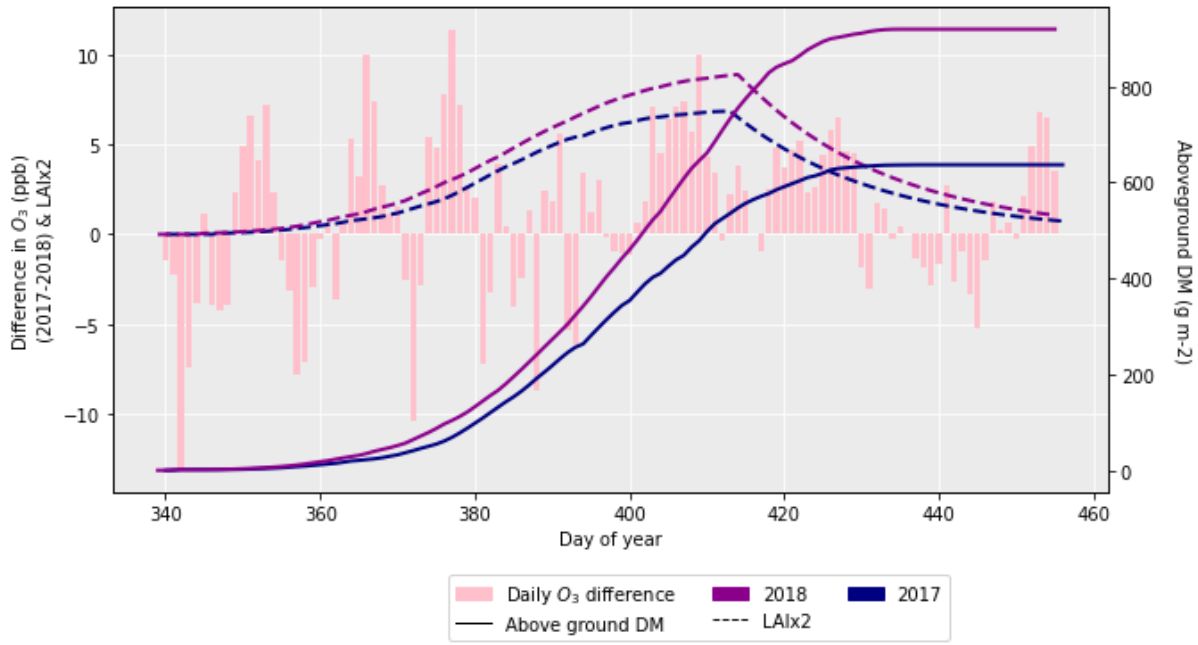

Figure 3.7: The difference in daily O_3 between 2017 and 2018 along with the difference in aboveground DM accumulation for the ambient treatment for both years and the LAI profiles. LAI has been multiplied by 2 to easier show the profile. The LAI and aboveground DM profiles are for the HUW234 cultivar.

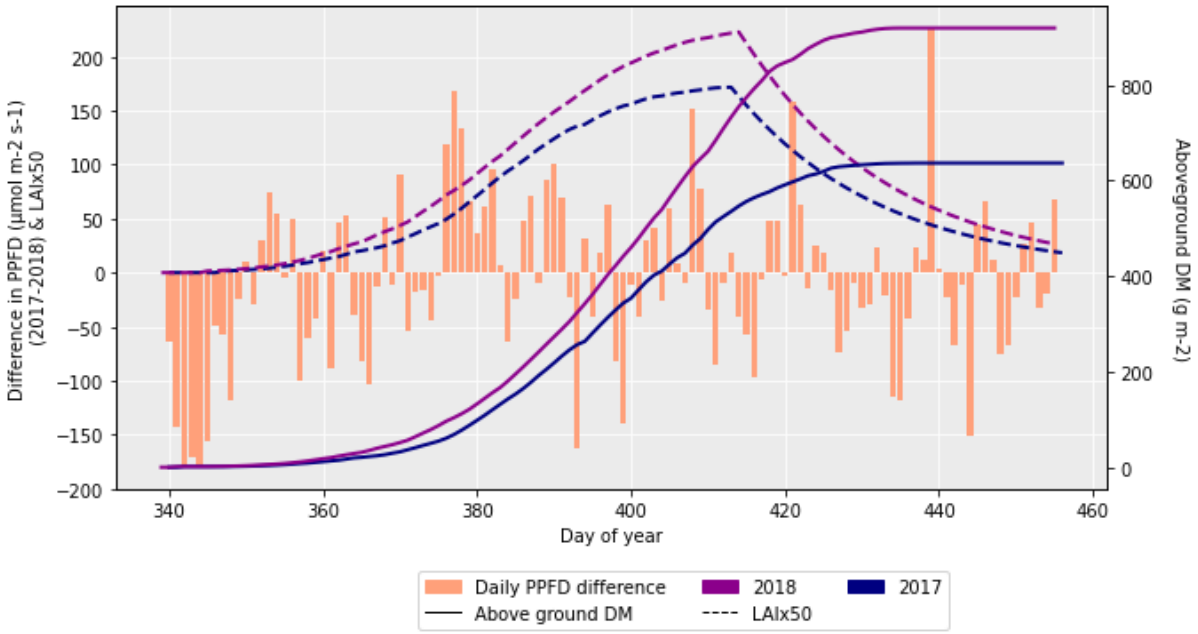

Figure 3.8: The difference in daily PPFD between 2017 and 2018 along with the difference in aboveground DM accumulation for the ambient treatment for both years and the LAI profiles. LAI has been multiplied by 50 to more clearly show the profile. The LAI and aboveground DM profiles are for the HUW234 cultivar.

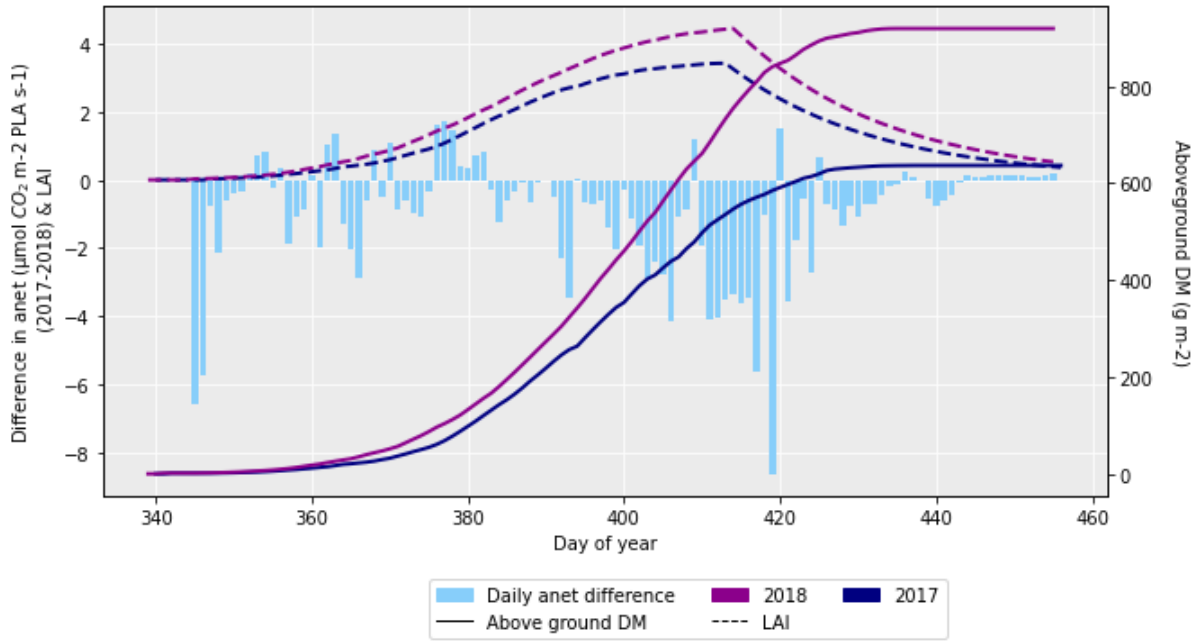

Figure 3.9: The difference in net photosynthetic rate for 2017 and 2018 along with the difference in aboveground DM accumulation and LAI for the ambient treatment for the 2 years. The LAI and aboveground DM profiles are for the HUW234 cultivar.

3.6 Discussion

We developed the DO_3SE-CropN model to address a current limitation in the ability of crop models to assess the effects of O_3 stress on not only crop yields, but also quality. We describe the further development and applications of the model to simulate O_3 effects on nutritionally important AA based on current understanding of antioxidant processes and implications for N remobilisation. This work is important since currently there are few models that consider

protein quality in their simulations. CN-Wheat considers AA from the perspective of being used for leaf, stem and grain protein production (Barillot, Chambon and Andrieu, 2016a). They do not explicitly consider the AA of the wheat grains, relevant for nutrition (Barillot, Chambon and Andrieu, 2016a). In SiriusQuality, Martre et al. (2006) consider the fractions of N that are split between gliadin, glutenin, albumin-globulin and other proteins in the wheat grains as a measure of wheat quality for bread production, not human nutrition. To our current knowledge, Liu et al. (2019) are the only authors who have extended a crop model to simulate protein quality, in the form of AA, from the perspective of human nutrition. In their work they extended the CERES-Wheat model to simulate lysine and other indispensable AA concentrations. Further, none of these crop models that consider crop quality have incorporated the effects of antioxidants. In our study we extend the equations used by Liu et al. (2019) to produce the first framework by which the effect of O_3 on protein quality (through antioxidants, AA and the DIAAS) can be captured.

3.6.1 Ability of the model to simulate DM and protein

The present model was able to reproduce the observed grain DM for 2018 but underestimated it for 2017 due to differences in meteorology that triggered earlier LAI development, leading to greater photosynthesis and biomass production in the model for 2018. The model was able to capture the RY loss of the HD3118 cultivar well for both years. However, the HUW234 cultivar experienced a large difference in RY loss between the two years, with the model only able to capture the RY loss well for one year. With only 2 years of data, it was not possible to determine which of the observed RY loss is the most common response for HUW234. Data for additional O_3 treatments and years are required to develop a more robust model parameterisation for different meteorological conditions and cultivars.

While the model underestimated the grain DM for 2017 by ~ 40%, there appears to have been no effect of this underestimation on the capacity of the model to capture grain protein concentration (100gProtein gDM^{-1}). A possible reason for this is that the lower photosynthesis in 2017, led to lower simulations of leaf and stem biomass. As a result, the N required by the leaf and stem for growth in the model was reduced, leading to lower N accumulation in these parts. Upon remobilisation to the grains, the reduction in N accumulated by the grains in 2017 compared to 2018, along with the reduced grain DM in 2017, led to similar protein concentrations. The model's ability to reproduce the observed grain protein concentration, despite yield discrepancies, suggests that the underlying N allocation and remobilisation equations reasonably approximate plant processes. This outcome supports the reliability of the equations, though further validation is needed to confirm their accuracy. Future work should focus on improving the model's estimates of protein yield and concentration so that O_3 threats to food security can be assessed with greater confidence.

In the model, there was a strong interdependence between the parameters controlling protein accumulation in the leaf and stem with grain protein, which is to be expected as protein remobilisation from the leaf and stem are key contributors to grain protein (Feller and Fischer, 1994; Gaju et al., 2014; Nehe et al., 2020). On calibrating the model, this interdependence meant that any attempt to improve the model's accuracy in capturing the decrease in leaf protein under elevated O_3 resulted in a reduced model accuracy in capturing the decrease in grain protein under elevated O_3, and vice-versa (see Fig.'s 4b and 4d). This meant that there was a trade-off between calibrating leaf and grain RP loss under O_3 exposure. No data was available on stem RP loss, so the accuracy of the stem parameterisation is unclear. Given this study focussed on grain quality, capturing the grain RP loss under O_3 was prioritised over the leaf. If

the model is not able to match the decrease in leaf protein with the corresponding decrease in grain protein under O_3 exposure for a given cultivar, then it implies a problem with the parameterisation or model construct. Regarding the parameterisation, leaf DM data were not available which would affect leaf N, and hence protein, accumulation. Therefore, in the future leaf (and stem) DM data at anthesis and harvest would aid in parameterising the equations describing the partitioning of photosynthate each day and could improve simulations of RP loss.

3.6.2 Modelling antioxidant processes under O_3 exposure

The first iteration of the DO_3SE-CropN model simulated the decrease in grain protein yield (gProtein m^{-2}), and increase in grain protein concentration (100gProtein gDM^{-1}) experienced by European and Chinese wheat cultivars (Broberg et al., 2015; Section 2 of this thesis). However, Indian wheat has been shown to experience a decrease in both protein yield and concentration under O_3 exposure (Yadav et al., 2020; Mishra, Rai and Agrawal, 2013). Through the incorporation of antioxidant processes, the present model is now able to capture the decrease in protein concentration, and yield, of protein in Indian wheat under O_3 exposure, improving the regional applicability and nutritional relevance of the model.

The design of the antioxidant equations has several benefits which make it useful for further applications. Firstly, the structure of Equation 3.1 means that it could be easily translated to other ROS mediated stressors, provided the corresponding equation parameters are identified, meaning the framework is flexible. Secondly, the modelling framework is simple. It does not require a large number of additional parameters, which reduces the complexity of the modelling process and makes it easier for other modellers to introduce into their models. Thirdly, it is compatible with the structure of other models that simulate plant N. The equations can be used to simply divide leaf and stem N into pools that are accessible or inaccessible (antioxidants) to the grain. Following this, the modeller only needs to ensure that any N remobilised from the leaf and stem to the grain comes from the accessible pool.

It was hypothesised that the introduction of the antioxidant processes would replace the previous O_3 effect on leaf and stem residual N that was parameterised in Section 2 of this thesis, as it was previously hypothesised that the increase in residual N occurred as a result of antioxidant production (Brewster, Fenner and Hayes, 2024; Sarkar et al., 2010; Section 2 of this thesis). However, during model calibration it was noted that the simulations of leaf and grain protein were improved when both processes were used in combination (see model parameterisation in supplementary information). There are two potential explanations for this: 1) The shape of the antioxidant response to O_3 is such that the two effects working in combination are a more effective approximation, meaning further data to investigate the effect could provide insight into the truer shape of the response, 2) O_3 has an effect on N remobilisation from the leaf and stem to the grains that is separate to antioxidant production. For example, ROS have been shown to oxidise proteins which would decrease protein concentrations but lead to greater residual N in the leaf and stem (Gill and Tuteja, 2010). Given this, and the previously described trade-off when calibrating leaf and grain RP loss, there is clearly a knowledge gap in our current understanding of antioxidant production and remobilisation of nutrients under O_3 exposure. Therefore, a study with multiple O_3 treatments that identifies the proportion of N in the leaf and stem at anthesis, and the leaf, stem and grains at harvest, as well as the corresponding proportion of proteins, would allow identification of how much N is associated with proteins, and whether this fraction changes under O_3 exposure and affects N remobilisation. Such data would also allow further development of the antioxidant equations in this study, as for simplicity, and lack of data to test a more complex

relationship, we have assumed linearity, but this may not be the case. Additionally, identification of the N associated with antioxidants at anthesis and harvest, and how these change under O_3 exposure, would also allow further development of the antioxidant equations. If combined with protein measurements at anthesis and harvest, mechanistic understanding of O_3 impacts on protein, antioxidant processes and grain filling with N could be developed further and used to refine existing model processes.

3.6.3 Antioxidant processes and grain quality

For consideration of O_3 effects on nutrition, it is important to consider the protein quality, in addition to its concentration. From a dietary perspective, indispensable AA, such as lysine and methionine, are the most important to consider when thinking about protein quality as they cannot be produced by the body and must be obtained through diet (Elango, Ball and Pencharz, 2008; Shewry and Hey, 2015). Lysine and methionine are key as they are the AA available in the lowest quantity in wheat exposed to O_3, and therefore limit the body's capacity to produce proteins from them (Yadav et al., 2020). If a person does not consume enough, or a high enough quality, of protein, then they are at risk of wasting and loss of muscle function (Medek, Schwartz and Myers, 2017). Understanding how O_3 induced changes to wheat protein will affect protein quality, and hence quality of diet, is key in understanding O_3 effects on human nutrition and its potential role exacerbating malnutrition.

The regressions from Liu et al. (2019) were used to simulate grain lysine and methionine concentrations as these were the most limiting for protein production under O_3 exposure (Yadav et al., 2020). However, there is variability in the response of AA in wheat grains under O_3 due to the differential activation of metabolic pathways under stress (Ali et al., 2019; Li et al., 2024; Wang et al., 2018; G A et al., 2024). Yadav et al. (2020) found that while overall protein concentrations decreased under elevated O_3, lysine and methionine concentrations decreased, while grain serine concentrations increased. The responses also differed between cultivars with HUW234 having an increase in threonine, while HD3118 had a decrease (Yadav et al., 2020). During stress conditions, the concentrations of AA vary to enhance plant defence mechanisms against abiotic stressors (Ali et al., 2019; Li et al., 2024; Wang et al., 2018; G A et al., 2024). In HUW234 and HD3118, lysine concentrations decreased under elevated O_3, due to its breakdown for energy production and plant defence (Ali et al., 2019; Yadav et al., 2020). Lysine breakdown produces proline, the concentration of which increased in both cultivars, which has been shown to protect against ROS-induced oxidative damage (Nayyar and Walia, 2003; Yadav et al., 2020; Yang, Zhao and Liu, 2020). Additionally, the concentration of methionine decreased in both cultivars under elevated O_3 (Yadav et al., 2020). The decrease is likely due to methionine's role as an antioxidant, and that it is very sensitive to oxidation by ROS (Ali et al., 2019). The changes in AA aid in the maintenance of photosynthetic rate and protection of photosynthetic pigments from ROS (Kaur and Kapoor, 2021; Naidu et al., 1991; Simon-Sarkadi and Galiba, 1996). The specific response of an AA to abiotic stress is cultivar specific and depends on the intensity of the stress (Ali et al., 2019). As a result, grain AA concentrations are linked to the stress response of the plant under O_3. Measurements of AA concentrations under multiple O_3 treatments would help to elucidate the shape of the response of AA's to O_3 stress. This is a field which has largely been neglected with only Yadav et al. (2020) having investigated it so far. Such data would allow the effect of O_3 on nutrition to be better understood.

3.6.4 Protein quality estimates using the DIAAS

Through extending DO_3SE-CropN to simulate the DIAAS, estimates of protein quality are translated into a metric that is commonly used to assess dietary quality in the nutrition field (e.g. Kurpad and Thomas (2020)). Using the observed data, the HUW234 cultivar experienced the greatest loss in protein quality under increased O_3 concentrations, despite showing the smallest RP and RY loss. The reason for this is that HUW234 experienced the greatest decrease in lysine concentrations, and lysine is the most limiting AA in wheat (Meybodi et al., 2019; Siddiqi et al., 2020). The DO_3SE-CropN model was not able to reproduce the reduction in protein quality calculated through the DIAAS as it was not able to reproduce the magnitude of the decrease in protein and lysine concentrations under elevated O_3 for either cultivar (Table 3.1, Figures 3.5b and 3.5d). Using the observed data, the calculations of DIAAS were the same for both cultivars due to the scaling factor used for the AA (see section 3.4.1) but, in reality, the DIAAS would differ between the cultivars. While using the simulations of grain protein and AA's was able to produce a difference in DIAAS between cultivars, it was only able to reproduce the DIAAS calculated from the observed data for the HD3118 cultivar in the ambient O_3 treatment, as the protein and lysine concentrations were captured well for this cultivar and treatment. To develop crop models that use the DIAAS to understand the reduction in protein quality under abiotic stress, the reduction in grain protein and the most limiting AA's for protein production under that stress need to be understood.

3.6.5 Data requirements for effective model calibration

Initially in this study, the data were split in half, and the 2017 data were used for model calibration and the 2018 for evaluation. However, due to the model overfitting to the 2017 dataset (see supplementary data), the decision was made to utilise all available data for calibration. This allowed the paper to focus on the development of the antioxidant processes and protein quality simulations. Should future work utilise the antioxidant or protein quality framework presented in this work, a thorough model calibration and evaluation is recommended. Calibrations that use data from contrasting growing conditions, such as different growing seasons/years, sowing dates or experimental conditions have been shown to reduce the chance of multiple combinations of parameters giving the same answer (equifinality), reduce model uncertainty, and improve simulation accuracy (He et al., 2017; Zhang et al., 2023). This is likely a result of achieving a truer parametrisation for the cultivar, leading to improved generalisation of the model upon application (Wallach, 2011). Hence, if there are few growing seasons of data available, it would be helpful to have data spanning a range of crop treatments.

3.6.6 Further work for understanding O_3 effects on wheat nutrition

Understanding cultivar-specific responses to increasing O_3 concentrations will be important for food security in order to breed cultivars that can maintain yields and protein quantity, as well as quality, in the future. Additionally, it can be seen in the calculations of the DIAAS score, and reflected in the wider literature, that the quality of protein in wheat is low, even without the impact of O_3, which will exacerbate protein deficiencies in consumers who rely on wheat based diets (Swaminathan, Vaz and Kurpad, 2012). Therefore, to reduce malnutrition, cultivars with a high protein quality, that can maintain yields and protein concentration under O_3 exposure should be investigated for their potential to maintain wheat supply and quality under conditions of elevated O_3 concentration. Additionally, existing barriers to diet diversification need to be

overcome, so that individuals may have access to higher quality protein sources (Agrawal et al., 2019).

To develop an understanding of cultivar specific responses to abiotic stress, a modelling approach similar to that used in this study would be useful, as such a model can capture the effect of antioxidant processes under stress on grain quality. To ensure the applicability of the model in addressing this goal there are a few existing barriers identified in this study:

1) Before model application, models need to be thoroughly calibrated and evaluated. To perform a thorough calibration and evaluation, a range of treatments and/or years of data need to be available to provide a set of calibration parameters that are more general for that cultivar and prevent over-fitting. Additionally, obtaining leaf and stem DM anthesis and harvest will aid in parameterising partitioning and remobilisation of photosynthate.
2) Differences in meteorological conditions between the two years of experiments in the present study had a large effect on simulations of grain DM. The effect of meteorology on simulations of photosynthetic processes and biomass production in crop models should be further investigated in the future to ascertain crop model sensitivity to input data choices.
3) To advance the antioxidant equations, and understand O_3 effects on grain quality, an experiment measuring N and protein concentrations in the leaf and stem at anthesis, and harvest, should be conducted. The proportion of N associated with antioxidants under the same O_3 treatments should also be obtained to improve mechanistic understanding of plant antioxidant response to O_3 which can be used to further develop the model.
4) Relationships linking grain protein to grain AA concentrations should be investigated for how they change under the influence of O_3. The modified equations could be integrated in the model so improve its ability to simulate AA concentrations under stress, and hence provide more trustworthy estimates of protein quality.

Reliable estimates of DIAAS would allow dietary protein quality to be incorporated into O_3 risk assessments. Performing yield and nutrition-based risk assessments utilising AA and DIAAS simulations under future O_3 scenarios would allow for assessment of which wheat growing areas will experience a decrease in wheat protein quality as well as yield. Such results could then be combined with dietary surveys to evaluate adult's and children's risk of not getting enough, or a high enough quality of, food under increasing O_3.

3.7 Conclusion

In summary, the present study has developed a framework by which the antioxidant response of wheat under O_3 exposure can be incorporated into wheat quality simulations in the existing crop model DO_3SE-CropN. The key benefits of the framework are that it is flexible, simple and compatible with other crop models provided they simulate leaf and stem N. The AA's most limiting for human nutrition under O_3 exposure were found to be lysine and methionine. The new modelling framework allowed the effect of high O_3 concentrations leading to a decrease in grain protein, lysine and methionine concentrations of Indian wheat to be simulated. Through calculations of the AA's, the FAO recommended metric for simulating wheat quality, the DIAAS, can be calculated. To improve the present model, we identified key experimental data needed to test and refine model formulations and parametrisations for a wider range of meteorological conditions and wheat cultivars. These include greater calibration data across multiple years and

treatments with leaf and stem DM and N measurements, mechanistic understanding of plant antioxidant response, and further development of relationships linking grain protein concentrations to AA concentrations under elevated O_3.

3.8 Supplementary information

3.8.1 Comparison of meteorological for 2017 and 2018

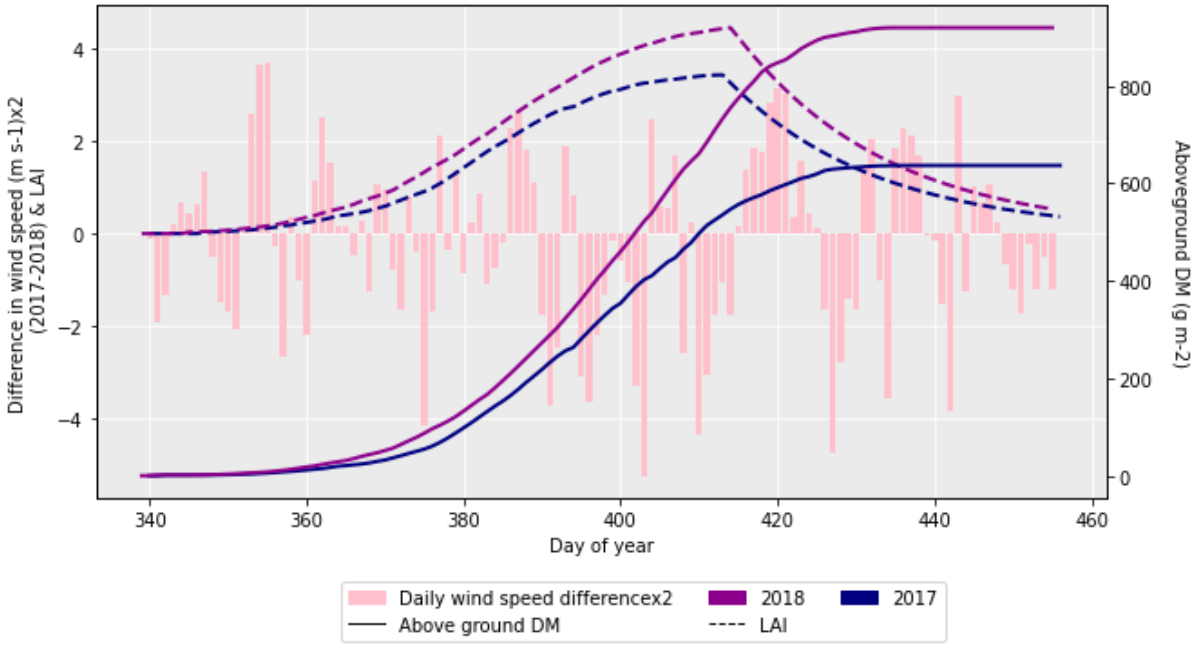

Figure S3.1: Daily mean difference in wind speed multiplied by 2, along with the difference in aboveground DM and LAI for the model run using the parameterisation noted "calibration method 2", which used all available data.

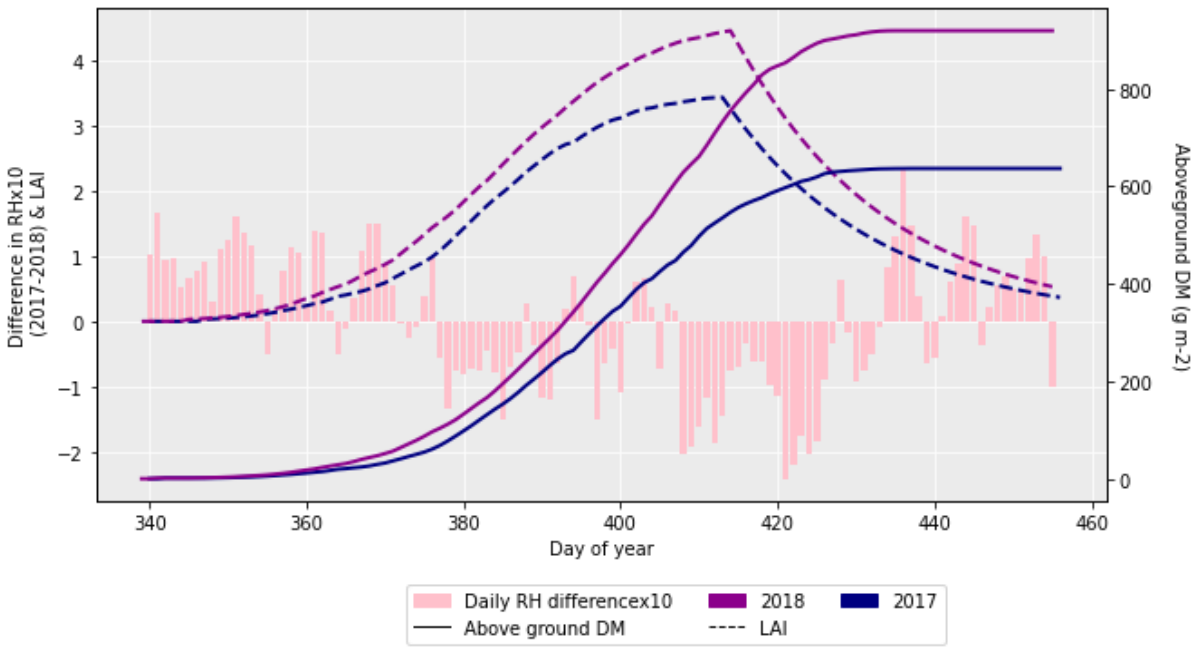

Figure S3.2: Daily mean difference in RH multiplied by 10, along with the difference in aboveground DM and LAI for the model run using the parameterisation noted "calibration method 2", which used all available data.

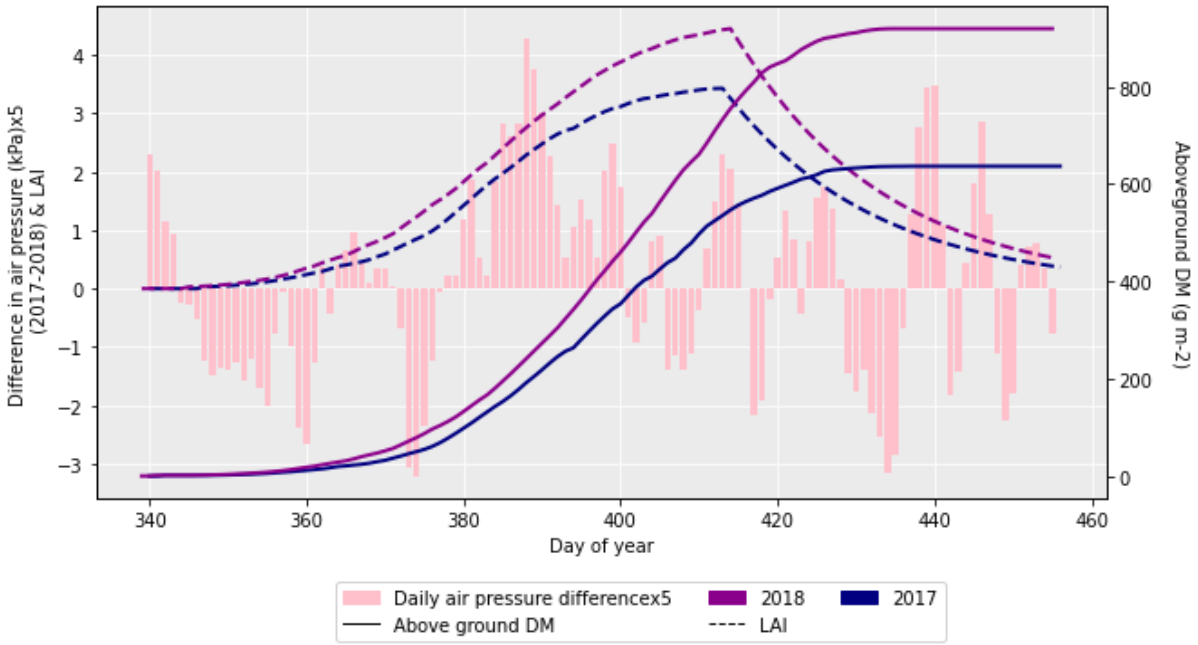

Figure S3.3: Daily mean difference in air pressure multiplied by 5, along with the difference in aboveground DM and LAI for the model run using the parameterisation noted "calibration method 2", which used all available data.

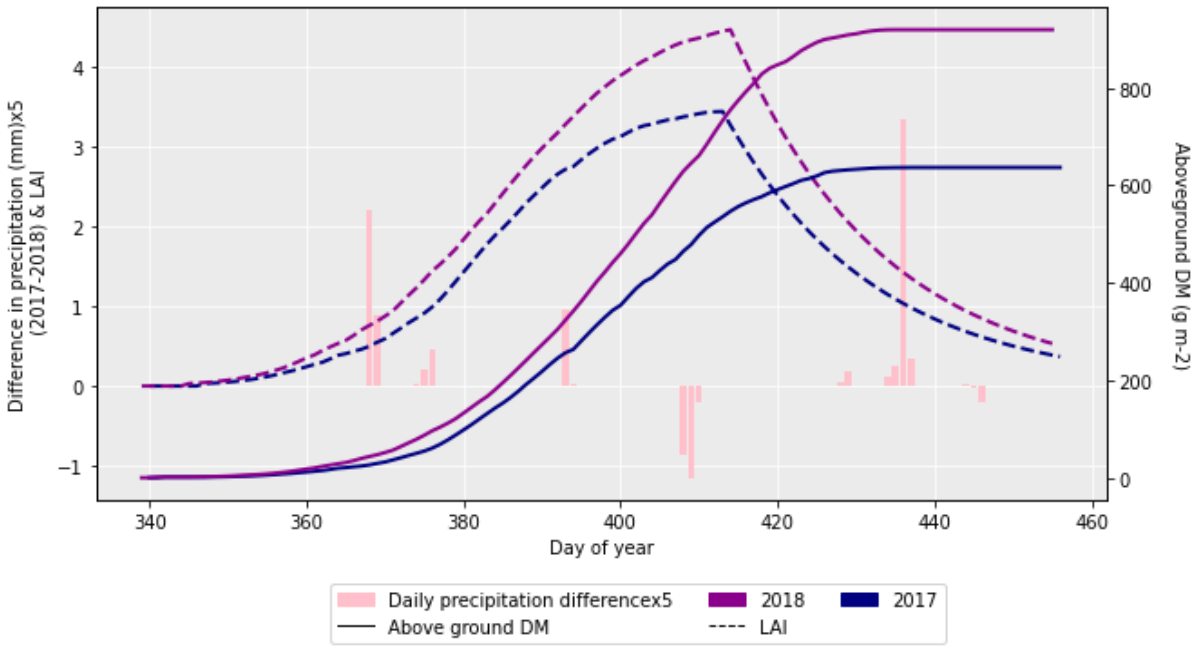

Figure S3.4: Daily mean difference in precipitation multiplied by 5, along with the difference in aboveground DM and LAI for the model run using the parameterisation noted "calibration method 2", which used all available data. Wheat was assumed to be irrigated so lack of rain was not an issue in model runs

3.8.2 Comparison of photosynthetic processes

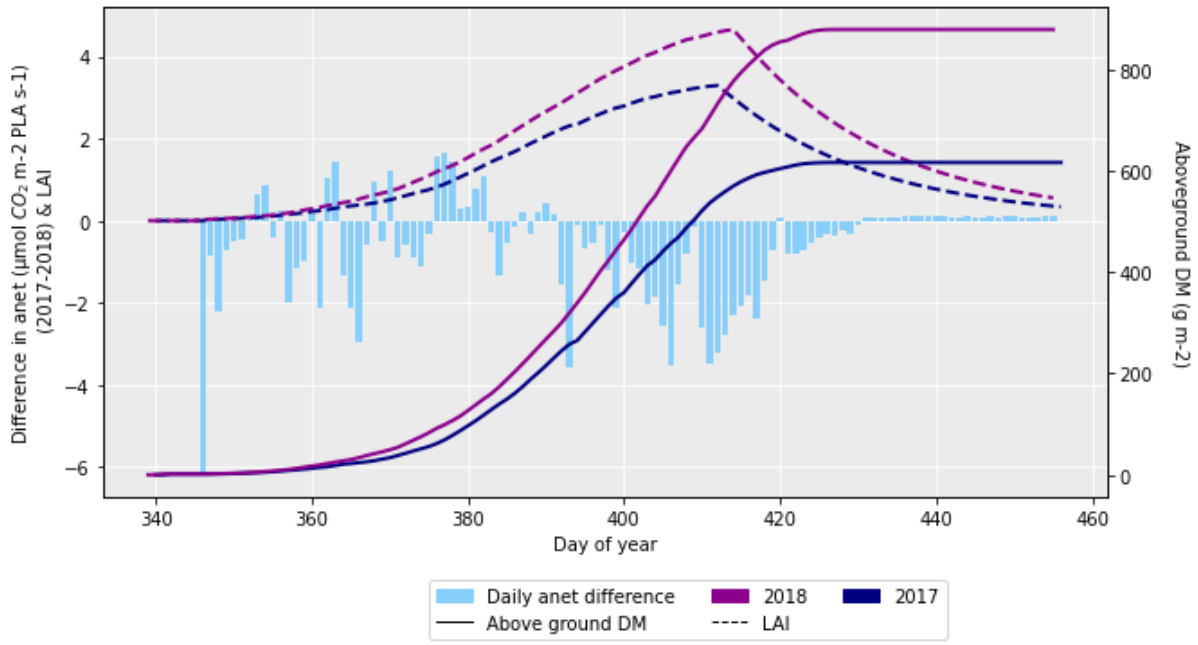

Figure S3.5: The difference in net photosynthetic rate for 2017 and 2018 along with the difference in aboveground DM accumulation and LAI for the ambient treatment for the 2 years. The LAI and aboveground DM profiles are for the HD3118 cultivar.

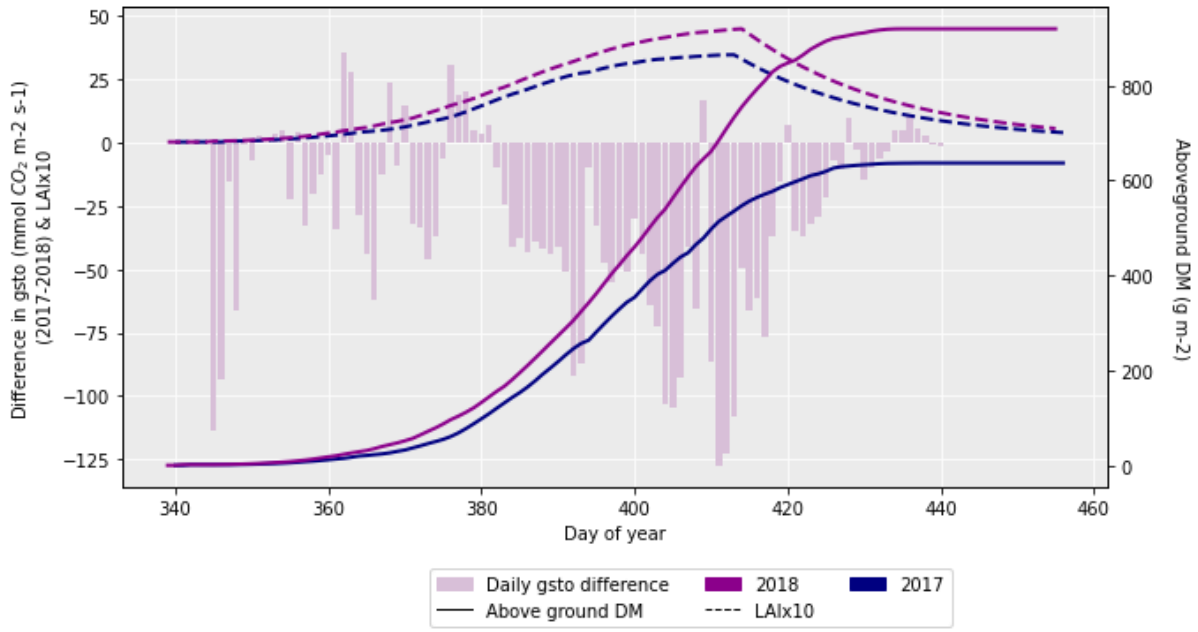

Figure S3.6: The difference in sunlit stomatal conductance for 2017 and 2018 HUW234 cultivar along with the aboveground DM accumulation and LAI for both years. This run used the parameterisation of "calibration method 2" where all available data was used for calibration

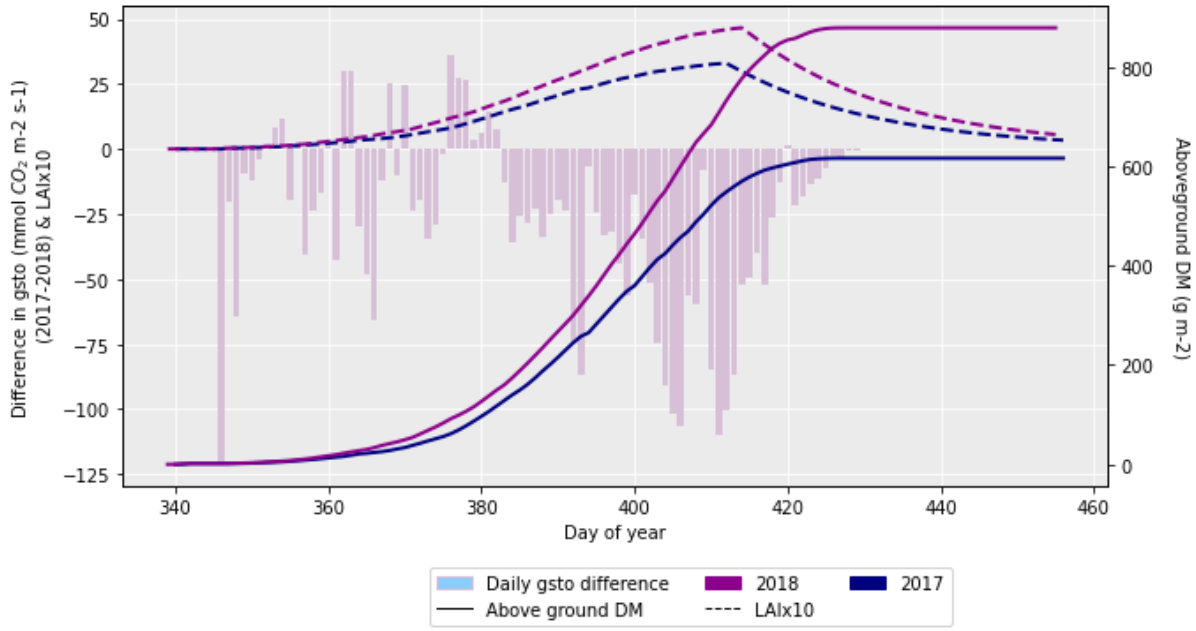

Figure S3.7: The difference in sunlit stomatal conductance for 2017 and 2018 HD3118 cultivar along with the aboveground DM accumulation and LAI for both years. This run used the parameterisation of "calibration method 2" where all available data was used for calibration

3.8.3 Model calibration

Initially, the input data was split into 2 groups. The 2017 data was used to calibrate the model and the 2018 data was used to evaluate the model. However, with such limited data the 2017 calibration dataset was subject to overfitting and the parameterisation obtained in the calibration did not give good results for the 2018 evaluation dataset. The parameterisation using the 2017 data for calibration and 2018 for evaluation is referred to as calibration method 1, and the parameterisation used in the main body of the paper, which used all available data to develop a parameterisation, is referred to as calibration method 2.

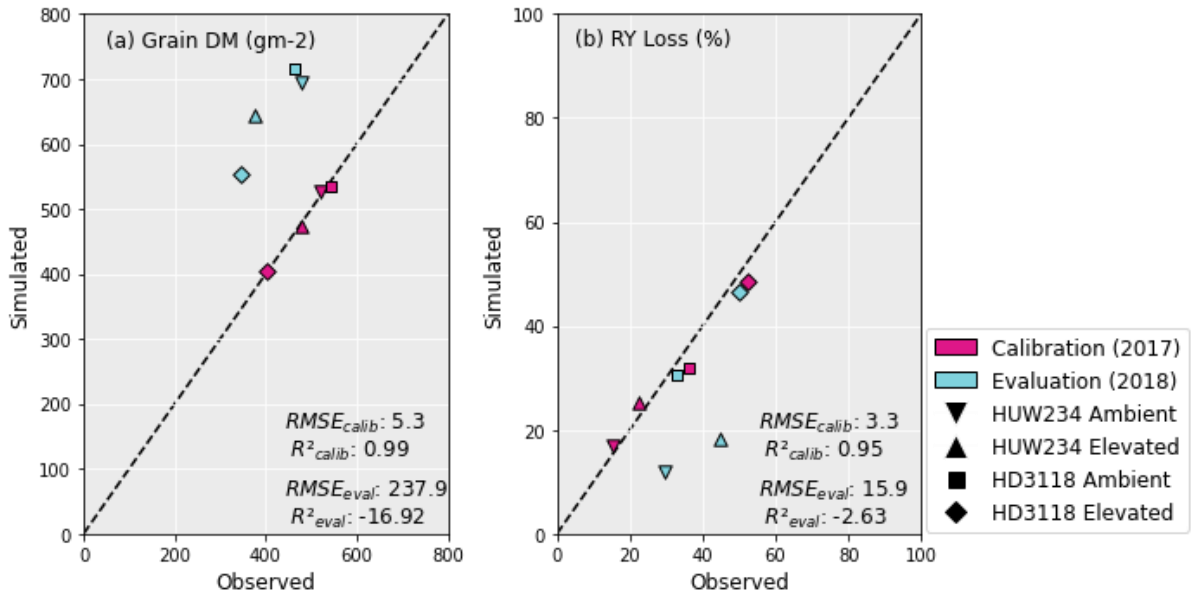

Figure S3.8: Calibration and evaluation of grain DM and RY loss using the DO_3SE-Crop model for the Varanasi dataset when using calibration method 1. RY loss was calculated comparative to preindustrial O_3 concentrations of 10 ppb (CLRTAP, 2017).

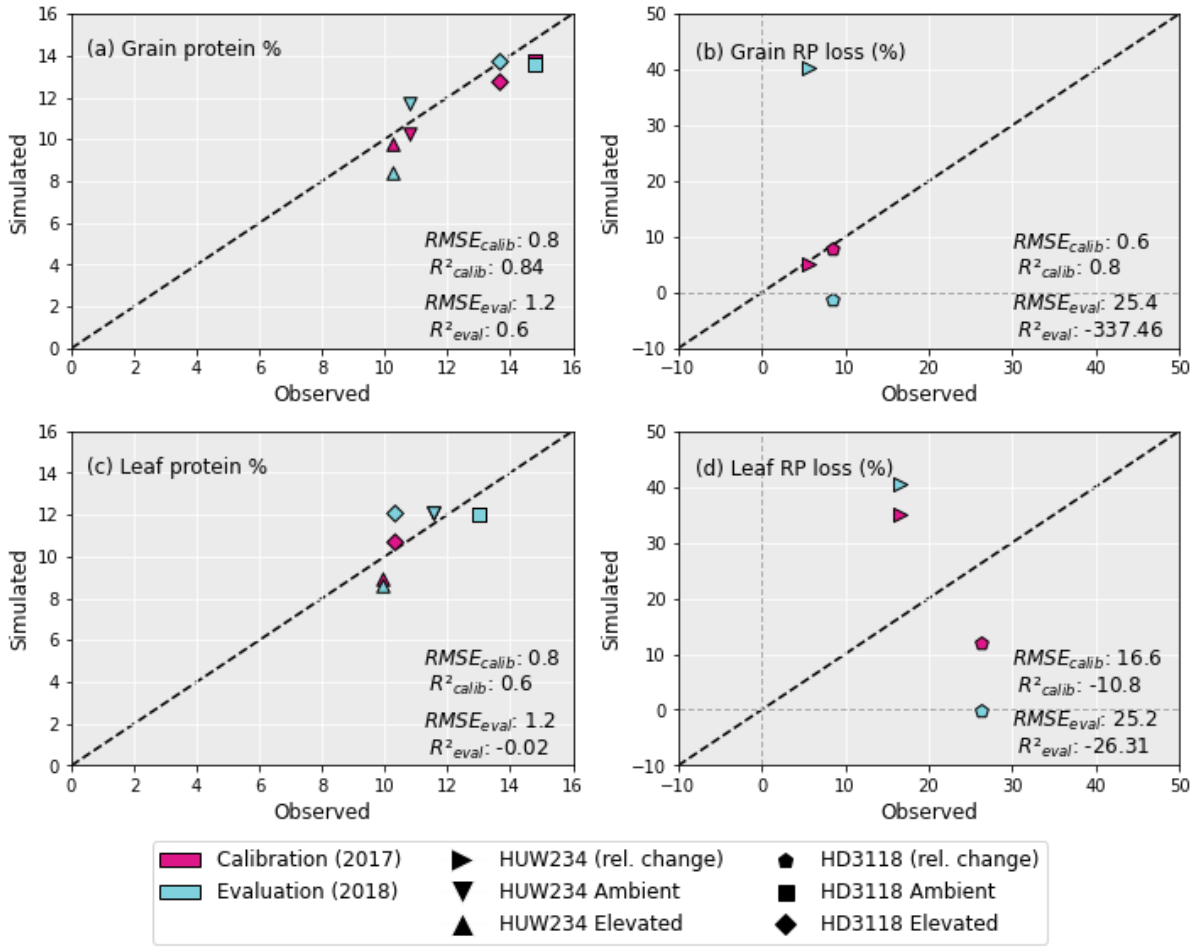

Figure S3.9: Calibration and evaluation of the concentration of grain (a) and leaf (c) protein of HUW234 and HD3118 cultivars under ambient and elevated O_3. Calibration and evaluation of the relative change in grain (b) and leaf (d) protein percentage. In figure (c) the ambient leaf protein % for the HUW234 and HD3118 cultivars in the calibration and evaluation were almost identical, hence the overlaid points. RMSE and R^2 of both the calibration and evaluation are indicated on the plot. These results use calibration method 1.

3.8.4 Correcting for the heating effect of the open top chamber

Data on the internal chamber and ambient air temperatures in Delhi, over the course of the wheat growing season in December 2018 to March 2019 were regressed against each other to obtain a regression with which to correct the input temperature data in the present study, as the air temperature sensor was external to the chambers.

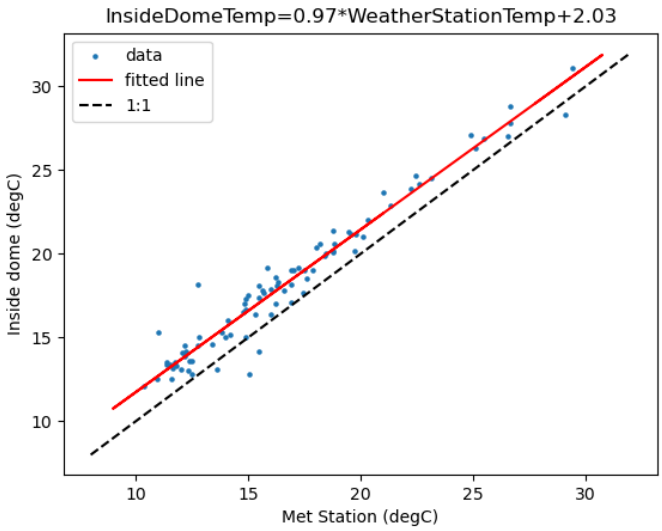

Figure S3.10: Regression between the air temperature as measured at the meteorological weather monitoring station and internal to the open top chambers in Delhi, during the wheat growth period 2018 to 2019. On average the open top chambers were approximately 2 degrees warmer than the ambient air.

3.8.5 Model parameterisation for calibration methods 1 and 2

Both the HUW234 and HD3118 cultivars were ran assuming the number of layers in the canopy was 4, and that there was 1 leaf population (nL=4, nP=1). The HUW234 cultivar parameterisation is given in Table S3.1, and the HD3118 cultivar parameterisation is given in Table S3.2.

Table S3.1: The parameters that were calibrated for (changed from the default parameterisation) in DO$_3$SE-CropN Model for both calibration methods for the HUW234 cultivar

Process	Parameter description	Calibrated Values		Unit
		Method 1	Method 2	
Phenology	Base temperature (T_b)	7	7	°C
	Optimum temperature (T_o)	25.99	25.99	°C
	Maximum temperature (T_m)	42.637	42.637	°C
	Plant emergence (TT_{emr})	80	80	°C days
	Flag emergence ($TT_{flag,emr}$)	792	792	°C days
	Start anthesis (TT_{astart})	1109	1109	°C days
	Mid-anthesis (TT_{amid})	1181	1181	°C days
	Harvest (TT_{harv})	1668	1668	°C days
Photo-synthesis	Maximum carboxylation capacity at 25 °C ($V_{cmax,25}$)	99.3	99.3	$\mu mol\ CO_2\ m^{-2}s^{-1}$
	Leaf vertical N co-efficient (kN)	0	0	-
	Maximum rate of electron transport at 25 °C ($J_{max,25}$)	138	138	$\mu mol\ CO_2\ m^{-2}s^{-1}$
	Parameter describing the variation in relative stomatal conductance with VPD (VPD_0)	2.95	2.75	kPa
	m (m)	7.4	7.4	-
Respiration	dark respiration (R_{dcoeff})	0.00972	0.00972	-

	growth respiration (R_g)	0.15	0.15	-
DM parameters	Coefficient for determining DM partitioning (α_{root})	16.5	16.64	-
	Coefficient for determining DM partitioning (β_{root})	-21	-20.5	-
	Coefficient for determining DM partitioning (α_{leaf})	20.477	18	-
	Coefficient for determining DM partitioning (β_{leaf})	-24.5	-20	-
	Coefficient for determining DM partitioning (α_{stem})	16.853	15.48	-
	Coefficient for determining DM partitioning (β_{stem})	-17	-14.69	-
	Coefficient determining specific leaf area (Ω)	22.2	22.2	$m^2\ kg^{-1}$
	Fraction of stem carbon in the reserve pool (τ)	0.75	0.75	-
	Fraction of DM in the harvest pool that goes to the grains (rest goes to the ear) (E_g)	0.85	0.85	-
Ozone damage	O_3 long term damage coefficient ($\gamma 3$)	0.0000325	0.0000325	$(\mu mol\ O_3\ m^{-2})^{-1}$
	O_3 long term damage coefficient determining senescence onset ($\gamma 4$)	4.2553	3.1811	-
	O_3 long term damage coefficient determining maturity ($\gamma 5$)	0.944	0.7742	-
	Critical accumulated stomatal O3 flux that determines the onset of leaf senescence (cL_{O_3})	8000	8500	$\mu mol\ O_3\ m^{-2}$
N uptake	Pre-anthesis maximum N uptake ($NUP_{pre,max}$)	0.55	0.55	$g\ N\ m^{-2}\ day^{-1}$
	Post-anthesis maximum N uptake ($NUP_{post,max}$)	0.3	0.3	$g\ N\ m^{-2}\ day^{-1}$
Leaf and stem N parameters	Target leaf N concentration ($[N_{leaf,target}]$)	1	1	$\frac{g\ N\ m^{-2}}{leaf\ area}$
	Target stem N concentration ($[N_{stem,target}]$)	0.017	0.017	$N\ g^{-1}\ DW$

	Ratio of N in grain to ear (f_{N,ear_grain})	0.95	0.95	-
Grain N parameters	Alpha parameter controlling sigmoid N grain filling function (α_N)	23	23	-
	Beta parameter controlling sigmoid N grain filling function (β_N)	1.2	1.2	-
N re-mobilisation	Gradient of N remobilisation from the leaf under O_3 exposure (m_{leaf})	0.6	0.2	-
	Intercept of N remobilisation from the leaf under O_3 exposure (c_{leaf})	10.89	10.89	-
	Gradient of N remobilisation from the stem under O_3 exposure (m_{stem})	0.0325	0.0325	-
	Intercept of N remobilisation from the stem under O_3 exposure (c_{stem})	0.2293	0.2293	-
Antioxidant processes	Accumulated stomatal O_3 flux above which N is only allocated to antioxidant pool (fst_{end})	45000	45000	mmol $O_3 m^{-2}$
	Modifier to customise the O_3 effect on antioxidants on the leaf (a_{leaf})	1	1	-
	Modifier to customise the O_3 effect on antioxidants on the stem (a_{stem})	2	2	-

Table S3.2: The parameters that were calibrated for (changed from the default parameterisation) in DO₃SE-CropN model for both calibration methods for the HD3118 cultivar

Process	Parameter description	Calibrated Values		Unit
		Method 1	Method 2	
Phenology	Base temperature (T_b)	6.992	6.992	°C
	Optimum temperature (T_o)	23	23	°C

	Maximum temperature (T_m)	43	43	°C
	Plant emergence (TT_{emr})	80	80	°C days
	Flag emergence ($TT_{flag,emr}$)	764	764	°C days
	Start anthesis (TT_{astart})	1050	1050	°C days
	Mid-anthesis (TT_{amid})	1093	1093	°C days
	Harvest (TT_{harv})	1450	1450	°C days
Photo-synthesis	Maximum carboxylation capacity at 25 °C ($V_{cmax,25}$)	101.6	101.6	$\mu mol\ CO_2\ m^{-2}s^{-1}$
	Leaf vertical N co-efficient (kN)	0	0.2	-
	Maximum rate of electron transport at 25 °C ($J_{max,25}$)	144	144	$\mu mol\ CO_2\ m^{-2}s^{-1}$
	Parameter describing the variation in relative stomatal conductance with VPD (VPD_0)	3.85	3	kPa
	m (m)	8.1	7.586	-
Respiration	dark respiration (R_{dcoeff})	0.00726	0.00726	-
	growth respiration (R_g)	0.2	0.15	-
DM parameters	Coefficient for determining DM partitioning (α_{root})	16	16	-
	Coefficient for determining DM partitioning (β_{root})	-21.5	-20.5	-
	Coefficient for determining DM partitioning (α_{leaf})	17.5	18	-
	Coefficient for determining DM partitioning (β_{leaf})	-19.921	-20	-
	Coefficient for determining DM partitioning (α_{stem})	15.15	16.6	-
	Coefficient for determining DM partitioning (β_{stem})	-15.714	-16.5	-
	Coefficient determining specific leaf area (Ω)	22.2	22.2	$m^2\ kg^{-1}$
	Fraction of stem carbon in the reserve pool (τ)	0.7	0.7	-
	Fraction of DM in the harvest pool that goes to the grains (rest goes to the ear) (E_g)	0.85	0.85	-
Ozone damage	O_3 long term damage coefficient ($\gamma 3$)	0.00008	0.0000377	$(\mu mol\ O_3\ m^{-2})^{-1}$
	O_3 long term damage coefficient determining senescence onset ($\gamma 4$)	0.9938	6.81	-
	O_3 long term damage coefficient determining maturity ($\gamma 5$)	0.92	1.4	-

	Critical accumulated stomatal O3 flux that determines the onset of leaf senescence (cL_{O_3})	12000	8500	$\mu mol\ O_3\ m^{-2}$
N uptake	Pre-anthesis maximum N uptake ($NUP_{pre,max}$)	0.65	0.5	$g\ N\ m^{-2}\ day^{-1}$
	Post-anthesis maximum N uptake ($NUP_{post,max}$)	0.4	0.2	$g\ N\ m^{-2}\ day^{-1}$
Leaf and stem N parameters	Target leaf N concentration ($[N_{leaf,target}]$)	1	1.2	$\frac{g\ N\ m^{-2}}{leaf\ area}$
	Target stem N concentration ($[N_{stem,target}]$)	0.025	0.02	$N\ g^{-1}\ DW$
Grain N parameters	Ratio of N in grain to ear (f_{N,ear_grain})	0.95	0.95	-
	Alpha parameter controlling sigmoid N grain filling function (α_N)	23	23	-
	Beta parameter controlling sigmoid N grain filling function (β_N)	1.2	1.2	-
N re-mobilisation	Gradient of N remobilisation from the leaf under O_3 exposure (m_{leaf})	0.2	0.2	-
	Intercept of N remobilisation from the leaf under O_3 exposure (c_{leaf})	10.89	10.89	-
	Gradient of N remobilisation from the stem under O_3 exposure (m_{stem})	0.2293	0.0335	-
	Intercept of N remobilisation from the stem under O_3 exposure (c_{stem})	0.03425	0.15	-

	Accumulated stomatal O_3 flux above which N is only allocated to antioxidant pool (fst_{end})	35000	75000	mmol $O_3 m^{-2}$
Antioxidant processes	Modifier to customise the O_3 effect on antioxidants on the leaf (a_{leaf})	0.6	1	-
	Modifier to customise the O_3 effect on antioxidants on the stem (a_{stem})	10	2	-

3.8.6 Senescence

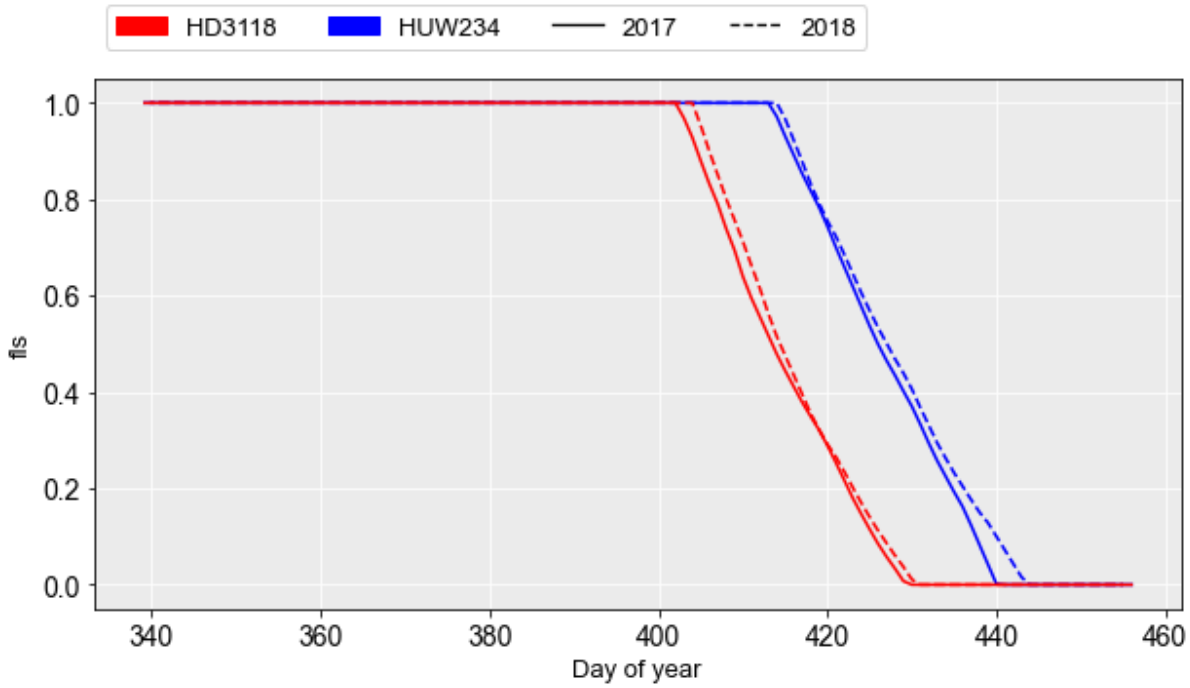

Figure S3.11: Graph of fls, the factor describing leaf senescence, where 0 is full senescence and 1 is no senescence, for both cultivars and years

4. Paper 3: Relative yield and protein estimates are highly sensitive to ozone risk assessment method and input data

4.1 Abstract

Tropospheric ozone (O_3) exposure reduces wheat yields and quality. Indian wheat experiences reductions in both protein content (gProtein m^{-2}) and concentration (gProtein gDM^{-1}) under elevated O_3. Previous risk assessments for India have mostly used concentration-response methods to estimate yield losses, but these methods neglect local meteorology which can

influence plant response to the stressor and have not considered wheat quality. This study evaluates O_3 effects on wheat yield and protein loss using a variety of O_3 risk assessment methods (concentration- and flux-response, and crop modelling) for Varanasi, in the Indo-Gangetic Plains where most of the wheat in India is grown. We used observational meteorology and O_3 data (December 2016–March 2017), alongside NASA Power and WRF-Chem modelled data, to understand the impact of input data variability on estimates of O_3 induced yield and protein losses. Additionally, we parameterised the flux-response and crop models for an O_3 tolerant and sensitive cultivar to see the effects of O_3 sensitivity on yield and protein losses. Concentration-response methods typically estimated greater relative yield (RY) losses, while flux-response and crop models gave lower estimates ($35.5 \pm 12\%$ vs. $18.8 \pm 4.0\%$ when concentration-response is excluded). Protein losses averaged 40% using the DO_3SE-CropN model, which was the only method currently available that can capture the response of Indian wheat grain protein content and concentration to O_3. Risk assessment method was the largest source of RY variability (with RY varying between 0 and 1 depending on method), followed by input data (where RY varied between 0 and 0.8). O_3 sensitivity contributed very little to variations in RY estimates (magnitude of 12 percentage points) but had a greater effect on protein (magnitude of ~40 percentage points). For protein content and concentration, risk assessment method contributed the most to variability, with input data choice and O_3 sensitivity still being substantial contributors. Accurate meteorological and O_3 inputs, in addition to well-parameterized models, are required to improve the reliability of O_3 yield and nutrition risk assessments for India, for which the lack of O_3 monitoring stations in India presents a challenge.

4.2 Introduction

Wheat provides approximately 20% of dietary calories and protein globally (Shiferaw et al., 2013). The threat of tropospheric ozone (O_3) to wheat yields has been widely studied in risk assessments, as O_3 induced yield losses have significant impacts on global food security (Mills et al., 2018b). The O_3 induced protein loss of wheat has received much experimental attention, but to-date no risk assessments have quantified regional or global losses (Broberg et al., 2015). Accurate risk assessments of yield and protein losses are crucial due to wheat's importance as a staple crop, providing calories for energy, sufficient and quality protein to prevent wasting and loss of muscle function, and vitamins and antioxidants that are overall beneficial to health (Medek, Schwartz and Myers, 2017; Peña-Bautista et al., 2017; Shewry and Hey, 2015). Policymakers and crop breeders rely on the results of risk assessments to direct policy recommendations and O_3 mitigation and adaptation strategies. The most common method for assessing O_3-induced yield reductions are concentration-response relationships, which only require canopy-level O_3 concentrations as their input. However, these methods often overestimate yield losses by failing to account for environmental modifiers that limit stomatal O_3 uptake (Pleijel, Danielsson and Broberg, 2022). More data-intensive methods, such as flux-response relationships and crop models, can provide more biologically relevant estimates, but due to high input data requirements (meteorology and O_3 concentrations) and model calibration requirements they are less commonly used. Risk assessments generally rely on input data from single-site observations or regionally interpolated observations, satellite re-analysis or atmospheric modelled data. The uncertainty surrounding yield and protein loss estimates, due to both risk assessment and input data choices, must be understood to ensure that policy recommendations and breeding strategies are based on the most reliable information.

4.2.1 Importance of wheat as a staple crop and the threat of O_3 to wheat yields and quality

Wheat is a key staple crop for global food security, providing 20% of daily calories and protein (Shiferaw et al., 2013). In Central and West Asia, and North Africa, wheat is even more important, providing at least 40% and 47% of daily calories and protein respectively (FAO, 2017). Wheat provides energy, protein, and essential amino acids, fibre, minerals, vitamins and antioxidants that are important for health and nutrition (Broberg et al., 2015; Shiferaw et al., 2013; Shewry and Hey, 2015; Peña-Bautista et al., 2017). If individuals do not consume enough volume, or a high enough quality, of food then they are at risk of wasting, stunting and loss of muscle function, lowering their immunity and increasing the risk of developing non-communicable diseases later in life (Medek, Schwartz and Myers, 2017; FAO et al., 2023; Briend, Khara and Dolan, 2015). Additionally, in developing countries, small scale wheat farming provides income to households as well as an easily accessible food source, supporting food security (El Bilali et al., 2019). As populations increase, the total demand for wheat is increasing, presenting challenges in the supply of wheat production meeting the demand (Shiferaw et al., 2013). India already faces challenges to food security with ~40% of the population unable to afford a nutritionally adequate diet (FAO et al., 2020; Herforth et al., 2020). Given that wheat is a staple food in the country, the threat of O_3 to wheat yields and quality needs to be investigated. Additionally, O_3 is expected to increase across the Indo-Gangetic Plains (IGP), where most of the wheat is grown, during the wheat-growing season, due to higher emissions of O_3 precursors and a changing climate which will promote O_3 production (Kumar et al., 2018; Fu and Tian, 2019; Rathore, Gopikrishnan and Kuttippurath, 2023). This gives even greater importance to investigating O_3 effects on wheat yields and quality.

Tropospheric O_3, that is formed when pre-cursor gases such as nitrogen oxides and methane react in the presence of UV light, threatens food security (Fowler et al., 2008; Broberg et al., 2015; Tai, Martin and Heald, 2014). O_3 diffuses into plants via the stomata, where it forms reactive oxygen species (ROS). These ROS trigger a series of reactions that have the effect of reducing photosynthesis and accelerating crop senescence (Emberson et al., 2018; Tiwari and Agrawal, 2018). As a result, crop yields and quality are reduced (Broberg et al., 2015). Globally, wheat yields are estimated to be reduced by ~9.2% due to O_3 pollution (Mills et al., 2018b). While in wheat producing countries such as India, where concentrations of O_3 pre-cursors are high, and climatic conditions for O_3 production are favourable, yield losses are estimated to range between 3.8%-41% depending on the method used to assess the risk (Ghude et al., 2014; Sinha et al., 2015; Mills et al., 2018b; Fowler et al., 2008; Rathore, Gopikrishnan and Kuttippurath, 2023). Additionally, several studies have shown a decrease in the yield of protein and other key minerals in O_3 exposed wheat (Broberg et al., 2015, 2023; Yadav et al., 2020; Piikki et al., 2008). The reduction in wheat yield and quality under O_3 exposure will present further problems to food security in regions where wheat production and O_3 concentrations are high, such as India and China (FAO et al., 2023; Wang et al., 2022; Mukherjee et al., 2021).

4.2.2 Development of risk assessment methods to assess O_3 threat

Several methods have been developed to assess the threat of O_3 to wheat yields and quality, of which the most common are summarised in Table 4.1 and are discussed in-turn in the following text. Traditional methods have made use of concentration-response relationships that link the O_3 concentrations crops are exposed to, to a corresponding yield or nutrient loss using experimental data (Mills et al., 2007; Broberg et al., 2015). The most common metrics which

quantify the O_3 exposure are M7 and AOT40, where M7 is the mean daylight O_3 concentration (generally between 9-4pm) over the wheat growing period, and AOT40 is the cumulative sum of O_3 concentrations more than 40 ppb during daylight hours (Sinha et al., 2015). In the USA W126 is also used; this metric gives increased weighting to the highest O_3 concentrations and better fits yield losses in the USA (Lefohn, Laurence and Kohut, 1988). The concentration-response relationships are the simplest methods for calculating yield and nutrient loss as they only require ground-level O_3 data as their input. Ideally, O_3 concentrations used to define these metrics would be provided at crop canopy height. Wind speed and O_3 measurement height can be used to translate these O_3 concentrations down to the canopy level as necessary (CLRTAP, 2018).

Another approach for estimating O_3 induced yield and nutrient losses are flux-response relationships (Grünhage et al., 2012; Yadav, Agrawal and Agrawal, 2021; Emberson et al., 2000a). These relationships were developed by linking the accumulated stomatal O_3 flux to the corresponding yield or nutrient loss. Calculations of stomatal conductance to calculate stomatal O_3 flux require hourly O_3 concentrations and meteorological variables such as radiation, temperature, vapor pressure deficit (VPD) and soil water content as well as crop phenology and effects of O_3 on leaf physiology which makes them more data heavy than the concentration-response approach (CLRTAP, 2017). However, since the calculation of the accumulated stomatal O_3 flux takes into consideration the influence of local environmental conditions on O_3 uptake that causes plant damage they are considered more biologically relevant (Pleijel, Danielsson and Broberg, 2022; Mills et al., 2011). The metric used to link accumulated O_3 flux to subsequent crop or nutrient loss is the phytotoxic O_3 dose above a threshold Y (POD_Y), and a simplified version of this metric (phytotoxic O_3 dose above a threshold Y for integrated assessment modelling)(POD_YIAM) is used to calculate fluxes at a regional level (CLRTAP, 2017; Mills et al., 2018b).

The final method by which yield, and nutrient losses are estimated is via crop models. Crop models are the most data heavy of the three approaches. They require hourly, or daily, meteorological and O_3 concentrations to estimate O_3 effects on seasonal crop development, growth and yield. There are two common methods by which O_3 damage has been integrated into crop models to-date. These methods are incorporating concentration-based metrics such as AOT40 or M7 (e.g. Xu et al., 2023; Guarin et al., 2019; Droutsas, 2020; Ren et al., 2007), or by calculating stomatal O_3 uptake (e.g. Nguyen et al., 2024; Pande et al., 2024). Calculation of short-term (photosynthesis) and/or long term (senescence) effects on crop growth can then be calculated from the concentration-based metrics or accumulated stomatal flux (Guarin et al., 2019b; Pande et al., 2024a; Ren et al., 2007; Nguyen et al., 2024). It is likely that crop models that use accumulated stomatal flux to estimate crop impacts are more realistic of the plant's physiological response to O_3 than crop models that uses concentration-based metrics (Emberson, 2020).

Table 4.1: Summary of the different risk assessment methods that can be used to estimate O_3 effects on crops

Risk assessment type	O_3 input	Growing season period	Stomatal O_3 uptake	O_3 damage estimate	References
Concentration-based	Canopy-level O_3*	Sowing to maturity	Not calculated	Parameterised concentration-response	(Mills et al., 2018c)

				relationship using e.g. AOT40 or M7	
Flux-based	Canopy level O_3*	Anthesis to maturity	Calculated by leaf physiology parameters and model inputs [PAR, VPD, precipitation, air pressure, temperature]	Parameterised flux-response relationship using POD_Y metrics	(CLRTAP, 2017)
Crop model using concentration-based methods	Current models use canopy-level O_3*	Sowing to maturity	Not calculated	AOT40 or M7 metrics are used to calculate short- and/or long-term O_3 effects, or they are used to develop a custom function for calculating RY	(Xu et al., 2023; Guarin et al., 2019b; Droutsas, 2020; Ren et al., 2007)**
Crop model using flux-based methods	Canopy-level O_3*	Sowing to maturity	Calculated by leaf physiology parameters and model inputs [PAR, VPD, precipitation, air pressure, temperature]	Parameterised O_3 damage module generally including short- and/or long-term O_3 effects	(Nguyen et al., 2024; Pande et al., 2024a; Tai et al., 2021; Schauberger et al., 2019; Tao et al., 2017; Zhou et al., 2018)**

** Canopy level O_3 can be calculated from other meteorological variables and O_3 measurement height*
*** No review or summary study has been performed so these citations refer to individual models that use these methods. All models simulate O_3 effects on key processes differently. For further detail please refer to the individual studies.*

4.2.3 Requirements of risk assessment methods

A summary of the requirements to perform the above risk assessments is given in Figure 4.1 and will be summarised in-turn in the following sections. Briefly, all risk assessments require O_3 concentration data to estimate O_3 damage. Flux-response and crop modelling methods additionally require meteorology to incorporate the modifying effect of the environment on stomatal O_3 uptake (Emberson et al., 2000a; Pande et al., 2024a). Concentration-response, flux-response and crop models are parameterised using experimental data that can come from O_3 filtration or fumigation experiments. The relative yield (RY) loss obtained from the differing risk assessments can be used to derive crop production loss and subsequent financial losses.

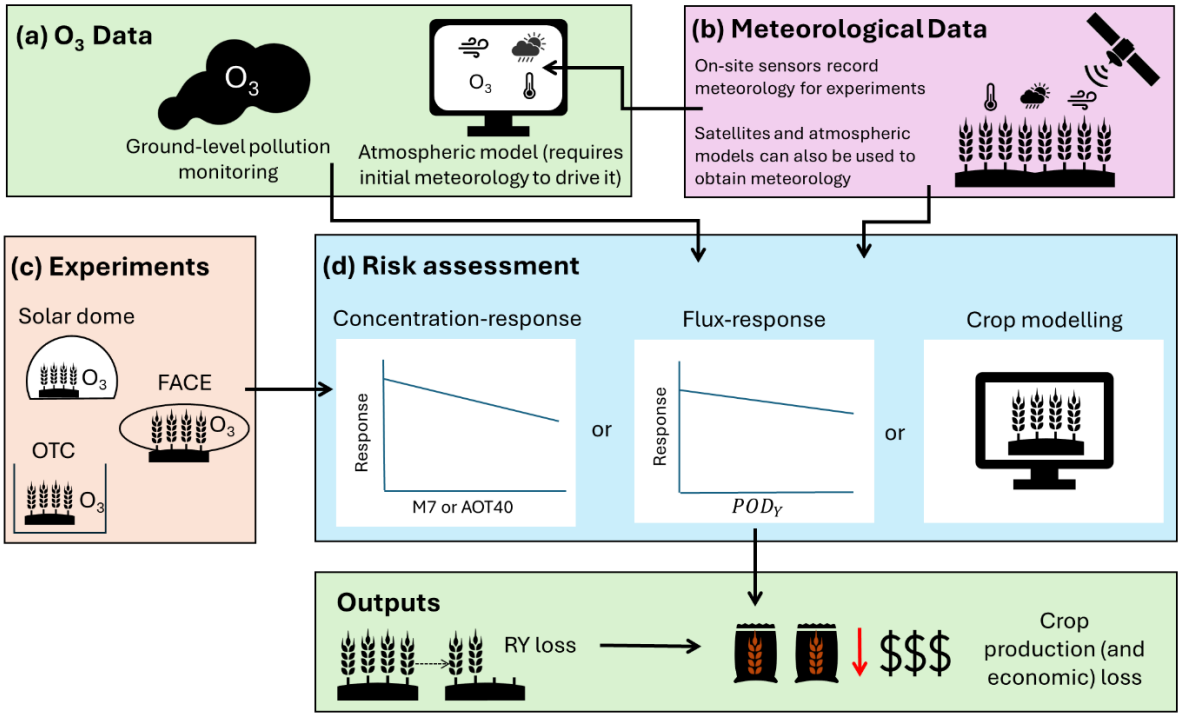

Figure 4.1: Summary of the requirements for performing risk assessments using concentration-, flux-response, or crop modelling methods.

(a) O_3 concentration data

All the risk assessment methods described above require O_3 concentration data for the site/sites under assessment. If observational O_3 concentrations are available then it is preferential to use these data (Sinha et al., 2015). For assessments across a larger region (e.g. sub-national or national) observed O_3 concentration data can be used but require linear interpolation for sites between O_3 monitoring locations. More commonly, O_3 concentration data for regional, continental and global assessments come from atmospheric chemistry or general circulation models (Ghude et al., 2014; Sharma et al., 2019; Tai et al., 2021). These models use O_3 precursor emissions data and meteorology to drive atmospheric chemistry reactions describing O_3 production, transport and deposition (Venkataraman et al., 2024). For O_3 risk assessments, O_3 concentrations are required at the canopy level. Canopy-level O_3 concentrations can be determined using a deposition scheme based on wind speed and measurement height or approximations of O_3 gradients for differing canopy types (CLRTAP, 2018, 2017).

(b) Meteorological data

For flux-response and crop modelling approaches, meteorological data are also required. These can be obtained from satellites, from sensors, weather stations located at/near the experimental site (Papers 1 and 2 of the present thesis). For risk assessments across larger regions, atmospheric models are more commonly used for meteorology (Mills et al., 2018b; Tai et al., 2021; Ghude et al., 2014; Sharma et al., 2019). To obtain meteorological data from satellites, satellite observations are input into an atmospheric re-analysis model along with surface land and ocean observations, and data from rawinsondes, to produce hourly estimates of meteorology. For example, NASA Power meteorological data are produced from the Modern Era Retrospective-Analysis for Research and Applications (MERRA-2) re-analysis model which uses land surface observations of air pressure, ocean surface observations of sea level

pressure and winds, upper air data (e.g. from rawinsondes), and finally geostationary satellite observations to produce hourly and daily modelled estimates of atmospheric variables with associated uncertainties available on the website (NASA, 2024b, 2024a). The validation of NASA Power meteorology from the atmospheric re-analysis model is performed by comparing the simulated meteorology with observational meteorology collated by the National Centre for Environmental Information. The observed meteorology come from different surface types (e.g. grasslands or forest), and over a wide range of locations globally (NASA, 2024a). To obtain meteorology from an atmospheric model, initial meteorological conditions are required to drive the model, along with specified boundary conditions (Sharma et al., 2019; Ghude et al., 2014; Venkataraman et al., 2024). The model then requires a "spin-up" period, where "spin-up" refers to the time-period used to achieve consistency in simulated versus realistic meteorology (Jerez et al., 2020; Venkataraman et al., 2024).

(c) Experimental fumigation/filtration data

Data from O_3 fumigation experiments are required by all risk assessments for method development. Commonly, plants are grown in solardomes (Brewster, Fenner and Hayes, 2024; Osborne et al., 2019), open top chambers (OTC) (Yadav et al., 2020; Sarkar and Agrawal, 2010), or free air CO_2/O_3 enrichment (FACE) set-ups (Feng et al., 2016). A disadvantage of solardomes and OTCs, are the altered temperature and humidity compared to outside conditions, which can accelerate plant growth (Emberson et al., 2009; Poorter et al., 2016; Leadley and Drake, 1993). Nevertheless, solardomes and OTCs allow for greater control over O_3 concentrations and exclusion of pests that could confuse interpretation of plant response to O_3. In contrast, FACE studies are suggested to be more realistic of conditions the crop would encounter in the field, but are limited in the range of O_3 treatments that can be applied and can suffer from pest damage (Feng et al., 2018; Kobayashi, 2022).

Regardless of their merits and drawbacks, all filtration/fumigation methods provide valuable information on crop response to O_3. A variety of wheat cultivars have been studied in solardomes, OTC and FACE systems under varying conditions including N or soil water availability, high temperatures and increased CO_2 (Piikki et al., 2008; Broberg et al., 2023; Brewster, Fenner and Hayes, 2024). These studies provide a deeper understanding of crop responses to O_3 by collecting data on phenology and senescence, photosynthesis, biomass, N status, yield and grain quality parameters (Brewster, Fenner and Hayes, 2024; Broberg et al., 2015; Feng et al., 2016).

4.2.4 Limitations of current risk assessment methods

Concentration-based studies have been criticised for ignoring cultivar-specific responses to stress and ignoring the interacting effects of the environment on O_3 induced damages, both of which result in a wide range of wheat sensitivities to O_3 between experiments, compared to flux-based or crop-modelling methods (Pleijel, Danielsson and Broberg, 2022; Emberson et al., 2000b; Emberson, 2020; Emberson et al., 2000a). Additionally, the neglect of environmental interactions in concentration-response risk assessments leads to differences in the estimates of spatial response of plants to O_3 stress, leading to differing identifications of at-risk areas (Mills et al., 2018b; Tai et al., 2021; Emberson et al., 2000a; Tarannum et al., 2024). Crop modelling methods can more mechanistically simulate O_3 effects on crops, and hence are more physiologically realistic than both flux- and concentration-based methods (Pande et al., 2024a). Nevertheless, some models integrate a concentration-response function into their modelling to simulate RY loss, which reduces the physiological relevance (e.g. GLAM-ROC,

DSSAT (Droutsas, 2020; Guarin et al., 2019b)), while others mechanistically simulate the stomatal uptake of O_3 and the subsequent effect on crops which is more physiologically relevant (e.g. DO_3SE-Crop, WOFOST, LINTULCC2 (Nguyen et al., 2024; Pande et al., 2024a)) (Emberson, 2020). However, all the models offer the capability of integrating environmental and O_3 effects on crop growth. Additionally, for performing risk assessments, input data can come from a wide variety of sources, such as atmospheric chemistry models, satellite re-analysis data or observations. Using different input data leads to differences in risk estimates, even for the same risk assessment method (Ghude et al., 2014; Sharma et al., 2019).

While several methods have been developed and applied to assess yield loss due to O_3 across a range of growing locations, risk assessments of wheat quality have not been performed despite some concentration- and flux-response relationships having been developed for protein (Broberg et al., 2015; Grünhage et al., 2012). To fully assess the threat of O_3 to food security, the effect of O_3 on crop quality needs to be incorporated into risk assessments, as O_3 affects both crop yield and quality.

4.2.5 Risk assessments performed for Indian wheat: Approaches and limitations

The aim of the present study is to compare different risk assessment methods and their sensitivity to variation in key input data (meteorology and O_3 concentrations). The comparison is made for Varanasi, India, which is in the IGP. The IGP is of particular interest as it is the highest wheat producing region in India, but it also experiences high O_3 concentrations (Mills et al., 2018c; Ministry of Agriculture & Farmers Welfare, 2023). Indian wheat is of particular interest with regards to O_3, as while several studies on European and Chinese wheat have shown an increase in protein concentration under elevated O_3 concentrations, Indian wheat has shown a decrease (Broberg et al., 2015; Yadav et al., 2020; Mishra, Rai and Agrawal, 2013). Several experiments have been performed at Varanasi which detail not only O_3 effects on wheat yields, but protein concentration, providing valuable data for developing flux-response and crop modelling methods for understanding O_3's effects on wheat quantity and quality, and estimating its impacts on food security (Yadav et al., 2020; Yadav, Agrawal and Agrawal, 2021; Section 3 of the present thesis).

Presently, a range of methods have been used in the literature to estimate relative yield (RY) loss across India. Table S4.2 and Figure S4.7 summarise the methods that have been used to find RY loss in India along with the absolute magnitude of the losses. The most common method is concentration-response relationships using M7 and AOT40 metrics, though with the exception of Sinha et al. (2015) these studies have not used equations developed for Indian wheat. To date only three flux-response methods (Mills et al., 2018b; Tang et al., 2013; Tai et al., 2021) and two crop models have been used to estimate RY losses at the country-level in India (Tai et al., 2021; Droutsas, 2020). Neither the flux-response nor crop modelling methods used to estimate RY loss were parameterised for Indian wheat. Further, no risk assessments looked at the response to the cultivar's sensitivity to O_3, or the effect of O_3 on protein, which will further exacerbate malnutrition in India. Additionally, due to sparse O_3 monitoring networks in India, it is difficult to determine "trust" in O_3 data, which can lead to under- or over-estimations of O_3 effects on wheat (Sharma et al., 2019).

4.2.6 Research questions

In the present study, we aim to understand the variability in estimates of yield loss due to differing input data choices and selection of risk assessment method. Particular focus is given to data sources that are available at a regional scale (satellite data and atmospheric chemistry modelling) to inform future data source and method selection for regional scale assessments in the country.

The research questions are:

1) Is the variability in O_3 concentrations and meteorological input data for the risk assessments within the bounds commonly used to assess the uncertainty of risk assessment methods?
2) How do estimates of RY, RP and RP concentration vary with different O_3 concentrations and meteorology?
3) How do estimates of RY, RP and RP concentration vary with different risk assessment methods when using the same O_3 concentrations and meteorological data?

We perform the above analysis for an O_3 tolerant and O_3 sensitive Indian wheat cultivar to address the question

4) Which risk assessment methods can differentiate wheat sensitivity to O_3?

Finally, answering the above questions allows us to answer the final question

5) Of differences in input data, risk assessment method and crop cultivar sensitivity to O_3, which is the greatest contributor to uncertainty on RY, RP and RP concentration estimates?

4.3 Methods

The data chosen to test how different input data choices affect risk assessment estimates in this study are satellite re-analysis meteorology data from NASA Power, atmospheric modelled meteorology and O_3 concentrations from WRF-Chem, and observational data (split into "OTC" and "field" data, see later sections). We begin by introducing each data source and explaining the method of estimating their associated uncertainty. Since the WRF-Chem O_3 concentrations were not measured at canopy-level, we explain how canopy-level O_3 concentrations are calculated with relevant equations. For performing the risk assessments, we detail how relevant O_3 metrics are calculated for each risk assessment type, and subsequently how these metrics are used to estimate relative yield, protein and protein concentration. The methods section concludes by bringing together existing protein data for Indian wheat to calculate a relative protein content and concentration to compare our results.

4.3.1 Input data sources

The input data in the present study were for the wheat growing period December 2016-March 2017. Observed meteorology and O_3 concentrations at Varanasi in the IGP from Yadav, Agrawal and Agrawal (2021) were available for this period, along with country-wide simulations of meteorology and O_3 from the atmospheric model WRF-Chem from which Varanasi data could be extracted. Further, to assess the use of satellite data in risk assessment estimates, meteorological data from NASA Power were also used. When comparing the meteorological variables and O_3 concentrations at Varanasi, January-March 2017 data were used. December 2016 was excluded due to not being directly simulated by WRF-Chem.

4.3.1.1 Observational O_3 and meteorology: Field and OTC

The observational meteorology and O_3 concentration data came from Yadav et al. (2021), who used an on-site sensor to record the temperature, air pressure, wind speed, O_3 concentrations, relative humidity (RH), photosynthetically active radiation (PAR) and rainfall on site at Varanasi, India (see Table 4.2 for a summary of measurement apparatus, height, location and duration). Measurements were taken hourly, and were gap-filled as necessary using a simplified linear-interpolation gap-filling method (Emberson et al., 2021). For a single missing value, the protocol averages the values that lie either side of it, for a days' worth of missing data, the protocol uses the hourly average of the day prior and the day after. For a longer period of missing data, the data for that equivalent day of the week prior and after are averaged for each hour where possible. For temperature, RH and air pressure, data were only available every 3rd hour. A linear model was fitted to each of the temperature and RH data and their equivalent NASA Power value for that hour to predict the parameter values for the missing hours at the site. If the gap-filling resulted in a large "jump" between in the observed and gap-filled data between hours, the linearly interpolated value replaced the observed value. Air pressure did not vary much between measurements so was kept constant over the hours of missing data.

For the datasets in this study, O_3 concentration data were not available for every day. Given the diurnal profile of O_3, a bell curve profile was used to gap fill O_3 concentrations with a nightly minimum of 5 ppb (Emberson et al., 2021). For running the risk assessment comparison, we use two datasets derived from the observational data; the first is termed "Field", the second "OTC" (open top chamber). The Field dataset consists of the gap-filled observed meteorology and O_3 concentrations at the Varanasi site. The OTC dataset consists of the gap-filled observed meteorology and O_3 concentrations at the Varanasi site, with an additional temperature correction applied to account for the warming effect of the OTC where the experiment was conducted. The OTC dataset was included as it was used to develop the DO_3SE-CropN model in Section 3 of the present thesis, and so can provide an idea of the impact of OTC effects on risk assessment estimates.

Table 4.2: The apparatus used to measure the observed data in Varanasi, along with the apparatus location and height with respect to the OTC and wheat, the measurement period, and the maximum and minimum observed values reported as: value prior to gap filling (value after gap filling) (Yadav, Agrawal and Agrawal, 2021; BHU, Department of Geophysics, 2009).

Variable	Measurement apparatus	Measurement location	Measurement height	Measurement period	% Data captured***
PAR	Radiometer (Model: PMA2100, Solar Light Company, Inc., Glenside, PA, USA)	Inside OTC	Top of canopy	December 2016-March 2017	22% total (58% 10am-5pm)****
O_3	O_3 analyser (Model APOA 370, HORIBA Ltd, Japan)	Inside OTC	45cm up to vegetative stage and 100cm at reproductive and post-reproductive stages	December 2016-March 2017	30% total (77% 10am-5pm)

			(~canopy height or just above)		
Temper-ature	AWS*	IMD**	1.2m	December 2016-March 2017	33% coverage (every 3rd hour)
Rainfall	AWS*	IMD**	1.2m	December 2016-March 2017	33% coverage (every 3rd hour)
RH	AWS*	IMD**	1.2m	December 2016-March 2017	33% coverage (every 3rd hour)
Wind speed	AWS*	IMD**	14m	December 2016-March 2017	33% coverage (every 3rd hour)****

**Automatic weather station (AWS), (specific instrumentation on the AWS unclear)*
***Indian meteorological division (IMD) Department of Geology and Geophysics, BHU, (~200m from experimental site)*
****Represents the percentage of the growing season for which data was available. All data gaps were gap-filled in accordance with the previously described protocol. PAR and O_3 data were only recorded between10am-5pm where data was available.*
*****While wind speed and PAR data was available the measurements were very dissimilar to NASA Power and so linear interpolation was performed for all of this data (Emberson et al., 2021).*

4.3.1.2 WRF-Chem data

The WRF-Chem data consists of simulated hourly RH, temperature, short-wave down radiation (converted to PAR by division of 0.45), air pressure, O_3 concentrations and wind speed available from the authors of Venkataraman et al. (2024). To obtain the simulations, the authors ran the WRF-Chem model using initial meteorology and boundary conditions from the ERA-Interim dataset, then MOZART-4 data was used to provide details for the chemical boundary conditions (Venkataraman et al., 2024). Following this December 2016 was used as a "spin-up" period. The WRF-Chem simulations were for the entirety of India, so the data for Varanasi was extracted using the latitude and longitude. The WRF-Chem grid cells are at a resolution of 27x27km and the grid cell did not cover substantially different topography so the cell meteorology and O_3 concentrations is assumed to be representative for Varanasi. The simulations from the study are considered some of the best to-date, as they cover the entirety of India with a fine spatial resolution and detailed emissions data (Venkataraman et al., 2024). Evaluations of the meteorological simulations showed that it recreated surface radiation, RH and temperature well (Venkataraman et al., 2024).

While WRF-Chem data for December 2016 were not available, the data for December 2017 were. We compared the observational meteorology and O_3 concentrations at Varanasi from Yadav, Agrawal and Agrawal (2021) and used these to determine the similarity between the two

months. Using this observational data, scaling factors were calculated for each meteorological variable which would convert the observed December 2017 meteorology to the observed December 2016 meteorology (see supplementary Table S4.1, and Figures S4.1-S4.6). These scaling factors were applied to the WRF-Chem December 2017 simulations to obtain an approximation of the simulated WRF-Chem meteorology for December 2016. Additionally, occasional values of the wind speed were missing in the WRF-Chem output, so gap filling was performed in accordance with the previously described gap filling protocol (Emberson et al., 2021).

4.3.1.3 NASA Power data

Hourly meteorological data from NASA Power for Varanasi were downloaded for the period December 2016 – March 2017 from NASA (2024). Parameters obtained from NASA (2024) were: "AllSkyPAR", "RH", "Temp", "Precip", "WindSpeed" and "Pressure". Precipitation was not used as we assume no water stress. It was not necessary to perform gap-filling for this dataset. However, since NASA Power does not record O_3 concentrations, the simulated WRF-Chem O_3 concentrations were substituted into this data. The WRF-Chem O_3 concentrations were used in-place of the observed O_3 data as they provide coverage across a larger spatial scale, in this case all of India (Venkataraman et al., 2024). The availability of NASA Power and WRF-Chem data across a larger scale makes them more suitable for risk assessments at a national level, where region wide meteorological and O_3 data are required as input. In the text, NASA Power meteorology with WRF-Chem O_3 concentration dataset is referred to as "NASA (WRF O_3)" to remind the reader that the O_3 concentrations were not from NASA Power.

4.3.2 Methodology for analysing the representativeness of the WRF-Chem and NASA (WRF-O_3) input data

To understand the uncertainty of the simulated WRF Chem data and the re-analysis NASA (WRF O_3) data we compare the meteorology and O_3 concentrations to the observed data. To more effectively form the comparison, it is useful to know the uncertainty on typical modelled meteorology and O_3 concentrations to determine if they form within these bounds. A recent sensitivity study used uncertainties of ± 3°C, $\pm 30\%$ and $\pm 40\%$ for modelled temperature, humidity and O_3 concentrations respectively in comparison to observed surface values, which the authors obtained by consulting the literature on typical model uncertainties (Emmerichs et al., in prep.). The uncertainties are summarised in Table 4.3. Rainfall/soil moisture is excluded due to the assumption of well-watered wheat at Varanasi (Section 3 of the present thesis). As these uncertainties represent the bounds within which modelled data is expected to fall within when compared to observational data, these bounds are applied to the observed data to observe whether the modelled re-analysis NASA (WRF-O_3) and atmospheric modelled WRF-Chem temperature, RH and O_3 concentrations fall within them. This allows for an understanding of the representativeness of the WRF-Chem and NASA (WRF-O_3) datasets of surface conditions at Varanasi. Performing this comparison assumes that the observed meteorology and O_3 concentrations are correct.

The differences in model outputs attributed to the differing meteorology and O_3 concentrations of the NASA (WRF O_3), WRF-Chem, Field and OTC data are investigated by exploring the differences in the fundamental modelling processes (phenology, photosynthesis, senescence, DM and N remobilisation) attributed to these variations, plotted individually as supplementary figures and discussed in Section 4.5.3.

*Table 4.3: Summary of uncertainty ranges of meteorological and O_3 data from Emmerichs et al. (in prep.) *30% represents the percentage variation in relative humidity and not a change in humidity of ±0.3.*

Model type	Temperature	O_3	Relative Humidity
O_3 Flux-response	± 3 °C	$\pm 40\%$	$\pm 30\%$*

4.3.3 Obtaining canopy-level O_3 concentrations

O_3 concentrations from WRF-Chem were simulated at a height of 29m. The DO_3SE model can calculate canopy-level O_3 concentrations from an observed or modelled O3 concentration at a given reference height, $[O_3]_z$. Initially, the deposition velocity (V_d) is calculated by considering the aerodynamic resistance (R_a), along with the boundary and surface resistances (Equation (4.1)):

$$V_d = \frac{1}{R_a + R_b + R_{sur}} \tag{4.1}$$

The deposition velocity is then used to propagate the O_3 concentrations at the reference height (z), in this case 29m, to canopy level (Equation (4.2))

$$[O_3]_{canopy} = [O_3]_z \times \left(1 - (R_a \times V_d)\right) \tag{4.2}$$

R_a is the aerodynamic resistance between the reference height and the canopy height, R_b and R_{sur} are the boundary layer and surface resistances of the canopy. For the consideration of crops, where there are several layers, the resistances of layers are summed cumulatively for input into the calculations (Simpson et al., 2012; Pande et al., 2024a).

The calculations of resistances in the above equations involve direct meteorological influences from wind speed, and indirect meteorological influences through LAI on V_d, determined through photosynthesis, where photosynthetic rate is impacted by temperature, stomatal O_3 uptake, VPD (though RH and temperature) and radiation (Pande et al., 2024a). This means that even if the measured height O_3 concentrations are the same, canopy level O_3 concentrations may vary due to the influence of meteorology and the cultivar response. Once the DO_3SE model was run using the differing input data, the canopy level O_3 was extracted for calculations of M7 and AOT40.

4.3.4 Calculating concentration, flux and crop-modelling metrics

4.3.4.1 Concentration metrics: M7 and AOT40

M7 and AOT40 are concentration-based metrics. M7 is calculated by taking the mean O_3 concentration at the canopy height between 9-4pm for the wheat growing period as in Equation (4.3):

$$M7 = \frac{1}{n}\sum_i [O_3]_{canopy,i} \qquad 09{:}00 \leq i < 16{:}00 \tag{4.3}$$

where i is the hour of the day and n represents the total hours in the growing season (Hogsett, Tingey and Lee, 1988).

Whereas AOT40 is calculated by taking the cumulative sum of canopy height O_3 concentrations more than 40 ppb during daylight hours as shown inequation (4.4):

$$AOT40 = \sum_i \left([O_3]_{canopy,i} - 40\right)\ [O_3]_{canopy,i} > 40\ ppb \tag{4.4}$$

where hourly O_3 concentrations must also be in ppb and the summation is calculated over the entire growing season (Mills et al., 2007; Fuhrer, Skärby and Ashmore, 1997).

4.3.4.2 Flux metric POD_6

To calculate POD_6 the multiplicative DO_3SE (version 4.39.16) model was used (Bland, 2024b). Yadav et al. (2021) detail the process used to parameterise the multiplicative DO_3SE model for O_3 sensitive and O_3 tolerant Indian wheat cultivars. In this study we use their parameterisation for the HD3118 (O_3 sensitive) and HUW234 (O_3 tolerant) cultivars and change only the phenology to match that developed in Section 3 of the present thesis, which is the same phenology parameterisation used for DO_3SE-Crop runs in this study. This parameterisation means that stomatal accumulation of O_3 flux in the multiplicative model begins at anthesis whereas Yadav, Agrawal and Agrawal (2021) accumulated O_3 from sowing. In the multiplicative DO_3SE model, the stomatal conductance (g_{sto}) in units of mmol O_3 m^{-2} PLA s^{-1} (where PLA stands for per leaf area) is calculated as follows:

$$g_{sto} = g_{max} \times min\{f_{phen}, f_{O_3}\} \times f_{light} \times max\{f_{min}, f_{temp} \times f_{VPD} \times f_{SW}\} \tag{4.5}$$

g_{max} is the species specific maximum stomatal conductance (mmol O_3 m^{-2} PLA s^{-1}), and f_{phen}, f_{light}, f_{temp}, f_{VPD} and f_{SW} are factors that vary between 0 and 1, and represent the response of g_{sto} to variation in leaf age, irradiance, temperature, VPD and soil water respectively. f_{min} is the minimum daylight g_{sto} expressed as a fraction of g_{max} and f_{O_3} is fraction between 0 and 1 representing the modifying effect of O_3 concentrations on stomatal conductance (Büker et al., 2012; CLRTAP, 2017). For the purposes of the present study, the wheat was well-watered, and water was not considered limiting so f_{SW} was set to 1. The equations describing f_{phen}, f_{light}, f_{temp}, f_{VPD}, f_{SW} and f_{O_3} can be found in CLRTAP (2017). After calculating the stomatal conductance, the stomatal O_3 flux (f_{st} in nmol O_3 m^{-2} PLA s^{-1}) is calculated by propagating the canopy-level O_3 concentrations ($[O_3]_{canopy}$ in nmol m^{-3}) through the resistances to O_3 uptake, to determine the O_3 concentration at the leaf that is subsequently taken up as shown in Equation 4.6:

$$f_{st} = [O_3]_{canopy} \times \frac{g_{sto}}{41000} \times \frac{r_c}{r_b + r_c} \tag{4.6}$$

where r_c is the leaf surface resistance and r_b is the leaf level quasi-laminar resistance both in units of s m^{-1}. The division of g_{sto} by 41000 converts the stomatal conductance from units of mmol m^{-2} s^{-1} so m s^{-1} at standard temperature (20°C) and air pressure (1.013 x 10^5 Pa) (CLRTAP, 2017). To calculate POD_6, Equation (4.7) is used, where Y = 6 nmol O_3 m^{-2} PLA s^{-1} and the fluxes are summed over daylight hours when $f_{st} > Y$. The factor $\frac{1}{10^6}$ represents the conversion to obtain POD_Y in units of mmol m^{-2} PLA while the multiplication by 3600 allows for the calculation of hourly stomatal fluxes:

$$POD_Y = \frac{3600}{10^6} \times \sum_{\substack{f_{st}>Y \\ Day}} f_{st} - Y \quad (4.7)$$

4.3.4.3 Crop modelling metric: fst

The DO_3SE-Crop model is a coupled photosynthetic-stomatal conductance model, which means that alterations to photosynthetic rate will have a feedback effect on stomatal conductance, and hence O_3 uptake (Leuning, 1995; Pande et al., 2024a).

In DO_3SE-Crop, stomatal conductance (g_{CO_2} in μmol CO_2 m^{-2} s^{-1}) is calculated as follows:

$$g_{CO_2} = g_{min} + \frac{m \times A_{net} \times f_{VPD}}{c_s - \tau} \quad (4.8)$$

g_{min} is the minimum daytime stomatal conductance (μmol CO_2 m^{-2} s^{-1}), m is a dimensionless coefficient representing the sensitivity of stomatal conductance to assimilation rate and VPD, A_{net} is the net photosynthetic rate (μmol m^{-2} s^{-1}) and the relationship between stomatal conductance and VPD is given by f_{VPD}. It should be noted this f_{VPD} is slightly different to that in the multiplicative DO_3SE model described in Section 4.3.4.2, as it is curvilinear, while the multiplicative f_{VPD} is linear. The equation describing the f_{VPD} function for DO_3SE-Crop is found in Pande et al. (2024) and for the multiplicative DO_3SE model is found in CLRTAP (2017). Finally, c_s is the external CO_2 concentration at the leaf surface (mmol mol-1) and τ is the CO_2 compensation point where the rate of photosynthesis is equal to the rate of respiration (Pande et al., 2024a; Leuning, 1995). g_{CO_2} is converted to g_{O_3} in units of mmol O_3 m^{-2} s^{-1}, by dividing by 1000 and multiplying by 0.96 to account for the difference in diffusivities of the gases (Campbell and Norman, 1998).

Following calculation of stomatal conductance to O_3, the stomatal O_3 flux is calculated as in Equation (4.6). Stomatal O_3 flux is accumulated hourly and goes on to accelerate both the onset and rate of senescence, as well as reducing the instantaneous rate of photosynthesis, affecting calculations of stomatal conductance (Ewert and Porter, 2000; Pande et al., 2024a). Additionally, in the DO_3SE-CropN model, accumulated O_3 flux and the M7 metric are used to parameterise antioxidant and N remobilisation equations describing the allocation of N to the wheat grain, subsequently determining grain protein (Papers 1 and 2 of the present thesis).

4.3.5 Calculating relative yield, relative protein and relative protein concentration4.3.5.1 Concentration-response

To calculate the relative yield (RY) and relative protein concentration (RPC) (gProtein gDM^{-1}/gProtein gDM^{-1}) using M7 and AOT40, the equations given in Table 4.4 are used. For RY, the concentration-response equations used were either developed for India (Sinha et al., 2015) or have been applied in India previously (Lal et al., 2017; Ghude et al., 2014). Considering protein, few concentration-response relationships were found for RPC in the literature: Chang-Espino et al. (2024) and Grünhage et al. (2012). While neither relationship was developed for Indian wheat, the relationship developed by Grünhage et al. (2012) was part of a comprehensive meta-analysis synthesising several studies across Europe and Asia. The broad geographical scope means the relationship is generalisable to several locations and so it was included in the present study to provide a comparison of current methods of calculating RPC with DO_3SE-CropN.

4.3.5.2 Flux-response

After calculating POD_6, parameterised flux-response relationships are used to calculate either the RY or relative protein (RP) (gProtein m^{-2}/gProtein m^{-2}) (see Table 4.4). Only flux-response relationships developed for, or applied in, India were used to calculate RY (Yadav, Agrawal and Agrawal, 2021; Mills et al., 2018b). For RP, limited data are available. A flux-response relationship from Grünhage et al. (2012) was used as the authors used data from 5 wheat cultivars and 3 European countries. While it is a disadvantage that the relationship does not use Asian wheat, it provides a benchmark for comparison to DO_3SE-CropN estimates.

4.3.5.3 Crop model

To calculate RY, RP and RPC using the DO_3SE-CropN model the parameterisations for each cultivar were taken from Section 3 of the present thesis, which developed the DO_3SE-CropN model and parameterised it for the HUW234 and HD3118 wheat cultivars. The final model yield, protein and protein concentrations of the ambient run were divided by that for the run with 0 ppb of O_3 to obtain RY, RP and RPC. In this study version 4.39.16 of the DO_3SE-Crop model (Bland, 2024b), and version 2.0 of the N module for DO_3SE-Crop (Cook, 2024) were used.

Table 4.4: The equations used to calculate RY, RP and RPC, where M7 and AOT 40 are in ppb, and POD_6 is measured in mmol O_3 m^{-2}

Parameter	Index	Equation	Location	Source
RY	M7	$RY = \frac{\exp\left(-\left(\frac{M7}{186}\right)^{3.2}\right)}{\exp\left(-\left(\frac{25}{186}\right)^{3.2}\right)}$	North America	(Adams et al., 1989)
	M7	$RY = \frac{\exp\left(-\left(\frac{M7}{62}\right)^{4.5}\right)}{\exp\left(-\left(\frac{25}{62}\right)^{4.5}\right)}$	India	(Sinha et al., 2015)
	AOT40	$RY = (-0.0000161 \times AOT40) + 0.99$	Europe	(Mills et al., 2007)
	AOT40	$RY = (-0.000026 \times AOT40) + 1.01$	India	(Sinha et al., 2015)
	POD_6	$RY = 1 - (0.038 \times POD_6)$	Europe	(Grünhage et al., 2012)
	POD_6	$RY = 0.927 - (0.1272 \times POD_6)$	India	(Yadav, Agrawal and Agrawal, 2021)
RP	POD_6	$RP = 1.01 - (0.025 \times POD_6)$	Europe	(Grünhage et al., 2012)
RPC	M7	$RPC = 0.0029 \times M7 + 0.99$	Asia, North America, Europe	(Broberg et al., 2015)

Calculations of RY, RP and RPC less than 0 are physiologically impossible, but given the nature of the concentration and flux-response relationships they can be possible if O_3 concentrations or fluxes are high. If RY, RP or RPC < 0, they are reported as 0 in the risk assessment due to the unphysiological nature of a negative RY loss.

4.3.6 RP and RPC from the literature

To-date, only two studies have looked at the effect of O_3 on RP and RPC on Indian wheat: Yadav et al. (2020) and Mishra, Rai and Agrawal (2013). The authors measure protein concentration and grain yields under a control and elevated O_3 treatment, from which the protein yield in gm^{-2} can also be calculated. We use the data of Yadav et al. (2020) and Mishra, Rai and Agrawal (2013) to calculate the RP and RPC of the ambient O_3 for comparison with the results of the present study. To obtain the RP and RPC of the ambient treatment, the approximate M7 values for the ambient and elevated treatments were extracted from the papers. The protein concentrations and yields for each cultivar and study were regressed against the approximate M7 value, so that the protein yield and concentration at 0 ppb of O_3 could be obtained. The relevant protein and protein concentration were then obtained by dividing the value in the ambient treatment, by the corresponding value at 0 ppb.

4.3.7 Performing the sensitivity analysis

For the concentration-based assessment methods detailed in Section 4.3.5, the WRF-Chem and NASA (WRF-O_3) input data were input initially into the DO_3SE model to calculate the O_3 concentration at canopy-level (Section 4.3.3). The OTC and field datasets already had canopy-level O_3 concentrations. Following this, the M7 and AOT40 metrics were calculated as in Section 4.3.4, and used to calculate the RY and RPC for the different concentration-based methods.

For the flux-based risk assessment methods, the four different input data (O_3 and meteorology) were used to drive the multiplicative DO_3SE model, which for the WRF-Chem and NASA (WRF-O_3) data has built-in methods for calculating canopy-level O_3 (Section 4.3.3). The POD_6 value obtained from the model output was used to calculate RY and RP for the different flux-based risk assessment methods. The model was performed run twice for each input dataset using firstly the O_3 tolerant and secondly the O_3 sensitive cultivar parameterisation.

For the crop modelling method using the DO_3SE-CropN model, the four different input data (O_3 and meteorology) were used to drive it. Again, for the WRF-Chem and NASA (WRF-O_3) data the crop model has built-in methods for calculating canopy-level O_3 (Section 4.3.3). The model was run once with the 4 datasets described in Section 4.3.1, and then once with the same datasets where O_3 was set to 0 ppb. The resulting grain yield, grain protein and grain protein concentration were extracted for each run and used to calculate RY,RP and RPC as in Section 4.3.5.3. All crop modelling runs were performed twice for each input dataset and O_3 concentration (ambient or 0 ppb) using firstly the O_3 tolerant and secondly the O_3 sensitive cultivar parameterisation.

By using relative measures of O_3's impacts on yield, protein content and concentration, the O_3 impact as calculated using each risk assessment method is implicitly normalised to the same scale to allow ease of comparison of results.

4.4 Results

4.4.1 Variation of risk estimates with input data, risk assessment method and O_3 sensitivity parameterisation

RY

Combining the RYs for all risk assessments, input data, and cultivars, the mean RY loss was (mean $\pm$ standard error) 28.3 $\pm$ 4.0 %, matching the lower boundary of the inter-quartile range

of RY losses from the literature in Figure 4.2a. Excluding the concentration-response results, which do not include environmental effects or the plant's ability to detoxify some O_3 damage, the mean RY loss was 18.8 $\pm$ 4.0%, compared to 35.5 $\pm$ 12% when using only concentration-response methods. Figure 4.2a compares the RY using the differing risk assessment methods in the present study with current country-level estimates of Indian wheat RY loss using risk assessment methods from the literature (summarised in Table S4.2, covering the years 2000-2015). Figure S4.7 compares the RY loss ranges from the differing methods in the literature with experimental data to determine their validity. Most of the risk assessment methods in the present study for Varanasi obtained RY estimates that were within the range of current literature risk assessment estimates. Further, the flux-response and DO_3SE-Crop methods reproduced the greater sensitivity of the HD3118 cultivar to O_3 by allowing cultivar-specific O_3 sensitivity parameterisation.

In the concentration-based risk assessments (AOT40 and M7), the OTC and Field datasets had similar canopy-level O_3 concentrations resulting in comparable RY estimates. The WRF-Chem dataset had similar daytime mean O_3 concentrations to those in the OTC and Field datasets (Figure 4.8c), giving almost identical RYs when using M7 based methods. AOT40-based methods generally predicted greater yield losses than M7-based methods for the same data source. Indian M7 and AOT40 relationships showed greater yield losses and variability than the American M7 and European AOT40 methods, with the American M7 relationship heavily underestimating yield losses. Except for the NASA (WRF O_3) data, the Indian M7 and European AOT40 methods produced RYs within the literature's range. The Indian AOT40 relationship, along with NASA (WRF O_3) and WRF-Chem input data, gave very low RY values of 0 and 0.28, compared to the lowest value reported in the literature of ~0.6.

The European flux-response method showed a similar range of RY estimates to the DO_3SE-Crop method, both slightly higher than the range in the literature. The Indian flux-response relationship predicted RYs that were consistent with the literature only when using the OTC and Field data, while the NASA (WRF O_3) data and WRF-Chem data gave low RYs (0.3-0.5). The European flux-response method, and DO_3SE-Crop model showed minimal differences in RY estimates between data sources, with RYs ranging from 0.85-0.96 and 0.93-1.00 respectively.

Using NASA (WRF O_3) data, RY ranged from 0-1 across risk assessment methods, with 0 obtained when using the AOT40 relationships and 1 obtained from the DO_3SE-Crop model for the HUW234 cultivar. The largest variation due to data source within a risk assessment method occurred for the European AOT40 metric, where RY ranged from 0-0.8 regardless of O_3 sensitivity. While data sources contributed to large variations in RY estimates within methods, particularly for the AOT40 and Indian relationships, there was greater variability in RY between the risk assessment methods. The Indian flux-response relationship using the NASA (WRF O_3) and WRF-Chem data showed a 10-12 percentage point difference between cultivars, while the DO_3SE-Crop model had an 11 and 8 percentage point difference in RY of the 2 cultivars when using the OTC and NASA (WRF O_3) data respectively. Therefore, the greatest source of uncertainty on estimates of RY rises from the choice of risk assessment method. Cultivar sensitivity to O_3 contributed very little to the uncertainty on RY estimates in the present study.

RP and RPC

The mean RP was only consistent with data from the literature when using the DO_3SE-CropN model. The European flux-response relationship underestimated the RP loss under O_3 exposure. The M7 relationship predicts an increase in protein concentration (gProtein gDM^{-1}) under O_3

exposure, however for Indian wheat a decrease is observed, which only the DO_3SE-CropN model can capture. The mean RPC using DO_3SE-CropN, is on the lower end of current estimates from the literature. The reduction in both protein and protein concentration under O_3 exposure using the DO_3SE-CropN model was ~40%.

The RP flux-response relationship, and the RPC M7 relationship show little variability between input data sources for both cultivars ($0.9 \leq RP \leq 0.98$ and $1.1 \leq RPC \leq 1.2$), demonstrating robustness to changes in input data. When using the DO_3SE-CropN model the effect of input data choice was larger than the concentration- and flux-response methods, varying between 0.2-0.6 for the HUW234 RP and RPC. The choice of risk assessment method had a larger effect than input data choice, with $0.2 \leq RP \leq 0.9$ for the HUW234 cultivar using NASA (WRF O_3) data as input, and RPC varying between $0.2 \leq RPC \leq 1.2$ for the same cultivar and data source. Cultivar effect was of equivalent magnitude to the input data choice for RP and RPC (~0.2-0.65 using DO_3SE-CropN with NASA (WRF O_3) as input).

However, while the DO_3SE-CropN model shows greater variability in estimates of RP and RPC than the other methods, the results are much closer to the RP and RPC calculated from the existing literature. Nevertheless, the O_3 sensitivity is the wrong way round. HD3118 is shown by the literature to experience a lower RP and RPC, while the model predicted this for the HUW234 cultivar. The European flux-response relationship did correctly identify that the RP of the HD3118 cultivar should be lower. O_3 sensitivity has a greater effect on RP and RPC variability than it did for RY, but the variability in estimates attributed to input data and risk assessment choice is still larger, with the effect of risk assessment choice being largest.

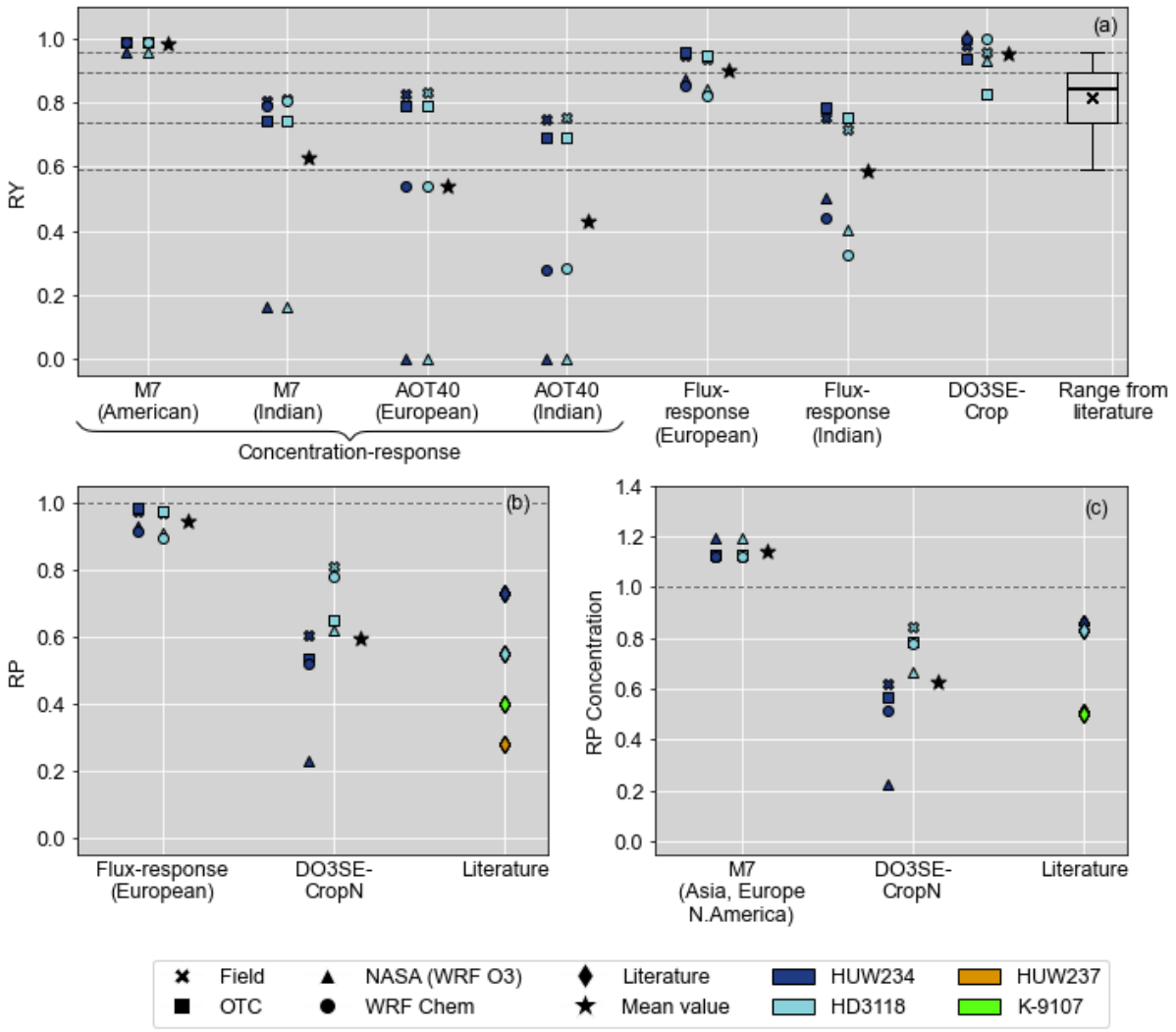

Figure 4.2: Comparison of risk assessment methods for estimating relative yield (RY), relative protein yield (RP), and relative protein concentration (RPC) under ambient O_3 concentrations. The different colours represent the yield losses for the different cultivars. The observed data for the HUW237 and K-9107 cultivars, and the HUW234 and HD3118 cultivars, comes from Mishra, Rai and Agrawal (2013) and Yadav et al. (2020) respectively, and was used to calculate RP and RP concentration as described in the methods. The 0 RYs using the AOT40 metric were below zero initially which is unphysiological and so were reported as 0. The mean for all input data sources and cultivars using each method is given to the right of the data as a star. The grey dashed lines are used to represent 1 on (b) and (c), and to indicate the boundaries of the boxplot on (a).

4.4.2 How does variability in input data affect key crop processes and hence risk estimates in crop modelling risk assessments

For the present study, we wanted to understand in greater detail how the differences in meteorological variables between inputs, affected grain DM and quality, LAI and gross primary productivity (GPP) in the crop model runs. This allows us to understand how the processes are affected by the differing meteorology's and O_3 concentrations in crop modelling risk assessment methods, and hence how and why risk estimates are affected by these differences in input data. The results are presented for O_3 tolerant (HUW234) and sensitive (HD3118) cultivars in Figures 4.3 and 4.4. Overall, LAI and GPP were reduced in the OTC run compared to the Field run (OTC data is 2°C warmer). Compared with the Field and OTC model runs, NASA (WRF O_3) and WRF-Chem reached anthesis ~20-25 days later due to lower temperatures slowing crop development. Using the WRF-Chem data as a model input gave the highest GPP

and LAI, though the peak LAI of the NASA (WRF O_3) run was similar to that using the WRF-Chem input for both cultivars. Regardless of cultivar parameterisation, simulations of LAI using NASA (WRF O_3) and WRF-Chem data were over twice as large as using the Field and OTC data. The final GPP using WRF-Chem as an input was ~3 times as large as the OTC dataset which had the lowest GPP overall.

The grain DM was greater when using the Field data as an input compared to the OTC data because of the greater GPP. The two cultivars responded differently to the NASA (WRF O_3) data as an input, with the HD3118 cultivar experiencing an increased grain DM, and the HUW234 cultivar having a lower grain DM, compared with using the OTC and Field data as model inputs. This difference may be attributed to the greater GPP accumulated by the HD3118 cultivar using the NASA (WRF O_3) input. Both the HUW234 and HD3118 cultivar had the highest GPP, and hence highest grain DM, using WRF-Chem data. Considering grain protein, the protein concentration (100gProtein gDM^{-1}) was generally robust to changes in input data sources.

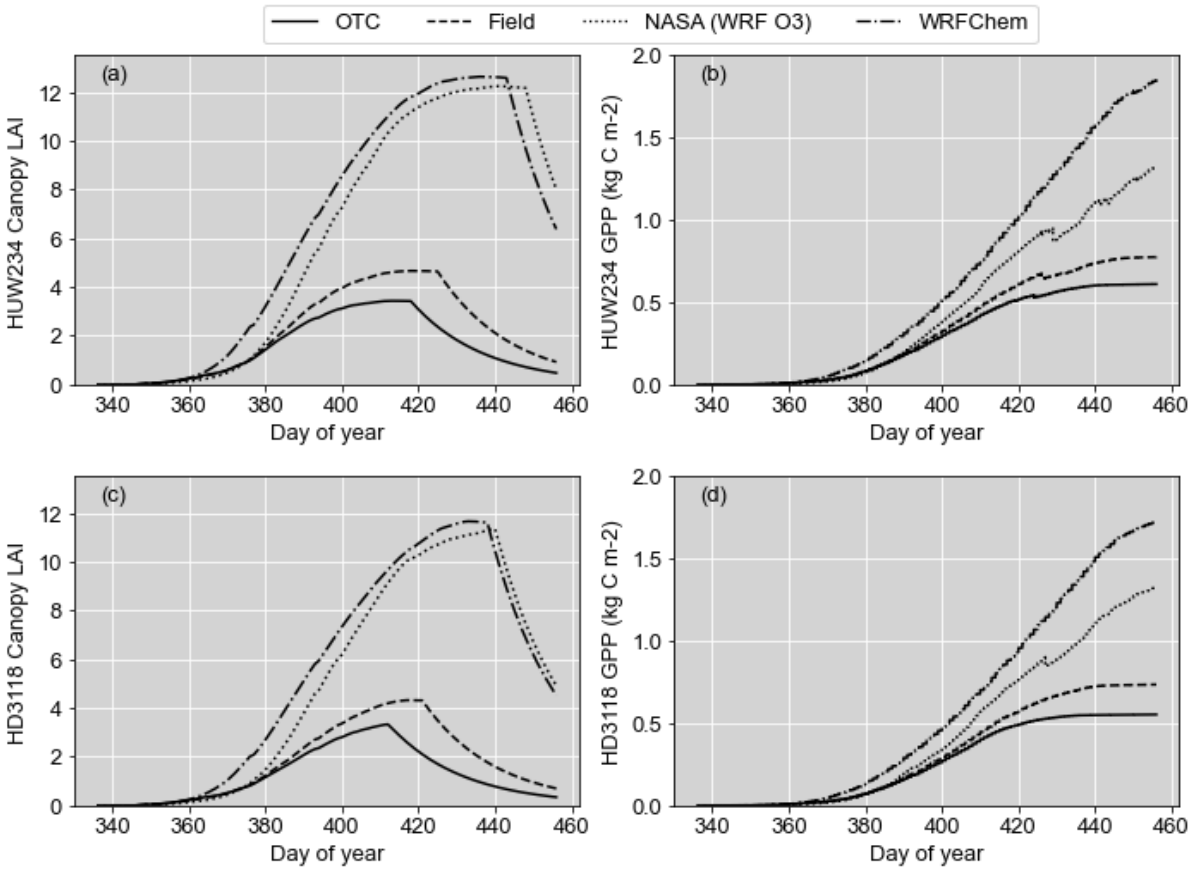

Figure 4.3: Profile of LAI (a, c) and GPP (b, d) for the HUW234 and HD3118 cultivars over the growing season in Varanasi (December 2016 to March 2017) using the different input sources. All profiles are for the ambient O_3 treatment. The different line-styles reflect the different input data sources.

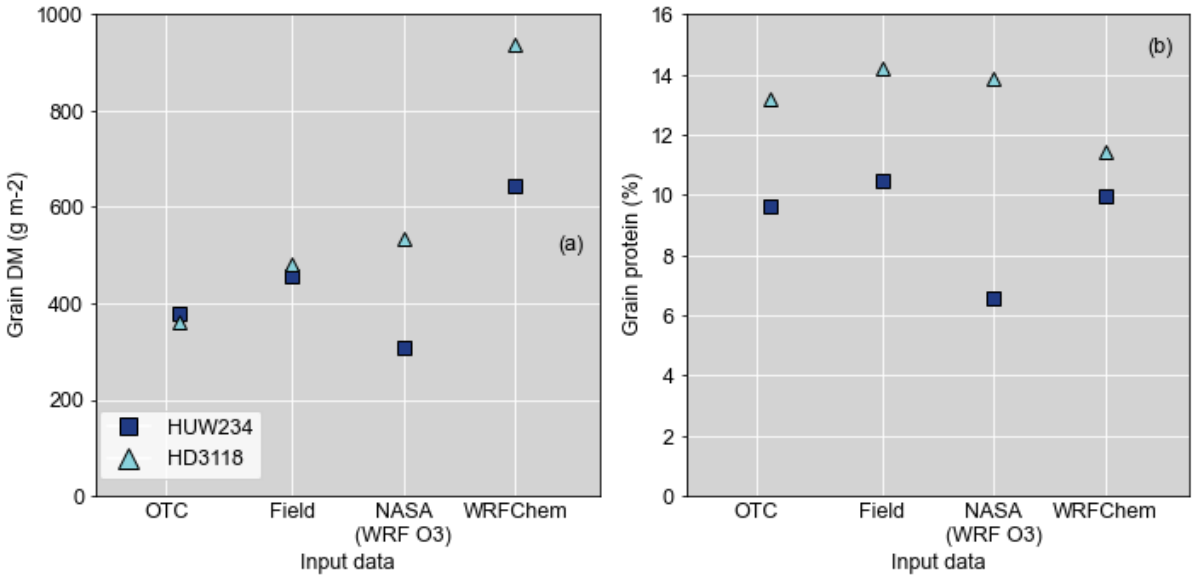

Figure 4.4: Difference in grain DM (a) and grain protein concentration (b) for the HD3118 and HUW234 cultivars using the different model outputs, where the runs using NASA (WRF O_3) data also used the O_3 concentration data from WRF-Chem. The different shaped and coloured markers represent the two cultivars. The O_3 concentrations for OTC and Field were the ambient O_3 concentrations from the sensors, and the WRF O_3 concentrations were the simulated ambient O_3.

4.4.3 Variability in O_3 concentrations and meteorological data used in the risk assessments

Hourly temperatures, RH, wind speed, air pressure and PAR from WRF-Chem and NASA (WRF O_3) generally followed the same pattern as the observed data, regardless of magnitude (Figures 4.5a, 4.6a, 4.7a, S4.8a and S4.9a). The absolute differences in meteorological variables and O_3 concentrations between the observed data, NASA (WRF O_3) and WRF-Chem are given in Figure S4.16. A summary of this information is presented as the percentage difference between the observed data and NASA (WRF O_3) and WRF-Chem data in Table 4.5. NASA (WRF O_3) and WRF-Chem air pressures closely matched observed values, averaging ~1 kPa (1%) lower (Table 4.5 and Figure's S4.8 and S4.16). NASA (WRF O_3) PAR closely followed the observed data, with daily means ~11% higher, while WRF-Chem's PAR was ~33.3% higher (Table 4.5 and Figure S4.9). NASA (WRF O_3) temperatures more closely aligned with observations at higher values but underestimated temperatures overall by ~4°C (17.6%), while WRF-Chem underestimated temperatures by ~5°C (20.4%) (Table 4.5 and Figure 4.5b). WRF-Chem temperatures generally did not fall within the $\pm$3°C uncertainty range, while NASA (WRF O_3) temperatures did fall within this range above 30°C. NASA (WRF O_3) temperatures are linear with the observed data due to the nature of the gap-filling but also because of the observed temperatures following the same increasing/ decreasing pattern as the NASA (WRF O_3) data. For RH below 0.5, NASA (WRF O_3) reproduced the observed RH well. For RH above 0.5 both NASA (WRF O_3) and WRF-Chem increasingly overestimated RH. In the observed data the RH did not exceed ~0.6, while NASA (WRF O_3) and WRF-Chem show RH ranging up to 0.8 and 0.9 respectively. WRF-Chem overestimated RH by ~0.2 (55.6%) and NASA (WRF O_3) by 10.3% (Table 4.5 and Figure 4.6). The RH in the NASA (WRF O_3) data was generally within the $\pm$30% uncertainty range while the WRF-Chem RH was overestimated.

WRF-Chem simulated wind speed at a height of 10m, which was propagated to canopy level through algorithms in the DO_3SE model. Figure 4.7 shows the WRF-Chem 10m wind speed

alongside canopy level wind speed for all data. Both NASA (WRF O_3) and WRF-Chem underestimated canopy-level wind speeds (Table 4.5 and Figure 4.7). NASA (WRF O_3) closely matched the observed data at lower wind speeds but deviated at higher speeds, while WRF-Chem's wind speeds were much lower, even at 10m. The average WRF-Chem canopy wind speed was 0.1 ms^{-1} (1.4 ms^{-1} at 10m), compared to 2.3 ms^{-1} (observed) and 1.8 ms^{-1} (NASA (WRF O_3)). On average, NASA (WRF O_3) underestimated canopy wind speed by 23.7%, while WRF-Chem almost entirely underestimated it (~100%) (Table 4.5).

While both WRF-Chem and NASA (WRF O_3) had the same input O_3 concentrations simulated by WRF-Chem at a height of 29m, the differing meteorology's resulted in a 6% reduction in O_3 concentrations at the canopy-level for NASA (WRF O_3), while for WRF-Chem O_3 concentrations were reduced by 33% and were more in-line with the observed data (Figure 4.8 and Figure S4.17). Hourly canopy-level O_3 concentrations from WRF-Chem and NASA (WRF O_3) did not mimic the shape of the observed data, experiencing troughs where the observed data show peaks, and peaks where the observed data show troughs (Figure 4.8a). The mean daily canopy O_3 concentrations for NASA (WRF O_3) and WRF-Chem were higher than observed, due to gap filling that assumed the minimum nighttime O_3 concentrations were 5 ppb, whereas the WRF-Chem and NASA (WRF O_3) data show higher canopy nighttime O_3 concentrations of ~45 and ~60 ppb respectively (Figure 4.8b). To better compare the daytime O_3 concentrations, the daily mean O_3 between 9am-4pm was computed and is displayed in Figure 4.8c. WRF-Chem's daytime canopy O_3 concentrations closely matched observed data, but for NASA (WRF O_3) were ~20 ppb higher. The WRF-Chem daily O_3 concentrations were mostly within the $\pm 40\%$ uncertainty range of the observed data while for NASA (WRF O_3) ~50% of the data was within this range. Overall, NASA (WRF O_3) 's daytime canopy O_3 was 59.3% higher than the gap-filled observed data, while WRF-Chem's O_3 simulations were consistent with observations.

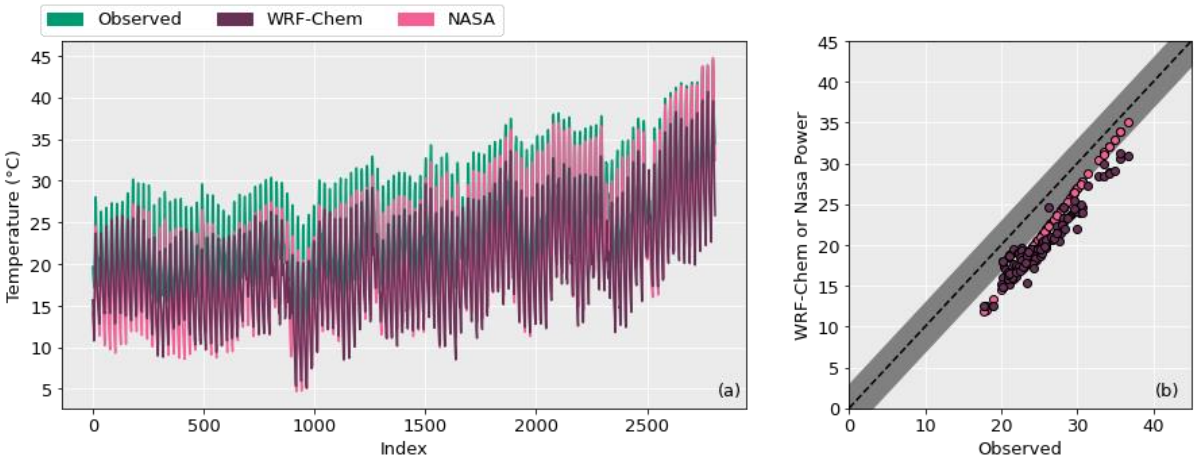

Figure 4.5: Comparison of the temperatures from January – March 2017 between the observational data, WRF-Chem data and NASA (WRF O_3) data. Fig. (a) shows the seasonal comparison and Fig. (b) shows the comparison of the WRF-Chem and NASA (WRF O_3) daily mean temperatures, with the dashed 1:1 line representing a perfect match between either WRF-Chem or NASA (WRF O_3), and the observed temperature. The shaded grey area represents ± 3°C for the uncertainty of the observed temperatures.

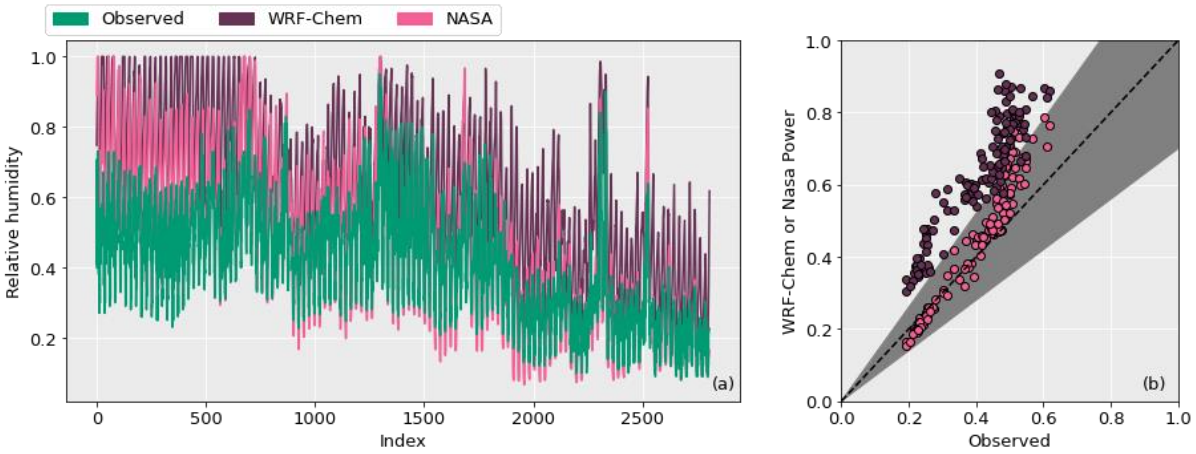

Figure 4.6: Comparison of the relative humidity (RH) from January – March 2017 between the observational data, WRF-Chem data and NASA (WRF O_3) data. Fig. (a) shows the seasonal comparison and Fig. (b) shows the comparison of the WRF-Chem and NASA (WRF O_3) daily mean RH, with the dashed 1:1 line representing a perfect match between either WRF-Chem or NASA (WRF O_3), and the observed RH. The shaded grey area represents ±30% for the uncertainty of the relative humidity.

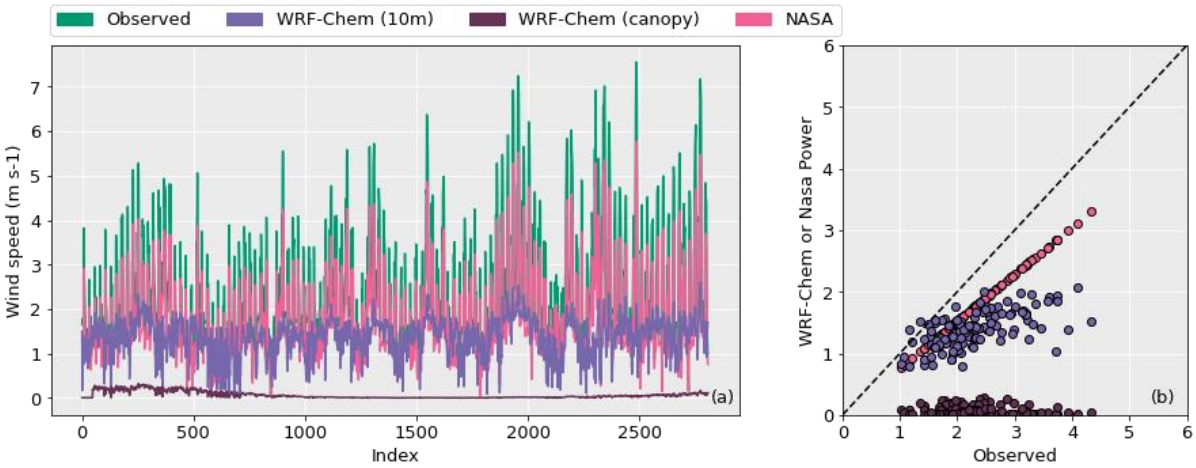

Figure 4.7: Comparison of the wind speed from January – March 2017 between the observational data, WRF-Chem data and NASA (WRF O_3) data. The WRF-Chem input wind speed data was at 10m and is plotted here with all other canopy level wind speeds as comparison to show the comparison of magnitude of WRF-Chem wind speeds with the observed and NASA (WRF O_3) data. Fig. (a) shows the seasonal comparison and Fig. (b) shows the comparison of the WRF-Chem (10m and canopy level) and NASA (WRF O_3) daily mean wind speed, with the dashed 1:1 line representing a perfect match between either WRF-Chem or NASA (WRF O_3), and the observed wind speed.

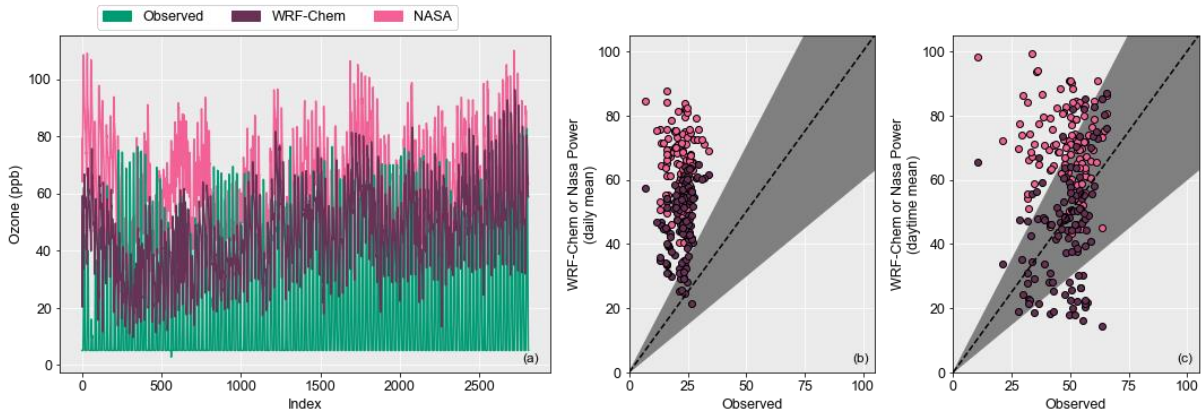

Figure 4.8: Comparison of the canopy level O_3 concentrations from January – March 2017 between the observational data, WRF-Chem data and NASA (WRF O_3) data. Fig. (a) shows the seasonal comparison and Fig. (b) shows the comparison of the WRF-Chem and NASA (WRF O_3) daily mean O_3, and (c) shows the daytime (9am-4pm) mean O_3 concentration, with the dashed 1:1 line representing a perfect match between either WRF-Chem or NASA (WRF O_3), and the observed O_3. While the NASA (WRF O_3) data had the same O_3 input as WRF-Chem, the O_3 concentration in WRF-Chem was at a height of 29m, when scaling down to canopy level the wind speed and resistances resulted in differing canopy deposition velocities, affecting the O_3 gradient and concentrations at canopy level. While canopy level O_3 concentrations were different between the OTC and Field dataset due to the temperature difference, the differences were minor and not plotted here. The shaded grey area ((b) and (c)) represents ±40% for the uncertainty of the observed O_3 concentrations.

Table 4.5: Percentage deviation of the daily NASA (WRF O_3) or WRF-Chem meteorology or O_3 concentrations as compared to the observed data. + represents that NASA (WRF O_3) or WRF-Chem simulates a greater value than the observed data, - means represents that NASA (WRF O_3) and WRF-Chem generally simulate lower values than reported in the literature. These values were calculated using daily values across the entire growing season.

Comparison	NASA (WRF O_3) deviation (%)	WRF-Chem deviation (%)
Canopy-level O_3 compared with non-gap filled O_3 data from Varanasi (9am-5pm)	+40.6%	+0.6%
Canopy-level O_3 compared with gap-filled observed data	+228%	+131%
Canopy level O_3 compared with gap-filled observed data for daylight hours only (9am-4pm)	+59.3%	+0.33%
Temperature	-17.6%	-20.4%
Wind speed	23.7%	-96.9%
Air pressure	-0.9%	-0.8%
PAR	+11.3%	+33.3%
RH	+10.3%	+55.6%

4.5 Discussion

Regardless of input choice, data source or O_3 sensitivity, the risk assessments showed that there is a large impact of O_3 on crop yield (averaging ~19% across different risk assessment methods and input data) and quality (reduction of ~40% in protein content and concentration using DO_3SE-CropN) for Varanasi. Considering Uttar Pradesh specifically (where Varanasi is located), Droutsas (2020), using an AOT40 based crop model obtained a RY loss of 15.5±1.9%,

while Tang et al. (2013), Tai et al. (2021) and Mills et al. (2018) using flux-based methods obtained RY losses of 12.7-27% and 3-8%, and 12.5-17.5% respectively. In the present study, only considering the flux-response estimates and crop model estimates, the mean RY loss at Varanasi, Uttar Pradesh, was 18.8±4% which is generally consistent with prior estimates, albeit a little higher. Mukherjee et al. (2021) summarise RY loss of Indian wheat cultivars under ambient O_3 from experimental studies, finding an average RY loss of 16±4.5%, which is consistent with the estimates of the present study, and most authors listed above. Tai et al. (2021) obtained lower estimates than the other authors which are also not consistent with Mukherjee et al. (2021). The authors comment that their relatively low estimates of yield loss compared to other flux-based studies occur due to differences in inputs and calculations of flux metrics as compared to previous approaches, further emphasising the importance of method and data considerations for O_3 risk assessments (Tai et al., 2021).

Addressing O_3 pollution would help to mitigate the yield and quality losses of wheat, leading to improved food security and nutrition. The substantial effects of O_3 on crop yields and quality demonstrate the urgency of improving risk assessments for the region to obtain realistic estimates of yield and protein loss, which are essential for policymakers and for identifying mitigation strategies. Understanding why risk estimates using different methods, data sources and parameterisations differ, and the implications of this, will help to improve the robustness of risk estimates for supporting policy development and interventions. Considering concentration-response methods, the differing O_3 concentrations led to differences in RY (gDM m^{-2}/gDM m^{-2}) and RPC (gProtein gDM^{-1}/gProtein gDM^{-1}) due to the equation structure. For the flux-response relationships, RY and RP (gProtein m^{-2}/ gProtein m^{-2}) estimates were variable due to the impacts of differing meteorology, O_3 concentrations and cultivar sensitivity to O_3 that affected the calculation of factors limiting stomatal conductance and O_3 uptake. While for the DO_3SE-Crop model, RY, RP and RPC varied with input data because of the effect of the differing meteorology, O_3 concentrations and cultivar parameterisation on the plant physiological processes and response to stress. Overall, while both input data choice, risk assessment method and cultivar parameterisations affected assessments of RY, RP and RPC for wheat in Varanasi, the choice of risk assessment method was more influential than input data choice, and the effect of the O_3 tolerant versus O_3 sensitive cultivar parameterisation was much smaller than the effect of either input data or risk assessment choice comparatively.

4.5.1 Sensitivity of risk assessment methods to meteorology, O_3 concentrations and O_3 sensitivity

The large differences in RY, RP and RPC between risk assessment methods and input data sources highlight the importance of data and method selection to accurately capture impacts on crop quality and yield. Both the present study and Tai et al. (2021) found that risk assessment choice introduced greater variability on RY estimates than input data choice. Currently, most methods used to estimate RY losses in India have been concentration-based studies, which generally estimates higher yield losses than flux-based studies (Tarannum et al., 2024; Tai et al., 2021; present study). Therefore, it is unsurprising that the RY estimates using the flux-response and crop modelling method in this study show lower RY losses than presently reported in the literature for India. The flux-based and DO_3SE-Crop model gave the lowest yield losses but were consistent with each other. The complimentary results obtained by the DO_3SE-Crop model and flux-based methods, in comparison with the differing flux and crop model results obtained by Tai et al. (2021), are likely due to the data availability that allowed DO_3SE-Crop and the multiplicative DO_3SE model to be well parameterised for Indian wheat (Section 3

of this thesis and section 2.4.2). Nevertheless, while the DO_3SE-Crop model is more mechanistic than the flux- or concentration-based studies, parameterisation is key to ensure realistic plant response.

Considering the differing input data sources, the Indian M7, AOT40 and flux-based risk-assessment methods were more sensitive to the differences in O_3 between datasets than the American M7, European AOT40 and flux relationships, representing the greater sensitivity of Indian wheat to O_3 (Emberson et al., 2009). Further, the yield losses in the present study using the Indian flux-response relationship were greater than in Yadav, Agrawal and Agrawal (2021), despite using almost identical parameterisations and the same input data. The reason for this is that the input data from Yadav, Agrawal and Agrawal (2021) had 11 days of missing O_3 data, and mostly recorded concentrations between 10am-5pm, with other times recorded as 0 ppb. In contrast, we gap-filled the data to match the diurnal O_3 profile with experimental data. Consequently, we accumulated a greater POD_6 (1.3 compared with 0.75 for the HUW234 cultivar and 1.4 compared with 0.7 for the HD3118 cultivar) leading to greater RY losses. Additionally, Yadav, Agrawal and Agrawal (2021) began accumulating POD_6 from sowing, but reached their maximum POD_6 10 days later, while in the present study we used the same phenology parameterisation to calculate POD_6 as we did for the DO_3SE-Crop model to ensure consistency. However, this parameterisation meant POD_6 accumulation began at anthesis. Marzuoli et al. (2024) mapped POD_6 accumulation for several wheat cultivars, finding it began ~2 months after sowing, and ~3-4 weeks before anthesis (Marzuoli et al., 2024). Therefore, it is recommended to revisit Yadav, Agrawal and Agrawal's (2021) flux-response parameterization with gap-filled O_3 data and appropriate timing for POD_6 accumulation, ensuring better estimates of yield loss and broader applicability for Indian agriculture.

O_3 sensitivity in the concentration-response studies was much larger than the flux- and crop-modelling based methods, indicating that flux-based and crop modelling methods are better at incorporating plant processes and environmental conditions to modify the O_3 dose a plant receives (Pleijel, Danielsson and Broberg, 2022). However, flux-response methods do this via a statistical relationship, rather than a mechanistic model (CLRTAP, 2017). RP and RPC estimates using DO_3SE-CropN were equally as sensitive to the changes in cultivar parameterisation as they were to input data source. While the variability in RP and RPC due to risk assessment method was larger (variation of magnitude 0.7 and 1 respectively), the variability in estimates due to data source and cultivar parameterisation was still large (magnitude of at least 0.4) highlighting the importance of obtaining accurate input data and reliable parameterisations for risk assessments.

4.5.2 Uncertainty on temperatures, RH, windspeed and daytime O_3 concentrations in the risk assessments

Uncertainties on meteorology and O_3 concentrations influence RY, RP and RPC estimates. Temperatures and RH from WRF-Chem exceeded typical model uncertainty ranges as outlined in Section 4.3.2. Previous WRF-Chem studies for India showed a mean absolute error (MAE) of 1.5-2.2°C for temperature and 0.08-0.13 for RH (Agarwal, Stevenson and Heal, 2024). NASA Power data showed a of 2.2°C with RH uncertainty estimated at $\pm$0.11 based on a 4.9% change in RH per 1°C (NASA, 2024a; Dai, 2006). The bounds used to represent uncertainty in the present analysis are larger than previously reported, so it is concerning that the temperatures and RH from WRF-Chem did not fall within the uncertainty range, as these uncertainties

propagate through the flux-based and crop-modelling risk assessments, leading to differences in RY, RP and RPC.

Surface wind speed uncertainties influence canopy-level O_3, and hence affect RY, RP and RPC estimates. While prior studies found WRF-Chem overestimated wind speeds (e.g. 1.5 ms^{-1} at night and 0.5-0.8 ms^{-1} during the day), this study found an underestimation of almost 100%. NASA's (WRF O_3) higher wind speeds resulted in a lower reduction in O_3 concentrations from 29m to canopy-level due to well-mixed air, whereas WRF-Chem's lower wind speeds led to a 33% reduction. This disparity affected RY estimates, with the European AOT40 relationship giving a RY of 0.8 and 0 for WRF-Chem and NASA (WRF-O_3) respectively.

WRF-Chem's wind speeds were not representative of the wheat growing conditions across India, as shown by the mismatch with the observed data. The 33% reduction in O_3 concentrations from a height of 29m to canopy-level in the WRF-Chem data implies an unrealistically high starting altitude of ~4000m above sea level (using Payra et al. (2022) and Soares(2014)) compared to Varanasi's 81m elevation. These findings suggest two key points. Firstly, WRF-Chem's wind speeds are O_3 concentrations are not representative for Varanasi, despite the model performing well across India (Venkataraman et al., 2024). Secondly, NASA's (WRF-O_3) more accurate wind-speeds resulted in only a small reduction in O_3 at canopy level, yet these concentrations remain much higher than observed. This suggests that WRF-Chem overestimated O_3 concentrations for Varanasi.

The large differences in RY and RPC estimates using NASA (WRF-O_3) and WRF-Chem data, in comparison with the field data, for concentration-response methods, shows the importance of having accurate surface O_3 concentration data for concentration-based risk assessments. Uncertainty on meteorology leads to differences in RY, RP and RPC for flux-based and crop modelling methods which incorporate the modifying effect of meteorology. Risk assessments do not typically incorporate uncertainty on the driving O_3 or meteorological data into their estimates. Since the present study has shown large differences in RY, RP and RPC estimates using different input data, and that different data do not always represent the observed surface conditions of the study location, it could be useful to perform risk assessments that take into consideration the uncertainty on the input data, to allow for an estimation of the uncertainty on risk assessment outputs.

4.5.3 Influences of different meteorology and O_3 concentrations in the crop modelling risk assessment

Crop modelling risk assessments are considered to be the most biologically relevant risk assessment method as they represent the effect of meteorology and O_3 concentrations on plant growth in a process-based manner. The variation in meteorology and canopy level O_3 concentrations between input data sources affected fundamental crop modelling processes in the crop model used in the present study, DO_3SE-CropN, leading to differences in GPP, LAI, grain DM and grain protein. The key modelling processes affected by the differences in input data leading to these outcomes are discussed in the following sections. The key processes were identified as stomatal conductance and photosynthesis, and crop development and senescence, and are discussed in turn.

4.5.3.1 Physiological processes that influence stomatal conductance and photosynthesis

The 2°C increased temperature of the OTC dataset led to higher VPD, affecting stomatal conductance and reducing photosynthesis, reducing the GPP of the OTC model run compared to the field run (Pande et al., 2024a; Leuning, 1995).The LAI, GPP, grain DM and protein concentrations in the NASA (WRF O_3) and WRF-Chem runs differed from the Field and OTC runs due to a complex combination of effects resulting from differences in temperature, RH, O_3 concentrations and wind speed. Differences in GPP between model runs using different input data were primarily due to differences in canopy level photosynthesis (Figure S4.14), driven by differences in stomatal conductance which affected leaf interior CO_2 concentrations (Figures S4.10 and S4.15). The large differences in GPP of the WRF-Chem and NASA (WRF O_3) compared to the Field and OTC runs were attributed to the large LAI and greater PAR which allowed for greater canopy-level photosynthesis.

Given that the flux-response and crop modelling approaches, which consider meteorological variables in addition to O_3, gave the lower RY losses (18.8% versus 28.3% when including concentration-response results), it is clear environmental conditions modified the O_3 that the plant was exposed to (Emberson, 2020; Fischer, 2019; Kobayashi, 2022). This could be because of temperature and RH effects on VPD, reducing the stomatal conductance in the flux-based and DO_3SE-Crop approaches, limiting O_3 uptake. This effect was also found by Tang et al. (2013) in their estimates of O_3 loss under greater temperatures and VPD using flux-based approaches. Alternatively, it could be due to the wind speed affecting the dispersal of O_3 throughout the canopy (Section 4.5.2). Or a combination of these effects.

4.5.3.2 Physiological processes that influence crop development and senescence, and their subsequent impacts on crop growth

Risk assessment methods that accurately capture anthesis and senescence timing, such as DO_3SE-Crop, can provide risk estimates that more realistically represent the plant's response to O_3. Increased O_3 concentrations, however, accelerate senescence, as seen in the OTC dataset, where greater O_3 accumulation led to earlier senescence, shortening the grain-filling period (Pande et al., 2024a; Ewert and Porter, 2000). In the NASA (WRF O_3) dataset, the temperatures were lower than the Field dataset, which delayed development and senescence, despite total accumulated O_3 being similar (Figures S4.11 and S4.12) (Pande et al., 2024a; Savin and Slafer, 1991). Senescence onset was earlier in the OTC run compared with the Field run as total O_3 accumulation was greater. Grain DM of the OTC run was reduced comparative to the Field run due to the reduced GPP (section 4.3.1) and accelerated senescence shortening the grain filling period. Delayed phenological development in the WRF-Chem and NASA (WRF O_3) runs extended photosynthesis duration compared to the OTC and Field runs. In combination, extended photosynthesis, greater stomatal conductance, and greater interior leaf CO_2 concentrations (Figure's S4.10, S4.14 and S4.15) led to greater GPP and LAI in the NASA (WRF O_3) and WRF-Chem runs. These details are not captured by the concentration-response methods and are not captured in a mechanistic way by the flux-response methods. However, they illustrate how the inter-connected and complex nature of plant response to stress and environmental conditions can be incorporated in risk assessments to provide more biologically realistic estimates.

Generally, the DO_3SE-CropN model reproduced the RPC ranges, except when using the NASA (WRF O_3) data for the HUW234 cultivar, where delayed anthesis and later senescence reduced protein deposition to the grain. These large differences in RP and RPC illustrate the importance

of phenology and senescence on protein deposition and protein yields, which cannot be captured by concentration-response models, and cannot be captured mechanistically by flux-response methods. Capturing stomatal conductance, photosynthetic, phenological and senescence processes is essential for ensuring risk assessments more realistically capture the effects of climate and O_3 on wheat yields and quality for more reliable risk estimates.

4.5.4 Considerations for O_3 risk assessments in India for simulating RY, RP and RPC

Increasing O_3 concentrations and climate change in India will reduce wheat yields and quality, further exacerbating malnutrition and worsening food security in the country. O_3 risk assessments allow for reduction in wheat yields and associated financial impact of O_3 induced yield reductions on growers, consumers and the government to be quantified (Tarannum et al., 2024; Pandey et al., 2023). Additionally, incorporating a focus on wheat nutrition will allow the risk assessments to be extended to include dietary impacts due to food quality, in addition to food availability. Yield and protein-based risk assessments provide key data that can be used to inform policy and allow for targeted and effective mitigation strategies for O_3 pollution. For instance, targeted reductions in NO_x emissions at agricultural sites could lower O_3 production and concentrations, mitigating the adverse effects on crop productivity and nutritional quality (Fowler et al., 2008). Comprehensive risk assessments of O_3 effects on yield and crop quality will support the development of air quality and food security policy to protect individuals' food security and the agricultural sector in India.

Flux-based and crop-modelling methods provide more realistic estimates than concentration-response methods of O_3 induced yield losses due to incorporating cultivar parameterisation as well as environmental conditions (Emberson et al., 2000b; Pleijel, Danielsson and Broberg, 2022; Mills et al., 2011; Tai et al., 2021; Tarannum et al., 2024). Flux-based and crop-modelling methods will be more appropriate for O_3 risk assessments under a changing climate (Tai et al., 2021). At present, the DO_3SE-CropN model is the only risk assessment method that captures the decrease in protein yield and concentration of Indian wheat under O_3 exposure. Additionally, mechanistic crop models simulate a more realistic plant response to the changing climate and increasing O_3 concentrations than the other risk assessment methods in the present study.

For performing a risk assessment, meteorological and O_3 concentration data are required for all wheat growing areas as modelling input. National scale input data are often obtained from atmospheric chemistry models, such as WRF-Chem (Mills et al., 2018b; Tai et al., 2021). Before using such data, it is important to validate the simulated meteorology and O_3 concentrations to identify whether bias correction is necessary. The tropospheric O_3 assessment report (TOAR) (https://igacproject.org/activities/TOAR) produced a global database of tropospheric O_3 concentrations (https://zam2061.zam.kfa-juelich.de/dashboard). Using this database, we can see that for India, the data is sparse, both spatially and over time. Such limited O_3 monitoring sites prevents country-wide validations of simulated O_3. However, there are several studies that have tested emissions inventories, chemical mechanisms and physics parameterisations of atmospheric models for India so these can be used to inform model parameterisation (Sharma et al., 2017; Govardhan, Nanjundiah and Satheesh, 2015; Agarwal, Stevenson and Heal, 2024). Additionally, it could be beneficial to incorporate uncertainty on the meteorological and O_3 concentration input data into the assessment to provide an uncertainty range on RY, RP and RPC outputs.

Crop models applied for risk assessment are often calibrated for one site and then applied at a larger scale. In such a case, additional uncertainty is introduced upon application due to the variability of the environment the model is being applied across. Crop models applied across a larger scale tend to select major growing areas for calibration or application, and given that major growing areas become major by producing high yields, this leads to a scaling dependency in modelling. Solutions to scaling dependencies are beyond the scope of this paper, but for further information on this topic the reader is referred to Hansen and Jones (2000) and Challinor, Parkes and Ramirez-Villegas (2015).

4.6 Conclusion

In summary, this study highlighted that the method and data chosen for performing a risk assessment can result in highly varied estimates of RY and protein. Cultivar sensitivity to O_3 contributed very little to variations in estimates of RY, but had an effect equal in magnitude to the input data choice on estimates of RP and RPC. The magnitude of the RY loss was reduced when using flux-response and crop modelling studies that can incorporate the modifying effect of meteorology on O_3 uptake and damage processes. NASA Power's meteorology more closely aligned with the observational data than WRF-Chem's. However, WRF-Chem simulations of O_3 and wind speed were not realistic for Indian growing conditions. Further, evaluations of O_3 concentration data in WRF-Chem are limited by the lack of O_3 monitoring stations in India. The highly variable estimates of RY, RP and RPC between methods and input data underscore the need for accurate meteorological inputs and well-parameterised models that incorporate meteorological effects to improve the reliability of O_3 risk assessments.

4.7 Supplementary information

4.7.1 Scaling factors

The scaling factors were calculated by comparing the observed values recorded by sensors for December 2016 and December 2017. The scaling factors were applied to WRF-Chem 2017 December data, to obtain the December 2016 data.

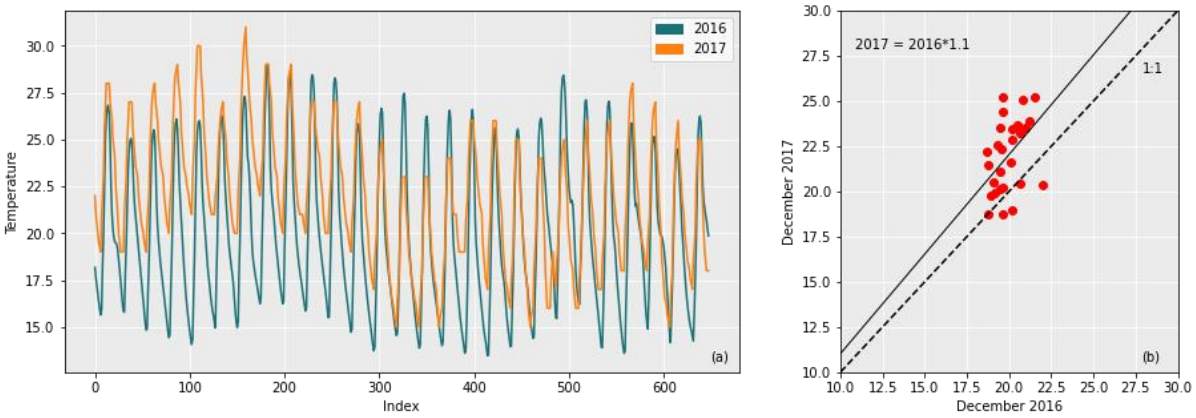

Figure S4.1: The time series comparison between hourly temperature in December 2016 and December 2017 (a) and the calculation of a scaling factor to convert between the two years (b), where the dashed line represents the 1:1 line and the solid line represents the equation indicated in the figure and the markers represent the average daily temperature.

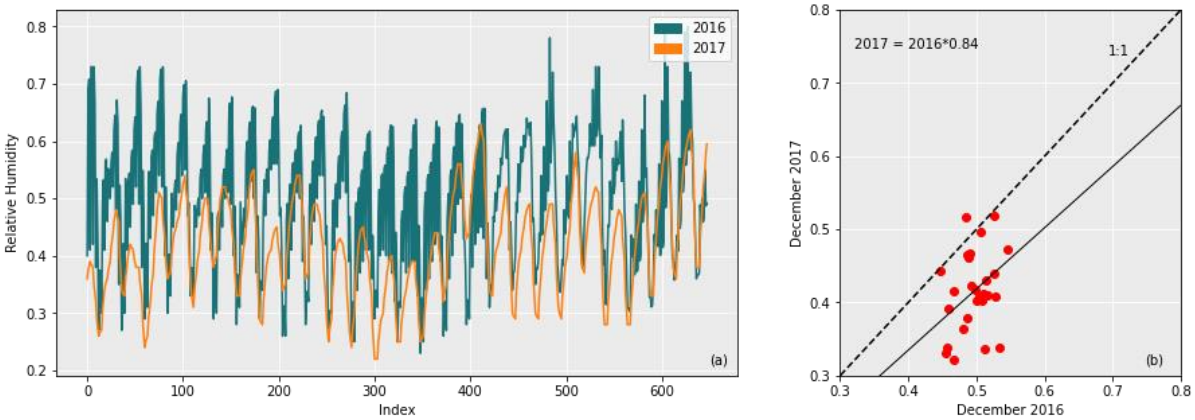

Figure S4.2: The time series comparison between hourly relative humidity in December 2016 and December 2017 (a) and the calculation of a scaling factor to convert between the two years (b), where the dashed line represents the 1:1 line and the solid line represents the equation indicated in the figure and the markers represent the average daily relative humidity

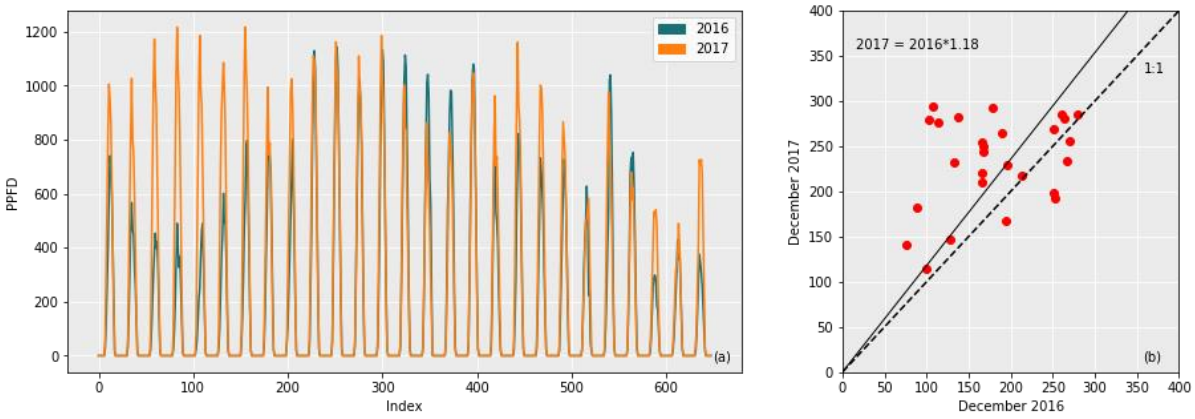

Figure S4.3: The time series comparison between hourly PPFD in December 2016 and December 2017 (a) and the calculation of a scaling factor to convert between the two years (b), where the dashed line represents the 1:1 line and the solid line represents the equation indicated in the figure and the markers represent the average daily PPFD

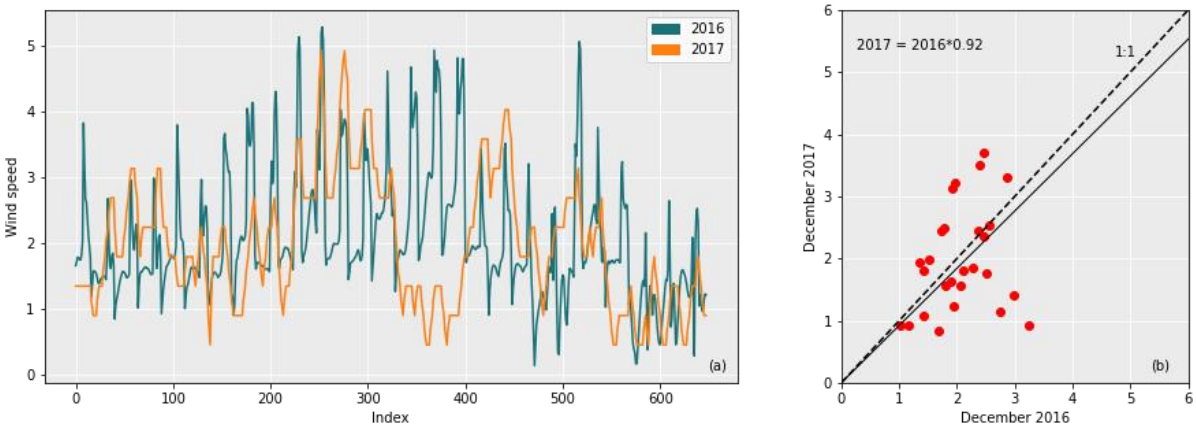

Figure S4.4: The time series comparison between hourly wind speed in December 2016 and December 2017 (a) and the calculation of a scaling factor to convert between the two years (b), where the dashed line represents the 1:1 line and the solid line represents the equation indicated in the figure and the markers represent the average daily wind speed

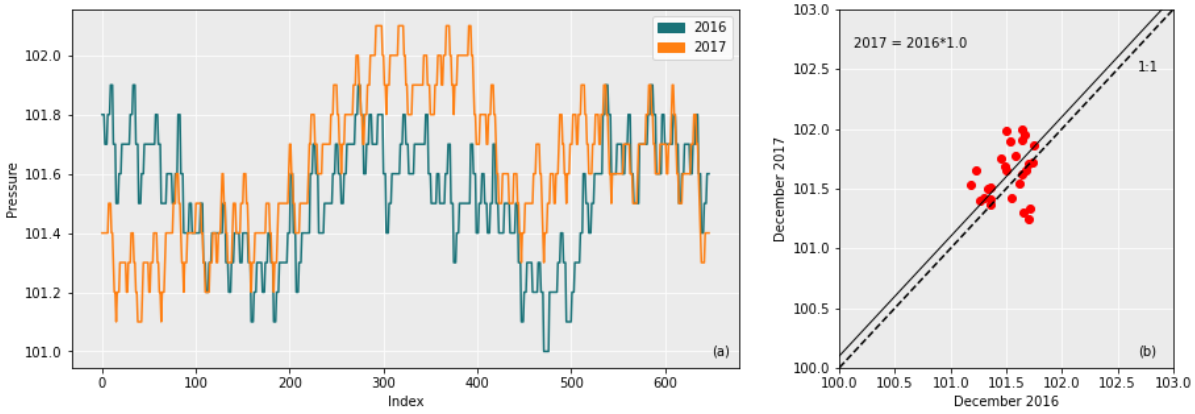

Figure S4.5: The time series comparison between hourly air pressure in December 2016 and December 2017 (a) and the calculation of a scaling factor to convert between the two years (b), where the dashed line represents the 1:1 line and the solid line represents the equation indicated in the figure and the markers represent the average daily air pressure

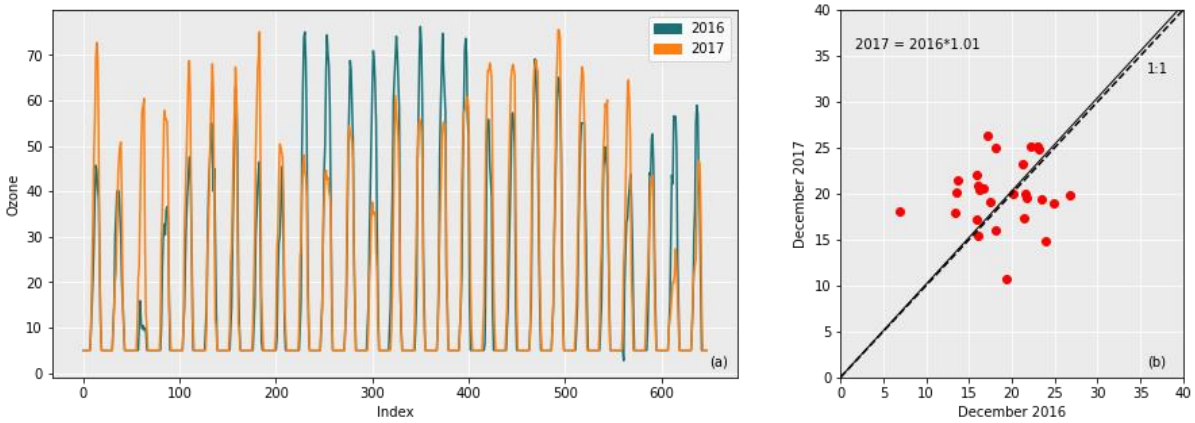

Figure S4.6: The time series comparison between hourly ozone concentrations in December 2016 and December 2017 (a) and the calculation of a scaling factor to convert between the two years (b), where the dashed line represents the 1:1 line and the solid line represents the equation indicated in the figure and the markers represent the average daily ozone concentrations

Table S4.1: Summary of factors used to scale the December 2017 WRF-Chem data to represent December 2016

Parameter	Factor
Temperature	1/1.1
Relative Humidity	1/0.84
Shortwave down radiation	1/1.18 (factor derived for PPFD but conversion factors cancel)
Wind speed	1/0.92
Air pressure	1
O_3	1/1.01
Precipitation and soil water	Zero water stress assumed so no scaling factor applied. Precipitation assumed zero and soil water content kept constant at 0.297 $m^3\ m^{-3}$

4.7.2 Relative yield (RY) loss of Indian Wheat

Table S4.2: Summary of the different approaches that have been used to estimate the relative yield loss of wheat due to O_3 exposure across India. Where ranges were reported these are given, otherwise just the average is given

Location	% Wheat prod. 2021	Study	Method	Year	RY Loss
Uttar Pradesh	31.40%	Mills et al. (2018)	Flux-response	2010-2012**	15-20%
		Droutsas (2020)	AOT40 Transp Model*	1980-2009***	15.5%
		Ghude et al. (2014)	Concentration-response	2005	2.70% (AOT40)
		Sharma et al. (2019)	Concentration-response	2014-2015	21% (AOT40)
Punjab	16.30%	Mills et al. (2018)	Flux-response	2010-2012**	10-20%
		Droutsas (2020)	AOT40 Transp Model*	1980-2009***	9.8%
		Ghude et al. (2014)	Concentration-response	2005	1% (AOT40)
		Sharma et al. (2019)	Concentration-response	2014-2015	16% (AOT40)
Haryana	11.10%	Mills et al. (2018)	Flux-response	2010-2012**	10-20%
		Droutsas (2020)	AOT40 Transp Model*	1980-2009***	10.5%
		Ghude et al. (2014)	Concentration-response	2005	1% (AOT40)
		Sharma et al. (2019)	Concentration-response	2014-2015	16% (AOT40)
Northern IGP		Lal et al. (2017)	Concentration-response	2012-2013	4% (M7), 13% (AOT40)
Rajasthan	10.10%	Mills et al. (2018)	Flux-response	2010-2012**	5-15%
		Droutsas (2020)	AOT40 Transp Model*	1980-2009***	15.3%
		Ghude et al. (2014)	Concentration-response	2005	4% (AOT40)
		Sharma et al. (2019)	Concentration-response	2014-2015	19% (AOT40)
Gujarat	3.10%	Mills et al. (2018)	Flux-response	2010-2012**	5-10%
		Ghude et al. (2014)	Concentration-response	2005	8% (AOT40)
Maharashtra	1.70%	Mills et al. (2018)	Flux-response	2010-2012**	5-10%
		Ghude et al. (2014)	Concentration-response	2005	17% (AOT40)
West		Lal et al. (2017)	Concentration-response	2012-2013	6% (M7), 27% (AOT40)
Bihar (Lower IGP)	5.20%	Mills et al. (2018)	Flux-response	2010-2012**	15-28%
		Droutsas (2020)	AOT40 Transp Model*	1980-2009***	18.9%
		Ghude et al. (2014)	Concentration-response	2005	3.60% (AOT40)
East		Lal et al. (2017)	Concentration-response	2012-2013	3% (M7), 7% (AOT40)
Madhya Pradesh	18.20%	Mills et al. (2018)	Flux-response	2010-2012**	5-15%
		Droutsas (2020)	AOT40 Transp Model*	1980-2009***	18.5%
		Ghude et al. (2014)	Concentration-response	2005	8% (AOT40)
		Sharma et al. (2019)	Concentration-response	2014-2015	23% (AOT40)
Average of studied locations		Mills et al. (2018)	Flux-response	2010-2012**	12.20%
		Droutsas (2020)	AOT40 Transp Model*	1980-2009***	16.20%
		Ghude et al. (2014)	Concentration-response	2005	3.8-6.2% (AOT40)
		Lal et al. (2017)	Concentration-response	2012-2013	4.2% (M7), 15% (AOT40)
		Avnery et al. (2011)	Concentration-response	2000	8-10% (M12), 25-30% (AOT40)
		Van Dingenen et al. (2009)	Concentration-response	2000	13.2% (M7), 27.6% (AOT40)
		Sinha et al. (2015)	Concentration-response	2011-2012	24.5% (M7), 41% (AOT40)

	Sinha et al. (2015)	Concentration-response	2012-2013	11% (M7), 27% (AOT40)
	Sharma et al. (2019)	Concentration-response	2014-2015	21% (AOT40)

[*]Droutsas (2020) modified the GLAM-Parti model to include O_3 effects on transpiration using AOT40 and included a plant adjustment to O_3 stress

[**]estimated yield loss relative to preindustrial O_3

[***] To estimate yield loss they ran the model with, and without the O_3 functions turned on

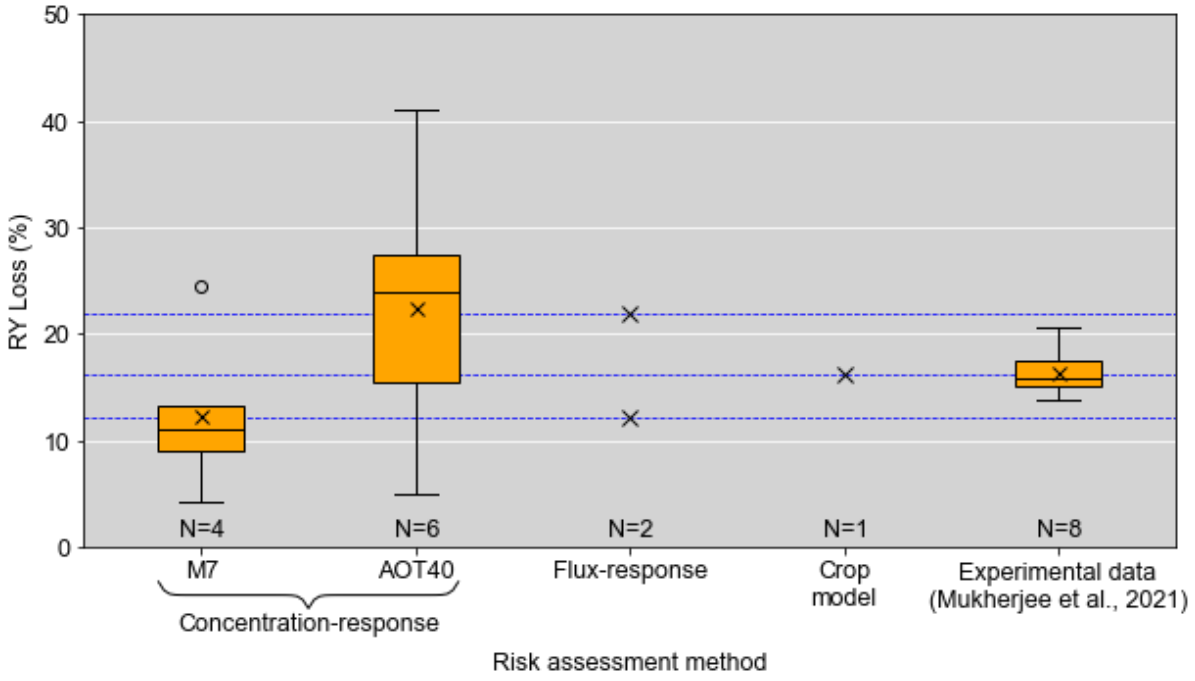

Figure S4.7: Boxplot showing the range of estimates of RY loss (%) for India for the different risk assessment metrics using data from Table S4.2. Experimental data of ambient RY loss in India is shown from Mukherjee et al. (2021)

Estimates of RY loss using the AOT40 metric are generally higher and more variable than those using the M7 metric, suggesting a greater consistency in RY loss estimates when using M7. The RY loss estimates using flux-response relationships were consistent with the mean RY loss of the M7 concentration-response relationship for Mills et al. (2018) and with the AOT40 relationship for Tang et al. (2013). Droutsas (2020), who applied an AOT40-based transpiration crop model produced RY loss estimates approximately midway between the estimates of Mills et al. (2018a) and Tang et al. (2013), and on the lower end of concentration-response estimates using AOT40. These differences underscore the importance of metric choice when performing O_3 risk assessments. Compared to the experimental data on RY loss of wheat under ambient O3 in India, M7 underestimates RY loss, while AOT40 over-estimates it. The average response of the flux-response relationship aligns well with the experimental data, while Droutsas' (2020) crop model obtains a RY loss almost identical to the mean RY loss of the experimental data.

4.7.3 Comparison of meteorological inputs

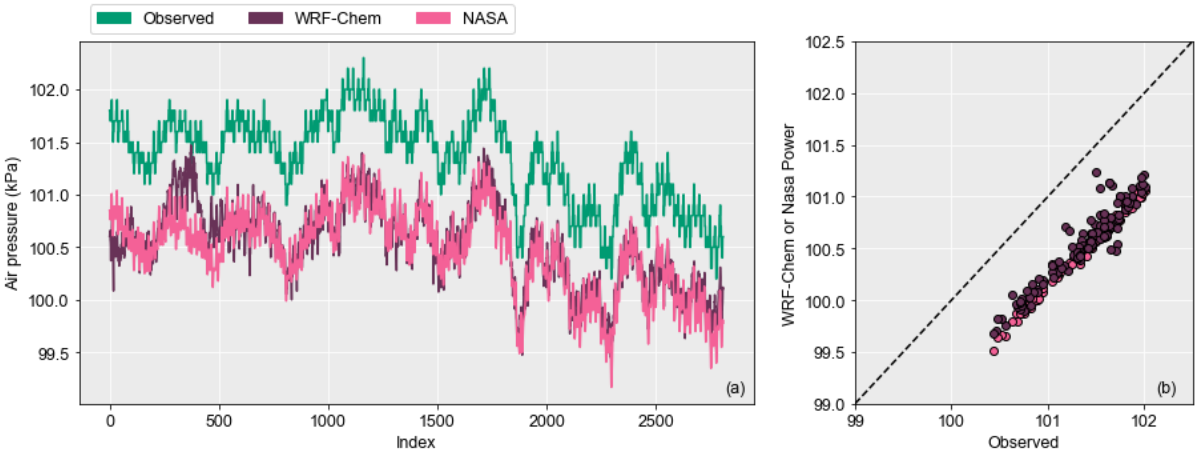

Figure S4.8: Comparison of the air pressure from January – March 2017 between the observational data, WRF-Chem data and NASA Power data. Fig. (a) shows the seasonal comparison and Fig. (b) shows the comparison of the WRF-Chem and NASA Power daily mean air pressure, with the dashed 1:1 line representing a perfect match between either WRF-Chem or NASA Power, and the observed air pressure.

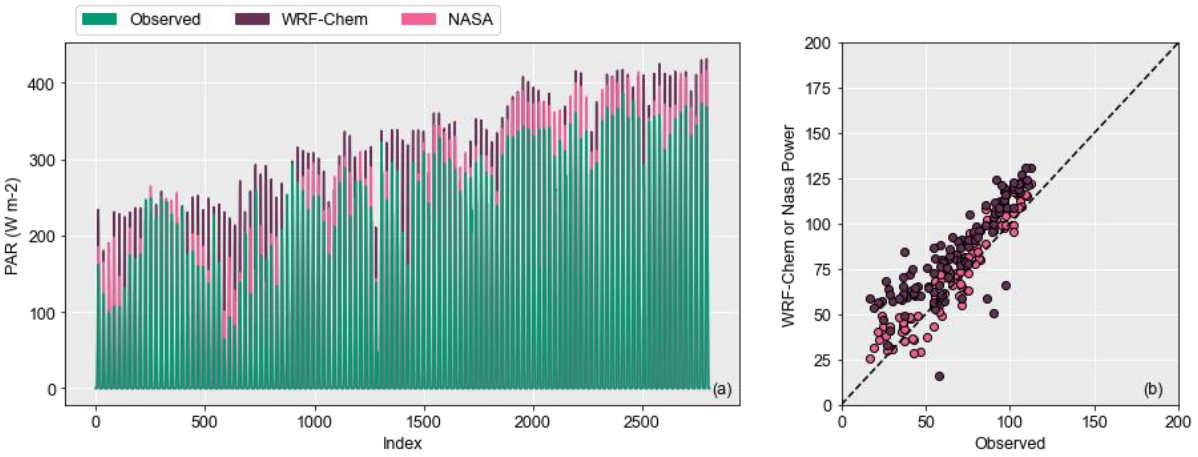

Figure S4.9: Comparison of photosynthetically active radiation (PAR) from January – March 2017 between the observational data, WRF-Chem data and NASA Power data. Fig. (a) shows the seasonal comparison and Fig. (b) shows the comparison of the WRF-Chem and NASA Power daily mean PAR, with the dashed 1:1 line representing a perfect match between either WRF-Chem or NASA Power, and the observed PAR.

4.7.4 Modelling outputs for discussion

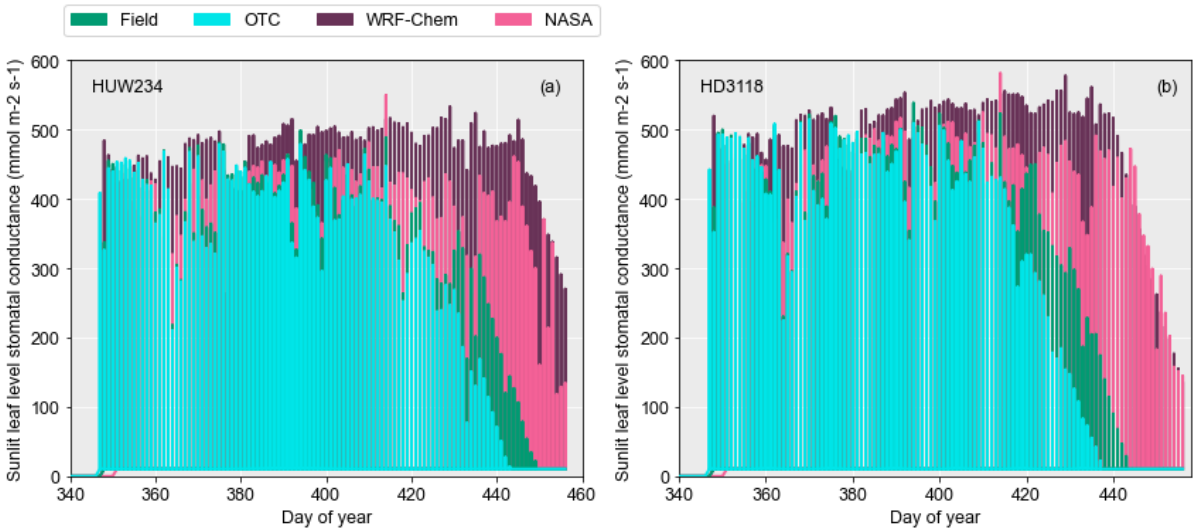

Figure S4.10: Comparison of simulated sunlit leaf level stomatal conductance for the HUW234 cultivar (a) and the HD3118 cultivar (b) across all input datasets

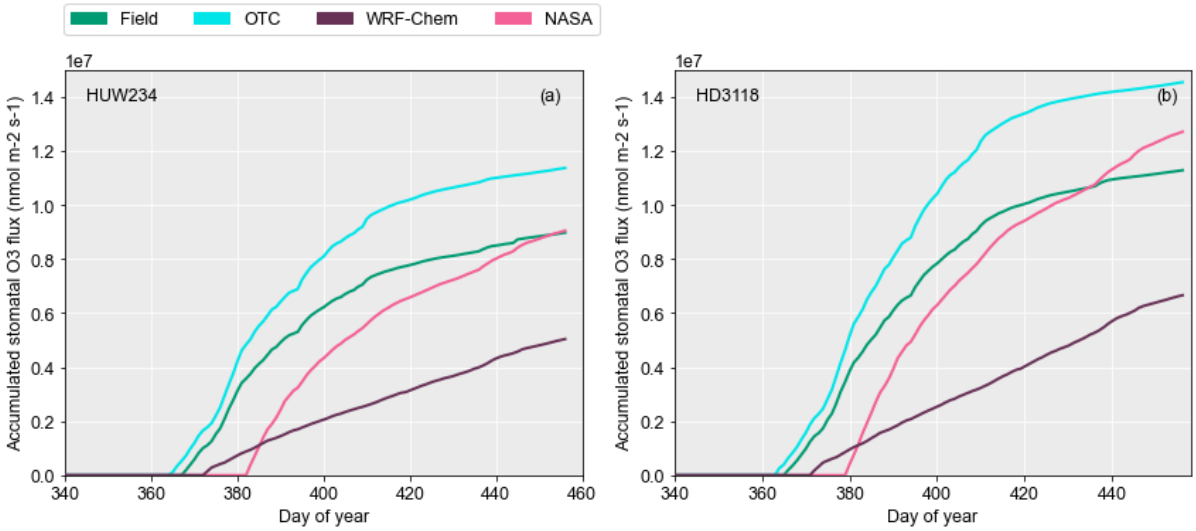

Figure S4.11: Comparison of accumulated stomatal O_3 flux for the HUW234 cultivar (a) and the HD3118 cultivar (b) across all input datasets

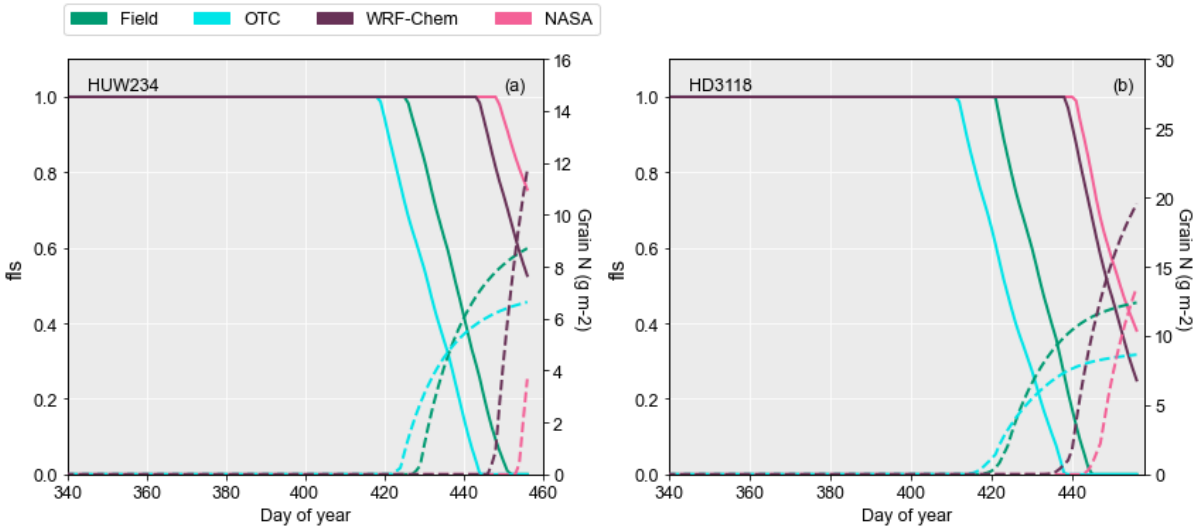

Figure S4.12: Comparison of fls (solid line) and grain N deposition (dashed line) for the HUW234 cultivar (a) and the HD3118 cultivar (b) across all input datasets. Where fls is a factor describing the progression of leaf senescence, with 1 being no senescence and 0 being complete senescence (Pande et al., 2024a).

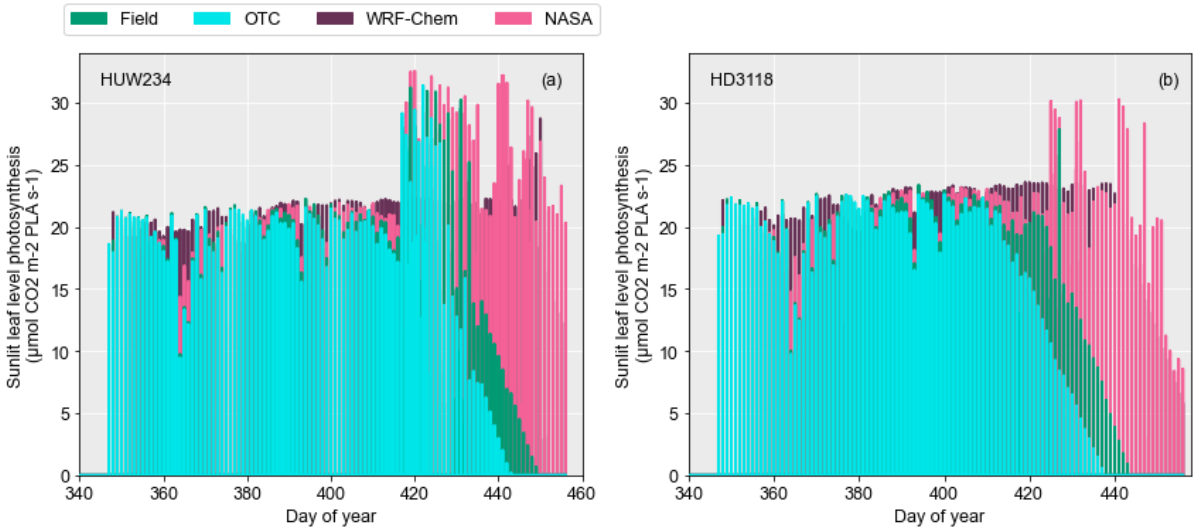

Figure S4.13: Comparison of sunlit leaf level photosynthesis for the HUW234 cultivar (a) and the HD3118 cultivar (b) across all input datasets

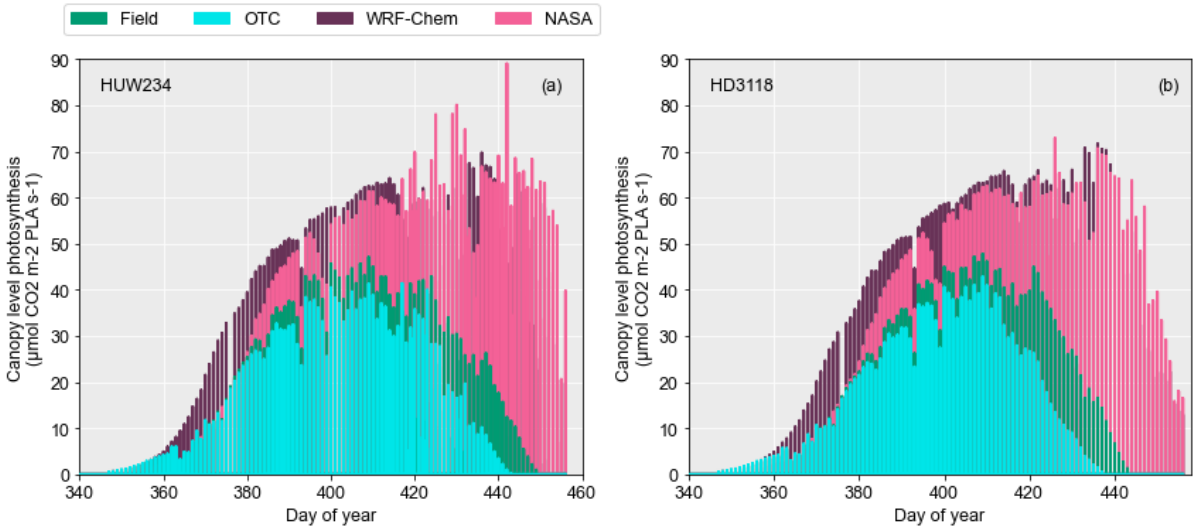

Figure S4.14: Comparison of canopy level photosynthesis for the HUW234 cultivar (a) and the HD3118 cultivar (b) across all input datasets

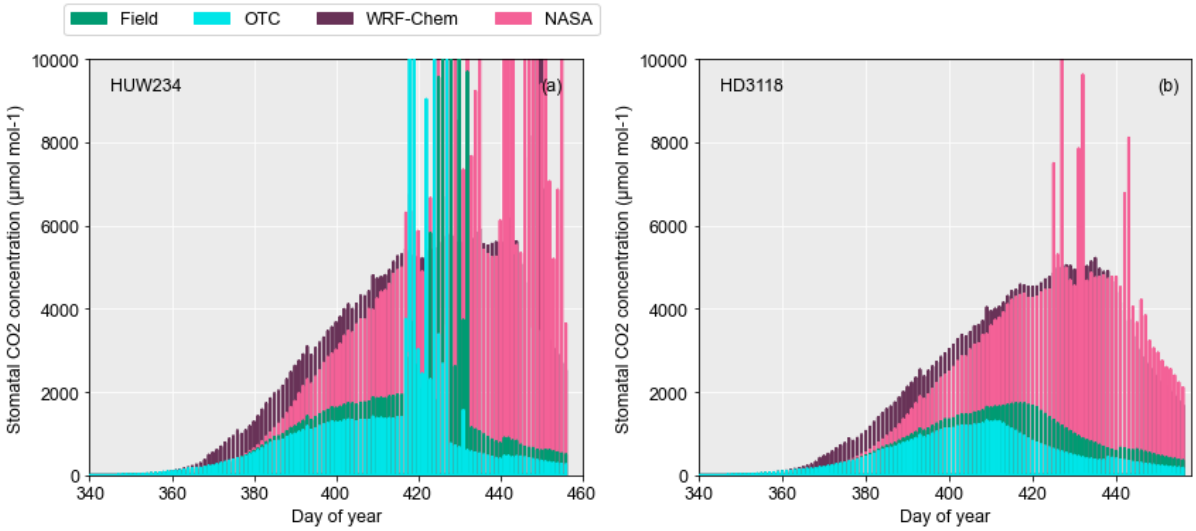

Figure S4.15: Comparison of stomatal or interior leaf CO_2 concentrations for the HUW234 cultivar (a) and the HD3118 cultivar (b) across all input datasets

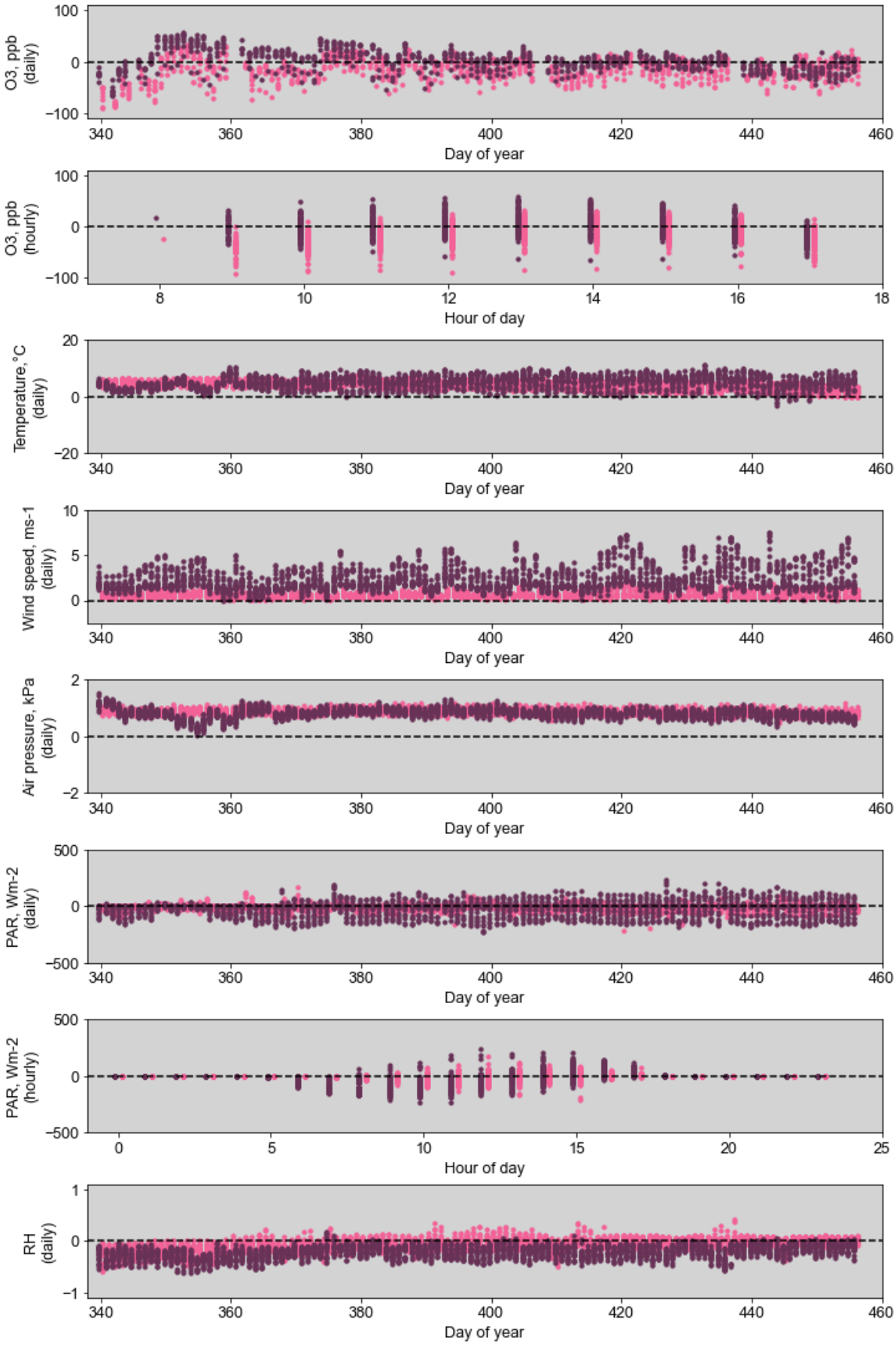
O3, ppb (daily)
100
0
−100
340
360
380
400
420
440
460
Day of year
O3, ppb (hourly)
100
0
−100
8
10
12
14
16
18
Hour of day
Temperature, °C (daily)
20
0
−20
340
360
380
400
420
440
460
Day of year
Wind speed, ms-1 (daily)
10
5
0
340
360
380
400
420
440
460
Day of year
Air pressure, kPa (daily)
2
0
−2
340
360
380
400
420
440
460
Day of year
PAR, Wm-2 (daily)
500
0
−500
340
360
380
400
420
440
460
Day of year
PAR, Wm-2 (hourly)
500
0
−500
0
5
10
15
20
25
Hour of day
RH (daily)
1
0
−1
340
360
380
400
420
440
460
Day of year

Figure S4.16: Deviation of the NASA Power and WRF-Chem O_3 concentrations and meteorological variables from the non gap-filled observed O3 data, and the observed meteorological variables.

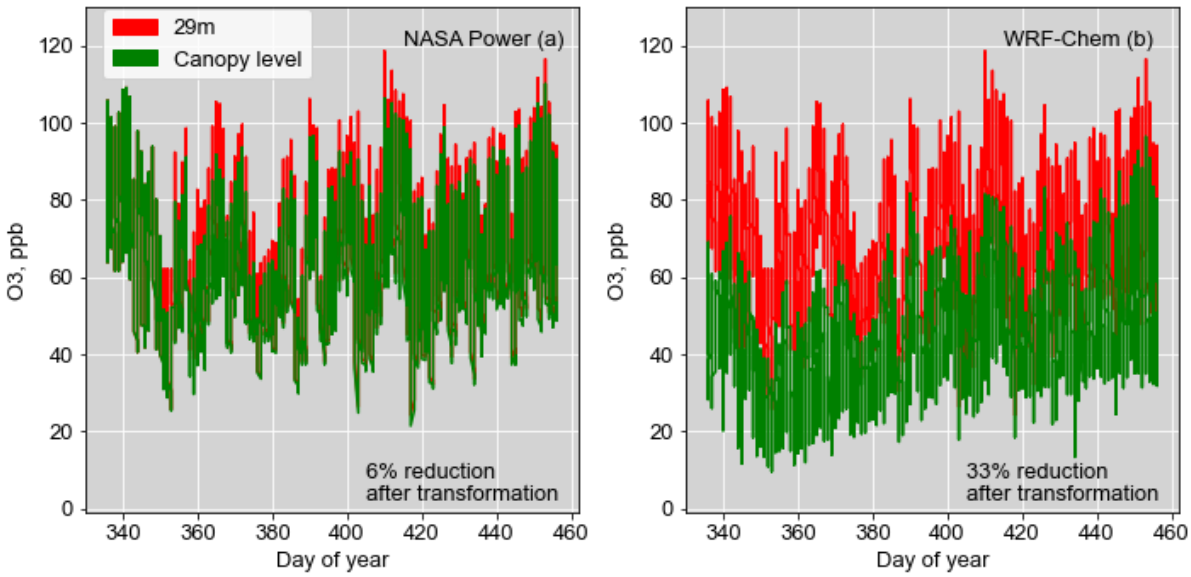

Figure S4.17: The difference in O_3 concentrations at the 29m height and canopy level in WRF-Chem and NASA Power runs. Indicated on the plot is the reduction in O_3 concentration that occurred after transforming the O_3 from the measured height at 29m to the canopy-level.

5. Synthesis

5.1 Overview

Ozone (O_3) poses a threat to both wheat yields and quality. Wheat is a key staple food globally, with a large proportion of the global population relying on it for calories and nutrition. The decrease in both wheat yields and quality under O_3 exposure is of particular concern for wheat producing countries, such as India, where O_3 concentrations are increasing. Given that wheat provides a substantial portion of daily calories and protein in India, a country already prone to malnutrition, a reduction in the availability or quality of wheat has the potential to exacerbate food insecurity and nutritional deficiencies

This thesis builds on the existing DO_3SE-Crop model, extending the model to include the effect of O_3 on N remobilisation and antioxidants, based on existing knowledge of the interactions between O_3 damage processes and nitrogen (N). The resulting DO_3SE-CropN model simulates the leaf, stem and grain N and protein concentrations, as well as important grain amino acid (AA) concentration (i.e. lysine and methionine). The Food and Agricultural Organisation of the United Nations (FAO) recommended metric for measuring protein quality, the dietary indispensable AA score (DIAAS), can be calculated from DO_3SE-CropN model outputs. This makes the DO_3SE-CropN model a good candidate for performing regional level risk assessments of O_3 effects on wheat quality. Such risk assessments are incredibly valuable as they provide information relevant to policymakers in terms of the effects that O_3 has on crops, as well as growers or breeders who may be interested in altering the cultivars they grow or management conditions in order to minimise O_3 damage to crop yields. However, such risk assessments are only as good as the data available for model parameterisation and model input. Therefore, this thesis additionally explores the issues of data availability and accuracy in both the development and application of the DO_3SE-CropN model.

This final chapter summarises the key findings of this thesis, the novelty of these results and their implications, as well as common themes and avenues for future research.

5.2 Summary of key research findings

5.2.1 Key findings from Paper 1: New ozone-nitrogen model shows early senescence onset is the primary cause of ozone-induced reduction in grain quality of wheat

5.2.1.1 Development of model simulating O_3-N interactions

In Section 2 (Paper 1) of this thesis, the interactions between O_3 damage processes and N were mapped and their interactions were explored for inclusion in the DO_3SE-Crop model. The key N processes associated with crop growth were reviewed from existing crop models and incorporated into a N module for DO_3SE-Crop. The resulting model was called DO_3SE-CropN. The O_3 inhibition of N remobilisation was incorporated through a linear regression combining data from Broberg et al. (2017) and Brewster, Fenner and Hayes (2024). The newly developed model was calibrated and evaluated using 3 years of data spanning 4 O_3 treatments using the Skyfall cultivar. The model was able to capture anthesis leaf and stem N concentrations, and the effect of O_3 on grain N. However, the effect of O_3 on leaf and stem N concentrations at harvest was exaggerated. It was suggested that the effect of O_3 on N remobilisation was not in fact linear, but potentially hormetic. Hormesis occurs when a stressor, such as O_3 initially has a positive impact on the plant, potentially encouraging greater remobilisation, and then past a threshold the stressor has a negative effect, limiting remobilisation (Agathokleous, Kitao and Calabrese, 2019). Currently, there is not enough data to parameterise a hormetic minimum for incorporating the non-linear response of N remobilisation into the DO_3SE-CropN model. It is recommended that future experiments investigating O_3 effects on N remobilisation focus on O_3 concentrations between 30-60 ppb as the data of Brewster, Fenner and Hayes (2024) indicate this is where the effect may occur.

5.2.1.2 Model development and identification of early senescence onset as the key factor affecting wheat quality under O_3 exposure

On finalising the DO_3SE-CropN model, a sensitivity analysis was conducted. This identified senescence onset as the key factor affecting grain N content and concentration under O_3 exposure, followed by senescence end/ duration. The effect of O_3 on N remobilisation did not strongly influence grain N content and concentration. The results align with existing literature as earlier senescence onset under O_3 exposure reduces the grain filling duration, leading to less time for N remobilisation (Havé et al., 2017). Additionally, as senescence onset is the starting point for which leaf N begins to be remobilised to the grain, it has a larger influence on grain N than senescence end (Havé et al., 2017). The implications of the findings from the sensitivity analysis are that breeders should focus their attention on stay-green wheat cultivars that do not experience a decrease in grain protein with the corresponding increase in yield. Such cultivars could maintain both yield and grain quality under O_3 exposure.

5.2.2 Key findings from Paper 2: Modelling the nutritional implications of O_3 on wheat protein and amino acids

5.2.2.1 Development of a framework to simulate antioxidants and protein quality

In Section 3 (Paper 2), antioxidant processes were integrated into the N module for DO_3SE-Crop by defining the N released from leaf senescence, and the N released from the stem, as either available to the grain, or unavailable (as N is a component of antioxidants). The fraction of N that was associated with antioxidants was calculated through a linear function that increases once the threshold of accumulated stomatal flux exceeded the threshold at which O_3 begins to accelerate senescence. The model was adapted to simulate lysine and methionine as these were found to be the key, nutritionally relevant AAs affected by O_3. Additionally, metrics to calculate protein quality through AA and the FAO recommended metric, the DIAAS, were integrated into the model to allow simulations of protein quality under O_3 exposure. Regressions between grain protein and AA concentration from Liu et al. (2019) were used to calculate grain AA concentrations, and the DIAAS equation from FAO (2013) was modified to incorporate the parameters simulated by DO_3SE-CropN.

The model was calibrated and evaluated for Indian wheat using data from Varanasi from Yadav et al.(2020) and Yadav, Agrawal and Agrawal (2021) and presents the first crop modelling framework able to incorporate the antioxidant response of wheat to O_3 exposure and its effect on N content. Varanasi was focussed on due to the nature of the experimental data that was available for this location. It is the first site globally to have investigated the effect of O_3 on wheat AA concentrations which allowed for integration of O_3 effects on AA into the DO_3SE-CropN model. The framework is simple, flexible and transferable to other crop models provided they simulate leaf and stem N. The decrease in the concentrations of grain protein and the nutritionally relevant AA lysine and methionine under O_3 exposure was captured by the model, though the magnitude of the decrease was generally underestimated. Through model estimates of grain lysine and methionine under O_3 exposure, grain quality using the DIAAS metric was calculated, though model estimates of AA and protein concentrations under O_3 exposure should be improved before using this metric in further risk assessments.

5.2.2.2 Further work necessary for understanding O_3 effects on wheat nutrition

The development of the framework described above led to identification of several knowledge and data gaps required for deeper understanding of O_3 effects on wheat quality and effects of meteorology on crop modelling processes. Although it was hypothesised that the new antioxidant processes would be a more mechanistic way of describing the effect of O_3 on reducing N remobilisation, superseding the equations developed in Section 2, the best results for leaf and grain protein were obtained when using both sets of equations in combination. Either the shape of the antioxidant response to O_3 is such that the two sets of equations work in combination to give the best approximation of the process, or there is an additional effect of O_3 on N remobilisation that is separate to the antioxidant response, such as the oxidisation of proteins by reactive oxygen species (ROS). Additionally, the variation in grain AA concentrations is likely linked to plant antioxidant processes, as methionine is considered an antioxidant and is easily oxidised by ROS, and lysine breaks down to proline, which protects against ROS damage. Investigation of how N, protein, AA's and antioxidant processes interact under O_3 exposure will help to improve mechanistic understanding and further model development. Additionally, the DO_3SE-Crop model showed large differences in photosynthetic rate and stomatal conductance for both cultivars between the two years of experiments in the present study, affecting biomass

simulations, which could have been caused by changes in the meteorology. It was recommended that the effect of varying input data variables on crop model outputs is investigated.

5.2.3 Key findings from Paper 3: Relative yield and protein estimates are more sensitive to ozone risk assessment choice than input data and cultivar parameterisation

5.2.3.1 Differences in meteorology and O_3 concentrations of risk assessment inputs and the effect of these on DO_3SE-CropN processes

In Section 4 (Paper 3), data sources with differing meteorology and O_3 concentrations were used to test their effects on key modelling processes in DO_3SE-CropN. Temperatures affected crop development (growth rate, anthesis, senescence timing and grain filling duration), while temperature, relative humidity (RH) and wind speed affected stomatal conductance and hence photosynthesis due to the coupled nature of the DO_3SE-Crop model. Photosynthetically active radiation (PAR) also affected photosynthesis, with differences in photosynthetic rate and LAI (determining canopy-level photosynthesis) affecting total biomass. Differences to phenology, photosynthesis and senescence subsequently affected grain yield and protein.

5.2.3.2 Sensitivity of risk assessment results to differences in input data and method choice

Risk assessments of relative yield (RY), relative protein (RP) (gProtein m^{-2}/gProtein m^{-2}) and relative protein concentration (RPC) (gProtein gDM^{-1}/ gProtein gDM^{-1} where DM stands for dry matter) were performed using concentration-based, flux-based and crop modelling methods (using the modified DO_3SE-CropN model from Section 3). Estimates of RY loss using concentration-response metrics were generally greater than when using DO_3SE-Crop and the flux-based methods, due to the lack of incorporation of environmental interactions which modify plant response to O_3, and capacity of the plant to recover from some O_3 stress. Estimates of RY using flux-based and crop modelling methods were less affected by input data variability as the higher vapor pressure deficit (VPD) reduced stomatal conductance and O_3 uptake.

Currently, few methods exist by which to measure RP and RPC under O_3 exposure. Broberg et al. (2015) developed an M7 relationship using data from Europe, Asia and North America, predicting an increase in RPC under O_3 exposure contrary to the observed decrease in India (Mishra, Rai and Agrawal, 2013; Yadav, Agrawal and Agrawal, 2021). A flux-response relationship from European wheat by Grünhage et al. (2012) was used to estimate RP, but results did not align well with estimates of Indian wheat RP. However, DO_3SE-CropN reproduced RP estimates consistent with literature values. While estimates of RP and RPC were more variable between input data sources when using DO_3SE-CropN than the flux- or concentration-response methods, the DO_3SE-CropN model is currently the only method that can reproduce realistic RP and RPC values for Indian wheat due to being parameterised and developed for this location.

5.2.3.3 Performing a nutrition-based risk assessment for O_3 effects on Indian wheat

The DO_3SE-CropN model incorporates the modifying effect of the environment on plant development, stomatal uptake of O_3 and photosynthetic rate, as well as the effect of O_3 on photosynthesis, senescence and N remobilisation. It does this in a mechanistic way which means it is more representative of the plant's biological processes than a flux-based method. Concentration-response relationships do not include environmental interactions, making them

unsuitable for assessing yield loss due to O_3 under India's changing climate (Tai et al., 2021; Emberson, 2020). Further, for assessing RP and RPC losses across India under O_3, currently only the DO_3SE-CropN model provides estimates in-line with the current literature as it has been parameterised and developed for Indian wheat. Altogether, these factors mean that the DO_3SE-CropN model has potential to be well-suited for performed a nutrition-based risk assessment of Indian wheat. Nevertheless, performance of such a risk assessment is currently limited by the availability of data for model calibration and input. Presently, the DO_3SE-CropN model has been developed and tested for only one site in India, Varanasi. While yield data are available at the district level and could be used for calibration of grain DM, there is no equivalent data for grain quality or protein, which make calibrating the nutritional quality of the grain difficult. Additionally, only aboveground biomass data were available for the experiment performed at Varanasi and these were not separated into leaf and stem DM data. While leaf N concentration data were available, no data was available for stem N. Given the difficulties in calibrating the model in Section 3, and the absence of some data highlighted above, further development and calibration of the DO_3SE-CropN model is necessary before it is used for a nutrition-based risk assessment. Additionally, before performing a risk assessment, suitable input data need to be obtained with which to run the model. These input data also need to be validated before use to determine their suitability at approximating the meteorological conditions and O_3 concentrations across the country. The limitations to validated input data include a lack of O_3 monitoring stations across India, which means it is difficult to validate simulations of O_3 from atmospheric models.

5.3 Novelty of key results

5.3.1 Process-based mapping of how O_3 and N interact

The first paper of this PhD developed a novel process-based map of how N and O_3 interact to influence plant growth, quality and O_3 damage. In the second paper, further understanding of O_3 – N processes was developed. The following section combines the understanding developed in papers 1 and 2 of O_3-N interactions.

Initially, O_3 diffuses into wheat leaves via the stomata, dissolving to form ROS (Emberson et al., 2018). While antioxidants neutralise some ROS, excess ROS attack the cell plasma membrane, degrade Rubisco and destroy photosynthetic pigments, reducing photosynthesis (Emberson et al., 2018; Rai and Agrawal, 2012; Khanna-Chopra, 2012). The reduction in photosynthesis reduces plant biomass (Emberson et al., 2018). Accelerated leaf senescence shortens grain filling duration which, along with the decreased plant biomass, leads to a reduction in crop yield (Gelang et al., 2000; Emberson et al., 2018; Broberg et al., 2015).

N taken up from the soil is stored in the leaf and stem and used to produce proteins (Lawlor, 2002; Pilbeam, 2010). Under stress, nutrient uptake decreases as allocation of photosynthate to repair damage is prioritised over allocation to the root for growth (Emberson et al., 2018; Pandey et al., 2018). A higher leaf N can delay the onset of senescence and increase photosynthetic rate; hence offering some protective capacity against O_3 (Pilbeam, 2010; Brewster, Fenner and Hayes, 2024; Nehe et al., 2020). However, under N deficiency the structure and function of chloroplasts is damaged which could exacerbate the negative impacts of O_3 on senescence and photosynthetic rate (Kang et al., 2023).

After senescence begins, N is remobilised from the leaves to the grains, and after anthesis N remobilisation begins from the stem (Havé et al., 2017; Gaju et al., 2014; Nehe et al., 2020;

Barraclough, Lopez-Bellido and Hawkesford, 2014). However, O_3 increases the residual N in the leaves and stem, reducing remobilisation to the grain (Brewster, Fenner and Hayes, 2024). It was suspected the increase in residual N is due to proteins being broken down and used for antioxidant production, and therefore not being remobilised to the grain (Brewster, Fenner and Hayes, 2024; Sarkar et al., 2010; Yadav et al., 2019b). However, Section 3 of this thesis highlighted that there could also be an additional process involved, such as the degradation of proteins by ROS (Gill and Tuteja, 2010). Reduced N remobilization lowers grain N and protein content, with variable impacts on grain N/protein concentration depending on yield loss, as seen in European vs. Indian wheat (Yadav et al., 2020; Mishra, Rai and Agrawal, 2013; Broberg et al., 2015).

5.3.2 Development of model to simulate O_3-N interactions

From the mapping of O_3-N interactions, the N module in Section 2 was developed. Equations were selected by reviewing existing crop models that incorporate N processes to determine which of their N mechanisms made sense physiologically and were easily integrable into DO_3SE-Crop. Studies by Brewster, Fenner and Hayes (2024) and Broberg et al. (2017) found that increasing O_3 concentrations increased residual N and reduced N remobilisation. Their data were combined into a linear regression to allow simulation of the O_3 effect on N remobilisation.

In the second paper of this thesis, it was hypothesised that elevated O_3 increases residual N due to its use in antioxidant production making it unavailable to the grain. A linear relationship between accumulated stomatal O_3 flux and the proportion of N associated with antioxidants was developed, where the proportion of N associated with antioxidants increases as stomatal O_3 flux increases above a threshold. The newly developed antioxidant processes were more mechanistic than the previous processes developed to incorporate the effect of O_3 on N remobilisation in Section 2, but performed better in combination with the mechanism developed in Section 2.

5.3.3 O_3 affects wheat protein quality, in addition to protein content and concentration

In Section 3, a method to assess O_3 effects on protein quality was developed. Research has shown that the concentrations of several essential and non-essential AA decrease under O_3 while others increase (Yadav et al., 2020). The differential response is due to the varying roles of AAs in plant stress response and defence, as well as their differing vulnerabilities to ROS (Ali et al., 2019). Additionally, AA response to stress is cultivar specific and means that stressors, such as O_3, influence wheat protein quality differently between cultivars. The most limiting AA's to protein production in wheat are lysine and methionine, with lysine often termed the most limiting (Shivakumar et al., 2019; Yadav et al., 2020; Meybodi et al., 2019; Siddiqi et al., 2020). A reduction in the most limiting AA under O_3 exposure reduces protein production which, given the reliance on wheat-based diets in India, could exacerbate existing malnutrition in the country. By using existing linear relationships between grain protein and AA concentrations (Liu et al., 2019b), the decrease in lysine and methionine concentration under O_3 exposure was simulated. The magnitude of the decrease in the AA under O_3 exposure was not well captured and requires further parameterisation.

5.3.4 O_3 effects on protein quality can be assessed using metrics recommended by the FAO

Section 3 presents a method by which simulated AA concentrations can be used to calculate the FAO recommended metric for measuring protein quality, the DIAAS (FAO, 2013). Due to the structure of the DIAAS equation, wheat protein quality was reduced by the same percentage under O_3 for both adults and children. However, since children require a greater quality of protein, the result of O_3 exposure is a lower wheat protein quality for children than adults.

The requirements for simulating the DIAAS are simple: simulate the most limiting AA, and the protein concentration of the crop. This means that the method will be easily transferrable to other crop models which incorporate simulations of grain N. Provided the model can capture the effect of an abiotic stressor on grain N and AA, the DIAAS will be easily simulated using the method shown in Section 3 of this thesis.

5.3.5 Comparison of risk assessment methods for determining relative yield, protein and protein concentrations of wheat exposed to O_3

In Section 4, existing methods for assessing RY, RP and RPC were compared to determine their sensitivity to differing sources of input data, and to compare the values obtained by the different methods when using the same input data. While previous studies have compared risk assessment methods used to estimate grain yield (see Tai et al. (2021), and Tarannum et al. (2024)), this study is unique in that it incorporates methods for estimating the protein yield (gProtein m^{-2}) and protein concentration (gProtein gDM^{-1}) loss under O_3 exposure. It also incorporates a wider range of risk assessment methods including concentration- and flux-response relationships and the DO_3SE-Crop model. Concentration-response relationships, which have been most commonly used for estimating RY of Indian wheat, produce higher estimates of yield loss as they don't account for the plant's detoxification capacity and local meteorological effects on stomatal O_3 uptake. Flux-response and crop modelling methods have been less commonly used for Indian wheat, but provide more biologically relevant estimates of yield loss by incorporating environmental interactions (Pleijel, Danielsson and Broberg, 2022). No comparisons of the relatively few risk assessment methods for estimating RP or RPC had been performed prior to this study.

Mukherjee et al. (2021) collected data from OTC experiments on RY loss of Indian wheat under ambient O_3, finding an average RY loss of $16 \pm 4.5\%$. Section 4 showed current estimates of national RY loss estimates for India from risk assessments in the literature, in comparison to Mukherjee et al.'s (2021) data. Previous risk assessments using M7 generally underestimated RY loss, while AOT40 mostly overestimated yield loss comparative to the experimental range from Mukherjee et al. (2021). The average flux-response and crop modelling RY estimates for India fall within the range of the experimental data. In Section 4, upon testing the risk assessment methods for Varanasi, the American M7 relationship underestimated RY loss comparative the experimental range from the literature, while all other concentration-response estimates heavily over-estimated RY loss in comparison ($17\% \leq RY \leq 100\%$). The European flux-response estimates in Section 4 gave an average RY loss of 10%, while the Indian flux-response method overestimated yield loss (compared to the experimental data) as 40%. The DO_3SE-Crop model underestimated RY loss with an average RY loss of 5%. The average RY loss of the non-concentration response studies, which are more representative of plant growing conditions since they incorporate the effects of local meteorology, was $18.8 \pm 4\%$, which agrees with the

average RY loss estimate from Mukherjee et al. (2021). Our findings also validated previous studies that found concentration-response methods tend to give larger estimates of RY loss than flux- and crop modelling-based methods (Tai et al., 2021; Tarannum et al., 2024).

The findings of Section 4 showed RY loss estimates using the European flux-response relationship and DO_3SE-Crop model, regardless of input data, were consistent with each other. However, as the European flux-response relationship was not designed for India this may be coincidence. The Indian flux-response relationship is more sensitive to O_3, reflecting the greater sensitivity of Indian wheat to O_3. However, the data used to develop the relationship was not gap-filled, and there were 11 days of missing measurements. While using mostly the same multiplicative DO_3SE model parameterisation (only phenology was different) and input data as Yadav, Agrawal and Agrawal (2021), the POD_6 found in Section 4 was higher, as a result of the gap-filling (1.3 compared with 0.75 for the HUW234 cultivar and 1.4 compared with 0.7 for the HD3118 cultivar), which led to greater RY loss estimates. Additionally, Yadav, Agrawal and Agrawal (2021) began accumulating POD_6 at sowing, whereas in Section 4 POD_6 accumulation, using the same phenology parameterisation as the DO_3SE-Crop runs to ensure consistency, began at anthesis. Marzuoli et al. (2024) found POD_6 accumulation begins ~2 months after sowing and 3-4 weeks before anthesis. Given the illustrated discrepancies, it is recommended that the Indian flux-response relationship is re-visited and re-parameterised using O_3 concentration data that is not prone to large gaps, and with appropriate timing for POD_6 accumulation, ensuring better estimates of RY loss to make the relationship more generally applicable to Indian conditions.

The RP and RPC estimates were much closer to those from the literature when using DO_3SE-CropN, which is unsurprising given the model was parameterised and developed further for Indian wheat in Section 3 of this thesis. The European RP relationship heavily underestimated the protein loss of Indian wheat under O_3 exposure, while the M7 concentration-response relationship predicted an increase in grain protein concentration, an effect seen in many countries, but not in India (Broberg et al., 2015; Mishra, Rai and Agrawal, 2013; Yadav et al., 2020). While the range of estimates of RP and RPC varied considerably depending on data source using the DO_3SE-CropN model, it gives more realistic estimates of the response of Indian wheat to O_3 and therefore it is recommended that for estimating O_3 induced protein loss for Indian wheat the DO_3SE-CropN model is used.

5.3.6 Uniqueness of the DO_3SE-CropN model

The model developed in papers 1 and 2 of this thesis, DO_3SE-CropN, is unique in several respects. It is the first crop model to…

1) …simulate the interaction between N processes and O_3 damage
2) …incorporate antioxidant processes in N dynamics
3) …simulate the effect of O_3 on wheat nutritional quality
4) …simulate the effect of O_3 on wheat protein quality, and only the second model to simulate wheat protein quality from a nutrition perspective
5) …incorporate the FAO recommended metric for determining protein quality, the DIAAS, which can estimate the quality of protein for different age groups
6) …be developed with the goal of application for nutrition-based risk assessments

These unique aspects make DO_3SE-CropN an ideal candidate for nutrition-based risk assessments of O_3 effects on crops provided sufficient data are available for model calibration.

5.4 Common themes

5.4.1 O_3-N interactions will influence food and nutrition security

O_3-N interactions are key for food security as O_3 reduces wheat yields, protein yields (gProtein m^{-2}) and, in India specifically, protein concentration (gProtein gDM^{-1}) is also reduced. N is a key component of protein and so understanding how O_3 affects N processes in wheat leads to a deeper understanding of how wheat protein is affected by O_3.

Countries such as India, which have a greater dietary reliance on wheat and experience higher O_3 concentrations, leading to greater yield loss, will be most affected by increasing O_3 concentrations (Van Dingenen et al., 2009; Mills et al., 2018b). The effect of O_3 on protein quality will exacerbate existing malnutrition, putting consumers at further risk of developing non-communicable diseases and lowered immunity (FAO et al., 2023). This is particularly concerning for children, who have greater protein quality requirements for growth and are at greater risk of stunting and wasting, which can increase mortality in later life (Briend, Khara and Dolan, 2015; FAO et al., 2023; Shewry and Hey, 2015). Further, people who are pregnant or in poorer socio-economic circumstances require higher quality protein for growth and fighting off infection (Minocha, Thomas and Kurpad, 2017b).

Understanding how O_3 and N interact can be used to inform methods, such as crop modelling, to understand the impacts of O_3 pollution on wheat yields and quality. Applied in different locations, such a model would be able to identify wheat growing regions or countries where quality and yield will be reduced by O_3 pollution. In combination with existing dietary data, it will be possible to understand the broader effects of O_3-N interactions on food and nutrition security.

5.4.2 Recommendations for crop model calibration

In papers 1 and 2 of this thesis model calibration was performed sequentially: phenology, leaf level photosynthesis and respiration, canopy level DM partitioning and O_3 damage parameters, and finally, N parameters. This approach ensures that foundational processes (phenology, photosynthesis and respiration) are fixed, so the DM and O_3 parameters can be more reliably calibrated. Key parameters for calibration are selected based on the modellers pre-existing knowledge of the model, or can be identified through a sensitivity analysis, which determines the most influential parameters for a chosen output (Vazquez-Cruz et al., 2014; Saltelli et al., 2008; Section 2 of this thesis). In DO_3SE-Crop, the DM and O_3 parameters must be calibrated simultaneously, as papers 1 and 2 of this thesis found effects of O_3 on yield in the low (Section 2) and ambient (Section 3) treatments. The N parameters were calibrated last as the N module for DO_3SE-CropN relies on the output of the DO_3SE-Crop model.

A combination of genetic algorithm and by-eye calibration approaches were used in this thesis. The genetic algorithm calibrates the model by adjusting selected parameters, within specified ranges, to maximize the R^2 between simulated and observed outputs. The genetic algorithm can give parameterisations that provide a good fit to chosen outputs. However, it can often give parameterisations that result in unrealistic simulations of the crop. For example, the yield may be reasonable, but the leaf area index (LAI) may be 20. To avoid this, the calibration can be run again by choosing different start points for each model parameter; this prevents the algorithm calibrating to a local maxima or minima. Alternatively, a by-eye calibration can be performed by manually altering parameters and visually inspecting the outputs to determine suitability.

Sometimes a by-eye approach is used in combination with a genetic algorithm to get close to the parameterisation, then a small variation range for model parameters is chosen to achieve a final calibration.

Model calibration and evaluation were limited in Section 3 due to only being available for 2 years and 2 O_3 treatments, compared to Section 2 of this thesis, where 4 treatments and 3 years of data were available. Multiple datasets from contrasting growing conditions are ideal for model parameterisation and evaluation to improve the generalisability of the model upon application (He et al., 2017; Zhang et al., 2023; Wallach, 2011).

5.4.3 Effect of meteorology and O_3 concentrations on crop modelling processes

The differences in meteorology and O_3 between the years used for model runs in Section 3 led to differences in simulations of LAI, biomass, grain DM, plant N, protein yield (gN m^{-2}) and concentration (gN gDM^{-1}). The simulations showed the grain DM in 2018 was greater than 2017, when the experimental data showed the reverse, which was attributed the differences in radiation, temperature and RH in the model input. In Section 4 of this thesis, differing sources of model input data were used, along with the parameterisation developed in Section 3, to understand how the differences in model input data affect crop modelling processes and subsequently key modelling outputs.

Generally, the key processes impacted by the changes in meteorology and O_3 concentrations were phenology, photosynthesis and senescence. Alterations to these processes subsequently affected LAI, gross primary productivity (GPP), grain DM and protein yield. Phenology was impacted by alterations to temperature which affected growth rate. Slowed development led to delayed anthesis and senescence, and later leaf area development. Since all model runs had the same harvest date, and senescence is when DM and N remobilisation from the leaves to the grains begins, delayed senescence led to reduced grain filling duration, and reduced grain DM and protein. Senescence onset and rate can be accelerated by increased O_3 concentrations in DO_3SE-Crop. So, while increased O_3 concentrations can bring forward the start of nutrient remobilisation to the grains, accelerated phenological development and increased O_3 concentrations can shorten the grain filling period, reducing grain DM and protein. The main meteorological factors affecting photosynthetic rate were temperature and RH effects on VPD, wind speed and PAR. Increased temperature and reduced RH increased VPD, which reduced stomatal conductance, and hence photosynthesis due to the coupled photosynthetic-stomatal conductance nature of DO_3SE-Crop. Additionally, greater canopy wind speeds, which can be affected by temperature and VPD, mean the air is more “well-mixed” which increases stomatal conductance and hence carbon dioxide (CO_2) and O_3 uptake. Increased CO_2 concentrations inside the leaf lead to greater production of GPP and LAI. The exact effect will depend on the concentrations of the gases.

5.5 Limitations

5.5.1 Model development

5.5.1.1 Development of N processes for DO_3SE-CropN

There are several areas of this thesis that would benefit from a greater focus by experimentalists to enable a better understanding of O_3 effects on wheat quality which can be used to improve the DO_3SE-CropN model.

1) There are currently no data describing seasonal profiles of leaf, stem, and grain N under O_3 exposure. Multiple measurements of the N concentration of the leaf and stem pre-anthesis, and grain post-anthesis, under varying O_3 concentrations would be beneficial to understand the temporal effect of O_3 on plant N.
2) It would be useful to explore the potential hormetic effect of O_3 on N remobilisation by examining O_3 concentrations ranging from 30 to 60 ppb to identify the minimum threshold for the hormetic response. This would enable improved specification of the equation describing N remobilisation under O_3 exposure.
3) It would be beneficial to have a greater understanding of the proportions of N in the leaf, stem and grain and the proportion of protein and antioxidants in the same plant parts under O_3 exposure. This would allow further understanding of how O_3 affects the N associated with antioxidants and proteins in wheat, and how this subsequently affects grain quality.
4) For modelling wheat nutritional quality, more data on the effect of O_3 on AA concentrations, particularly the most limiting AAs in wheat (lysine and methionine), would enable construction and parameterisation of equations describing the reduction in AAs under O_3 exposure. Such equations would help the model to simulate the effect of O_3 on wheat protein quality.
5) Very few studies to date have looked at the effect of O_3 on Indian wheat quality. Mishra, Rai and Agrawal (2013) and Yadav et al. (2020) are the only authors to have done so, with the work of Yadav et al. (2020) used in Section 3 of this thesis. To improve the wider applicability of the model for Indian wheat, it would be helpful to have the data described in points 1-4 above for multiple locations across the country. Data from multiple growing locations would allow for development of a model parameterisation and construct that is more generalisable for Indian wheat, and hence is more suitable for performing nutrition-based O_3 risk assessments.

5.5.1.2 Developing DO_3SE-Crop to simulate the co-occurring effects of climate change and O_3 pollution

This thesis highlighted the effects of O_3 on protein yield (gProtein m^{-2}) and concentration (gProtein gDM^{-1}). However, the climate is currently changing. Heat and drought stress, and increased CO_2 concentrations, will co-occur with O_3 pollution to impact plant productivity and nutritional quality (Broberg et al., 2023; Naaz et al., 2022). This changing climate will impact O_3 production and interact with O_3 damage processes to further damage plants. While high temperatures and drought stress decrease stomatal conductance, leading to lesser O_3 uptake, they increase ROS accumulation which could exacerbate O_3 damage to photosynthetic pigments, reducing photosynthesis and accelerating senescence (Suryavanshi and Buttar, 2016; Bota, Medrano and Flexas, 2004; Farooq et al., 2011; Lal et al., 2022; Rijal et al., 2020; Khanna-Chopra, 2012). The acceleration of senescence could be partially offset by increased CO_2 which reduces stomatal conductance and hence O_3 uptake (Ewert and Pleijel, 1999). However, some studies have shown an acceleration of flag leaf senescence in wheat under elevated CO_2, due to photosynthetic acclimation to the higher gas concentration (McKee, Bullimore and Long, 1997; Nie et al., 1995; Zhu et al., 2012, 2009). Therefore, the direction of the effect of elevated CO_2 on senescence is unclear. Elevated CO_2 stimulates photosynthesis and improves carbon assimilation, which may offset the reduction in photosynthesis under heat stress, drought stress and increased O_3 concentrations (Wall et al., 2006; Mulholland et al., 1997; Broberg et al., 2019; Yadav et al., 2019a). Nitrate assimilation, the process by which nitrate ions are converted to organic N compounds to form useful proteins like Rubisco, is

impaired under elevated CO_2 (Bloom et al., 2010). Further, ribosomes (where protein synthesis takes place) and translocation factors (that determine how AA chains are synthesised) are reduced under heat stress (Wang et al., 2018). Additionally, there is a decrease in the enzymes controlling the precursors involved in protein synthesis under heat stress (Wang et al., 2018).

The above processes all interact and combine to affect the yield and quality of wheat. Heat stress, water stress and increased O_3 concentrations decrease the grain protein yield (gProtein m^{-2}) but increase the concentration (gProtein gDM^{-1}) (Mariem et al., 2021; Broberg et al., 2015; Broberg, Högy and Pleijel, 2017; Broberg et al., 2023). Whereas heat, water and O_3 stress decrease grain starch concentration but CO_2 increases it (Mariem et al., 2021; Broberg et al., 2015). Yadav et al. (2019) found that higher CO_2 can offset O_3 induced decreases in yield components but the same is not true for wheat quality. The decrease in protein concentration of wheat grains under higher CO_2 cannot be offset by increased O_3 as in addition to the dilution effect, elevated CO_2 impairs nitrate assimilation (Bloom, 2015). Naaz et al. (2022) assessed the combined impact of elevated CO_2, temperature and O_3 on wheat yields using 2050 projections for India, finding that yields were significantly reduced compared to present conditions.

The DO_3SE-Crop model incorporates the effects of temperatures on accelerating crop development, soil water stress, temperature and RH (through VPD) effects on stomatal conductance, and increased CO_2 concentrations on accelerating photosynthesis. Therefore, it is already able to assess some of the effects of a changing climate, and its interactions with O_3 on crop quality and yield. However, currently, the effect of increased temperatures and drought stress on increasing ROS, and therefore accelerating senescence, is not included in the model. Neither is the effect of elevated CO_2 on reducing stomatal conductance and hence O_3 uptake. Senescence and stomatal conductance are key processes in DO_3SE-Crop, so in order to improve its suitability for assessing the effect of climate-O_3 interactions on yields and quality, the model should be further developed to include the climate effect on these processes. Additionally, there is no process currently in the N module that would account for the decrease in protein concentration under elevated CO_2, but if drought and heat stress effects on senescence and photosynthesis are included into DO_3SE-Crop, these should translate into equivalent decreases in N accumulation and concentration due to the model structure. Overall, the combination of climate change and O_3 effects on crop growth, yield and quality in differing scenarios can be investigated using the DO_3SE-Crop model, but further development would improve the reliability of the model assessment.

5.5.2 Model calibration

An issue common for all crop modellers is obtaining sufficient data for model calibration. In Section 3 of this thesis, this issue was highlighted as only 2 years of data with 2 O_3 treatments were available. Initially the 2017 data were used for calibration and the 2018 for evaluation, but this meant the model over-fitted to the 2017 data. To focus on model development both years were used for model development. This contrasts with Section 2, where the 3 years and 4 O_3 treatments allowed for sufficient calibration data across years without overfitting. For future calibrations, data from contrasting growing conditions, such as greater number of O_3 treatments, different growing seasons/ years, altered sowing dates or other experimental conditions will reduce the likelihood of overfitting (He et al., 2017; Zhang et al., 2023).

Further, as there are such large data requirements for model calibration, only 3 wheat cultivars were calibrated for in the present study, the UK cultivar Skyfall in Section 2, and the Indian cultivars HUW234 and HD3118 in Section 3. Different cultivars will have different

parameterisations (e.g. different $V_{cmax,25}$, $J_{max,25}$, anthesis timing, grain filling rates and more). To parameterise the models for different cultivars would require more experimental data detailing the physiology and response to stress of these cultivars. When applying the model over a region or country, a representative parameterisation or cultivar can be chosen based on properties or varieties of wheat commonly grown in the area.

There are also measurements that are commonly not taken, or could be taken at a greater frequency to improve model calibration:

1) When performing measurements for crop modelling, LAI, leaf DM and stem DM should also be recorded so that DM can be appropriately partitioned between these sinks, and the N associated with that plant part can be captured more accurately.
2) If it is possible to measure LAI, leaf DM, stem DM and grain DM at multiple time-points, then the model can be calibrated to be a more realistic approximation of plant growth.
3) N data for the leaf, stem and grain at multiple time points would aid in appropriate allocation of N between sinks and a more realistic approximation of plant N.
4) Root DM is commonly not measured, but DM in DO_3SE-Crop is partitioned between roots, leaves, stems and the grains. Obtaining root DM data would aid in partitioning total biomass, making simulations more representative of the cultivar.
5) Similarly, while photosynthesis data is often measured, DO_3SE-Crop also needs respiration data, particularly the rate of dark respiration, to parameterise respiration equations. Appropriate parameterisation of the respiration equations is required to prevent the simulated plant from "respiring away" all the photosynthesis it performed throughout the day, leaving less for growth. When dark respiration is incorrectly parameterised it results in early development of LAI to compensate and photosynthesise more to produce the same yield (see Nguyen et al. (2024)).

5.5.3 Model application

5.5.3.1 Input data requirements for regional risk assessments in India

To apply DO_3SE-Crop across a country requires gridded meteorological and O_3 concentration data. In Section 4, the performance of DO_3SE-CropN was tested for yield and nutrition risk assessments using output from the atmospheric chemistry model WRF-Chem, and satellite data from NASA Power, to understand differences in source data for risk assessment. Since NASA Power doesn't record O_3 concentrations, the O_3 concentrations from WRF-Chem were substituted for this run. The WRF-Chem O_3 concentrations were used in place of the observed O_3 as for a national risk assessment, atmospheric modelled O_3 concentrations are more accessible due to limited O_3 monitoring data across India. RH, PAR, wind speeds and temperatures were captured better by the NASA Power data than for WRF-Chem. In the WRF-Chem dataset, the wind speed was heavily underestimated. However, WRF-Chem's canopy-level O_3 concentrations matched the observed data better than NASA Power. The variability in the NASA Power and WRF-Chem datasets affected estimates of RY, RP and RPC. Section 4 only compared the differences in meteorology and O_3 concentrations for one location only, Varanasi. To identify which data is more suitable for performing a risk assessment, the meteorological and O_3 concentrations need to be evaluated for several wheat growing locations.

Meteorological data can be evaluated through comparisons with ground-level or satellite observations. However, O_3 concentrations cannot be directly measured by satellites. While a total O_3 column concentration can be obtained, a model would be required to calculate O_3 at different heights, and hence obtain surface O_3. Evaluating surface O_3 concentrations will be

difficult due to the lack of observational O_3 concentrations across India. The tropospheric O_3 assessment report (TOAR) produced a database of global O_3 concentrations available as an easily usable dashboard (https://zam2061.zam.kfa-juelich.de/dashboard). Using the database, we can see that surface O_3 data for India is spatially and temporally sparse, with very limited observation sites. For sites that measure O_3 concentrations, the data is generally not recorded consistently on an hourly basis throughout the wheat growing season. Since the DO_3SE-Crop model requires hourly O_3 concentrations to simulate the instantaneous effect of O_3 on photosynthesis, as well as the long-term accumulation effect on senescence, O_3 measurements need to be reliable and consistent.

5.5.3.2 Performing a nutrition-based risk assessment of Indian wheat

Given the new DO_3SE-Crop model simulates the effect of O_3 on wheat yields, and the newly developed N module simulates the O_3 effect on wheat protein and protein quality, the DO_3SE-CropN model has the capacity to perform a nutrition focussed risk assessment of O_3 effects on wheat. The results of RY, RP and RPC estimates, along with simulations of wheat protein quality through metrics such as the DIAAS could be interpreted alongside local dietary data to determine the threat of O_3 to individuals' diet. Such assessments can reveal regionally in which areas O_3 induced reductions in protein and protein quality will exacerbate existing malnutrition. The results of such analyses could aid in identifying local and national scale interventions that either limit O_3 pollution or mitigate damages to yields and quality caused by interactions between O_3 pollution and the climate.

Section 4 found that the DO_3SE-CropN model was the only model that could produce the RP and RPC of Indian wheat, largely due to the model having been designed and parameterised for two Indian wheat cultivars. Therefore, it has potential to be well-suited for performing a nutrition-based risk assessment of Indian wheat. The DO_3SE-Crop model incorporates meteorological processes, making it suitable for simulating wheat under differing climates in India, and it incorporates the capacity of the plant to recover from some O_3 damage, making it more biologically relevant than concentration-response relationships. Further experimental data on O_3-N or O_3-protein interactions from several sites in India to calibrate and develop the N module would be useful to ensure the robustness of the DO_3SE-CropN model for application in the country.

5.6 Implications of key results

5.6.1 O_3 effects on N remobilisation are key for...

5.6.1.1 ...Crop modellers

To date, DO_3SE-CropN, developed in this thesis, is the only model that simulates the effect of O_3 on plant N processes, and subsequently on wheat protein and protein quality. However, there are many existing crop models that simulate O_3 effects on crop yields. Inclusion of N processes and the O_3 influence in these models would allow modellers to not only estimate yield losses but improve the nutritional relevance of their simulations. This is key for addressing global food security, as maintaining yield and nutritional quality are vital for sustaining human health. Additionally, several of these models have been, or are currently, involved in model intercomparison projects. The projects involve training and evaluating multiple models on the same datasets for more robust risk assessments, or testing of agricultural adaptations for differing scenarios. Integration of O_3-N processes into these models would allow for nutrition-based intercomparison projects to evaluate O_3 effects on wheat quality at national and global

scales. However, in order to properly calibrate and evaluate these processes, datasets that include the effect of O_3 on plant N or protein would need to be available for calibration and evaluation. Further, agricultural strategies that mitigate yield and nutrient loss under O_3 exposure could be identified. A nutrition-based intercomparison project of O_3 effects on wheat would have several benefits: reduced uncertainty of model predictions which means more reliable data for policymakers and researchers, mitigation strategies could be investigated to aid farmers in maintaining yield and reducing nutrient loss under O_3 exposure. These would lead to the protection of human nutrition under increasing O_3 concentrations.

5.6.1.2 ...Breeders

Currently, stay-green cultivars have been identified for their potential to maintain yield under abiotic stress (Kamal et al., 2019). However, it was found in Section 2 of this thesis that the early onset of senescence is the key determinant of grain protein concentration under O_3 exposure, and early senescence leads to lower protein deposition to the grain (Sultana et al., 2021; Nehe et al., 2020; Bogard et al., 2011). Therefore, breeders need to be aware of O_3-N interactions in order to develop stay-green wheat cultivars that do not experience a protein penalty as a potential adaptation to O_3 stress. The mechanistic understanding of O_3-N interactions developed in Section 2 of this thesis will aid breeders in developing such cultivars.

5.6.1.3 ...Growers

Following on from section 5.6.1.2, breeders and growers need to work together in developing cultivars that maintain nutritional quality as well as yield under O_3 exposure. Globally, wheat is grown under a wide range of climates so breeders will need to make sure that any developed wheat varieties are climatically suitable, particularly under the future changing climate, and have the appropriate growing season length for the region. The DO_3SE-CropN model takes hourly meteorological and O_3 inputs, allowing for the growth of a cultivar in different climates and environments to be tested. Additionally, cultivar-specific parameters are calibrated, making the model suitable for testing how well different cultivars perform under the same conditions. Therefore, with sufficient data to calibrate cultivar response, the DO_3SE-CropN model is an ideal candidate for growers to test the suitability of cultivars for maintaining yields and protein content and quality under differing O_3 and environmental conditions.

5.6.1.4 ...Governments and consumers

Given O_3 reduces crop yields, protein content and quality, O_3-N interactions affect an individual's food and nutrition security. This is of critical importance to both governments and consumers as achieving Sustainable Development Goal 2 requires that all individuals have safe, nutritious and sufficient food, and that all forms of malnutrition are eradicated, by 2030 (FAO et al., 2023). Increasing O_3 concentrations in countries such as India, where wheat production is high, threaten achievement of this goal, as wheat yields, and nutrition will be reduced. Governments need to be aware of the implications of increasing O_3 concentrations on malnutrition, food and nutrition security to develop effective policies, design and implement appropriate mitigation strategies, and invest in agricultural practices that can adapt to or counteract these negative effects.

5.6.2 Wider implications for policy

5.6.2.1 Food security policies in India

The present thesis has highlighted the issues posed by O_3 pollution to both crop yields and quality. This is of critical importance in India given that wheat is a staple crop responsible for

both energy and nutrition, meaning that reductions in yield and crop quality have the potential to exacerbate existing malnutrition in the country. Currently, there are several policies/ schemes in India that aim to reduce food insecurity. The minimum support price (MSP) is the minimum price paid by the government to farmers for produce when the price of the crop is less than the costs of growing the crop, providing income protection for farmers (Aditya et al., 2017). The Public Distribution System (PDS) is linked to the MSP and provides grains to poorer consumers at reduced prices (Pingali, Mittra and Rahman, 2017). The Integrated Child Development Scheme (ICDS) offers food, nutrition, health education and check-ups to young children and pregnant or breast-feeding mothers (Chakrabarti et al., 2019). The Mid-Day Meal Scheme (MDMS) provides primary school children with meals meeting nutritional standards for their age (Ramachandran, 2019). The National Food Security Act (NFSA) subsidises grain prices for a significant proportion of the population and offers free meals and monetary payments to pregnant women (Pingali, Mittra and Rahman, 2017). Jain (2015) found that ICDS improved child growth in rural areas while Afridi (2010) and Ramachandran (2019) found that the MDMS reduced protein, calorie and iron deficiencies. Despite these benefits, challenges to the schemes including infrastructure, training, food safety, nutritional value, and the exclusion of rural and tribal communities threaten their success (Deodhar et al., 2010; Kamali, 2014; Chudasama et al., 2016).

Since O_3 concentrations are projected to increase in India (Rathore, Gopikrishnan and Kuttippurath, 2023), wheat yields and quality will reduce further, threatening current schemes tackling food insecurity. The ICDS and MDMS may need to re-evaluate their nutritional profiles to reflect the poorer quality of wheat under increasing O_3. Additionally, the reduction in wheat yields will mean less wheat is available for all previously listed schemes. Under increased O_3 the price of wheat is likely to increase for consumers and governments (Pandey et al., 2023). Further, the reduction in crop yields will lead to a lower income for rural farmers, who are already at a high risk of poverty and food insecurity in India (Pingali et al., 2019). Insufficient nourishment from sufficient and high quality of food puts individuals at an increased risk of malnutrition which can lead to disease (Swaminathan, Vaz and Kurpad, 2012; Minocha, Thomas and Kurpad, 2017b). The government needs to be aware of the potential impact of O_3 on exacerbating existing malnutrition in India to ensure that current food security policies can be adapted and remain effective if the quantity and quality of wheat available changes. Further, existing policies supporting farmers, such as the MSP, may require reconsideration if the production of wheat decreases due to O_3 exposure.

5.6.2.2 Emissions policies globally and in India

Given O_3 reduces crop yields and quality, governments in countries where O_3 pollution poses threats to crops need to focus on mitigating O_3 damage. Globally, ~5% of countries have adopted world health organisation (WHO) guidelines into law for O_3 pollution, and ~ 40% weaker standards than recommended (UNEP, 2021). While 56% of countries globally have established national ambient air quality standards, enforcement is inconsistent (UNEP, 2016). Furthermore, only 38% of countries globally have specific air quality policies, yet existing guidelines are designed for human health not vegetation (UNEP, 2016). There may be some reduced O_3 damage afforded to vegetation through these health metrics, but they are likely not stringent enough to protect vegetation. Additionally, India does not have metrics designed to moderate O_3 concentrations for human health (Emberson, 2020).

In India, financial incentives and awareness programs have reduced agricultural residue burning, and the introduction of a national clean air program aims to reduce particulate matter

(Ministry of Environment, Forest & Climate Change, 2020; Chhabra et al., 2019). In 2009, India distributed over 2.7 million liquid petroleum gas cook stoves to reduce air pollution, as 20-50% of ambient air pollution in India is thought to originate from fuel burning for cooking (UNEP, 2016; Chafe and Chowdhury, 2021; Patnaik, Tripathi and Jain, 2019; Chowdhury et al., 2019). The scheme successfully reduced emissions but environmental benefits are uncertain (Singh, Pachauri and Zerriffi, 2017). While there are no specific policies in India targeting O_3 pollution, the previously described methods may limit emissions of O_3 precursors and hence reduce O_3 formation, but this is not certain (Ministry of Environment, Forest & Climate Change, 2019, 2020). As the present thesis has highlighted the threats posed by O_3 pollution to crop yields and quality, development of pollution control measures relating to O_3 and its precursors are essential for protecting food security in India.

5.7 Final remarks

This thesis has developed the first crop model to simulate O_3-N interactions and simulate O_3 effects on wheat grain and protein quality. O_3-N interactions are important for human nutrition, as increasing O_3 concentrations not only reduce wheat yields, but wheat protein, and protein quality. To date, no O_3 risk assessments have focussed on protein, despite wheat providing up to 20% of dietary protein globally. The N module for DO_3SE-Crop, developed in this thesis, provides a crop modelling framework for nutrition-based risk assessments as it integrates the O_3 effect on yield with O_3 effects on protein and protein quality. Several research gaps have also been revealed, particularly in understanding O_3 effects on plant N, antioxidants and protein quality, which are key for model development and parameterisation but also for developing adaptation strategies to O_3. Despite this, the mechanisms and frameworks presented in this thesis lay a foundation for other crop modellers to integrate O_3-N interactions in their models to simulate wheat quality. The model has been parameterised and tested for European and Indian wheat which experience different responses to O_3 concentrations, showing the robustness of the initial model design. The DO_3SE-CropN model takes meteorological inputs and CO_2 concentrations, meaning it can simulate the interaction of climate and O_3 effects on wheat quality, though further development of the model would improve the reliability of these simulations. Regional applications of the DO_3SE-CropN model for India are limited by the availability of validated input data due to the lack of O_3 monitoring networks in India, and limited calibration data to develop a general parameterisation for Indian wheat. Overall, this thesis provides a foundational framework by which O_3 effects on crop quality can be further understood. Through discussion of current limitations to model development and experimental understanding of O_3 effects on crop quality, this thesis identifies the key areas necessary for future research to focus on to develop a deeper understanding of the threat posed by O_3 to human nutrition.

6. List of references

Abdelhakim, L. O. A. et al. (2021). The effect of individual and combined drought and heat stress under elevated CO2 on physiological responses in spring wheat genotypes. *Plant Physiology and Biochemistry*, 162, pp.301–314. [Online]. Available at: doi:10.1016/j.plaphy.2021.02.015.

Adams, R. M. et al. (1989). A reassessment of the economic effects of ozone on U.S. Agriculture. *Journal of the Air Pollution Control Association*, 39 (7), pp.960–968. [Online]. Available at: doi:10.1080/08940630.1989.10466583.

Aditya, K. S. et al. (2017). Awareness about Minimum Support Price and Its Impact on Diversification Decision of Farmers in India. *Asia and the Pacific Policy Studies*, 4 (3), pp.514–526. [Online]. Available at: doi:10.1002/app5.197.

Afridi, F. (2010). Child welfare programs and child nutrition: Evidence from a mandated school meal program in India. *Journal of Development Economics*, 92 (2), pp.152–165. [Online]. Available at: doi:10.1016/j.jdeveco.2009.02.002.

Agarwal, P., Stevenson, D. S. and Heal, M. R. (2024). Evaluation of WRF-Chem-simulated meteorology and aerosols over northern India during the severe pollution episode of 2016. *Atmospheric Chemistry and Physics*, 24 (4), pp.2239–2266. [Online]. Available at: doi:10.5194/acp-24-2239-2024.

Agathokleous, E., Kitao, M. and Calabrese, E. J. (2019). Hormesis: A Compelling Platform for Sophisticated Plant Science. *Trends in Plant Science*, 24 (4), pp.318–327. [Online]. Available at: doi:10.1016/j.tplants.2019.01.004.

Aggarwal, P. K. et al. (2006). InfoCrop: A dynamic simulation model for the assessment of crop yields, losses due to pests, and environmental impact of agro-ecosystems in tropical environments. I. Model description. *Agricultural Systems*, 89 (1), pp.1–25. [Online]. Available at: doi:10.1016/j.agsy.2005.08.001.

Agrawal, S. et al. (2019). Socio-economic patterning of food consumption and dietary diversity among Indian children: evidence from NFHS-4. *European Journal of Clinical Nutrition*, 73 (10), pp.1361–1372. [Online]. Available at: doi:10.1038/s41430-019-0406-0.

Ainsworth, E. A. and Rogers, A. (2007). The response of photosynthesis and stomatal conductance to rising [CO2]: Mechanisms and environmental interactions. *Plant, Cell and Environment*, 30 (3), pp.258–270. [Online]. Available at: doi:10.1111/j.1365-3040.2007.01641.x.

Ali, Q. et al. (2019). Role of Amino Acids in Improving Abiotic Stress Tolerance to Plants. In: *Plant Tolerance to Environmental Stress*. pp.175–204. [Online]. Available at: doi:10.1201/9780203705315-12.

Andersson, A. (2005). *Nitrogen redistribution in spring wheat: root contribution, spike translocations and protein quality*. (10), Alnarp, Sweden.

Archibald, A. T. et al. (2020a). Tropospheric ozone assessment report: A critical review of changes in the tropospheric ozone burden and budget from 1850 to 2100. *Elementa*, 8 (1), pp.1–53. [Online]. Available at: doi:10.1525/elementa.2020.034.

Archibald, A. T. et al. (2020b). Tropospheric Ozone Assessment Report: On the changes in surface ozone over the twenty-first century: sensitivity to changes in surface temperature and chemical mechanisms: 21st century changes in surface ozone. *Philosophical Transactions of the Royal Society A: Mathematical, Physical and Engineering Sciences*, 378 (2183). [Online]. Available at: doi:10.1098/rsta.2019.0329.

Asseng, S. et al. (2015). Rising temperatures reduce global wheat production. *Nature Climate Change*, 5 (2), pp.143–147. [Online]. Available at: doi:10.1038/nclimate2470.

Asseng, S. et al. (2019). Climate change impact and adaptation for wheat protein. *Global Change Biology*, 25 (1), pp.155–173. [Online]. Available at: doi:10.1111/gcb.14481.

Avnery, S. et al. (2011). Global crop yield reductions due to surface ozone exposure: 1. Year 2000 crop production losses and economic damage. *Atmospheric Environment*, 45 (13), pp.2284–2296. [Online]. Available at: doi:10.1016/j.atmosenv.2010.11.045.

Bal, P. K. et al. (2016). Climate change projections over India by a downscaling approach using PRECIS. *Asia-Pacific Journal of Atmospheric Sciences*, 52 (4), pp.353–369. [Online]. Available at: doi:10.1007/s13143-016-0004-1.

Balla, K. et al. (2014). Changes in the photosynthetic efficiency of winter wheat in response to abiotic stress. *Open Life Sciences*, 9 (5), pp.519–530. [Online]. Available at: doi:10.2478/s11535-014-0288-z.

Balla, K. et al. (2019). Heat stress responses in a large set of winter wheat cultivars (Triticum aestivum L.) depend on the timing and duration of stress. *PLoS ONE*, 14 (9), pp.1–20. [Online]. Available at: doi:10.1371/journal.pone.0222639.

Baqasi, L. A. et al. (2018). Effects of low concentrations of ozone (O3) on metabolic and physiological attributes in wheat (Triticum aestivum L.) pants. *Biomedical and Pharmacology Journal*, 11 (2), pp.929–934. [Online]. Available at: doi:10.13005/bpj/1450.

Barillot, R., Chambon, C. and Andrieu, B. (2016a). CN-Wheat, a functional-structural model of carbon and nitrogen metabolism in wheat culms after anthesis. I. Model description. *Annals of Botany*, 118 (5), pp.997–1013. [Online]. Available at: doi:10.1093/aob/mcw143.

Barillot, R., Chambon, C. and Andrieu, B. (2016b). CN-Wheat, a functional-structural model of carbon and nitrogen metabolism in wheat culms after anthesis. II. Model evaluation. *Annals of Botany*, 118 (5), pp.1015–1031. [Online]. Available at: doi:10.1093/aob/mcw144.

Barraclough, P. B., Lopez-Bellido, R. and Hawkesford, M. J. (2014). Genotypic variation in the uptake, partitioning and

remobilisation of nitrogen during grain-filling in wheat. *Field Crops Research*, 156, pp.242–248. [Online]. Available at: doi:10.1016/j.fcr.2013.10.004.
Barutcular, C. et al. (2016). Quality traits performance of bread wheat genotypes under drought and heat stress conditions. *Fresenius Environmental Bulletin*, 25 (12), pp.6159–6165.
Bazargani, M. M. et al. (2011). A proteomics view on the role of drought-induced senescence and oxidative stress defense in enhanced stem reserves remobilization in wheat. *Journal of Proteomics*, 74 (10), pp.1959–1973. [Online]. Available at: doi:10.1016/j.jprot.2011.05.015.
Bellini, E. and De Tullio, M. C. (2019). Ascorbic acid and ozone: Novel perspectives to explain an elusive relationship. *Plants*, 8 (5), pp.1–12. [Online]. Available at: doi:10.3390/plants8050122.
Bertheloot, J. et al. (2008). A process-based model to simulate nitrogen distribution in wheat (Triticum aestivum) during grain-filling. *Functional Plant Biology*, 35 (10), pp.781–796. [Online]. Available at: doi:10.1071/FP08064.
Bertheloot, J., Martre, P. and Andrieu, B. (2008). Dynamics of light and nitrogen distribution during grain filling within wheat canopy. *Plant Physiology*, 148 (3), pp.1707–1720. [Online]. Available at: doi:10.1104/pp.108.124156.
Best, M. J. et al. (2011). The Joint UK Land Environment Simulator (JULES), model description – Part 1: Energy and water fluxes. *Geoscientific Model Development*, 4 (3), pp.677–699. [Online]. Available at: doi:10.5194/gmd-4-677-2011.
BHU Department of Geophysics. (2009). *Placement Brochure: Department of Geophysics, Banaras Hindu University, Varanasi, India*. Varanasi, India.
Bielenberg, D. G., Lynch, J. P. and Pell, E. J. (2002). Nitrogen dynamics during O3-induced accelerated senescence in hybrid poplar. *Plant, Cell and Environment*, 25 (4), pp.501–512. [Online]. Available at: doi:10.1046/j.1365-3040.2002.00828.x.
El Bilali, H. et al. (2019). Food and nutrition security and sustainability transitions in food systems. *Food and Energy Security*, 8 (2), pp.1–20. [Online]. Available at: doi:10.1002/fes3.154.
Bland, S. (2024a). *SEI-DO3SE/pyDO3SE-open: V4.39.11 (v4.39.11)*. Zenodo. [Online]. Available at: doi:10.5281/zenodo.11620482.
Bland, S. (2024b). *SEI-DO3SE/pyDO3SE-open: V4.39.16 (v4.39.16)*. Zenodo. [Online]. Available at: doi:10.5281/zenodo.11620501.
Von Bloh, W. et al. (2018). Implementing the nitrogen cycle into the dynamic global vegetation, hydrology, and crop growth model LPJmL (version 5.0). *Geoscientific Model Development*, 11 (7), pp.2789–2812. [Online]. Available at: doi:10.5194/gmd-11-2789-2018.
Bloom, A. J. et al. (2010). Carbon Dioxide Enrichment Inhibits Nitrate Assimilation in Wheat and Arabidopsis. *Science*, 328 (May), pp.899–904.
Bloom, A. J. (2015). Photorespiration and nitrate assimilation: A major intersection between plant carbon and nitrogen. *Photosynthesis Research*, 123, pp.117–128. [Online]. Available at: doi:10.1007/s11120-014-0056-y.
Bogard, M. et al. (2011). Anthesis date mainly explained correlations between post-anthesis leaf senescence, grain yield, and grain protein concentration in a winter wheat population segregating for flowering time QTLs. *Journal of Experimental Botany*, 62 (10), pp.3621–3636. [Online]. Available at: doi:10.1093/jxb/err061.
Bota, J., Medrano, H. and Flexas, J. (2004). Is photosynthesis limited by decreased Rubisco activity and RuBP content under progressive water stress? *New Phytologist*, 162 (3), pp.671–681. [Online]. Available at: doi:10.1111/j.1469-8137.2004.01056.x.
Brestenský, M. et al. (2019). Dietary Requirements for Proteins and Amino Acids in Human Nutrition. *Current Nutrition & Food Science*, 15, pp.638–645. [Online]. Available at: doi:10.2174/1573401314666180507123506.
Brewster, C. (2023). *Ground level ozone and wheat: an exploration of effects on yield, interactions with nitrogen, and potential sources of sensitivity and tolerance*. [Online]. Available at: https://research.bangor.ac.uk/portal/en/theses/ground-level-ozone-and-wheat-an-exploration-of-effects-on-yield-interactions-with-nitrogen-and-potential-sources-of-sensitivity-and-tolerance(88cc93b5-e504-4006-a0a9-69613e730e8c).html.
Brewster, C., Fenner, N. and Hayes, F. (2024). Chronic ozone exposure affects nitrogen remobilization in wheat at key growth stages. *Science of the Total Environment*, 908 (168288). [Online]. Available at: doi:10.1016/j.scitotenv.2023.168288.
Briend, A., Khara, T. and Dolan, C. (2015). Wasting and stunting-similarities and differences: Policy and programmatic implications. *Food and Nutrition Bulletin*, 36 (1), pp.S15–S23. [Online]. Available at: doi:10.1177/15648265150361S103.
Brisson, N. et al. (1998). STICS: A generic model for the simulation of crops and their water and nitrogen balances. I. Theory and parameterization applied to wheat and corn. *Agronomie*, 18 (5–6), pp.311–346. [Online]. Available at: doi:10.1051/agro:19980501.
Brisson, N. et al. (2003). An overview of the crop model STICS. *European Journal of Agronomy*, 18 (3–4), pp.309–332. [Online]. Available at: doi:10.1016/S1161-0301(02)00110-7.
Broberg, M. C. et al. (2015). Ozone effects on wheat grain quality - A summary. *Environmental Pollution*, 197, pp.203–213. [Online]. Available at: doi:10.1016/j.envpol.2014.12.009.
Broberg, M. C. et al. (2017). Fertilizer efficiency in wheat is reduced by ozone pollution. *Science of the Total*

Environment, 607–608, pp.876–880. [Online]. Available at: doi:10.1016/j.scitotenv.2017.07.069.
Broberg, M. C. et al. (2019). Effects of elevated CO2 on wheat yield: Non-linear response and relation to site productivity. *Agronomy*, 9 (5), pp.1–18. [Online]. Available at: doi:10.3390/agronomy9050243.
Broberg, M. C. et al. (2021). Harvest index and remobilization of 13 elements during wheat grain filling: Experiences from ozone experiments in China and Sweden. *Field Crops Research*, 271 (July). [Online]. Available at: doi:10.1016/j.fcr.2021.108259.
Broberg, M. C. et al. (2023). Effects of ozone, drought and heat stress on wheat yield and grain quality. *Agriculture, Ecosystems and Environment*, 352 (December 2022). [Online]. Available at: doi:10.1016/j.agee.2023.108505.
Broberg, M. C., Daun, S. and Pleijel, H. (2020). Ozone induced loss of seed protein accumulation is larger in soybean than in wheat and rice. *Agronomy*, 10 (3). [Online]. Available at: doi:10.3390/agronomy10030357.
Broberg, M. C., Högy, P. and Pleijel, H. (2017). CO2-induced changes in wheat grain composition: Meta-analysis and response functions. *Agronomy*, 7 (2), pp.1–18. [Online]. Available at: doi:10.3390/agronomy7020032.
Büker, P. et al. (2012). DO3SE modelling of soil moisture to determine ozone flux to forest trees. *Atmospheric Chemistry and Physics*, 12 (12), pp.5537–5562. [Online]. Available at: doi:10.5194/acp-12-5537-2012.
Bunce, J. A. (2000). Responses of stomatal conductance to light, humidity and temperature in winter wheat and barley grown at three concentrations of carbon dioxide in the field. *Global Change Biology*, 6 (4), pp.371–382. [Online]. Available at: doi:10.1046/j.1365-2486.2000.00314.x.
Campbell, G. S. and Norman, J. M. (1998). *An introduction to environmental biophysics*. 2nd ed. Springer.
Cariboni, J. et al. (2007). The role of sensitivity analysis in ecological modelling. *Ecological Modelling*, 203 (1–2), pp.167–182. [Online]. Available at: doi:10.1016/j.ecolmodel.2005.10.045.
Cavero, J. et al. (1998). Application of epic model to nitrogen cycling in irrigated processing tomatoes under different management systems. *Agricultural Systems*, 56 (4), pp.391–414. [Online]. Available at: doi:10.1016/S0308-521X(96)00100-X.
Chafe, Z. and Chowdhury, S. (2021). A deadly double dose for India's poor. *Nature Sustainability*, 4 (10), pp.835–836. [Online]. Available at: doi:10.1038/s41893-021-00752-0.
Chakrabarti, S. et al. (2019). India's integrated child development services programme; equity and extent of coverage in 2006 and 2016. *Bulletin of the World Health Organization*, 97 (4), pp.270–282. [Online]. Available at: doi:10.2471/BLT.18.221135.
Challinor, A. J. et al. (2018). Improving the use of crop models for risk assessment and climate change adaptation. *Agricultural Systems*, 159 (June 2017), pp.296–306. [Online]. Available at: doi:10.1016/j.agsy.2017.07.010.
Challinor, A. J., Parkes, B. and Ramirez-Villegas, J. (2015). Crop yield response to climate change varies with cropping intensity. *Global Change Biology*, 21 (4), pp.1679–1688. [Online]. Available at: doi:10.1111/gcb.12808.
Chang-Espino, M. et al. (2021). The effect of increased ozone levels on the stable carbon and nitrogen isotopic signature of wheat cultivars and landraces. *Atmosphere*, 12 (7), pp.1–25. [Online]. Available at: doi:10.3390/atmos12070883.
Chang-Espino, M. C. et al. (2024). Science of the Total Environment Nitrogen modulates the ozone response of Mediterranean wheat : Considerations for ozone risk assessment. *Science of the Total Environment*, 951. [Online]. Available at: doi:10.1016/j.scitotenv.2024.175718.
Chenu, K. et al. (2017). Contribution of Crop Models to Adaptation in Wheat. *Trends in Plant Science*, 22 (6), pp.472–490. [Online]. Available at: doi:10.1016/j.tplants.2017.02.003.
Chhabra, A. et al. (2019). Monitoring of Active Fire Events Due To Paddy Residue Burning in Indo-Gangetic Plains Using Thermal Remote Sensing. *The International Archives of the Photogrammetry, Remote Sensing and Spatial Information Sciences*, XLII-3/W6, pp.649–657. [Online]. Available at: doi:10.5194/isprs-archives-xlii-3-w6-649-2019.
Chhetri, N. and Chaudhary, P. (2011). Green Revolution: Pathways to food security in an era of climate variability and change? *Journal of Disaster Research*, 6 (5), pp.486–497. [Online]. Available at: doi:10.20965/jdr.2011.p0486.
Cho, K. et al. (2011). *Tropospheric ozone and plants: Absorption, responses, and consequences*. [Online]. Available at: doi:10.1007/978-1-4419-8453-1_3.
Chowdhury, S. et al. (2019). *The Contribution of Household Fuels to Ambient Air Pollution in India - A Comparison of Recent Estimates*. New Delhi.
Chudasama, R. K. et al. (2016). Evaluation of integrated Child Development Services program in Gujarat, India for the years 2012 to 2015. *Indian journal of public health*, 60 (2), pp.124–130. [Online]. Available at: doi:10.4103/0019-557X.184544.
Clark, D. B. et al. (2011). The Joint UK Land Environment Simulator (JULES), model description – Part 2: Carbon fluxes and vegetation dynamics. *Geoscientific Model Development*, 4 (3), pp.701–722. [Online]. Available at: doi:10.5194/gmd-4-701-2011.
CLRTAP. (2017). Chapter 3: Mapping critical levels for vegetation. In: *Manual on methodologies and criteria for modelling and mapping critical loads and levels and air pollution effects, risks and trends*. [Online]. Available at: https://unece.org/fileadmin/DAM/env/documents/2017/AIR/EMEP/Final__new_Chapter_3_v2__August_2017_.pdf.
CLRTAP. (2018). Supplementary material for Mapping critical levels for vegetation. *Manual on Methodologies and Criteria for Modelling and Mapping Critical Loads and Levels and Air Pollution Effects, Risks and Trends*. [Online]. Available at: https://icpvegetation.ceh.ac.uk/sites/default/files/ScientificBackgroundDocumentAOct2018.pdf.

Cohen, I. et al. (2021). Meta-analysis of drought and heat stress combination impact on crop yield and yield components. *Physiologia Plantarum*, 171 (1), pp.66–76. [Online]. Available at: doi:10.1111/ppl.13203.
Cook, J. (2024). *JoCook1997/DO3SE-CropN: Initial release (v2.0)*. Zenodo. [Online]. Available at: doi:10.5281/zenodo.13771475.
Cook, J. et al. (2024). New ozone-nitrogen model shows early senescence onset is the primary cause of ozone-induced reduction in grain quality of wheat. *EGUSphere [preprint]*, (May), pp.1–43. [Online]. Available at: doi:10.5194/egusphere-2024-1311.
Cooper, O. R. et al. (2014). Tropospheric Ozone Assessment Report: Global distribution and trends of tropospheric ozone: An observation-based review. *Elementa: Science of the Anthropocene*, 2, pp.1–28. [Online]. Available at: doi:10.12952/journal.elementa.000029.
Corbellini, M. et al. (1997). Effect of the Duration and Intensity of Heat Shock During Grain Filling on Dry Matter and Protein Accumulation, Technological Quality and Protein Composition in Bread and Durum Wheat. *Australian Journal of Plant Physiology*, 24.
Dai, A. (2006). Recent climatology, variability, and trends in global surface humidity. *Journal of Climate*, 19 (15), pp.3589–3606. [Online]. Available at: doi:10.1175/JCLI3816.1.
Dai, L. et al. (2019). Nitrogen availability does not affect ozone flux-effect relationships for biomass in birch (Betula pendula) saplings. *Science of the Total Environment*, 660, pp.1038–1046. [Online]. Available at: doi:10.1016/j.scitotenv.2019.01.092.
DEFRA et al. (2018). *UKCP18 Guidance: Representative Concentration Pathways*. [Online]. Available at: https://www.metoffice.gov.uk/binaries/content/assets/metofficegovuk/pdf/research/ukcp/ukcp18-guidance---representative-concentration-pathways.pdf.
Demirevska-Kepova, K. et al. (2005). Heat stress effects on ribulose-1,5-bisphosphate carboxylase/oxygenase, Rubisco binding protein and Rubisco activase in wheat leaves. *Biologia Plantarum*, 49 (4), pp.521–525. [Online]. Available at: doi:10.1007/s10535-005-0045-2.
Deodhar, S. Y. et al. (2010). An evaluation of mid day meal scheme. *Journal of Indian School of Political Economy*, 22 (1–4), pp.33–48. [Online]. Available at: http://www.iimahd.ernet.in/~satish/MDMJISPEPaper(2).pdf.
Desmos. (2023). *Desmos calculator*. [Online]. Available at: https://www.desmos.com/calculator [Accessed 1 January 2023].
Development Initiatives. (2020a). *2020 Global nutrition report: action on equity to end malnutrition*. Bristol, UK.
Development Initiatives. (2020b). *Global Nutrition Report | Country Nutrition Profiles - Global Nutrition Report*. [Online]. Available at: https://globalnutritionreport.org/resources/nutrition-profiles/asia/southern-asia/india/.
Van Dingenen, R. et al. (2009). The global impact of ozone on agricultural crop yields under current and future air quality legislation. *Atmospheric Environment*, 43 (3), pp.604–618. [Online]. Available at: doi:10.1016/j.atmosenv.2008.10.033.
Droutsas, I. (2020). *How do climate, ozone and crops interact to impact on health and nutrition?* University of Leeds.
Duncan, B. N. et al. (2015). A space-based, high-resolution view of notable changes in urban NOx pollution around the world (2005–2014). *Journal of Geophysical Research: Atmospheres*, 121. [Online]. Available at: doi:10.1002/2014JC010485.Received.
Ebi, K. L. et al. (2021). Nutritional quality of crops in a high CO2 world: an agenda for research and technology development. *Environmental Research Letters*, 16 (6), p.064045. [Online]. Available at: doi:10.1088/1748-9326/abfcfa.
Elango, R., Ball, R. O. and Pencharz, P. B. (2008). Indicator amino acid oxidation: Concept and application. *Journal of Nutrition*, 138 (2), pp.243–246. [Online]. Available at: doi:10.1093/jn/138.2.243.
Elshorbany, Y. et al. (2024). Tropospheric Ozone Precursors: Global and Regional Distributions. *[preprint]*, pp.1–57. [Online]. Available at: doi:10.5194/egusphere-2024-720.
Emberson, L. et al. *Simulating the impacts of ground level ozone (O3) on wheat productivity by AgMIP-O3 crop models at sites across the Northern Hemisphere*.
Emberson, L. (2020). Effects of ozone on agriculture, forests and grasslands: Improving risk assessment methods for O3. *Philosophical Transactions of the Royal Society A: Mathematical, Physical and Engineering Sciences*, 378 (2183). [Online]. Available at: doi:10.1098/rsta.2019.0327.
Emberson, L. et al. (2021). *Methodology for gap-filling and standardisation of data for AgMIP Ozone V8*. [Online]. Available at: https://agmipdatahub.files.wordpress.com/2021/10/agmip-gap-filling-protocol_-v8.docx.pdf [Accessed 17 April 2024].
Emberson, L. D. et al. (2000a). Modelling stomatal ozone flux across Europe. *Environmental Pollution*, 109 (3), pp.403–413. [Online]. Available at: doi:10.1016/S0269-7491(00)00043-9.
Emberson, L. D. et al. (2000b). Modelling stomatal ozone flux across Europe. *Environmental Pollution*, 109 (3), pp.403–413.
Emberson, L. D. et al. (2009). A comparison of North American and Asian exposure-response data for ozone effects on crop yields. *Atmospheric Environment*, 43 (12), pp.1945–1953. [Online]. Available at: doi:10.1016/j.atmosenv.2009.01.005.
Emberson, L. D. et al. (2018). Ozone effects on crops and consideration in crop models. *European Journal of*

Agronomy, 100 (June), pp.19–34. [Online]. Available at: doi:10.1016/j.eja.2018.06.002.
Emmerichs, T. et al. *Comparison of existing stomatal ozone flux models: sensitivity to land cover parameterisations and key input variables*.
Ewert, F. and Pleijel, H. (1999). Phenological development, leaf emergence, tillering and leaf area index, and duration of spring wheat across Europe in response to CO2 and ozone. *European Journal of Agronomy*, 10 (3–4), pp.171–184. [Online]. Available at: doi:10.1016/S1161-0301(99)00008-8.
Ewert, F. and Porter, J. R. (2000). Ozone effects on wheat in relation to CO2: Modelling short-term and long-term responses of leaf photosynthesis and leaf duration. *Global Change Biology*, 6 (7), pp.735–750. [Online]. Available at: doi:10.1046/j.1365-2486.2000.00351.x.
Faisal, S. et al. (2017). Morpho-physiological assessment of wheat (Triticum aestivum L.) genotypes for drought stress tolerance at seedling stage. *Pakistan Journal of Botany*, 49 (2), pp.445–452.
Fanzo, J. (2018). The role of farming and rural development as central to our diets. *Physiology and Behavior*, 193 (January), pp.291–297. [Online]. Available at: doi:10.1016/j.physbeh.2018.05.014.
FAO. (2013). *Dietary protein quality evaluation in human nutrition: Report of an FAO Expert Consultation*. Rome.
FAO. (2017). *The future of food and agriculture: trends and challenges*. Rome. [Online]. Available at: https://www.fao.org/policy-support/tools-and-publications/resources-details/en/c/472484/.
FAO et al. (2020). *The State of Food Security and Nutrition in the World 2020. Transforming food systems for affordable healthy diets*. Rome: FAO. [Online]. Available at: https://www.fao.org/policy-support/tools-and-publications/resources-details/en/c/1298217/.
FAO et al. (2023). *The state of food security and nutrition in the world*. [Online]. Available at: doi:10.1016/S2213-8587(22)00220-0.
Farooq, M. et al. (2011). Heat stress in wheat during reproductive and grain-filling phases. *Critical Reviews in Plant Sciences*, 30 (6), pp.491–507. [Online]. Available at: doi:10.1080/07352689.2011.615687.
Farquhar, G. D., Caemmerer, S. and Berry, J. A. (1980). A biochemical model of photosynthetic CO2 assimilation in leaves of C3 species. *Planta*, 149 (1), pp.78-90–90. [Online]. Available at: doi:10.1007/BF00386231.
Fatima, A. et al. (2018). Variability in defence mechanism operating in three wheat cultivars having different levels of sensitivity against elevated ozone. *Environmental and Experimental Botany*, 155 (June), pp.66–78. [Online]. Available at: doi:10.1016/j.envexpbot.2018.06.015.
Fatima, A. et al. (2019). Ascorbic acid and thiols as potential biomarkers of ozone tolerance in tropical wheat cultivars. *Ecotoxicology and Environmental Safety*, 171 (January), pp.701–708. [Online]. Available at: doi:10.1016/j.ecoenv.2019.01.030.
Feller, U. and Fischer, A. (1994). Nitrogen metabolism in senescing leaves. *Critical Reviews in Plant Sciences*, 13 (3), pp.241–273. [Online]. Available at: doi:10.1080/07352689409701916.
Feng, Z. et al. (2011). Differential responses in two varieties of winter wheat to elevated ozone concentration under fully open-air field conditions. *Global Change Biology*, 17 (1), pp.580–591. [Online]. Available at: doi:10.1111/j.1365-2486.2010.02184.x.
Feng, Z. et al. (2016). Differential effects of ozone on photosynthesis of winter wheat among cultivars depend on antioxidative enzymes rather than stomatal conductance. *Science of the Total Environment*, 572, pp.404–411. [Online]. Available at: doi:10.1016/j.scitotenv.2016.08.083.
Feng, Z. et al. (2018). Comparison of crop yield sensitivity to ozone between open-top chamber and free-air experiments. *Global Change Biology*, 24 (6), pp.2231–2238. [Online]. Available at: doi:10.1111/gcb.14077.
Feng, Z. and Kobayashi, K. (2009). Assessing the impacts of current and future concentrations of surface ozone on crop yield with meta-analysis. *Atmospheric Environment*, 43 (8), pp.1510–1519. [Online]. Available at: doi:10.1016/j.atmosenv.2008.11.033.
Feng, Z., Kobayashi, K. and Ainsworth, E. A. (2008). Impact of elevated ozone concentration on growth, physiology, and yield of wheat (Triticum aestivum L.): A meta-analysis. *Global Change Biology*, 14 (11), pp.2696–2708. [Online]. Available at: doi:10.1111/j.1365-2486.2008.01673.x.
Fischer, T. (2019). Wheat yield losses in India due to ozone and aerosol pollution and their alleviation: A critical review. *Outlook on Agriculture*, 48 (3), pp.181–189. [Online]. Available at: doi:10.1177/0030727019868484.
Fowler, D. et al. (2008). *Ground-level ozone in the 21st century: future trends, impacts and policy implications*. (October). [Online]. Available at: https://royalsociety.org/news-resources/publications/2008/ground-level-ozone/.
Fu, T. M. and Tian, H. (2019). Climate Change Penalty to Ozone Air Quality: Review of Current Understandings and Knowledge Gaps. *Current Pollution Reports*, 5 (3), pp.159–171. [Online]. Available at: doi:10.1007/s40726-019-00115-6.
Fuhrer, J. et al. (1990). Effects of ozone on the grain composition of spring wheat grown in open-top field chambers. *Environmental Pollution*, 65 (2), pp.181–192. [Online]. Available at: doi:10.1016/0269-7491(90)90183-D.
Fuhrer, J., Skärby, L. and Ashmore, M. R. (1997). Critical levels for ozone effects on vegetation in Europe. *Environmental Pollution*, 97 (1–2), pp.91–106. [Online]. Available at: doi:10.1016/S0269-7491(97)00067-5.
G A, N. et al. (2024). Unraveling the effect of drought and heat stresses on grain quality of wheat (Triticum aestivum). *The Indian Journal of Agricultural Sciences*, 94 (5), pp.489–494. [Online]. Available at: doi:10.56093/ijas.v94i5.142783.

Gaju, O. et al. (2014). Nitrogen partitioning and remobilization in relation to leaf senescence, grain yield and grain nitrogen concentration in wheat cultivars. *Field Crops Research*, 155, pp.213–223. [Online]. Available at: doi:10.1016/j.fcr.2013.09.003.
Galmés, J. et al. (2013). Variation in Rubisco content and activity under variable climatic factors. *Photosynthesis Research*, 117 (1–3), pp.73–90. [Online]. Available at: doi:10.1007/s11120-013-9861-y.
Gandin, A., Dizengremel, P. and Jolivet, Y. (2021). Integrative role of plant mitochondria facing oxidative stress: The case of ozone. *Plant Physiology and Biochemistry*, 159 (December 2020), pp.202–210. [Online]. Available at: doi:10.1016/j.plaphy.2020.12.019.
Gao, M. et al. (2018). Photosynthetic and antioxidant response of wheat to di(2-ethylhexyl) phthalate (DEHP) contamination in the soil. *Chemosphere*, 209, pp.258–267. [Online]. Available at: doi:10.1016/j.chemosphere.2018.06.090.
Gelang, J. et al. (2000). Rate and duration of grain filling in relation to flag leaf senescence and grain yield in spring wheat (Triticum aestivum) exposed to different concentrations of ozone. *Physiologia Plantarum*, 110 (3), pp.366–375. [Online]. Available at: doi:10.1111/j.1399-3054.2000.1100311.x.
Ghude, S. D. et al. (2014). Reductions in India's crop yield due to ozone. *Geophysical Research Letters*, 41 (15), pp.5685–5691. [Online]. Available at: doi:10.1002/2014GL060930.
Gill, S. S. and Tuteja, N. (2010). Reactive oxygen species and antioxidant machinery in abiotic stress tolerance in crop plants. *Plant Physiology and Biochemistry*, 48 (12), pp.909–930. [Online]. Available at: doi:10.1016/j.plaphy.2010.08.016.
Godwin, D. C. and Allan Jones, C. (1991). Nitrogen Dynamics in Soil-Plant Systems. In: Hanks, J. and Ritchie, J. T. (Eds). *Modeling plant and soil systems*. pp.287–321. [Online]. Available at: doi:10.2134/agronmonogr31.c13.
Gonmei, Z. and Toteja, G. S. (2018). Micronutrient status of Indian population. *Indian Journal of Medical Research*, 148 (5), pp.511–521. [Online]. Available at: doi:10.4103/ijmr.IJMR_1768_18.
Govardhan, G., Nanjundiah, R. S. and Satheesh, S. K. (2015). Performance of WRF-Chem over Indian region. *Journal of Earth System Science*, 124 (4), pp.875–896.
Grant, R. F. (1998). Simulation in ecosys of root growth response to contrasting soil water and nitrogen. *Ecological Modelling*, 107 (2–3), pp.237–264. [Online]. Available at: doi:10.1016/S0304-3800(97)00221-4.
Griffiths, P. T. et al. (2021). Tropospheric ozone in CMIP6 simulations. *Atmospheric Chemistry and Physics*, 21 (5), pp.4187–4218. [Online]. Available at: doi:10.5194/acp-21-4187-2021.
Groot, J. J. R. (1987). *Simulation of nitrogen balance in a system of winter wheat and soil*. [Online]. Available at: https://research.wur.nl/en/publications/simulation-of-nitrogen-balance-in-a-system-of-winter-wheat-and-so.
Grünhage, L. et al. (2012). Updated stomatal flux and flux-effect models for wheat for quantifying effects of ozone on grain yield, grain mass and protein yield. *Environmental Pollution*, 165, pp.147–157. [Online]. Available at: doi:10.1016/j.envpol.2012.02.026.
Guarin, J. R. et al. (2019a). Impacts of tropospheric ozone and climate change on Mexico wheat production. *Climatic Change*, 155 (2), pp.157–174. [Online]. Available at: doi:10.1007/s10584-019-02451-4.
Guarin, J. R. et al. (2019b). Modeling the effects of tropospheric ozone on wheat growth and yield. *European Journal of Agronomy*, 105 (February), pp.13–23. [Online]. Available at: doi:10.1016/j.eja.2019.02.004.
Guarin, J. R. et al. (2024). Modeling the effects of tropospheric ozone on the growth and yield of global staple crops with DSSAT v4.8.0. *Geoscientific Model Development*, 17 (7), pp.2547–2567. [Online]. Available at: doi:10.5194/gmd-17-2547-2024.
Guo, J. et al. (2021). Proteomics reveals the effects of drought stress on the kernel development and starch formation of waxy maize. *BMC Plant Biology*, 21 (1), pp.1–14. [Online]. Available at: doi:10.1186/s12870-021-03214-z.
Hansen, J. W. and Jones, J. W. (2000). Short Survey: Scaling-up crop models for climate variability. *Agricultural Systems*, 65 (1), pp.43–72.
Hansen, S. et al. (1991). Simulation of nitrogen dynamics and biomass production in winter wheat using the Danish simulation model DAISY. *Fertilizer Research*, 27 (2–3), pp.245–259. [Online]. Available at: doi:10.1007/BF01051131.
Harper, L. A. et al. (1987). Nitrogen Cycling in a Wheat Crop: Soil, Plant, and Aerial Nitrogen Transport. *Agronomy Journal*, 79 (6), pp.965–973. [Online]. Available at: doi:10.2134/agronj1987.00021962007900060004x.
Havé, M. et al. (2017). Nitrogen remobilization during leaf senescence: Lessons from Arabidopsis to crops. *Journal of Experimental Botany*, 68 (10), pp.2513–2529. [Online]. Available at: doi:10.1093/jxb/erw365.
He, D. et al. (2017). Data requirement for effective calibration of process-based crop models. *Agricultural and Forest Meteorology*, 234–235, pp.136–148. [Online]. Available at: doi:10.1016/j.agrformet.2016.12.015.
Held, A. A., Mooney, H. A. and Gorham, J. N. (1991). Acclimation to ozone stress in radish: leaf demography and photosynthesis. *New Phytologist*, 118 (3), pp.417–423. [Online]. Available at: doi:10.1111/j.1469-8137.1991.tb00023.x.
Herforth, A. et al. (2020). Cost and affordability of nutritious diets across and within countries. *Background paper for The State of Food Security and Nutrition in the World.*, Rome.
Herman, J. and Usher, W. (2019). *SALib Documentation*. [Online]. Available at: https://salib.readthedocs.io/_/downloads/en/latest/pdf/.

Hogsett, W. E., Tingey, D. T. and Lee, E. H. (1988). Ozone exposure indices: concepts for development and evaluation of their use. In: Heck, W. W., Taylor, O. C. and TIngey, D. T. (Eds). *Assessment of crop loss from air pollutants*. Elsevier Ltd. pp.107–140.

Hoshika, Y. et al. (2020). Flux-based ozone risk assessment for a plant injury index (pii) in three european cool-temperate deciduous tree species. *Forests*, 11 (1), pp.1–12. [Online]. Available at: doi:10.3390/f11010082.

Hunt, L. A. and Pararaiasingham, S. (1995). CROPSIM — WHEAT: A model describing the growth and development of wheat. *Canadian Journal of Plant Science*, 75 (3), pp.619–632.

ICP Vegetation. (2014). *Examples of ozone damage in crops*.

Jacob, D. J. and Winner, D. A. (2009). Effect of climate change on air quality. *Atmospheric Environment*, 43 (1), pp.51–63. [Online]. Available at: doi:10.1016/j.atmosenv.2008.09.051.

Jain, A. et al. (2023). Food deprivation among adults in India: an analysis of specific food categories, 2016–2021. *eClinicalMedicine*, 66, p.102313. [Online]. Available at: doi:10.1016/j.eclinm.2023.102313.

Jain, M. (2015). India's struggle against malnutrition-is the ICDS program the answer? *World Development*, 67, pp.72–89. [Online]. Available at: doi:10.1016/j.worlddev.2014.10.006.

Janardanan, R. et al. (2024). Country-level methane emissions and their sectoral trends during 2009-2020 estimated by high-resolution inversion of GOSAT and surface observations. *Environmental Research Letters*, 19 (3). [Online]. Available at: doi:10.1088/1748-9326/ad2436.

Jerez, S. et al. (2020). On the Spin-Up Period in WRF Simulations Over Europe: Trade-Offs Between Length and Seasonality. *Journal of Advances in Modeling Earth Systems*, 12 (4), pp.1–18. [Online]. Available at: doi:10.1029/2019MS001945.

Jones, D. B. (1941). Factors for converting percentages of nitrogen in foods and feeds into percentages of proteins. *United States Department of Agriculture*, Washington, D.C.

Kamal, N. M. et al. (2019). Stay-green trait: A prospective approach for yield potential, and drought and heat stress adaptation in globally important cereals. *International Journal of Molecular Sciences*, 20 (23). [Online]. Available at: doi:10.3390/ijms20235837.

Kamali, R. (2014). *Untouchable food for untouchable women: The inclusion and exclusion of women and their children in the public distribution system and the mid-day meal scheme in Block Jaisinagar, Madhya Pradesh, India*.

Kang, H. et al. (2021). Elevated CO2 Enhances Dynamic Photosynthesis in Rice and Wheat. *Frontiers in Plant Science*, 12 (October). [Online]. Available at: doi:10.3389/fpls.2021.727374.

Kang, J. et al. (2023). Physiological mechanisms underlying reduced photosynthesis in wheat leaves grown in the field under conditions of nitrogen and water deficiency. *Crop Journal*, 11 (2), pp.638–650. [Online]. Available at: doi:10.1016/j.cj.2022.06.010.

Kangasjärvi, J., Jaspers, P. and Kollist, H. (2005). Signalling and cell death in ozone-exposed plants. *Plant, Cell and Environment*, 28 (8), pp.1021–1036. [Online]. Available at: doi:10.1111/j.1365-3040.2005.01325.x.

Kaur, R. and Kapoor, N. (2021). Role of Amino Acids other than Proline in Abiotic Stress Amelioration in Plants. *Journal of University of Shanghai for Science and Technology*, 23 (2), pp.271–291. [Online]. Available at: doi:10.51201/Jusst12616.

van Keulen, H. and Seligman, N. H. (1987). *Simulation of water use, nitrogen nutrition and growth of a spring wheat crop*. Wageningen: Pudoc. [Online]. Available at: doi:10.1017/S0021859600081582.

Khan, A. et al. (2021). Rising atmospheric temperature impact on wheat and thermotolerance strategies. *Plants*, 10 (1), pp.1–24. [Online]. Available at: doi:10.3390/plants10010043.

Khanna-Chopra, R. (2012). Leaf senescence and abiotic stresses share reactive oxygen species-mediated chloroplast degradation. *Protoplasma*, 249 (3), pp.469–481. [Online]. Available at: doi:10.1007/s00709-011-0308-z.

Khatkar, B. S., Chaudhary, N. and Dangi, P. (2015). *Production and Consumption of Grains: India*. 2nd ed. Elsevier Ltd. [Online]. Available at: doi:10.1016/B978-0-12-394437-5.00044-9.

Kobayashi, K. (2022). Effects of ozone on agricultural crops. In: *Handbook of air quality and climate change*. [Online]. Available at: doi:10.1007/978-4-431-56438-6_4.

Kong, L. et al. (2016). Remobilization of vegetative nitrogen to developing grain in wheat (Triticum aestivum L.). *Field Crops Research*, 196, pp.134–144. [Online]. Available at: doi:10.1016/j.fcr.2016.06.015.

Kropff, M. J. and Laar, H. H. van. (1993). *Modelling Crop-Weed Interactions*. Wallingford, UK: CAB International. [Online]. Available at: doi:10.23919/FRUCT.2017.8071355.

Kumar, K. S. K. and Parikh, J. (2001). Socio-economic Impacts of Climate Change on Indian Agriculture. *International Review for Environmental Strategies*, 2 (2), pp.277–293.

Kumar, R. et al. (2018). How Will Air Quality Change in South Asia by 2050? *Journal of Geophysical Research: Atmospheres*, 123 (3), pp.1840–1864. [Online]. Available at: doi:10.1002/2017JD027357.

Kurpad, A. V. and Thomas, T. (2020). Protein Quality and its Food Source in the Diets of Young Indian Children. *Journal of Nutrition*, 150 (6), Oxford University Press., pp.1350–1351. [Online]. Available at: doi:10.1093/jn/nxaa100.

Lægdsmand, M. (2011). *Crop Simulation Model*. [Online]. Available at: https://www.fasset.dk/Upload/Fasset/Document/Crop model.pdf.

Lal, M. K. et al. (2022). Physiological and molecular insights on wheat responses to heat stress. *Plant Cell Reports*, 41 (3), pp.501–518. [Online]. Available at: doi:10.1007/s00299-021-02784-4.

Lal, S. et al. (2017). Loss of crop yields in India due to surface ozone: an estimation based on a network of observations. *Environmental Science and Pollution Research*, 24 (26), pp.20972–20981. [Online]. Available at: doi:10.1007/s11356-017-9729-3.
Lawlor, D. W. (2002). Carbon and nitrogen assimilation in relation to yield: Mechanisms are the key to understanding production systems. *Journal of Experimental Botany*, 53 (370), pp.773–787. [Online]. Available at: doi:10.1093/jxb/53.370.773.
Leadley, P. W. and Drake, B. G. (1993). Open top chambers for exposing plant canopies to elevated CO2 concentration and for measuring net gas exchange. *Vegetatio*, 104/105, pp.3–15. [Online]. Available at: doi:10.1007/BF00048141.
Lefohn, A. S., Laurence, J. A. and Kohut, R. J. (1988). A comparison of indices that describe the relationship between exposure to ozone and reduction in the yield of agricultural crops. *Atmospheric Environment*, 22 (6), pp.1229–1240. [Online]. Available at: doi:10.1016/0004-6981(88)90353-8.
Leuning, R. (1995). A critical appraisal of combine stomatal model C3 plants. *Plant, Cell & Environment*, 18, pp.339–355. [Online]. Available at: http://www.unc.edu/courses/2010spring/geog/595/001/www/Leuning95b-PCE.pdf%0Apapers2://publication/uuid/B8B998AB-EB42-4E09-A609-B192084D13EE.
Li, F., Kang, S. and Zhang, J. (2004). Interactive effects of elevated CO2, nitrogen and drought on leaf area, stomatal conductance, and evapotranspiration of wheat. *Agricultural Water Management*, 67 (3), pp.221–233. [Online]. Available at: doi:10.1016/j.agwat.2004.01.005.
Li, G. et al. (2024). Amino acid metabolism response to post-anthesis drought stress during critical periods of elite wheat (Triticum aestivum L.) endosperm development. *Environmental and Experimental Botany*, 218 (November 2023). [Online]. Available at: doi:10.1016/j.envexpbot.2023.105577.
Li, H. et al. (2022a). *Climate-driven deterioration of future ozone pollution in Asia predicted by machine learning with multisource data*. 2019 (September), pp.1–40. [Online]. Available at: doi:10.5194/acp-23-1131-2023.
Li, J. et al. (2022b). Effects of light quality on growth, nutritional characteristics, and antioxidant properties of winter wheat seedlings (Triticum aestivum L.). *Frontiers in Plant Science*, 13 (September), pp.1–15. [Online]. Available at: doi:10.3389/fpls.2022.978468.
Liu, B. et al. (2019a). Global wheat production with 1.5 and 2.0°C above pre-industrial warming. *Global Change Biology*, 25 (4), pp.1428–1444. [Online]. Available at: doi:10.1111/gcb.14542.
Liu, J. et al. (2018). The effects of nitrogen and water stresses on the nitrogen-to-protein conversion factor of winter wheat. *Agricultural Water Management*, 210 (February), pp.217–223. [Online]. Available at: doi:10.1016/j.agwat.2018.07.042.
Liu, J. et al. (2019b). Modeling wheat nutritional quality with a modified CERES-wheat model. *European Journal of Agronomy*, 109 (September 2018), p.125901. [Online]. Available at: doi:10.1016/j.eja.2019.03.005.
Liu, Y. et al. (2020). Dynamic responses of accumulation and remobilization of water soluble carbohydrates in wheat stem to drought stress. *Plant Physiology and Biochemistry*, 155 (July), pp.262–270. [Online]. Available at: doi:10.1016/j.plaphy.2020.07.024.
Lobell, D. B., Sibley, A. and Ivan Ortiz-Monasterio, J. (2012). Extreme heat effects on wheat senescence in India. *Nature Climate Change*, 2 (3), pp.186–189. [Online]. Available at: doi:10.1038/nclimate1356.
Lu, X. et al. (2018). Lower tropospheric ozone over India and its linkage to the South Asian monsoon. *Atmospheric Chemistry and Physics*, 18 (5), pp.3101–3118. [Online]. Available at: doi:10.5194/acp-18-3101-2018.
Mariem, S. Ben et al. (2021). Climate Change, Crop Yields, and Grain Quality of C3 Cereals: A Meta-Analysis of [CO2], Temperature , and Drought Effects. *Plants*, 10 (6), pp.1–19. [Online]. Available at: doi:10.3390/plants10061052.
Mariotti, F., Tomé, D. and Mirand, P. P. (2008). Converting nitrogen into protein - Beyond 6.25 and Jones' factors. *Critical Reviews in Food Science and Nutrition*, 48 (2), pp.177–184. [Online]. Available at: doi:10.1080/10408390701279749.
Martre, P. et al. (2006). Modelling protein content and composition in relation to crop nitrogen dynamics for wheat. *European Journal of Agronomy*, 25 (2), pp.138–154. [Online]. Available at: doi:10.1016/j.eja.2006.04.007.
Martre, P. (2014). *Modelling Dry Matter and Nitrogen Accumulation and Vertical Distribution within Wheat Canopies in SiriusQuality2*.
Marzuoli, R. et al. (2024). Phytotoxic Ozone Dose – Response Relationships for Durum Wheat (Triticum durum, Desf.). *Plants*, 13 (5). [Online]. Available at: doi:10.3390/plants13050573.
McDuffie, E. E. et al. (2020). A global anthropogenic emission inventory of atmospheric pollutants from sector- And fuel-specific sources (1970-2017): An application of the Community Emissions Data System (CEDS). *Earth System Science Data*, 12 (4), pp.3413–3442. [Online]. Available at: doi:10.5194/essd-12-3413-2020.
McKee, I. F., Bullimore, J. F. and Long, S. P. (1997). Will elevated CO2 concentrations protect the yield of wheat from O3 damage? *Plant, Cell and Environment*, 20 (1), pp.77–84. [Online]. Available at: doi:10.1046/j.1365-3040.1997.d01-1.x.
Medek, D. E., Schwartz, J. and Myers, S. S. (2017). Estimated effects of future atmospheric co2 concentrations on protein intake and the risk of protein deficiency by country and region. *Environmental Health Perspectives*, 125 (8), pp.1–8. [Online]. Available at: doi:10.1289/EHP41.

Medlyn, B. E. et al. (2002). Temperature response of parameters of a biochemically based model of photosynthesis. II. A review of experimental data. *Plant, Cell and Environment*, 25 (9), pp.1167–1179. [Online]. Available at: doi:10.1046/j.1365-3040.2002.00891.x.
Meehl, G. A. et al. (2018). Future heat waves and surface ozone. *Environmental Research Letters*, 13 (6). [Online]. Available at: doi:10.1088/1748-9326/aabcdc.
Meybodi, N. M. et al. (2019). Wheat Bread: Potential Approach to Fortify its Lysine Content. *Current Nutrition & Food Science*, 15 (7). [Online]. Available at: doi:10.2174/1573401315666190228125241.
Mikkelsen, T. N. and Ro-Poulsen, H. (1994). Exposure of Norway spruce to ozone increases the sensitivity of current year needles to photoinhibition and desiccation. *New Phytologist*, 128 (1), pp.153–163. [Online]. Available at: doi:10.1111/j.1469-8137.1994.tb03998.x.
Mills, G. et al. (2007). A synthesis of AOT40-based response functions and critical levels of ozone for agricultural and horticultural crops. *Atmospheric Environment*, 41 (12), pp.2630–2643. [Online]. Available at: doi:10.1016/j.atmosenv.2006.11.016.
Mills, G. et al. (2011). New stomatal flux-based critical levels for ozone effects on vegetation. *Atmospheric Environment*, 45 (28), pp.5064–5068. [Online]. Available at: doi:10.1016/j.atmosenv.2011.06.009.
Mills, G. et al. (2018a). Closing the global ozone yield gap: Quantification and cobenefits for multistress tolerance. *Global Change Biology*, 24 (10), pp.4869–4893. [Online]. Available at: doi:10.1111/gcb.14381.
Mills, G. et al. (2018b). Ozone pollution will compromise efforts to increase global wheat production. *Global Change Biology*, 24 (8), pp.3560–3574. [Online]. Available at: doi:10.1111/gcb.14157.
Mills, G. et al. (2018c). Tropospheric Ozone Assessment Report: Present-day ozone distribution and trends relevant to human health. *Elementa: Science of the Anthropocene*, 6 (47). [Online]. Available at: doi:10.1525/elementa.302.
Ministry of Agriculture & Farmers Welfare. (2022). *Agricultural Statistics at a Glance 2021*. New Delhi.
Ministry of Agriculture & Farmers Welfare. (2023). Agricultural Statistics at a Glance 2022. *Department of Agriculture & Farmers Welfare Economics & Statistics Division*.
Ministry of Environment Forest & Climate Change. (2019). *NCAP: National Clean Air Programme*. New Delhi. [Online]. Available at: doi:10.1002/9783527678679.dg08246.
Ministry of Environment Forest & Climate Change. (2020). *National Ambient Air Quality Status & Trends 2019*. New Delhi.
Ministry of Statistics and Programme Information. (2012). *Household Consumption of Various Goods and Services in India: NSS 68th Round*. [Online]. Available at: http://mospi.nic.in/sites/default/files/publication_reports/Report_no558_rou68_30june14.pdf.
Minocha, S., Thomas, T. and Kurpad, A. V. (2017a). Dietary protein and the health-nutrition-agriculture connection in India. *Journal of Nutrition*, 147 (7), American Society for Nutrition., pp.1243–1250. [Online]. Available at: doi:10.3945/jn.116.243980.
Minocha, S., Thomas, T. and Kurpad, A. V. (2017b). Dietary protein and the health-nutrition-agriculture connection in India. *Journal of Nutrition*, 147 (7), pp.1243–1250. [Online]. Available at: doi:10.3945/jn.116.243980.
Mishra, A. K., Rai, R. and Agrawal, S. B. (2013). Individual and interactive effects of elevated carbon dioxide and ozone on tropical wheat (Triticum aestivum L.) cultivars with special emphasis on ROS generation and activation of antioxidant defence system. *Indian Journal of Biochemistry and Biophysics*, 50 (2), pp.139–149. [Online]. Available at: https://pubmed.ncbi.nlm.nih.gov/23720888/.
Moss, R. H. et al. (2010). The next generation of scenarios for climate change research and assessment. *Nature*, 463 (7282), pp.747–756. [Online]. Available at: doi:10.1038/nature08823.
Mukherjee, A. et al. (2021). Ozone a persistent challenge to food security in India: Current status and policy implications. *Current Opinion in Environmental Science and Health*, 19, p.100220. [Online]. Available at: doi:10.1016/j.coesh.2020.10.008.
Mulholland, B. J. et al. (1997). Effects of elevated carbon dioxide and ozone on the growth and yield of spring wheat (Triticum aestivum L.). *Journal of Experimental Bota*, 48 (306), pp.113–122.
Myers, S. S. et al. (2017). Climate Change and Global Food Systems: Potential Impacts on Food Security and Undernutrition. *Annual Review of Public Health*, 38, pp.259–277. [Online]. Available at: doi:10.1146/annurev-publhealth-031816-044356.
Naaz, S. et al. (2022). Bioclimatic modeling and FACE study forecast a bleak future for wheat production in India. *Environmental Monitoring and Assessment*, 195 (1). [Online]. Available at: doi:10.1007/s10661-022-10551-5.
Nagarajan, S. et al. (1999). Effect of Post-Anthesis Water Stress on Accumulation of Dry Matter, Carbon and Nitrogen and Their Partitioning in Wheat Varieties Differing in Drought Tolerance. *Journal of Agronomy & Crop Science*, 183, pp.129–136. [Online]. Available at: doi:10.1046/j.1439-037x.1999.00326.x.
Naidu, B. P. et al. (1991). Amino acid and glycine betaine accumulation in cold-stressed wheat seedlings. *Phytochemistry*, 30 (2), pp.407–409. [Online]. Available at: doi:10.1016/0031-9422(91)83693-F.
NASA. (2023). *Nasa Power Data*. [Online]. Available at: https://power.larc.nasa.gov/ [Accessed 21 November 2023].
NASA. (2024a). *Meteorological Data Assessment Process*. [Online]. Available at: https://power.larc.nasa.gov/docs/methodology/meteorology/assessment/#hourly-assessment [Accessed 19 September 2024].

NASA. (2024b). *Meteorological data overview*. [Online]. Available at: https://power.larc.nasa.gov/docs/methodology/meteorology/ [Accessed 19 September 2024].
NASA. (2024c). *NASA Power Data*. [Online]. Available at: https://power.larc.nasa.gov/ [Accessed 10 June 2024].
Nayyar, H. and Walia, D. P. (2003). Water stress induced proline accumulation in contrasting wheat genotypes as affected by calcium and abscisic acid. *Biologia Plantarum*, 46 (2), pp.275–279. [Online]. Available at: doi:10.1023/A:1022867030790.
Nehe, A. S. et al. (2020). Nitrogen partitioning and remobilization in relation to leaf senescence, grain yield and protein concentration in Indian wheat cultivars. *Field Crops Research*, 251 (November 2019), p.107778. [Online]. Available at: doi:10.1016/j.fcr.2020.107778.
Nguyen, T. H. et al. (2024). Assessing the spatio-temporal tropospheric ozone and drought impacts on leaf growth and grain yield of wheat across Europe through crop modeling and remote sensing data. *European Journal of Agronomy*, 153 (September 2023). [Online]. Available at: doi:10.1016/j.eja.2023.127052.
Nie, G. Y. et al. (1995). Effects of free-air CO2 enrichment on the development of the photosynthetic apparatus in wheat, as indicated by changes in leaf proteins. *Plant, Cell & Environment*, 18 (8), pp.855–864. [Online]. Available at: doi:10.1111/j.1365-3040.1995.tb00594.x.
O'Neill, B. C. et al. (2014). A new scenario framework for climate change research: The concept of shared socioeconomic pathways. *Climatic Change*, 122 (3), pp.387–400. [Online]. Available at: doi:10.1007/s10584-013-0905-2.
Osborne, S. et al. (2019). New insights into leaf physiological responses to ozone for use in crop modelling. *Plants*, 8 (4). [Online]. Available at: doi:10.3390/plants8040084.
Osborne, T. et al. (2015). JULES-crop: A parametrisation of crops in the Joint UK Land Environment Simulator. *Geoscientific Model Development*, 8 (4), pp.1139–1155. [Online]. Available at: doi:10.5194/gmd-8-1139-2015.
Pan, J. et al. (2006). Modeling plant nitrogen uptake and grain nitrogen accumulation in wheat. *Field Crops Research*, 97 (2–3), pp.322–336. [Online]. Available at: doi:10.1016/j.fcr.2005.11.006.
Pande, P. (2023). *Developing and applying the DO3SE-crop model to assess ozone impacts on wheat*. University of York.
Pande, P. et al. (2024a). Developing the DO3SE-crop model for Xiaoji , China. *EGUsphere [preprint]*. [Online]. Available at: doi:10.5194/egusphere-2024-694.
Pande, P. et al. (2024b). Ozone dose-response relationships for wheat can be derived using photosynthetic-based stomatal conductance models. *Agricultural and Forest Meteorology*, 356 (August 2023), p.110150. [Online]. Available at: doi:10.1016/j.agrformet.2024.110150.
Pandey, A. K. et al. (2018). Effect of elevated ozone and varying levels of soil nitrogen in two wheat (Triticum aestivum L.) cultivars: Growth, gas-exchange, antioxidant status, grain yield and quality. *Ecotoxicology and Environmental Safety*, 158 (April), pp.59–68. [Online]. Available at: doi:10.1016/j.ecoenv.2018.04.014.
Pandey, D. et al. (2023). Assessing the costs of ozone pollution in India for wheat producers, consumers and government food welfare policies. *PNAS*, 120 (32).
Pandiyan, A., Barbhai, M. and Medithi, S. (2019). A Review on Green Revolution, Nutritional Transition, Diabetes and Millet Movement in India. *The Indian Journal of Nutrition and Dietetics*, 56 (4), p.455. [Online]. Available at: doi:10.21048/ijnd.2019.56.4.23713.
Panozzo, J. F. and Eagles, H. A. (1999). Rate and duration of grain filling and grain nitrogen accumulation of wheat cultivars grown in different environments. *Australian Journal of Agricultural Research*, 50 (6), pp.1007–1015. [Online]. Available at: doi:10.1071/AR98146.
Paoletti, E. and Grulke, N. E. (2010). Ozone exposure and stomatal sluggishness in different plant physiognomic classes. *Environmental Pollution*, 158 (8), pp.2664–2671. [Online]. Available at: doi:10.1016/j.envpol.2010.04.024.
Pathak, H. et al. (2003). Modelling the quantitative evaluation of soil nutrient supply, nutrient use efficiency, and fertilizer requirements of wheat in India. *Nutrient Cycling in Agroecosystems*, 65 (2), pp.105–113. [Online]. Available at: doi:10.1023/A:1022177231332.
Patnaik, S., Tripathi, S. and Jain, A. (2019). *A Roadmap for Access to Clean Cooking Energy in India*. New Delhi. [Online]. Available at: doi:10.18003/ajpa.20189.
Payra, S. et al. (2022). Changes in tropospheric ozone concentration over Indo-Gangetic Plains: the role of meteorological parameters. *Meteorology and Atmospheric Physics*, 134 (6), pp.1–11. [Online]. Available at: doi:10.1007/s00703-022-00932-3.
Pedregosa, F. et al. (2011). Scikit-learn: Machine Learning in Python Fabian. *Journal of Machine Learning Research*, 12, pp.2825–2830. [Online]. Available at: doi:10.48550/arXiv.1201.0490.
Peña-Bautista, R. J. et al. (2017). Wheat-based foods: Their global and regional importance in the food supply, nutrition, and health. *Cereal Foods World*, 62 (5), pp.231–249. [Online]. Available at: doi:10.1094/CFW-62-5-0231.
Piikki, K. et al. (2008). The grain quality of spring wheat (Triticum aestivum L.) in relation to elevated ozone uptake and carbon dioxide exposure. *European Journal of Agronomy*, 28 (3), pp.245–254. [Online]. Available at: doi:10.1016/j.eja.2007.07.004.
Pilbeam, D. J. (2010). *The Utilization of Nitrogen by Plants: A Whole Plant Perspective*. [Online]. Available at: doi:10.1002/9781444328608.ch13.

Pingali, P. et al. (2019). *Food Systems for a Rising India. Palgrave Studies in Agricultural Economics and Food Policy*. Palgrave Macmillan, Cham. [Online]. Available at: doi:https://doi.org/10.1007/978-3-030-14409-8_4.

Pingali, P., Mittra, B. and Rahman, A. (2017). The bumpy road from food to nutrition security – Slow evolution of India's food policy. *Global Food Security*, 15 (April), pp.77–84. [Online]. Available at: doi:10.1016/j.gfs.2017.05.002.

Pleijel, H., Danielsson, H. and Broberg, M. C. (2022). Benefits of the Phytotoxic Ozone Dose (POD) index in dose-response functions for wheat yield loss. *Atmospheric Environment*, 268 (September 2021), p.118797. [Online]. Available at: doi:10.1016/j.atmosenv.2021.118797.

Pleijel, H. and Uddling, J. (2012). Yield vs. Quality trade-offs for wheat in response to carbon dioxide and ozone. *Global Change Biology*, 18 (2), pp.596–605. [Online]. Available at: doi:10.1111/j.1365-2486.2011.2489.x.

Poorter, H. et al. (2016). Pampered inside, pestered outside? Differences and similarities between plants growing in controlled conditions and in the field. *New Phytologist*, 212 (4), pp.838–855. [Online]. Available at: doi:10.1111/nph.14243.

Porter, J. R. (1993). AFRCWHEAT2: A model of the growth and development of wheat incorporating responses to water and nitrogen. *European Journal of Agronomy*, 2 (2), pp.69–82.

Porter, J. R. et al. (2014). Food security and food production systems. In: Field, C. B. et al. (Eds). *Climate Change 2014: Impacts, Adaptation, and Vulnerability. Part A: Global and Sectoral Aspects. Contribution of Working Group II to the Fifth Assessment Report of the Intergovernmental Panel on Climate Change*. Cambridge: Cambridge University Press. pp.485–533. [Online]. Available at: doi:10.1017/CBO9781107415379.012.

Porter, J. R. and Gawith, M. (1999). Temperatures and the growth and development of wheat: a review. *European Journal of Agronomy*, 10, pp.23–36. [Online]. Available at: %5C%5CGRAEFE%5CJournals%5CEuropean_Journal_of_Agronomy%5C_3.pdf.

Priesack, E., Gayler, S. and Hartmann, H. P. (2006). The impact of crop growth sub-model choice on simulated water and nitrogen balances. *Nutrient Cycling in Agroecosystems*, 75 (1–3), pp.1–13. [Online]. Available at: doi:10.1007/s10705-006-9006-1.

Raghunathan, K., Headey, D. and Herforth, A. (2020). Affordability of nutritious diets in rural India. *Food Policy*, 99. [Online]. Available at: doi:10.1016/j.foodpol.2020.101982.

Raghunathan, R. and Chandrasekaran, D. (2020). The Association Between the Attitude of Food-Waste-Aversion and BMI: An Exploration in India and the United States. *Journal of Consumer Psychology*. [Online]. Available at: doi:10.1002/jcpy.1168.

Rai, R. and Agrawal, M. (2012). Impact of tropospheric ozone on crop plants. *Proceedings of the National Academy of Sciences India Section B - Biological Sciences*, 82 (2), pp.241–257. [Online]. Available at: doi:10.1007/s40011-012-0032-2.

Ramachandran, P. (2019). School Mid-day Meal Programme in India: Past, Present, and Future. *Indian Journal of Pediatrics*, 86 (6), pp.542–547.

Rathore, A., Gopikrishnan, G. S. and Kuttippurath, J. (2023). Changes in tropospheric ozone over India: Variability, long-term trends and climate forcing. *Atmospheric Environment*, 309 (December 2022), p.119959. [Online]. Available at: doi:10.1016/j.atmosenv.2023.119959.

Reiling, K. and Davison, A. W. (1995). Effects of ozone on stomatal conductance and photosynthesis in populations of Plantago major L. *New Phytologist*, 129 (4), pp.587–594. [Online]. Available at: doi:10.1111/j.1469-8137.1995.tb03026.x.

Ren, W. et al. (2007). Effects of tropospheric ozone pollution on net primary productivity and carbon storage in terrestrial ecosystems of China. *Journal of Geophysical Research Atmospheres*, 112 (22), pp.1–17. [Online]. Available at: doi:10.1029/2007JD008521.

Rijal, B. et al. (2020). Drought Stress Impacts on Wheat and Its Resistance Mechanisms. *Malaysian Journal of Sustainable Agriculture*, 5 (2), pp.67–76. [Online]. Available at: doi:10.26480/mjsa.02.2021.67.76.

Ritchie, H., Rosado, P. and Roser, M. (2023). Agricultural Production. *Our World in Data*.

Rosenzweig, C. et al. (2018). Coordinating AgMIP data and models across global and regional scales for 1.5°C and 2.0°C assessments. *Philosophical Transactions of the Royal Society A: Mathematical, Physical and Engineering Sciences*, 376 (2119). [Online]. Available at: doi:10.1098/rsta.2016.0455.

Ruane, A. C. and Rosenzweig, C. (2019). Climate Change Impacts on Agriculture. In: Serraj, R. and Pingali, P. (Eds). *Agriculture & Food Systems to 2050*. First. London: World Scientific Publishing Co. Pte. Ltd. pp.161–192.

Rupa Kumar, K. et al. (2006). High-resolution climate change scenarios for India for the 21st century. *Current Science*, 90 (3), pp.334–345.

Saini, H., Sedgley, M. and Aspinall, D. (1983). Effect of Heat Stress During Floral Development on Pollen Tube Growth and Ovary Anatomy in Wheat (Triticum aestivum L.). *Australian Journal of Plant Physiology*, 10 (2). [Online]. Available at: doi:10.1071/PP9830137.

Saltelli, A. et al. (2008). *Global Sensitivity Analysis: The Primer*. Chichester: John Wiley & Sons Ltd. [Online]. Available at: doi:10.1111/j.1751-5823.2008.00062_17.x.

Salunke, P. et al. (2023). Future projections of seasonal temperature and precipitation for India. *Frontiers in Climate*, 5. [Online]. Available at: doi:10.3389/fclim.2023.1069994.

Sanchez-Bragado, R., Serret, M. D. and Araus, J. L. (2017). The nitrogen contribution of different plant parts to wheat

grains: Exploring genotype, water, and nitrogen effects. *Frontiers in Plant Science*, 7 (January), pp.1–14. [Online]. Available at: doi:10.3389/fpls.2016.01986.
Sarkar, A. et al. (2010). Investigating the impact of elevated levels of ozone on tropical wheat using integrated phenotypical, physiological, biochemical, and proteomics approaches. *Journal of Proteome Research*, 9 (9), pp.4565–4584. [Online]. Available at: doi:10.1021/pr1002824.
Sarkar, A. and Agrawal, S. B. (2010). Elevated ozone and two modern wheat cultivars: An assessment of dose dependent sensitivity with respect to growth, reproductive and yield parameters. *Environmental and Experimental Botany*, 69 (3), pp.328–337. [Online]. Available at: doi:10.1016/j.envexpbot.2010.04.016.
Savin, R. and Slafer, G. A. (1991). Developmental base temperature in different phenological phases of wheat (Triticum aestivum). *Journal of Experimental Botany*, 42 (241), pp.1077–1082. [Online]. Available at: http://jxb.oxfordjournals.org/.
Schauberger, B. et al. (2019). Global historical soybean and wheat yield loss estimates from ozone pollution considering water and temperature as modifying effects. *Agricultural and Forest Meteorology*, 265 (October 2018), pp.1–15. [Online]. Available at: doi:10.1016/j.agrformet.2018.11.004.
Schultz, M. G. et al. (2017). Tropospheric Ozone Assessment Report: Database and metrics data of global surface ozone observations. *Elementa: Science of the Anthropocene*, 5 (58). [Online]. Available at: doi:10.1525/elementa.244.
scikit-learn developers. (2023). *sklearn.metrics.r2_score; scikit-learn 1.3.2 documentation*. [Online]. Available at: https://scikit-learn.org/stable/modules/generated/sklearn.metrics.r2_score.html [Accessed 17 April 2024].
Shah, N. H. and Paulsen, G. M. (2003). Interaction of drought and high temperature on photosynthesis and grain-filling of wheat. *Plant and Soil*, 257 (1), pp.219–226. [Online]. Available at: doi:10.1023/A:1026237816578.
Shaheen, N. et al. (2016). Amino acid profiles and digestible indispensable amino acid scores of proteins from the prioritized key foods in Bangladesh. *Food Chemistry*, 213, pp.83–89. [Online]. Available at: doi:10.1016/j.foodchem.2016.06.057.
Sharkey, T. D. et al. (2007). Fitting photosynthetic carbon dioxide response curves for C3 leaves. *Plant, Cell and Environment*, 30 (9), pp.1035–1040. [Online]. Available at: doi:10.1111/j.1365-3040.2007.01710.x.
Sharma, A. et al. (2017). WRF-Chem simulated surface ozone over south Asia during the pre-monsoon: Effects of emission inventories and chemical mechanisms. *Atmospheric Chemistry and Physics*, 17 (23), pp.14393–14413. [Online]. Available at: doi:10.5194/acp-17-14393-2017.
Sharma, A. et al. (2019). Revisiting the crop yield loss in India attributable to ozone. *Atmospheric Environment: X*, 1 (December 2018), p.100008. [Online]. Available at: doi:10.1016/j.aeaoa.2019.100008.
Shewry, P. R. and Hey, S. J. (2015). The contribution of wheat to human diet and health. *Food and Energy Security*, 4 (3), pp.178–202. [Online]. Available at: doi:10.1002/FES3.64.
Shiferaw, B. et al. (2013). Crops that feed the world 10. Past successes and future challenges to the role played by wheat in global food security. *Food Security*, 5 (3), pp.291–317. [Online]. Available at: doi:10.1007/s12571-013-0263-y.
Shivakumar, N. et al. (2019). Protein-quality evaluation of complementary foods in Indian children. *American Journal of Clinical Nutrition*, 109 (5), pp.1319–1327. [Online]. Available at: doi:10.1093/ajcn/nqy265.
Shukla, A. K., Tiwari, P. K. and Prakash, C. (2014). Micronutrients Deficiencies vis-a-vis Food and Nutritional Security of India. *Indian Journal of Fertilisers Indian J. Fert*, 10 (12), pp.94–112.
Sicard, P. et al. (2017). Projected global ground-level ozone impacts on vegetation under different emission and climate scenarios. *Atmospheric Chemistry and Physics*, 17 (19), pp.12177–12196. [Online]. Available at: doi:10.5194/acp-17-12177-2017.
Siddiqi, R. A. et al. (2020). Diversity in Grain, Flour, Amino Acid Composition, Protein Profiling, and Proportion of Total Flour Proteins of Different Wheat Cultivars of North India. *Frontiers in Nutrition*, 7. [Online]. Available at: doi:10.3389/fnut.2020.00141.
Sillmann, J. et al. (2021). Combined impacts of climate and air pollution on human health and agricultural productivity. *Environmental Research Letters*, 16 (9). [Online]. Available at: doi:10.1088/1748-9326/ac1df8.
Silvestro, P. C. et al. (2017). Sensitivity analysis of the Aquacrop and SAFYE crop models for the assessment of water limited winter wheat yield in regional scale applications. *PLoS ONE*, 12 (11), pp.1–30. [Online]. Available at: doi:10.1371/journal.pone.0187485.
Simon-Sarkadi, L. and Galiba, G. (1996). Reflection of Environmental Stresses. *Periodica Polytechnica: Chemical Engineering*, 40 (1–2), pp.79–86.
Simpson, D. et al. (2012). The EMEP MSC-W chemical transport model – Technical description. *Atmospheric Chemistry and Physics*, 12 (16), pp.7825–7865. [Online]. Available at: doi:10.5194/acp-12-7825-2012.
Singh, D., Pachauri, S. and Zerriffi, H. (2017). Environmental payoffs of LPG cooking in India. *Environmental Research Letters*, 12 (11). [Online]. Available at: doi:10.1088/1748-9326/aa909d.
Singh, N., Dey, S. and Knibbs, L. D. (2023). Spatio-temporal patterns of tropospheric NO2 over India during 2005–2019. *Atmospheric Pollution Research*, 14 (3), p.101692. [Online]. Available at: doi:10.1016/j.apr.2023.101692.
Sinha, B. et al. (2015). Assessment of crop yield losses in Punjab and Haryana using 2 years of continuous in situ ozone measurements. *Atmospheric Chemistry and Physics*, 15 (16), pp.9555–9576. [Online]. Available at:

doi:10.5194/acp-15-9555-2015.
Sitch, S. et al. (2003). Evaluation of ecosystem dynamics, plant geography and terrestrial carbon cycling in the LPJ dynamic global vegetation model. *Global Change Biology*, 9 (2), pp.161–185. [Online]. Available at: doi:10.1046/j.1365-2486.2003.00569.x.
Soares, C. (2014). Chapter 19: Basic Design Theory. In: *Gas Turbines: A handbook of Air, Land and Sea Applications*. 2nd Editio. pp.913–958.
Soltani, A. and Hoogenboom, G. (2007). Assessing crop management options with crop simulation models based on generated weather data. *Field Crops Research*, 103 (3), pp.198–207. [Online]. Available at: doi:10.1016/j.fcr.2007.06.003.
Soltani, A. and Sinclair, T. R. (2012). *Modeling physiology of crop development, growth and yield*. Soltani, A. and Sinclair, T. R. (Eds). CAB International. [Online]. Available at: doi:10.1079/9781845939700.0001.
Somvanshi, P. S., Pandiaraj, T. and Singh, R. P. (2020). An unexplored story of successful green revolution of India and steps towards ever green revolution. *Journal of Pharmacognosy and Phytochemistry*, 9 (1), pp.1270–1273. [Online]. Available at: http://www.phytojournal.com.
Stevenson, D. S. et al. (2013). Tropospheric ozone changes, radiative forcing and attribution to emissions in the Atmospheric Chemistry and Climate Model Intercomparison Project (ACCMIP). *Atmospheric Chemistry and Physics*, 13 (6), pp.3063–3085. [Online]. Available at: doi:10.5194/acp-13-3063-2013.
Stöckle, C. O., Donatelli, M. and Nelson, R. (2003). CropSyst, a cropping systems simulation model. *European Journal of Agronomy*, 18 (3–4), pp.289–307. [Online]. Available at: doi:10.1016/S1161-0301(02)00109-0.
Stone, P. J. and Nicolas, M. E. (1995). A survey of the effects of high temperature during grain filling on yield and quality of 75 wheat cultivars. *Australian Journal of Agricultural Research*, 46 (3), pp.475–492. [Online]. Available at: doi:10.1071/AR9950475.
Sultana, N. et al. (2021). Wheat leaf senescence and its regulatory gene network. *Crop Journal*, 9 (4), pp.703–717. [Online]. Available at: doi:10.1016/j.cj.2021.01.004.
Suryavanshi, P. and Buttar, G. S. (2016). Mitigating Terminal Heat Stress in Wheat. *International Journal of Bio-resource and Stress Management*, 7 (1), pp.142–150. [Online]. Available at: doi:10.23910/ijbsm/2016.7.1.1333f.
Swaminathan, S., Vaz, M. and Kurpad, A. V. (2012). Protein intakes in India. *British Journal of Nutrition*, 108 (SUPPL. 2), pp.50–58. [Online]. Available at: doi:10.1017/S0007114512002413.
Szopa, S. et al. (2021). Short-lived Climate Forcers. In: Masson-Delmotte, V. et al. (Eds). *Climate Change 2021: The Physical Science Basis. Contribution of Working Group I to the Sixth Assessment Report of the Intergovernmental Panel on Climate Change*. Cambridge, United Kingdom and New York, USA: Cambridge University Press. pp.817–922. [Online]. Available at: doi:10.1017/9781009157896.008.817.
Tai, A. P. K. et al. (2021). Impacts of Surface Ozone Pollution on Global Crop Yields: Comparing Different Ozone Exposure Metrics and Incorporating Co-effects of CO2. *Frontiers in Sustainable Food Systems*, 5 (March), pp.1–18. [Online]. Available at: doi:10.3389/fsufs.2021.534616.
Tai, A. P. K. and Martin, M. V. (2017). Impacts of ozone air pollution and temperature extremes on crop yields: Spatial variability, adaptation and implications for future food security. *Atmospheric Environment*, 169, pp.11–21. [Online]. Available at: doi:10.1016/j.atmosenv.2017.09.002.
Tai, A. P. K., Martin, M. V. and Heald, C. L. (2014). Threat to future global food security from climate change and ozone air pollution. *Nature Climate Change*, 4 (9), pp.817–821. [Online]. Available at: doi:10.1038/nclimate2317.
Tang, H. et al. (2013). A projection of ozone-induced wheat production loss in China and India for the years 2000 and 2020 with exposure-based and flux-based approaches. *Global Change Biology*, 19 (9), pp.2739–2752. [Online]. Available at: doi:10.1111/gcb.12252.
Tao, F. et al. (2017). Effects of climate change , CO2 and O3 on wheat productivity in Eastern China, singly and in combination. *Atmospheric Environment*, 153, pp.182–193. [Online]. Available at: doi:10.1016/j.atmosenv.2017.01.032.
Tarannum, N. et al. (2024). Assessing the impact of surface ozone on wheat yield and economic losses in Rajasthan India: A comparitive analysis of concentration- and flux-based metrics. *[preprint]*.
Tarasick, D. et al. (2019). Tropospheric Ozone Assessment Report: Tropospheric ozone from 1877 to 2016, observed levels, trends and uncertainties. *Elementa: Science of the Anthropocene*, 7 (39). [Online]. Available at: doi:10.1525/elementa.376.
Tcherkez, G. et al. (2020). Elevated CO2 has concurrent effects on leaf and grain metabolism but minimal effects on yield in wheat. *Journal of Experimental Botany*, 71 (19), pp.5990–6003. [Online]. Available at: doi:10.1093/jxb/eraa330.
Tian, H. et al. (2015). Climate extremes and ozone pollution: a growing threat to China' s food security. *Ecosystem Health and Sustainability*, 2 (1). [Online]. Available at: doi:10.1002/ehs2.1203.
Tiwari, S. and Agrawal, M. (2018). *Tropospheric Ozone and its Impacts on Crop Plants*. Cham, Switzerland: Springer International Publishing. [Online]. Available at: doi:10.1007/978-3-319-71873-6.
Tkachuk, R. (1969). Nitrogen-to-protein conversion factors for cereals and oilseed meals. *Cereal Chemistry*, 46, pp.419–424. [Online]. Available at: https://www.cerealsgrains.org/publications/cc/backissues/1969/Documents/chem46_419.pdf.

Tomer, R. et al. (2015). Impact of elevated ozone on growth, yield and nutritional quality of two wheat species in northern india. *Aerosol and Air Quality Research*, 15 (1), pp.329–340. [Online]. Available at: doi:10.4209/aaqr.2013.12.0354.
Triboi, E. and Triboi-Blondel, A. M. (2002). Productivity and grain or seed composition: A new approach to an old problem - Invited paper. *European Journal of Agronomy*, 16 (3), pp.163–186. [Online]. Available at: doi:10.1016/S1161-0301(01)00146-0.
Tripathi, A. and Mishra, A. K. (2017). The Wheat Sector in India: Production, Policies and Food Security. In: *The Eurasian Wheat Belt and Food Security: Global and Regional Aspects*. pp.275–296. [Online]. Available at: doi:10.1007/978-3-319-33239-0_17.
UNEP. (2016). *Actions on air quality: Policies and programmes for improving air quality around the world*.
UNEP. (2021). *Actions on Air Quality: A Global Summary of Policies and Programmes to Reduce Air Pollution*. Nairobi. [Online]. Available at: https://www.unep.org.
US Department of Agriculture. (2024). *Production - Wheat*. [Online]. Statista. Available at: https://fas.usda.gov/data/production/commodity/0410000 [Accessed 28 May 2024].
Vazquez-Cruz, M. A. et al. (2014). Global sensitivity analysis by means of EFAST and Sobol' methods and calibration of reduced state-variable TOMGRO model using genetic algorithms. *Computers and Electronics in Agriculture*, 100, pp.1–12. [Online]. Available at: doi:10.1016/j.compag.2013.10.006.
Venkataraman, C. et al. (2024). Drivers of PM2.5 Episodes and Exceedance in India: A Synthesis From the COALESCE Network. *Journal of Geophysical Research: Atmospheres*, 129 (14), pp.1–18. [Online]. Available at: doi:10.1029/2024JD040834.
Waggoner, P. E. (1971). Plants and polluted air. *Bioscience*, 21 (10), pp.455–459.
Wall, G. W. et al. (2006). Interactive effects of elevated carbon dioxide and drought on wheat. *Agronomy Journal*, 98 (2), pp.354–381. [Online]. Available at: doi:10.2134/agronj2004.0089.
Wallach, D. (2011). Crop model calibration: A statistical perspective. *Agronomy Journal*, 103 (4), pp.1144–1151. [Online]. Available at: doi:10.2134/agronj2010.0432.
Wang, E. (1997). Mathematical description of the dynamic processes simulated in SPASS. In: *Development of a generic process-oriented model for simulation of crop growth*. Munich: Herbert Utz Verlag Wissenschaft. pp.28–83.
Wang, E. and Engel, T. (2002). Simulation of growth, water and nitrogen uptake of a wheat crop using the SPASS model. *Environmental Modelling and Software*, 17 (4), pp.387–402. [Online]. Available at: doi:10.1016/S1364-8152(02)00006-3.
Wang, L. et al. (2015). Diurnal variation of apoplastic ascorbate in winter wheat leaves in relation to ozone detoxification. *Environmental Pollution*, 207, pp.413–419. [Online]. Available at: doi:10.1016/j.envpol.2015.09.040.
Wang, P. et al. (2023a). Air pollution governance in China and India: Comparison and implications. *Environmental Science and Policy*, 142 (April 2022), pp.112–120. [Online]. Available at: doi:10.1016/j.envsci.2023.02.006.
Wang, R. et al. (2023b). Onset and severity thresholds of drought impacts on wheat. *Agricultural Water Management*, 281 (March), p.108259. [Online]. Available at: doi:10.1016/j.agwat.2023.108259.
Wang, X. et al. (2018). Metabolic adaptation of wheat grain contributes to a stable filling rate under heat stress. *Journal of Experimental Botany*, 69 (22), pp.5531–5545. [Online]. Available at: doi:10.1093/jxb/ery303.
Wang, Y. et al. (2017). Elevated ozone level affects micronutrients bioavailability in soil and their concentrations in wheat tissues. *Plant, Soil and Environment*, 63 (8), pp.381–387. [Online]. Available at: doi:10.17221/323/2017-PSE.
Wang, Y. et al. (2022). Reductions in crop yields across China from elevated ozone. *Environmental Pollution*, 292 (August 2021). [Online]. Available at: doi:10.1016/j.envpol.2021.118218.
Wang, Y. and Frei, M. (2011). Stressed food - The impact of abiotic environmental stresses on crop quality. *Agriculture, Ecosystems and Environment*, 141 (3–4), pp.271–286. [Online]. Available at: doi:10.1016/j.agee.2011.03.017.
Wheeler, T. and Von Braun, J. (2013). Climate Change Impacts on Global Food Security. *Science*, 341 (61645), pp.508–513. [Online]. Available at: http://dx.doi.org/10.1016/j.jsames.2011.03.003%0Ahttps://doi.org/10.1016/j.gr.2017.08.001%0Ahttp://dx.doi.org/10.1016/j.precamres.2014.12.018%0Ahttp://dx.doi.org/10.1016/j.precamres.2011.08.005%0Ahttp://dx.doi.org/10.1080/00206814.2014.902757%0Ahttp://dx.
Wild, O. et al. (2012). Modelling future changes in surface ozone: A parameterized approach. *Atmospheric Chemistry and Physics*, 12 (4), pp.2037–2054. [Online]. Available at: doi:10.5194/acp-12-2037-2012.
Williams, J. R. et al. (1989). EPIC crop growth model. *Transactions of the American Society of Agricultural Engineers*, 32 (2), pp.497–511. [Online]. Available at: doi:10.13031/2013.31032.
World Population Review. (2024). *Wheat consumption by country 2024*. [Online]. Available at: https://worldpopulationreview.com/country-rankings/wheat-consumption-by-country [Accessed 29 May 2024].
Wu, H. et al. (2016). Elevated ozone effects on soil nitrogen cycling differ among wheat cultivars. *Applied Soil Ecology*, 108, pp.187–194. [Online]. Available at: doi:10.1016/j.apsoil.2016.08.015.
Xu, B. et al. (2023). Impacts of meteorological factors and ozone variation on crop yields in China concerning carbon neutrality objectives in 2060. *Environmental Pollution*, 317 (September 2022). [Online]. Available at: doi:10.1016/j.envpol.2022.120715.

Xu, H. et al. (2007). Photosynthesis and yield responses of ozone-polluted winter wheat to drought. *Photosynthetica*, 45 (4), pp.582–588. [Online]. Available at: doi:10.1007/s11099-007-0100-7.
Xu, Z. et al. (2016). Elevated-CO2 response of stomata and its dependence on environmental factors. *Frontiers in Plant Science*, 7 (MAY2016), pp.1–15. [Online]. Available at: doi:10.3389/fpls.2016.00657.
Yadav, A. et al. (2019a). The effects of elevated CO2 and elevated O3 exposure on plant growth, yield and quality of grains of two wheat cultivars grown in north India. *Heliyon*, 5 (8), p.e02317. [Online]. Available at: doi:10.1016/j.heliyon.2019.e02317.
Yadav, D. S. et al. (2019b). ROS production and its detoxification in early and late sown cultivars of wheat under future O3 concentration. *Science of the Total Environment*, 659, pp.200–210. [Online]. Available at: doi:10.1016/j.scitotenv.2018.12.352.
Yadav, D. S. et al. (2020). Responses of an old and a modern Indian wheat cultivar to future O3 level: Physiological, yield and grain quality parameters. *Environmental Pollution*, 259. [Online]. Available at: doi:10.1016/j.envpol.2020.113939.
Yadav, D. S. et al. (2021). Diurnal variations in physiological characteristics, photoassimilates, and total ascorbate in early and late sown Indian wheat cultivars under exposure to elevated ozone. *Atmosphere*, 12 (12). [Online]. Available at: doi:10.3390/atmos12121568.
Yadav, D. S., Agrawal, S. B. and Agrawal, M. (2021). Ozone flux-effect relationship for early and late sown Indian wheat cultivars: Growth, biomass, and yield. *Field Crops Research*, 263 (December 2020), p.108076. [Online]. Available at: doi:10.1016/j.fcr.2021.108076.
Yang, Q., Zhao, D. and Liu, Q. (2020). Connections Between Amino Acid Metabolisms in Plants: Lysine as an Example. *Frontiers in Plant Science*, 11 (June), pp.1–8. [Online]. Available at: doi:10.3389/fpls.2020.00928.
Young, P. J. et al. (2013a). Corrigendum to 'Pre-industrial to end 21st century projections of tropospheric ozone from the atmospheric chemistry and climate model intercomparison project (ACCMIP)'. *Atmospheric Chemistry and Physics*, 13 (10), pp.5401–5402. [Online]. Available at: doi:10.5194/acp-13-5401-2013.
Young, P. J. et al. (2013b). Pre-industrial to end 21st century projections of tropospheric ozone from the Atmospheric Chemistry and Climate Model Intercomparison Project (ACCMIP). *Atmospheric Chemistry and Physics*, 13 (4), pp.2063–2090. [Online]. Available at: doi:10.5194/acp-13-2063-2013.
Zahra, N. et al. (2023). Impact of climate change on wheat grain composition and quality. *Journal of the Science of Food and Agriculture*, 103 (6), pp.2745–2751. [Online]. Available at: doi:10.1002/jsfa.12289.
Zanis, P. et al. (2022). Climate change penalty and benefit on surface ozone: A global perspective based on CMIP6 earth system models. *Environmental Research Letters*, 17 (2). [Online]. Available at: doi:10.1088/1748-9326/ac4a34.
Zhang, D. et al. (2023). Future climate change impacts on wheat grain yield and protein in the North China Region. *Science of the Total Environment*, 902 (August), p.166147. [Online]. Available at: doi:10.1016/j.scitotenv.2023.166147.
Zhang, J. et al. (2015). Wheat genotypic variation in dynamic fluxes of WSC components in different stem segments under drought during grain filling. *Frontiers in Plant Science*, 6 (AUG), pp.1–11. [Online]. Available at: doi:10.3389/fpls.2015.00624.
Zhao, D. et al. (2015). Overexpression of a NAC transcription factor delays leaf senescence and increases grain nitrogen concentration in wheat. *Plant Biology*, 17 (4), pp.904–913. [Online]. Available at: doi:10.1111/plb.12296.
Zheng, B. et al. (2015). *The APSIM-Wheat Module (7.5 R3008)*.
Zhou, S. S. et al. (2018). *Coupling between surface ozone and leaf area index in a chemical transport model : strength of feedback and implications for ozone air quality and vegetation health*. (x), pp.14133–14148. [Online]. Available at: doi:10.5194/acp-18-14133-2018.
Zhu, C. et al. (2009). Elevated CO2 accelerates flag leaf senescence in wheat due to ear photosynthesis which causes greater ear nitrogen sink capacity and ear carbon sink limitation. *Functional Plant Biology*, 36 (4), pp.291–299. [Online]. Available at: doi:10.1071/FP08269.
Zhu, C. et al. (2012). The temporal and species dynamics of photosynthetic acclimation in flag leaves of rice (Oryza sativa) and wheat (Triticum aestivum) under elevated carbon dioxide. *Physiologia Plantarum*, 145 (3), pp.395–405. [Online]. Available at: doi:10.1111/j.1399-3054.2012.01581.x.